

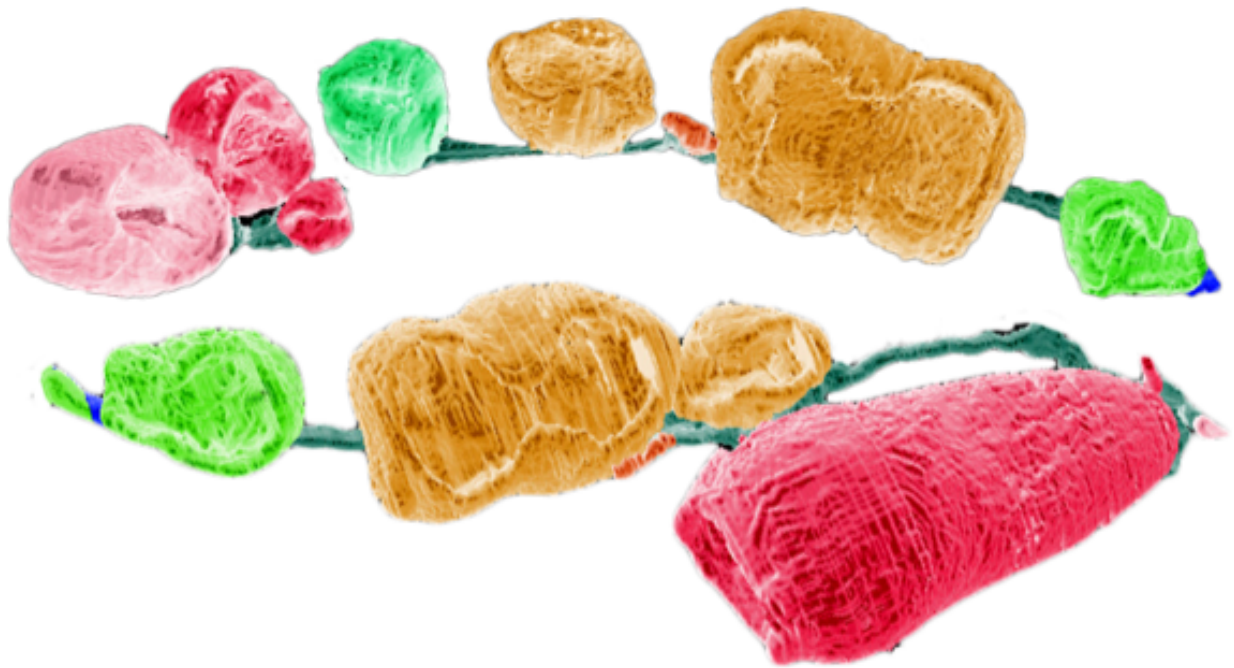


MONASH University

Developmental patterns behind mammalian tooth generation and evolution

Qamariya Nasrullah

BSc (Hons)



**A thesis submitted for the degree of Doctor of Philosophy at
Monash University in May 2018
School of Biological Sciences**

Under the Supervision of

**Dr. Alistair R. Evans — Monash University
Dr. Edwina McGlenn — ARMI, Monash University**

Courage doesn't
always roar.
Sometimes courage is
the quiet voice at the
end of the day saying,
'I will try again
tomorrow'.

- Mary Anne Radmacher

For Maryam, Bilal & Oliver
for giving me the courage.

Copyright notice

© The author (2018). Except as provided in the Copyright Act 1968, this thesis may not be reproduced in any form without the written permission of the author.

I certify that I have made all reasonable efforts to secure copyright permissions for third-party content included in this thesis and have not knowingly added copyright content to my work without the owner's permission.

Under the Copyright Act 1968, this thesis must be used only under the normal conditions of scholarly fair dealing. In particular, no results or conclusions should be extracted from it, nor should it be copied or closely paraphrased in whole or in part without the written consent of the author. Proper written acknowledgement should be made for any assistance obtained from this thesis.

ABSTRACT

Teeth are vital for a mammal's survival, helping it capture and process food. To be functional, teeth need to have precisely configured shapes and sizes to ensure fit within a jaw and for occlusion between the upper and lower jaws. Developmental processes, including molecular pathways, regulate tooth size, shape and replacement, and determine the number of generations produced. The current consensus asserts that the generation of replacement teeth occurs in the same manner in all mammals. Also, almost all mammals have a fixed number of teeth during their lifetime. However, some historical studies have suggested there are taxa that exhibit exceptions to the conventional replacement pattern, including the kangaroos and wallabies (Macropodidae). Investigating the three-dimensional relationships of developing teeth is made difficult by conventional two-dimensional techniques. Using the tammar wallaby (*Macropus eugenii*) as a study species, I sought to document the complete pattern of tooth development and replacement in three-dimensional space, using the stain and CT scan technique "diceCT". I also investigated unlimited tooth replacement within the nabarlek rock-wallaby (*Petrogale concinna*), in terms of its tooth size patterning from juvenile to adult by the inhibitory cascade, to determine how changes during development allow for this ability. Finally, I utilised the laboratory mouse (*Mus musculus*) to investigate how developmental interactions control shape and size by manipulating and *in-vitro* culturing of molar buds of different ages.

The diceCT technique enabled me to image 3D tissue-level resolution of developing tammar wallaby embryos and pouch young. I visualised both unmineralised and mineralised tooth structures *in situ*, following tooth development from bud-bell stages, and enamel and dentine deposition. Employing this technique, I documented tooth development and replacement within the tammar from before birth until dental maturity at four years of age. I discovered that the replacement tooth (the p3) developed anteriorly to its predecessor (dp3), and from the primary dental lamina, which differs from the general mammalian model of replacement. My other model macropodid, the nabarlek, also exhibited tooth development patterns that differed from its sister species. Both juveniles and adults of the other *Petrogale* species I examined, as well as juvenile nabarleks show an increasing tooth size pattern along the row. This pattern contrasts with the adult nabarleks, which instead shifted to molars of the same size. The nabarlek also had a more rapid tooth development pattern compared to its skull development. I found from our cultured mice molars that tooth-tooth inhibition influences the final size as well as shape of the tooth. By removing inhibition from the first molar (m1) from the second molar (m2), the m2 grew larger and developed an additional cusp, akin to the anteroconid cusp usually only found on the m1.

The unusual tooth replacement in the tammar wallaby raises issues with how tooth generations and successional lamina are currently defined. Furthermore, with the inclusion of past literature, we begin to see that many more marsupials and placentals also replace their teeth differently to the currently accepted model, highlighting the inability to generalise this model to all mammalian taxa. The nabarlek's ability to change its tooth size pattern from juvenile to adult indicates that molecular signals during development are being altered. Future explorations into these controlling factors are imperative to unlocking the key to continuous tooth generation, particularly for regenerative medicine. Finally, from the mice I find that molar tooth germs may all have equal size and shape potential and that it is the degree of inhibition along a gradient that produces morphological variation. I suggest the same inhibitory cascade mechanism may be responsible for shape variation seen in vertebrate forelimbs, digits and vertebrae, which previously have been shown to follow the IC for segment proportions, but not yet form.

General Declaration

Declaration for thesis based or partially based on conjointly published or unpublished work

I hereby declare that this thesis contains no material which has been accepted for the award of any other degree or diploma at any university or equivalent institution and that, to the best of my knowledge and belief, this thesis contains no material previously published or written by another person, except where due reference is made in the text of the thesis.

This thesis includes one original paper published in a peer reviewed journal and three unpublished papers. The core theme of the thesis is an exploration of developmental and evolutionary patterns of tooth size, shape and generation. The ideas, development and writing up of all the papers in the thesis were the principal responsibility of myself, the candidate, working within the School of Biological Science, Monash University, under the supervision of Associate Professor Alistair Evans.

The inclusion of co-authors reflects the fact that the work came from active collaboration between researchers and acknowledges input into team-based research.

In the case of chapters 2-5 my contribution to the work involved the following:

Thesis Chapter	Publication Title	Publication Status	Nature and % of student contribution	Co-author name(s) Nature and % of Co-author's contribution*	Co-author(s), Monash student Y/N*
2	Three-dimensional mammalian tooth development using diceCT	Published: Nasrullah, Q., Renfree, M. B., & Evans, A. R. (2018). Three-dimensional mammalian tooth development using diceCT. <i>Archives of oral biology</i> , 85, 183-191.	85%. Conception of study, data collection, processing and analysis, wrote manuscript and design and production of figures.	1) Alistair Evans, conception of study, collection of scan data, input into manuscript (10%) 2) Marilyn Renfree, Provided all wallaby specimens, input into methods section of manuscript (5%)	No
3	From embryo to adult: The complete development and "unusual" replacement of the tammar wallaby (<i>Macropus eugenii</i>) dentition	In preparation	85%. Conception of study, data collection, processing and analysis, wrote manuscript and design and	1) Alistair Evans, conception of study, collection of scan data, input into manuscript (10%) 2) Marilyn Renfree,	No

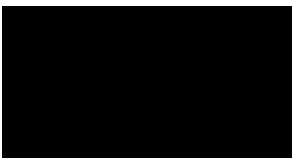
			production of figures.	Provided all wallaby specimens, input into methods section of manuscript (5%)	
4	Size pattern regulation of continuous tooth generation in the nabarlek (<i>Petrogale concinna</i>)	In preparation	90%. Conception of study, data collection, processing and analysis, wrote manuscript and design and production of figures.	1) Alistair Evans, conception of study, input into manuscript (10%)	No
5	Tooth shape patterns and the evolution of the anteroconid in Murid rodents	In preparation	75%. Conception of study, data collection, processing and analysis, wrote manuscript and design and production of figures.	1) Mona Christensen, conception of study, assistance in data collection and analysis of data (15%) 2) Alistair Evans, conception of study, input into manuscript (5%) 3) Jukka Jernvall, assistance in data collection (5%)	No

I have renumbered sections of the supplementary material, and reformatted references of Chapter 2 (the published paper) in order to generate a consistent presentation within the thesis.

Student signature: 

Date: 24 May 2018

The undersigned hereby certify that the above declaration correctly reflects the nature and extent of the student's and co-authors' contributions to this work. In instances where I am not the responsible author I have consulted with the responsible author to agree on the respective contributions of the authors.

Main Supervisor signature: 

Date: 23 May 2018

Appreciation is a
wonderful thing. It
makes what is
excellent in others
belong to us as well.

- Voltaire

Acknowledgements

Five years in the making and five pages of people to thank!



Firstly and foremostly, a warm and whole-hearted thank you to my supervisor, Alistair Evans, a talented scientist and fantastic lab head. Thank you for all the opportunities you have created for me, for nurturing my abilities, and for the skills and techniques you helped me to develop. I think together we have discovered some pretty cool things about teeth, but we only got to scratch the surface (microwear at best). These projects have opened up many more weird and wonderful questions about teeth to be answered and I hope that we get to collaborate on many more jaw-breaking discoveries in the future.



Thank you to my co-supervisor, Edwina McGlenn and your skilful team. It was an incredible experience to learn genetic techniques under your tutorage, and I now have these skills for life. I hope one day I can make proper use of them. A special thanks to Lisa Wong for her kindness and patience, and to the rest of the team Heidi, Eamon, Laura and Victoria for all their assistance and expertise.



To Marilyn Renfree, several of my chapters wouldn't be possible without you. You kindly donated an enormous amount of material, which we hopefully have put to good use and discovered some exciting things about macropodids. Your team have also been invaluable help to me on many occasions – Yu Chen and Stephen for genetic material and advice, and Chris for specimen collection and information.



A big thanks to my panel members, Rob Bryson-Richardson, Christen Mirth and John Bowman, for your feedback and guidance throughout my candidature. And a warm and heart-felt thank you to Fiona Hibbert, for keeping us calm and informed.



This was a truly unique and privileged PhD, where I got to spend some time in Finland, working with an incredible team at the University of Helsinki, during the pitch-black coldness of winter.

To my lab buddy Mona Christensen, I couldn't have done it without you! Not only did I enjoy

and benefit from our professional collaboration, but I will cherish our lifelong friendship. It was also a privilege to work under Jukka Jernvall's supervision, a brilliant developmental biologist, who has opened my eyes to an incredible branch of science I am keen to pursue a career in. I would also like to thank Susanna Sova for making me feel welcome in place far from home, Elodie Renvoise and Jacqueline Moustakas for their technical advice, and Agnes for taking the time to instruct me on how to do *in-situs*.



Another privilege of my PhD was also travelling around my own country, to collect the largest possible data set on the nabarlek wallaby. This was only feasible through the hospitality of the museum staff: Kenny Travouillon (WA Museum), David Stemmer (SA Museum), Karen Roberts, Katie Date and Ricky-Lee Erickson (Melbourne Museum), Gavin Dally (MAGNT), Leo Joseph and Robert Palmer (AWRC, CSIRO Canberra), and Sandy Ingleby (Australian Museum).



Collecting microCT data would have been a lot more difficult without Asadul Haque, for his maintenance and operations advice on the Xradia Versa scanner. Also, thanks to Karen Siu and Anton Maksimenko at the Australian Synchrotron for assistance in IMBL operations and processing of scans.



To Suresh and the SKB lab, thanks for saving my skin so many times during my tissue culturing experiments by allowing me to use your equipment when mine (many times) malfunctioned. A special thanks to Calvin for helping me with use of the incubator, and for Avilash for investigating CO₂ leaks with me.



To my fellow Adelaide expats, Elli and Andrew – thanks for introducing me to boreks, Coffea Café and the Dandenong Markets. Kat, you embraced Melbourne more in a few weeks than I did in several years, thanks for persuading me to give it a proper try. Erica – it was such a wonderful moment to be reunited with you at Bikram Yoga – friends who sweat together stay together. Leslie – sorry we didn't get to do more bike rides and brunch dates, but thanks for always being there for me. Michal, sorry I had to leave just as you arrived, but glad we got to dance to a few 90s numbers together.



I also wanted to thank my friends in Adelaide for staying put, if you had moved away, I wouldn't have your friendship to come home to. Rose, Sareen, Nellie and Ali, I hope we get to have many more gaming and farming dates. Kim and Tamara, thanks for your unwavering love and support for me, especially in chocolate form. Thanks Matt, for inspiring me to be more fierce and true to myself. Teagan and Wayne, we gotta hang out soon! Dennis – sharing this experience with you has helped me pull through, and congrats to you also! And Grace and Natalie – for being my inspiration in both academia and life. To the Flinders crew, Gav, Rach, Gully, Diana, Elen, Kailah, Aaron and Rod, thanks for always making time and space for me in your every-busy and growing lab!



Anjuli and Jarrod, my cosmopolitan comrades, thank for giving us a darn good reason to visit Canberra. I wish we had landed those jobs, but maybe we'll be working in the same place someday soon. Until then, I remain incredibly proud of you both, on the brave moves you'd made and the careers you've worked hard to set up for yourselves.



Doing a PhD is pretty tough, and when I was feeling most down, I got a job as receptionist for the MPA. This role gave me my confidence back and motivated me to persevere. Sometimes you have to step outside the science world to celebrate your successes and see how far you've really come. Thank you to Jess for seeing potential in me and to Jenny, Sunshine, Zuzanna, Ben, for your support, friendship and lots of laughs. You are an incredible bunch, and we (us students) are so lucky to have you.



Having worked five Royal Shows now during my PhD journey, and I would do 50 more because of my fantastic bosses, Caz and Susan. Thanks for being so supportive this whole time, you both are insanely good at your jobs and inspire me to try harder. Susie and Tari – looking forward to another crazy week with you!



I thought that the PhD journey would be a mores solitary one. I didn't expect to meet so many incredible people and make such good friends. Thank you to Emily, Julie, Kelsey, Cat and Mel for being there for me, sharing Uluru and Three Capes Hike with you are some of my most memorable experiences. Lotte and Stef, Netherlands should be proud they produced such inspiring and caring women. Stephen (and Savi), thanks for sharing the tough times, deep-dish

pie and the Labyrinth-sing along with me, here's to some celebratory beers soon (dance, magic, dance). Cass – whatever career you decide to do, you are going to kill it! It was truly awesome knowing you, and helped get me through, so thanks buddy! Also, thanks to Amanda, Evatt, Marie, Sonia, Cathy, Cat, Rowan, Toby, Louise, Helena, Ash, Viviana and anyone else I forgot! I couldn't have done it without each of you!



After having to move out from our beautiful Caulfield apartment, I was worried I would have nowhere to stay for my final few months. I was never homeless thanks to Nancy, Shane, Gem and Tiny, Clem and Michael – I wouldn't have been able to finish my data collecting or my thesis writing without your warm hospitality. You are also pretty fantastic company.



I wouldn't have lasted long without the support of my lab family. Travis and David, no matter how busy you were (raising children!) you always had time to help me. I was always inspired by your passion and enjoyment you got from science, maybe studying cool marine mammals helps? Alana, I was constantly wowed by your discoveries and methodical approaches to wombats and even bigger extinct wombats! You've been a wonderful role model and motivator. Matt, Michelle and Alan, thanks for helping me enjoy myself once in a while, whether it be all-you-can-eat Japanese, or weird taxidermy drinking games (no more feijoa or absinthe ever again, please). Angela and Kaitlyn, it was wonderful to have your company and support through the difficult times, and you both are exceptional scientists and people. I especially want to thank my dear friend Lap - it was such a pleasure to have got to spend some time with you. We miss you and hope you're enjoying your new job. Also, now that I'm done maybe we can finally make our movie show – seen any good films lately?



To the newbies: one of the few upsides of being first to the party and last to leave is being privy to all the fashionably late arrivals. James, Douglass and Alex, you are all such smart cookies and I expect you will do me and those crazy marsupials proud. Mark – you were just getting warmed up with insect segmentations – there's definitely a Nobel prize to be had in there. Billy – thanks for being such a lad and coming to my aid countless times, you'd do anything for a mate, and great things for Shep's rep. Silke, I wish I had got to know you better, but I am super excited to see what you find about snake teeth! And to my ladies (both prize winners and just winners in general): Tahlia, whose mind is as sharp as she dresses (like a

plagiaulacoid tooth with a high rake angle?) and Hazel, my modest friend, who has already taken the palaeo world by storm... you guys make me fulminate with admiration! Thank you to you all for making the final slog bearable, and even enjoyable. Love you to bits.



They say you can't choose your family but I think I lucked out. To my Aunty Nazli and her gorgeous and talented clan, thanks for taking care of me in your beautiful Coburg home and encouraging me to pursue my ambitions. To my sister Liz, thank you for being so kind and warm to a total stranger rocking up, spending hours talking about science, fashion and life with me, and always having so much confidence in me. Jon and Cathy, thanks for your continuous support and interest in my weird line of work, and for your warm hugs and home-cooked meals that kept me sustained.



To my brilliant brothers Tariq and Nur-El-Din, who are also my two best friends, even though I have always been so bossy and mad, you somehow have remained my unwavering fans, and have always cheered me on - I hope I have made you proud. To my dad Bilal and uncle Michael, I can't believe it is finally finished! Thanks for never letting me give up, for believing in me, and for helping me make sense of - and overcome difficult academic and administrative hurdles. To my mum, thanks for loving me no matter what, and for never doubting my abilities. You are a brilliant woman, and I would be lucky to inherit a fraction of your intelligence (dad's too). Hopefully some inklings of it can be seen throughout these pages!



And finally, to my partner Oliver ... Richard Dawkins says the chances of a person being born is a like a single grain of sand in a desert. Well at what odds did we end up in the same desert at the same time? I count myself lucky for meeting you every day. You have supported me from the start to end of my PhD and have somehow stuck by me through some incredibly stressful times. So, I hope I can repay you with a lifetime of happy memories. Here's to travelling and enjoying the world together.



Thank you all for your part, big or small, in this journey.



Table of Contents

ABBREVIATIONS	1
CHAPTER 1	3
INTRODUCTION	3
1.1 THESIS SUMMARY AND AIMS	4
1.2 REFERENCES	11
CHAPTER 2	14
THREE-DIMENSIONAL MAMMALIAN TOOTH DEVELOPMENT USING DICECT	14
ABSTRACT	15
2.1 INTRODUCTION	16
2.2 METHODS	19
2.3 RESULTS	23
2.4 DISCUSSION	33
2.5 ACKNOWLEDGMENTS	36
2.6 REFERENCES	37
CHAPTER 3	44
FROM EMBRYO TO ADULT: THE COMPLETE DEVELOPMENT AND UNUSUAL REPLACEMENT OF THE TAMMAR WALLABY (<i>MACROPUS EUGENI</i>) DENTITION.	44
ABSTRACT	45
3.1 INTRODUCTION	46
3.2 METHODS	52
3.3 RESULTS	55
3.4 DISCUSSION	65
3.5 CONCLUSIONS AND FUTURE DIRECTIONS	70
3.6 REFERENCES	71
CHAPTER 4	76
DEVELOPMENTAL PATTERNS OF CONTINUOUS TOOTH GENERATION IN THE NABARLEK (<i>PETROGALE CONCINNA</i>)	76
ABSTRACT	77
4.1 INTRODUCTION	78
4.2 METHODS	82

4.3 RESULTS	87
4.4 DISCUSSION	92
4.5 CONCLUSIONS AND FUTURE DIRECTIONS	96
4.6 REFERENCES	98
CHAPTER 5	102
PATTERNS OF TOOTH SHAPE DEVELOPMENT AND THE EVOLUTION OF THE ANTEROCONID IN MURID RODENTS.	102
ABSTRACT	103
5.1 INTRODUCTION	104
5.2 MATERIALS AND METHODS	109
5.3 RESULTS	111
5.4 DISCUSSION	114
5.5 CONCLUSIONS	118
5.6 REFERENCES	119
CHAPTER 6	123
DISCUSSION	123
6.1 DISCUSSION OF THESIS FINDINGS	124
6.2 CONCLUSIONS	139
6.3 REFERENCES	141
APPENDICES	151
FOR CHAPTERS 2-5	151
APPENDIX A	152
APPENDIX B	158
APPENDIX C	172
APPENDIX D	183

Abbreviations

When describing tooth identity, terminology was used as per Lockett and Wooley (1996): Incisor (I) Canine (C) Premolar (P) and Molar (M). Deciduous teeth were denoted by lowercase "d" (e.g. dP is a deciduous premolar). Upper teeth positions were annotated by a superscript number, and subscript for lower teeth (e.g. dP₃ is a lower deciduous premolar). When discussing both upper and lower teeth, normal font was used (e.g. dP3).

We must have
perseverance and
above all confidence in
ourselves. We must
believe that we are
gifted for something
and that this thing
must be achieved.

- Marie Curie

Chapter 1

Introduction

1.1 Thesis Summary and Aims

Modern and ancestral mammals collectively showcase great diversity in dental morphology, indicating adaptation to a variety of dietary niches. Mammals have also evolved more complex dentition, while limiting tooth replacement. These innovations have evolved in part through changes in developmental processes that determine the final tooth size, shape and number of tooth generations. Studying developmental patterns in multiple mammalian model organisms, I explore these innovations to shed light on their evolutionary pathways.

1.1.1 Mammalian Tooth Development

Tooth development transpires as interactions between the dental epithelium and underlying mesenchyme (Thesleff, 2003). Initiation begins from the primary dental lamina which thickens at localised points to form the future sites of teeth. Tooth buds go through bud, cap and bell stages, where some become mineralised, and those that become part of the functional dentition then erupt (Lockett, 1993b).

Successional generations and molars initiate differently, where they arise from a secondary extension of dental lamina. Known as the successional lamina, this extends posteriorly from the last deciduous premolar, and gives rise to the first molar (M1). The M1 in turn then produces a posterior extension of successional lamina, which then produces the next molar (M2). This patterns continues for the production of subsequent molars.

Similarly, replacement dentition is produced from the successional lamina. However, this lamina usually arises lingually from the tooth that it will replace (Lockett, 1993a) (Figure 1.1). This successional lamina degrades after giving rise to the replacement dentition (Štembírek *et al.*, 2010). This degradation is thought to be responsible for limiting the number of tooth generations in mammals.

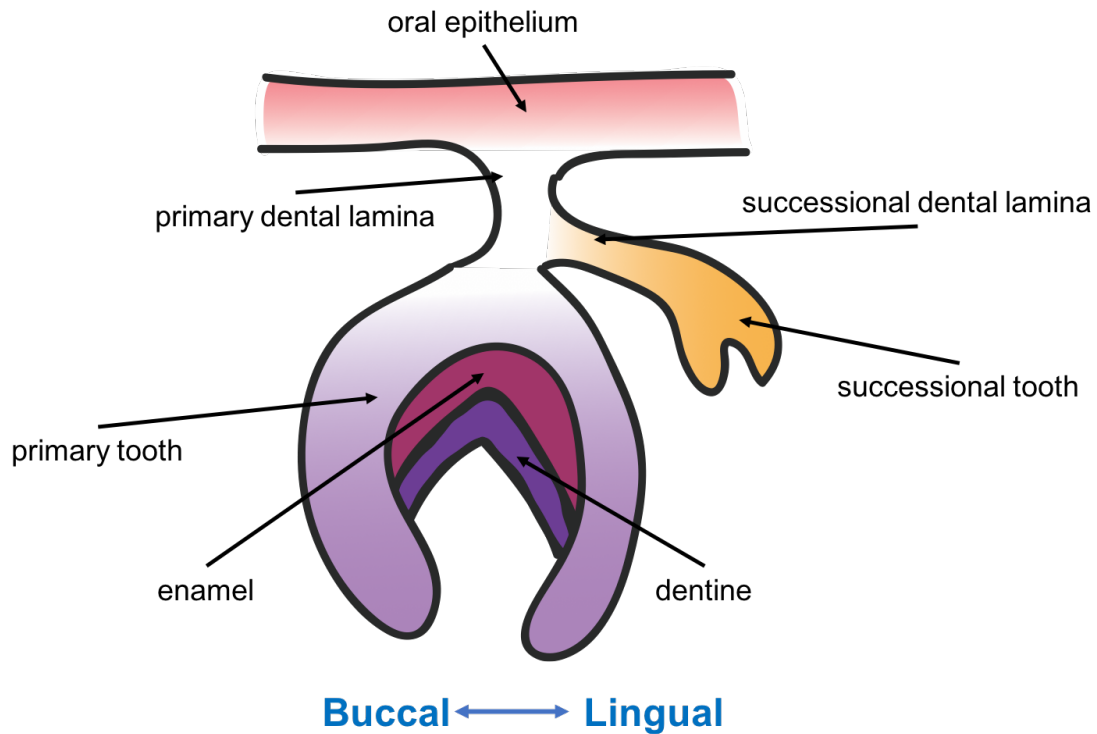


Figure 1.1 Tooth development of lower primary and secondary (successional) generations of teeth. The former develop from the primary dental lamina, the latter from the successional dental lamina, normally lingually from the tooth it replaces.

1.1.2 Marsupial Tooth Replacement Patterns

Most tooth development studies have examined the mouse *Mus musculus*, which does not have tooth replacement. Studies on non-model species with tooth replacement, such as the carnivorous marsupial *Antechinus flavipes*, suggest that mammalian tooth replacement may occur in different ways (Archer 1974). Unlike diphyodont placentals that have two sets of teeth per locus, marsupials only erupt one replacement tooth at the dP3 locus (third deciduous premolar), by the P3 (third permanent premolar).

A key study by Lockett (1993a) that included 13 orders of eutherians and four major marsupial families found homologies between these divergent groups. Lockett (1993a, b) deduced two rules about a true successional tooth within these mammals: that it develops from the successional lamina, and that it develops lingually from the deciduous predecessor. However, Lockett highlighted that there is conflict surrounding whether tooth succession occurs in this way or at all, especially within macropodids (kangaroos and wallabies). In some studies, it appears that the replacement tooth (P3) develops from the

primary dental lamina, and mesially from the dP3 it replaces (Berkovitz, 1966: 1972, Kirkpatrick, 1969). This pattern, if confirmed, would defy the convention that Lockett (1993a) proposed for all mammals.

One major reason macropodid tooth succession patterns remain contentious is because a complete documentation of their tooth development and replacement event is lacking. Most studies only provide snapshots of early stages, none so far having documented the P3 from initiation to eruption. Another issue is that most evidence provided for tooth replacement events are single 2D histological sections, which can be open to interpretation. The 3D visualisation of embryonic development is a challenge, especially imaging unmineralised tissue, a low density material difficult to pick up in X-ray CT scans. One solution to this problem has been to produce 3D models by combining microCT scanning with inorganic Lugol's Iodine Solution (I₂KI), a differential stain that targets epithelial cells (and thus some tooth tissues). Iodine accumulates in these cells creating a more differentiated grading of X-ray attenuation, increasing the visual contrast of unmineralised tissue.

The combination of microCT scanning with Lugol's solution is a relatively recent technique, first introduced by Metscher (2009), and termed diceCT (Diffusible Iodine-base Contrast-Enhanced Computed Tomography) by Gignac *et al.* (2016). Applications include the phenotyping of cardiovascular development in mouse embryos (Degenhardt *et al.*, 2010) and visualising the soft tissue anatomy of heads of post-embryonic archosaurs (Gignac and Kley, 2014). This has yet to be tested on marsupial young which undergo development both *in utero* and in the pouch.

In **Chapter 2** I test the potential of diceCT as a non-destructive technique to visualise and study the development of tooth classes, tooth generations, cusp morphogenesis and mineralisation *in situ*, using the tammar wallaby *Macropus eugenii* as a case study. The microCT scans of developing fetuses and pouch young are stained using Lugol's Iodine contrast agent. Stained versus unstained specimen comparisons are made to investigate whether staining had improved visualisation of structures. Scan slices are compared to histological sections to confirm the identity of tissues and structures. The tammar wallaby *Macropus eugenii* is an organism with relatively complex tooth shape and replacement, only

partially documented, making it an ideal model to test this technique and to gain insight into marsupial and other mammal tooth evolution and development.

In **Chapter 3**, using the diceCT method described in Chapter 2, I aim to provide a complete documentation of the tammar wallaby tooth development and replacement pattern, following tooth development from initiation (before birth) to completion (four years of age) when the fourth and final molars erupt. Tissue layers are digitally segmented to create 3D models. This series is potentially the most temporally and anatomically complete 3D digitisation of a mammalian tooth development and replacement sequence to date. Using these models, I can thus confirm whether the P3 is a true successor or not within this macropodid model, and whether its pattern conforms with Lockett's proposed conventions. These findings may shed further light on interpreting not only marsupial but mammalian replacement processes.

1.1.3 The Inhibitory Cascade Model

Mammalian molars have been observed to follow distinct size patterns, where sequential molars are produced in an increasing, decreasing or uniform size pattern. This control of molar size is proposed to be via an Inhibitory Cascade (IC) mechanism, where the growth of one molar dictates the size of the adjacent teeth through an interplay of activation and inhibition (Kavanagh *et al.*, 2007). Tissue culture experiments separating the first molar from the second molar resulted in teeth that grew larger and faster than normal. This effect appeared to be a result of a reduction in the inhibitor molecules from the M1 to the M2 (Figure 1.2), a flowthrough effect also seen with the M3. From these observed size patterns of molars, it appears that inhibition/activation occurs along a directional gradient, and that the M1 influences the M2, which influences the M3.

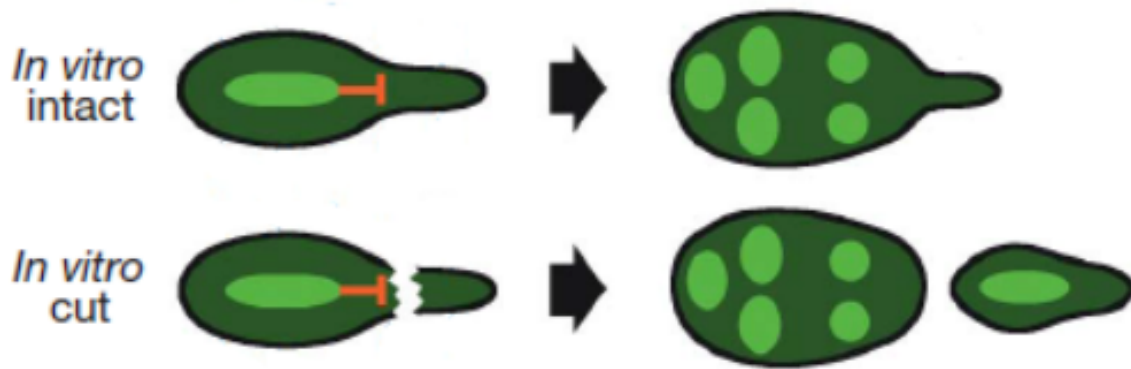


Figure 1.2 *In-vitro* culturing of M1 and M2, where posterior tail that forms M2 from M1 is cut, to test an inhibitory hypothesis. The M2 in the *in-vitro* cut develops more quickly and grows larger than the *in-vitro* intact. From Kavanagh *et al.* (2007).

1.1.4 The Case Of The Nabarlek

The IC provides a framework of developmental controls of tooth size, which may allow for such innovations as continuous tooth replacement. The nabarlek (*Petrogale concinna*) is a species of rock-wallaby and one of 5 mammalian species in the world that can continuously replace its teeth (Gomes Rodrigues *et al.*, 2011). The key to its ability may be the achievement of an activation/inhibition balance in its tooth development causing the newly grown posterior molars to grow a similar size and shape (Tate, 1948), allowing a seamless production line progressing from within the jaw.

While Chapters 2 and 3 focus on documenting the developmental pattern of the tammar wallaby, **Chapter 4** concentrates on determining the mechanisms behind the continuous tooth replacement ability of the nabarlek rock-wallaby, by looking at controls of its tooth size as it grows. Measuring the occlusal areas of nabarlek tooth rows provides quantitative data on this change in size gradient, from an increasing to equivalent size between teeth, as well as shows at what age this change occurs. I compare tooth row size patterns to the nabarlek's nearest relatives, *Petrogale brachyotis* and *Petrogale burbidgei* to establish that this pattern is unique to the nabarlek and a possible requisite trait for continuous tooth generation in mammals.

1.1.5 Molar Shape Influenced by Inhibition

Though the IC model suggests that tooth-tooth inhibition controls size, there is evidence that shape may also be affected, where dental complexity was shown to be highest in the middle of the tooth row, with shape becoming simpler anteriorly and posteriorly (Butler, 1939). If shape is also shown to follow a gradient, perhaps simpler teeth have the capacity to become more complex but are impeded in their development by inhibition; for example, the presence of a premolar may inhibit the potential complexity of the adjacent molar (Labonne *et al.*, 2012).

Provisional evidence of inhibition affecting shape has been found in the fossil record. In rodents a fifth cusp, known as the anteroconid, evolved on the M1. The appearance of the anteroconid occurred at the same time premolars disappeared around 55 million years ago (Peterková *et al.*, 2005). This has been suggested to have evolved through the integration of the premolar (P4) bud cells into the developing first molar (M1), providing the materials for the extra cusp (Prochazka *et al.*, 2010). The IC model, however, provides an alternate explanation to this, where I propose that the disappearance of the premolar freed the first molar from inhibition, permitting it to grow larger and more complex.

In **Chapter 5**, the IC is explored as a mechanism influencing tooth shape, where I extend the original mice tooth culture experiments (from Kavanagh *et al.*, 2007) to manipulate and produce more complex teeth through the simple removal of tooth-tooth inhibition. I dissect out M1s of e14 (embryonic day 14) mice, and M2s of e16 mice, which are of similar size, to culture next to each other *in-vitro*. By beginning with two similar sized molars, we can determine whether inhibition acts equally between the two teeth. By placing the M2 anterior to the M1, we can test whether inhibition only occurs uni-directionally and if the posteriorly-placed M1 will be unable to inhibit the M2.

In **Chapter 6**, in light of my findings from chapters 2-5, I discuss techniques of documenting tooth development, and developmental patterns of tooth size, shape and generation. I reflect on the future of morphological digitisation, and how it will contribute to the sharing of knowledge to verify developmental studies of teeth and other organs. I find that the current model of tooth replacement is not applicable to the tammar wallaby, let alone many more mammal species, which show a lot more variation than previously reported. I outline the adaptations the nabarlek and other species have to allow for

continuous tooth generation, and how these may benefit our understanding of evolution and potentially future medical applications. Furthermore, I propose that not only tooth size (which is well documented), but tooth shape can be controlled by the IC, which has great implication for our understanding of shape patterning, not just of teeth, but possibly other serial body parts. I also present my final conclusions of this thesis.

1.2 References

- Archer, M. (1974). The development of cheek teeth in *Antechinus flavipes* (Marsupialia, Dasyuridae). *Journal of the Royal Society of Western Australia*, 57, 54-63.
- Berkovitz, B. K. B. (1966). The homology of the premolar teeth in *Setonix brachyurus* (Macropodidae: Marsupialia). *Archives of oral biology*, 11(12), 1371-IN39.
- Berkovitz, B. K. B. (1972). Tooth development in *Protemnodon eugenii*. *Journal of dental research*, 51(5), 1467-1473.
- Butler, P. M. (1939). Studies of the Mammalian Dentition.—Differentiation of the Post-canine Dentition. *Journal of Zoology*, 109(1), 1-36.
- Degenhardt, K., Wright, A. C., Horng, D., Padmanabhan, A., & Epstein, J. A. (2010). Rapid three-dimensional phenotyping of cardiovascular development in mouse embryos by micro-CT with iodine staining. *Circulation: Cardiovascular Imaging, CIRCIMAGING*-109.
- Gignac, P. M., & Kley, N. J. (2014). Iodine-enhanced micro-CT imaging: Methodological refinements for the study of the soft-tissue anatomy of post-embryonic vertebrates. *Journal of Experimental Zoology Part B: Molecular and Developmental Evolution*, 322(3), 166-176.
- Gignac, P. M., Kley, N. J., Clarke, J. A., Colbert, M. W., Morhardt, A. C., Cerio, D., ... & Echols, M. S. (2016). Diffusible iodine-based contrast-enhanced computed tomography (diceCT): an emerging tool for rapid, high-resolution, 3-D imaging of metazoan soft tissues. *Journal of anatomy*, 228(6), 889-909.
- Gomes Rodrigues, H., Marangoni, P., Šumbera, R., Tafforeau, P., Wendelen, W., & Viriot, L. (2011). Continuous dental replacement in a hyper-chisel tooth digging rodent. *Proceedings of the National Academy of Sciences*, 108(42), 17355-17359.
- Kavanagh, K. D., Evans, A. R., & Jernvall, J. (2007). Predicting evolutionary patterns of mammalian teeth from development. *Nature*, 449(7161), 427-432.
- Kirkpatrick, T. H. (1969). The dentition of the marsupial family Macropodidae: with particular reference to tooth development in the grey kangaroo *Macropus giganteus* Shaw.

- Labonne, G., Laffont, R., Renvoise, E., Jebrane, A., Labruère, C., Chateau-Smith, C., ... & Montuire, S. (2012). When less means more: evolutionary and developmental hypotheses in rodent molars. *Journal of evolutionary biology*, 25(10), 2102-2111.
- Luckett, W. P. (1993a). An ontogenetic assessment of dental homologies in therian mammals. In *Mammal phylogeny* (pp. 182-204). Springer, New York, NY.
- Luckett, W. P. (1993b). Ontogenetic staging of the mammalian dentition, and its value for assessment of homology and heterochrony. *Journal of Mammalian Evolution*, 1(4), 269-282.
- Metscher, B. D. (2009). MicroCT for developmental biology: A versatile tool for high-contrast 3D imaging at histological resolutions. *Developmental dynamics*, 238(3), 632-640.
- Peterková, R., Lesot, H., Viriot, L., & Peterka, M. (2005). The supernumerary cheek tooth in *tabby/EDA* mice—a reminiscence of the premolar in mouse ancestors. *Archives of oral biology*, 50(2), 219-225.
- Prochazka, J., Pantalacci, S., Churava, S., Rothova, M., Lambert, A., Lesot, H., ... & Peterková, R. (2010). Patterning by heritage in mouse molar row development. *Proceedings of the National Academy of Sciences*, 107(35), 15497-15502.
- Štembírek, J., Buchtová, M., Král, T., Matalová, E., Lozanoff, S., & Míšek, I. (2010). Early morphogenesis of heterodont dentition in minipigs. *European journal of oral sciences*, 118(6), 547-558.
- Tate, G. H. H. (1948). Studies on the anatomy and phylogeny of the Macropodidae (Marsupialia). *Bulletin of the AMNH*; v. 91, article 2.
- Thesleff, I. (2003). Epithelial-mesenchymal signalling regulating tooth morphogenesis. *Journal of cell science*, 116(9), 1647-1648.

Know how to learn.
Then, want to learn.
- Katherine Johnson

Chapter 2

**Three-dimensional mammalian tooth development
using diceCT**

ABSTRACT

Objective: This study aims to develop the Diffusible Iodine-based Contrast-Enhanced CT (diceCT) method for non-destructive imaging of both soft and mineralised tissues. We sought to document the 3D spatio-temporal pattern of mammalian tooth development including multiple tooth classes and generations, using the tammar wallaby (*Macropus eugenii*) as a model species.

Design: We took microCT scans of developing fetuses and pouch young stained using Lugol's Iodine (I2KI) contrast agent. Stained versus unstained specimen comparisons were then made to investigate whether staining had improved visualisation of structures. Scan slices were compared to histological sections to confirm the identity of tissues and structures. Tissue layers were digitally segmented to create 3D models.

Results: DiceCT dramatically enhanced visual contrast of soft tissues, allowing differentiation between epithelial and mesenchymal layers. Subvolume scans at higher magnification achieved single-cell layer resolution within relatively large intact heads. We observed *in-situ* initiating teeth, which progressed through major stages of tooth

development including morphogenesis and mineralisation. In addition, we traced the development of other mineralized and unmineralised tissues, such as the cranial bones and the brain, eye and olfactory system.

Conclusions: DiceCT was time- and cost-effective in producing complex 3D models of the entire dentition of the tammar wallaby at each developmental stage with tissue-level resolution. The 3D view of soft and mineralised tooth structures allowed us to define tooth class and generation from a developmental perspective. Additionally, the development of other organs can also be documented using the same scans, demonstrating the efficiency and versatility of this technique.

2.1 Introduction

Tooth production, replacement and function are all products of precisely-controlled development, which in turn can be used as a model for understanding genetics, evolution, and oral health. Because teeth are part of living systems, they allow for real-time observation of developmental patterns, such as cusp formation (Vaahtokari *et al.*, 1996; Kangas *et al.*, 2004), as well as the investigation of signalling pathways shared with a variety of other structures, including hair follicles (Andl *et al.*, 2004), sweat glands (Tucker *et al.*, 2000), the palate (Satokata and Maas, 1994) and vertebrae (Peters *et al.*, 1998). In addition, knowledge of tooth and craniofacial development is essential in understanding and treating medical issues like cleft palate deformation (Celli *et al.*, 1999; Peters *et al.*, 1998), oligodontia (Nieminen *et al.*, 2001) and cleidocranial dysplasia (D'Souza *et al.*, 1999). Finally, from an evolutionary point of view, teeth have been instrumental in documenting morphological transitions in range of vertebrates, including primates (Smith 1989), hominids (Sofaer *et al.*, 1971; Evans *et al.*, 2016), and rodents (Peterková *et al.*, 2005; Peterková *et al.*, 2006; Prochazka *et al.*, 2010; Harjunmaa *et al.*, 2012; Gomes Rodrigues *et al.*, 2013).

Traditionally, paraffin sectioning has been employed to investigate tooth development, resulting in 3D reconstructions of serial sections based on hand drawn interpretations (Berkovitz 1972; Ooë, 1979), wax reconstructions (Berkovitz, 1978), cardboard cut-outs (Ooë, 1981), and thin section computer alignment (Lesot *et al.*, 1996; Peterková *et al.*, 1996; Vaahtokari *et al.*, 1996; Jernvall *et al.*, 1998). More recently Radlanski *et al.* (2016) completed 3D reconstructions of sectioned human fetus jaws and were able to partially model the tooth development pattern. However, the physical process of sectioning is inherently destructive and tends to distort the original morphology, making it an unfavourable technique for rare material.

Scanning technology has revolutionised developmental biology by allowing non-destructive 3D documentation of embryological material, though each method has its limitations. Magnetic resonance imaging (MRI) is effective for imaging soft tissue but does not allow high resolution (Sharpe, 2003), while optical projection tomography (OPT) is limited to

small-sized samples (Correia *et al.*, 2015). X-ray microcomputed tomography (microCT) produces high resolution images, but low attenuation levels can make it difficult to distinguish soft from mineralised tissues (Descamps *et al.*, 2014), let alone different soft tissue layers from each other.

One solution to this problem has been to combine microCT scanning with a differential stain, with candidates including: gallocyanin-chromalum, which targets cell nuclei; phosphotungstic acid (PTA), effective but with slow penetration rates (Metscher, 2009b); phosphomolybdic acid (PMA) which is also highly effective but again has slower penetration rates or osmium tetroxide (OsO₄) which is common but highly toxic (Descamps *et al.*, 2014); and inorganic Lugol's Iodine (I₂KI), which is a smaller molecular and has a much more rapid diffusion rate (Metscher, 2009a,b), has a high affinity for glycogen (Fennerty, 1999) and targets epithelial cells. The combination of microCT scanning with Lugol's solution is a relatively recent technique, first introduced by Metscher (2009b), and termed diceCT (Diffusible Iodine-base Contrast- Enhanced Computed Tomography) by Gignac *et al.* (2016). Applications include the phenotyping of cardiovascular development in mouse embryos (Degenhardt *et al.*, 2010) and visualising the soft tissue anatomy of heads of post-embryonic archosaurs (Gignac and Kley, 2014).

To date, diceCT has not been used to document tooth development, but potentially holds great promise. Lugol's specificity could help to visualise crucial interactions between the dental epithelium and the underlying mesenchyme (Neubüser *et al.* 1997; Thesleff, 2003; Soukup, *et al.*, 2008; Fraser *et al.*, 2009; Jernvall and Thesleff, 2012). In mammals, developing tooth germs pass through bud, cap and bell stages, and then become increasingly mineralised before erupting. These earlier "soft" stages are crucial for tooth shape formation, but, owing to their weak attenuation of X-rays, have often been difficult to visualise. With the aid of Lugol's solution, simultaneous, detailed imaging of soft tissues and incipient mineralisation should be possible.

The feasibility of a similar technique was demonstrated by Harjunmaa *et al.* (2012) who pioneered the combined use of microCT and staining to study teeth by producing 3D models of developing mouse molars with the help of phosphotungstic acid stain (PTA). Their approach allowed them to segment digitally the mesenchyme from the epithelium,

although their study was restricted to excised and cultured tooth germs. Although that study was a significant step forward, it only examined the epithelial-mesenchyme interface of bud to bell stages of unmineralised teeth. Teeth have many more differentiated tissue layers, including several that increasingly mineralise. These stages and layers also need to be included in order to completely document mammalian tooth development. PTA also does not appear to adhere to cartilage as well as Lugol's (Metscher, 2009a; Descamps *et al.*, 2014), and may not be able to visualise partially mineralised structures of developing teeth.

Another stain and scan study using a silver-based contrast agent (Protargol-S) effectively imaged developing teeth within e12-e15 mouse embryos (Raj *et al.* 2014). However, they found that penetration was sub-optimal in older mice (>e18), even when using synchrotron beam energy. While Lugol's has been shown to produce good contrast in more mineralised or larger specimens, even when using desk-top scanners. In addition, as with the Harjunmaa *et al.* (2012) study, because mice do not show tooth replacement and have only two tooth classes, they are a limited model for studying dental morphogenesis and replacement.

Here, we test the potential of diceCT as a non-destructive technique to visualise and study the development of tooth classes, tooth generations, cusp morphogenesis and mineralisation *in-situ*, using the tammar wallaby *Macropus eugenii* as a case study. Berkovitz (1972) used hand reconstructed paraffin sections to document the tooth development of *M. eugenii*, but could not conclusively capture complex 3D relationships, such as lamina connections between primary and secondary generations. Another previous study investigated the oral apparatus of the tammar using microCT alone, but only targeted the mineralised cranial elements, rather than the tooth development pattern (Goswami *et al.*, 2016). *Macropus eugenii* has four tooth classes (incisor, canine, premolars and molars), tooth replacement with two tooth generations at some positions, and, unusually among mammals, molar progression (anterior movement of molars through life; Sanson, 1989), making it an opportune model for studying tooth development within mammals.

2.2 Methods

2.2.1 Specimen Fixation and Staining

Macropus eugenii, the tammar wallaby, has a complex reproductive pattern. Tammars mate immediately post-partum, and the new conceptus enters embryonic diapause while the neonate enters the pouch and continues its development for ~9 months, supported by a dynamic and changing lactation (Tyndale-Biscoe and Renfree, 1987). Removal of the sucking stimulus by removing the pouch young (RPY) initiates development of the diapausing blastocyst, with birth 26.5 days later. Embryonic and fetal stages are timed from the day RPY. The day of birth was designated day 0 post-partum (pp). Heads of 16 wallaby fetuses (day 23 RPY to day 26 RPY) and pouch young ranging in age from the day of birth (day 0 pp) to 258 pp were collected as previously described (Renfree *et al.*, 1982; Hickford *et al.*, 2009) (Tables A2.1 and A2.2). Ages were recorded from either known day of birth or estimated from the head length growth curves of Poole *et al.*, (1991). Growth (head length versus age) do not differ between males and females until the time of puberty (Poole *et al.*, 1991), so the sexes were combined.

Specimens were fixed and gently agitated in 4% paraformaldehyde for 24 h, washed in PBS and stored in either 100% methanol or 70% ethanol. The specimens were stained in Lugol's solution (prepared by adding 10 g KI plus 5 g I₂ in 100 mL H₂O, then diluted to 10% in water, following Metscher 2009a, 2009b), making a working stock of 1.5% w/v. Most specimens were stained between 2 to 14 days, depending on their size (Tables A2.1 and A2.2), although our largest specimen took 28 days. Staining times were conservative based on those for smaller, less mineralized specimens such as mice (24–72 h, Degenhardt *et al.*, 2010; Wong *et al.*, 2013), or much larger, more mineralized animals, such as alligators (7–28 days, Gignac and Kley, 2014). Most specimens were placed on a gentle 2D rocker to assist penetration, with Lugol's solution replenished every day or two. After being scanned, all Lugol's-stained specimens were destained by being soaked in water for several days, then in 1% sodium thiosulfate for a week. They were then transferred back into their original storage solution (100% methanol or 70% ethanol).

2.2.2. MicroCT Scanning

Stained specimens were removed from Lugol's solution, rinsed in distilled water, patted dry with a paper towel, and wrapped in Parafilm to prevent dehydration. For larger specimens, we used transfer pipettes to remove water from the oesophagus, in order to prevent movement of the head during the scan. Specimens were positioned inside Eppendorf or Falcon tubes and mounted onto scanning platforms. Scans were conducted using the Australian Synchrotron Imaging and Medical Beamline (IMBL) X-ray microCT and the Monash University X-ray Microscope Facility for Imaging Geomaterials (XMFIG) Zeiss Xradia 520 Versa microCT.

Fourteen specimens were microCT scanned at the Monash XMFIG (Table A2.1). We also scanned one unstained specimen (4942) as a negative control, which was subsequently stained in Lugol's and then rescanned for comparison. Scans were performed using 80–130 kV, 7–24 μ A at 0.39 \times magnification, 1601–3201 projections with 1–16 s exposures. We trialled combinations of these parameters to determine optimal settings. Scan times ranged from 1 to 20 h, and resulted in 4.93–42.8 μ m cubic voxel reconstructions. For four of the specimens we also performed sub-volume scans of individual developing teeth, at higher magnification (4 \times) and/or closer proximity to the X-ray source, to see if higher resolution could be achieved. Six of the 14 specimens were scanned at the Australian Synchrotron using the IMBL in February 2014 (Table A2.2). To confirm the specificity of the stain, these specimens were scanned at 34 keV (just above the K-edge of iodine) at 1800 projections with 0.5 s exposure, producing 6.11 μ m cubic voxels. We also scanned specimen 4180 at 32 KeV (below the K-edge) for comparison.

Greyscale values in scan images were used as a proxy for comparing attenuation levels (see Metscher, 2009b), where low levels of attenuation produced darker values (approaching black), while higher attenuation approached white. Greyscale values were measured using histograms in ImageJ.

2.2.3. Histological Comparison

To confirm the identity of specific tissue and cell types identified in the diceCT sections, we removed the Lugol's staining from one previously scanned specimen (5964), stained it with Haematoxylin & Eosin (H & E) and then physically sectioned it in the coronal plane. As this specimen was young enough that mineralisation was only partial, it was not de-mineralised in order to preserve all original structures *in-situ*. We also used a separate H & E-stained histology collection of tammar wallaby heads of similar ages (up to 55 days-old pouch young) from Lockett (1993a) as additional comparative material. These sections were photographed using a Moto microscope camera, and then compared to equivalent segmented microCT scan slices. Next, we took three measurements (approximating the minimum, maximum, and middle range for the layer) of the thickness of each tissue layer for equivalent tooth sections, using ImageJ for histology sections and Avizo for microCT scan slices (at both 0.39× and 4×). We only measured structures that were thicker than twice the voxel size for that scan (Nyquist frequency), i.e. structures the same or smaller than the voxel size could not be measured accurately, and therefore were not measured. For example, in the whole-head scans at 0.39×, the resolution would be below the size of the single-cell layer OEE (voxel size larger than OEE width), while in the sub-volume scans at 4×, resolution would be greater than the thickness of the OEE (voxel size smaller than OEE width), therefore we could accurately measure this layer. We also measured head width (between the most lateral protrusions of cheeks), and the organ width of the lower left first incisor (the medial-caudal edge to the lateral-cranial edge of the OEE). Finally, we compared the averages of these for the microCT to those for the histology sections to determine whether the layers identified in the scans had similar dimensions.

2.2.4. 3D Reconstruction

MicroCT scans were reconstructed using Automatic Reconstructor (Zeiss, Oberkochen, Germany) for XFIG and XTRACT (CSIRO, Melbourne, Australia) for synchrotron scans. These were then segmented in 3D using Avizo 9.0.1 (FEI, Oregon, USA). We occasionally used despeckle and Nagao filters to improve contrast and sharpen outline of tooth germs (as indicated in figures). Using a combination of magic wand with thresholding, brush with

limited range, and the blow tool, unmineralised and mineralised dental tissues were segmented out and surfaces extracted to create 3D models. These were the primary and secondary laminae, and the tissues within the dental organs: the outer and inner enamel epithelium (OEE and IEE), the stellate reticulum, ameloblasts and odontoblasts; and mineralising tissues: enamel, dentine and predentine. When describing the whole tooth germs, we used staging from Lockett (1993) to describe the bud, cap and bell stages of their development.

2.3 Results

2.3.1 Specimen Fixation and Staining

In stained specimens, visual contrast was enhanced between unmineralised and mineralised tissues, as well as among soft tissues where graded attenuation was visible between tissue layers and structures (Figure 2.1a–b). The unstained specimen revealed only mineralised structures with high, relatively even attenuation: cranial bones, dentine, and enamel.

In terms of Lugol's staining efficacy, the stain penetrated to the centre of the specimen and consistently affected tissues of similar density throughout, indicating that both optimal Lugol's concentration and staining time had been achieved. Through experimenting with scanning parameters at the XMFIG, we found that a combination of high exposure time (3 s) and number of projections (3201) with relatively low power (80 kV) resulted in the most clearly defined soft tissue layers for our mid-range sized specimens without excessive scan times. Likewise, synchrotron scans conducted just above the k-edge (34 keV) (Figure 2.1d) produced much sharper images than scans below the k-edge (32 keV) (Figure 2.1c). The synchrotron scans show that what we are imaging is indeed a signal from the iodine-based stain.

Epithelial tissues, such as the primary epithelial band of the oral cavity that gives rise to the vestibular and dental laminae, were most strongly stained. Also visible were other developing organs such as the neuroepithelium-derived brain and eye lenses, and the ectoderm-derived inner ear and nasal cavities. However, the stain was not exclusive to epithelial tissues: tissue layer organisation of mesenchymal structures, such as the muscle fibres of the tongue, were also highly visible (Figure 2.1e–f).

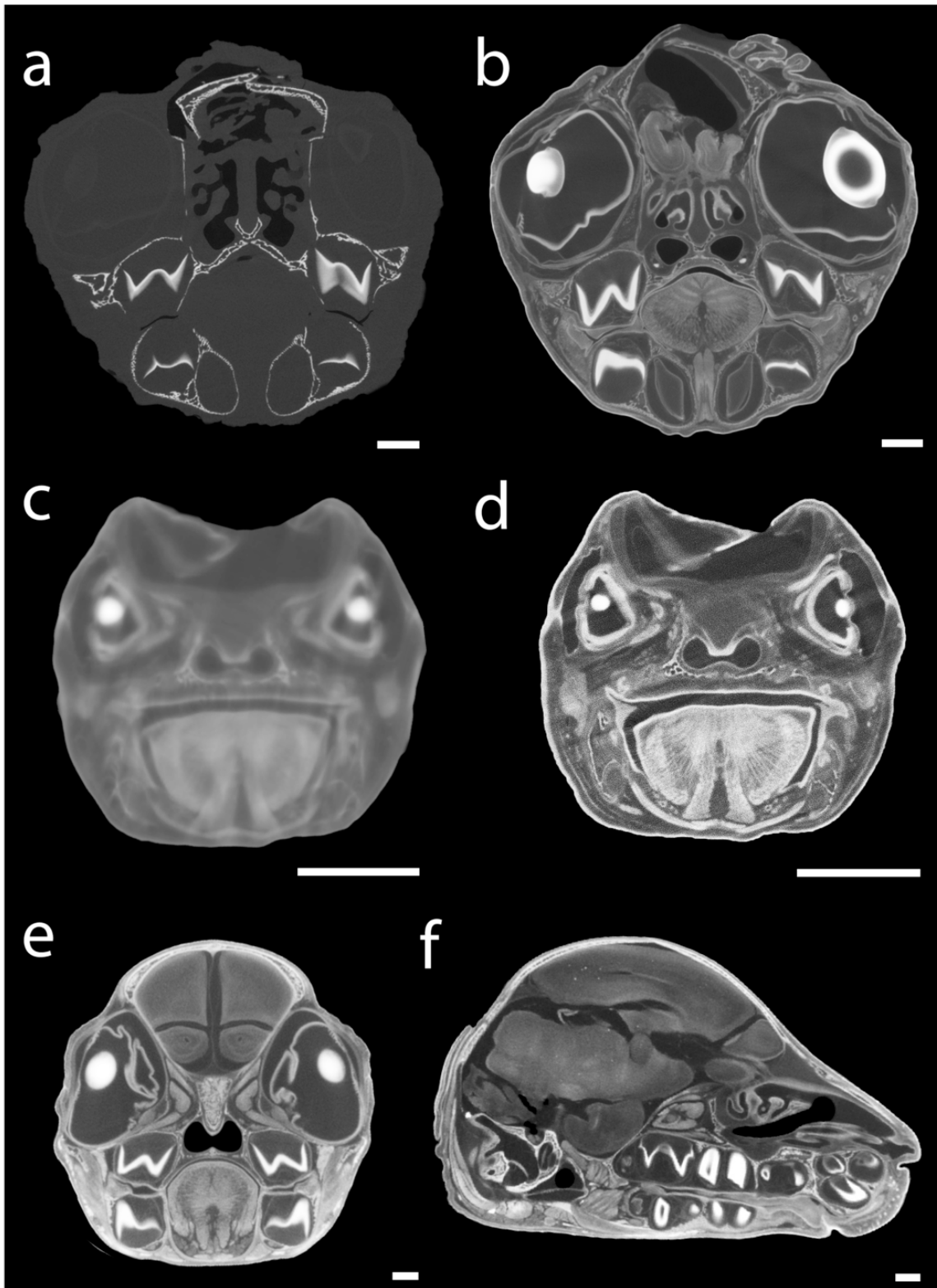


Figure 2.1 Comparison of 2D slices of CT scans of a) unstained and b) stained specimen 4942; both scanned at the XMFIG, Monash University, Comparison of specimen 4180 scanned at c) 32 and d) 34 keV; IMBL at the Australian Synchrotron. e) Coronal and f) lateral sections of specimen 5449, exhibiting soft and mineralised tissues and organs *in-situ*, both scanned at XMFIG. Scale bar = 2 mm length.

2.3.2. Histology Versus MicroCT

Qualitative Morphology

Our comparison of segmented scan slices and the histology slides showed strikingly close alignment in both morphology and size (Figure 2.2). An overview of the whole head clearly shows the position, density and tissue thickness of the maxillae, mandibles, tooth germs, and tongue, as well as the oral and nasal cavities (Figure 2.2a–b). Finer structures visualized by the stain include the oral mucosa that lines the oral cavity as well as distinct layers of squamous epithelium, lamina propria and textured muscularis propria in the tongue (Figure 2.2c–d). Within the tongue, it is possible to discern skeletal muscle fibres and salivary gland fibres. The mineralised palate and mandible show high attenuation, and both the vestibular and the dental laminae (which gives rise to the teeth) are clearly visible. A close-up view of a single tooth organ reveals several tissue layers in the microCT scan, but single-cell layers, such as the inner enamel epithelia and ameloblasts, can be difficult to distinguish (Figure 2.2e–f).

Quantitative Morphology

The head width and incisor organ width of the histology and microCT sections are virtually identical (Table A2.3). In addition, all measured tissue layers thicknesses had highly overlapping ranges between microCT and histology sections, for both whole-head and sub-volume scans (Tables A2.3 and A2.4; Figures A2.1 and A2.2).

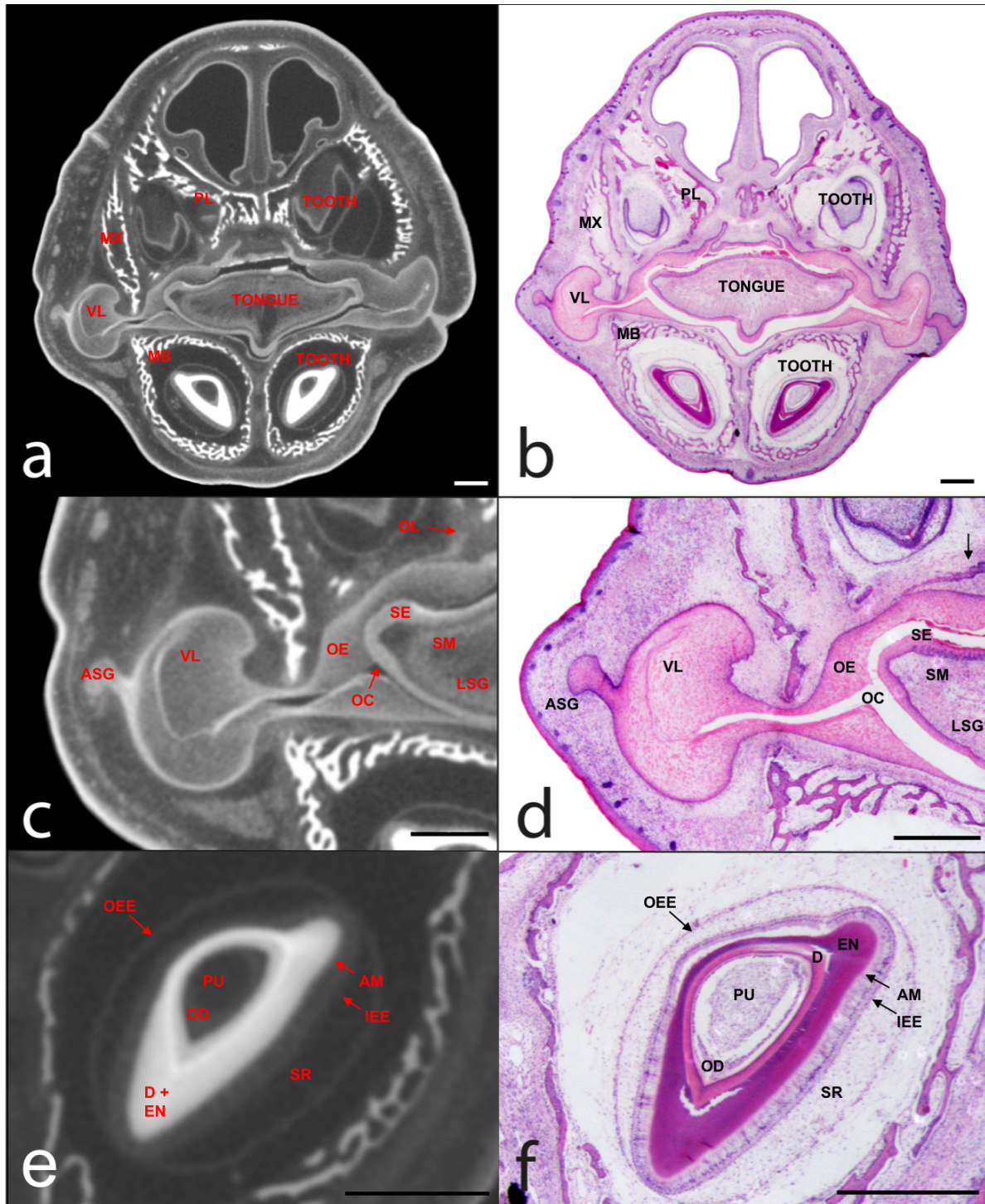


Figure 2.2 Comparison of organ morphology and tissue layers of specimen 5694 visualised using the diceCT method (left) and H&E histology sections (right); coronal section (2D slice) of whole head (a, b), subsection of oral cavity through the premaxilla and symphysis of the mandible (c, d) and incisor organ (e, f). Abbreviations: AM (Ameloblasts), ASG (Accessory Salivary Gland lamina), EN (Enamel), D (Dentine), DL (Dental Lamina), IEE (Inner Enamel Epithelium), LSG (Lingual Salivary Gland), MB (Mandible), MX (Maxilla), OC (Oral Cavity), OD (Odontoblasts), OE (Oral Epithelium), OEE (Outer Enamel Epithelium), PL (Palatine), PU (Pulp), SE (Squamous Epithelium), SR (Stellate Reticulum), SM (Skeletal Muscle), VL (Vestibular Lamina). Scale bar = 2 mm.

2.3.3. Tooth Development Patterns in Three Dimensions

Using the diceCT scans, we successfully reconstructed and mapped the *in-situ* 3D position and orientation of developing tooth structures. From before birth (23 RPY) to 258 days old, we produced 3D models of tooth rows of upper and lower jaws including segmented tissue layers.

We tracked the development of all tooth classes through major stages of mammalian tooth development – bud, cap and bell – and through to the mineralisation of a semi-complete functional set of teeth, including incisors, canines, deciduous premolars, permanent premolars and three (of four) molars in each quadrant (Figure 2.3). In particular, we observed the development of the enlarged pair of lower incisors, characteristic of the diprotodont dentition, as well as the vestigial upper canines (C^1), which develop to mid-bell stage and partially mineralise before being resorbed. In addition, we modelled the development of the deciduous premolars, dP2 and molariform dP3. One of the last teeth to appear, the permanent premolar (P3), is a plagiulacoid (blade-like) tooth, which will eventually replace the two deciduous premolars.

We could also determine primary and secondary dentition through tracking primary and secondary dental laminae connections. Thus, our scans reveal two generations of incisors: a non-functional, deciduous first incisor (dI^1) and a permanent first incisor (I^1), with the latter quickly outgrowing and replacing its predecessor to become the only functional generation. Finally, we could detect the difference between dP3, which originates from the primary dental lamina, and M1, which characteristically develops from a secondary posterior extension of the primary dental lamina.

Within the tooth buds we could segment out the tissues within the dental organs: the OEE, IEE, stellate reticulum, ameloblasts and odontoblasts; and mineralising tissues: enamel, dentine and predentine. We also successfully mapped in 3D the primary and secondary enamel knot development, capturing the shape and timing of cusp formation.

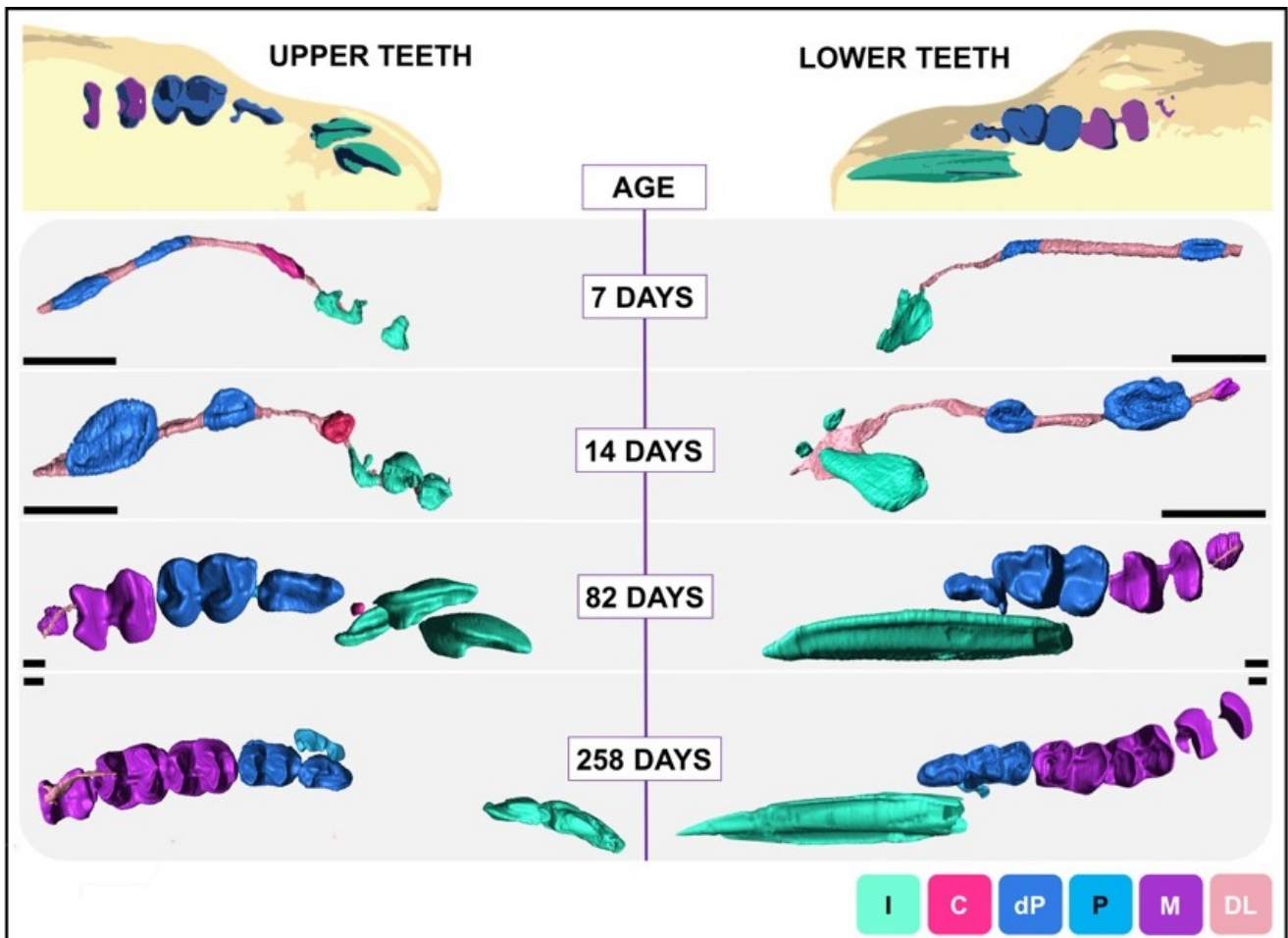


Figure 2.3 3D of tooth development of soft to mineralised tissue, using diceCT, within the right upper and lower quadrants of the tammar wallaby, from 7 to 258 days in pouch, in apical view (7-14 days) occlusal view (82-258 days). Abbreviations: C (Canine), DL (Dental lamina), dP (Deciduous Premolar), I (Incisor), M (Molar), P (Permanent Premolar). Specimens of 7 and 14 days were segmented around their inner and outer enamel epithelium, while specimens 82 and 258 days were segmented between their IEE and odontoblast layer. Scalebar = 1 mm.

Here, we will focus on the morphology of the developing teeth from the bud to the bell stages of mammalian tooth development, describing their gross and internal morphology as made visible by the diceCT protocol.

Bud Stage

The ectodermal and mesenchymal tissue layers, which produce tooth buds, markedly differ in levels of attenuation, and match their counterparts in the histology sections in both morphology and thickness. There are localised thickenings along the dental lamina which develop into nodular structures, signifying the bud stage (Figure 2.4a–d). These structures are essentially homogenous outgrowths in the microCT, with no internal layers visible.

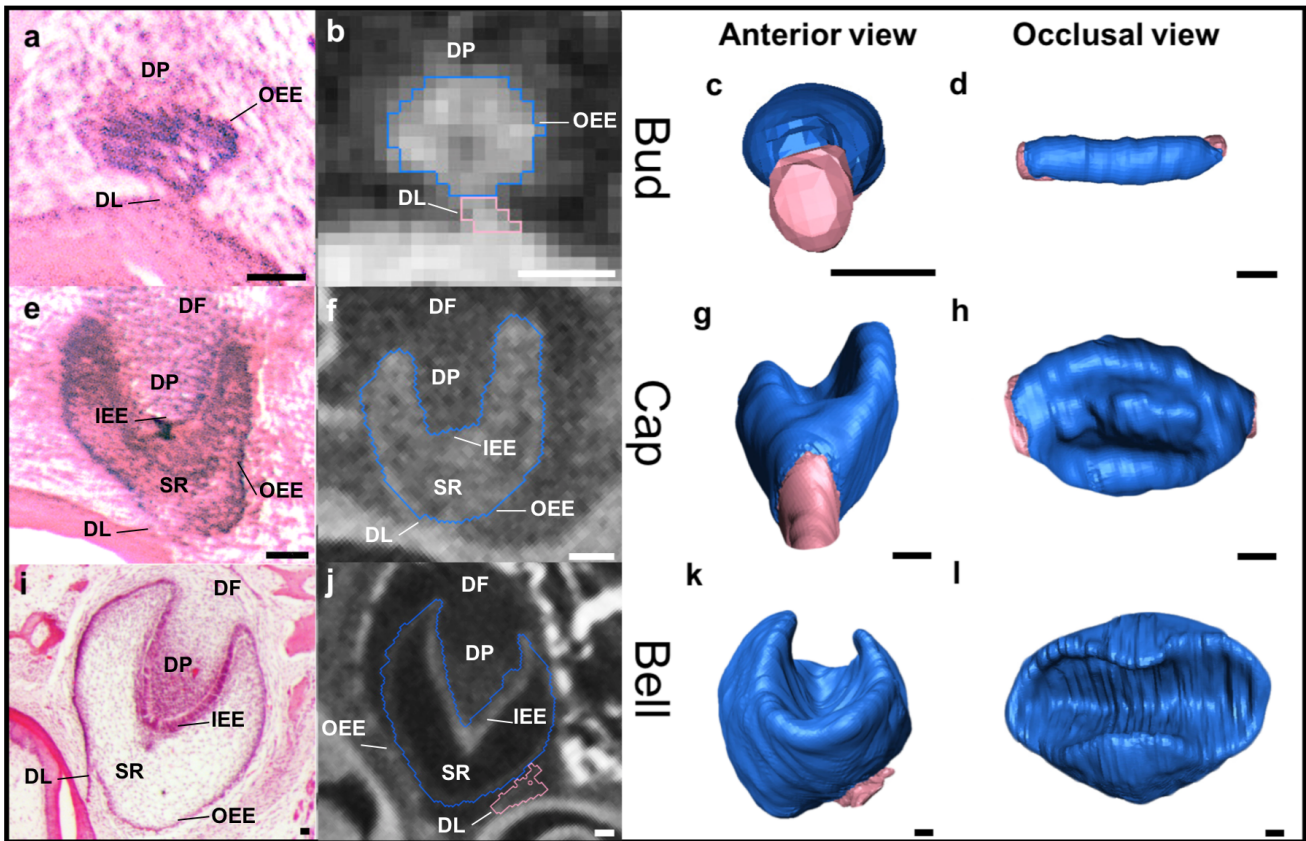


Figure 2.4 Histology sections (a, e, i), 2D diceCT sections with outlines of segmented layers (b, f, j) and 3D reconstructions from diceCT in anterior (c,g,k) and apical (d, h, l) views, of the upper right deciduous premolar (dP²) through the bud (a-d), cap (e-h) and bell (i-l) stages. In 2D and 3D sections, the dP² tooth germs are in blue and dental lamina in flesh pink. Abbreviations: Dental Lamina (DL), Dental Follicle (DF), Dental Papilla (DP), Inner Enamel Epithelium (IEE), Outer Enamel Epithelium (OEE), Stellate Reticulum (SR). Specimens were segmented around their inner and outer enamel epithelium. Scanned at the XMGIF, Monash University. Scale bar = 100 μ m.

Cap Stage

The growth and invagination of the tooth buds to form a cup-like shape signifies the cap stage (Figure 2.4e–h). The surrounding mesenchyme shows stronger attenuation than when at bud stage, indicating thickening of this tissue layer. The IEE and OEE of the cap stage organs also show increased attenuation compared to earlier developmental stages; however, the boundary between these layers is too indistinct to segment out in some tooth germs. The dental papilla is visible as a condensed orb of lower attenuation within the invagination. A fainter halo encircles the developing teeth, and can be confidently identified as condensed ectomesenchymal cells that form the dental follicle. The primary dental lamina stem still attaches to the oral epithelium at this stage.

Bell Stage

At bell stage, the inner enamel epithelium has undergone further invagination, beginning to form the inverse shape of the tooth it will produce, where subsequently mineralised layers will be deposited to produce the final functional product (Figure 2.4i–l). At early-to-mid bell stage, primary (for single-cusped teeth) and secondary (for multicusped teeth) enamel knots and cords become visible as bright cones at the in-folded curves of the inner enamel epithelium that closely match that seen in histology (Figure 2.5). They are positioned close to the centre of the tooth germ, viewed both occlusally and laterally. Dentine commences mineralisation before enamel and is initially the densest material present in the tooth. At day 57 (specimen 4946) dentine is already clearly discernible, whereas the enamel, ameloblasts and inner enamel epithelium all have similar density and appear relatively homogenous. The same is true of the enamel and odontoblast layers (premineralisation), which cannot be separated out (Figure 2.6). At late bell stage, enamel becomes the densest material, and individual layers become more clearly defined.

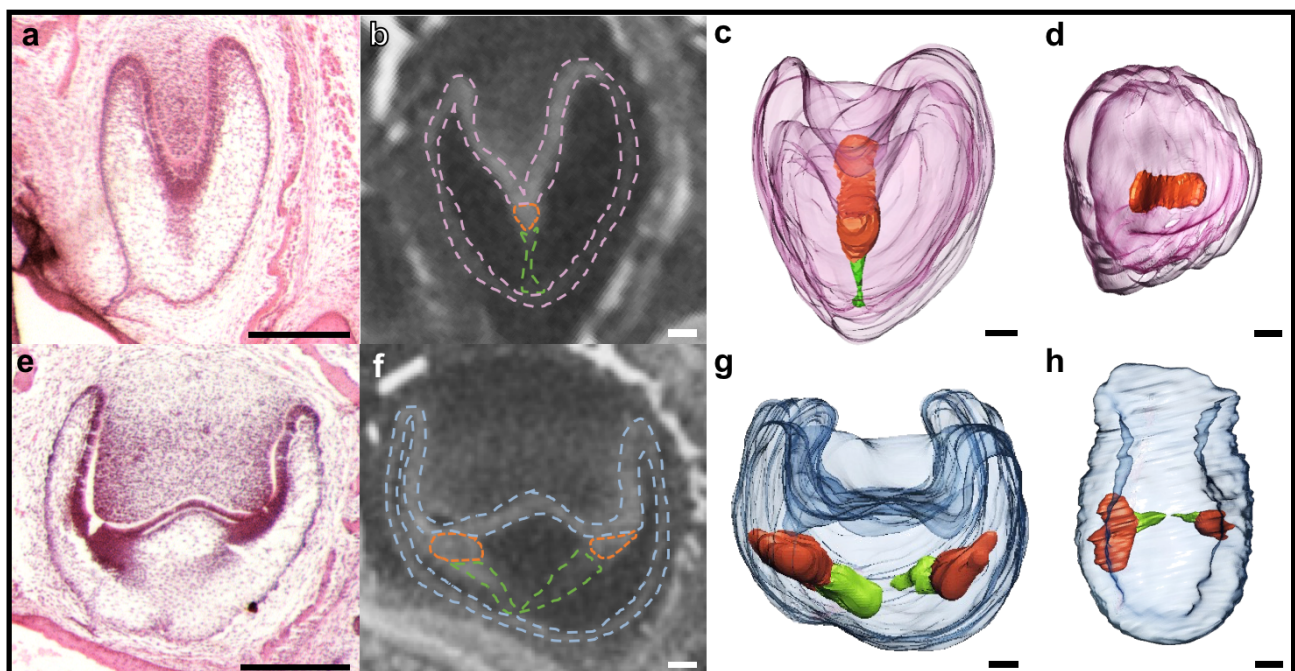


Figure 2.5 H & E stained histology (a, e), 2D diceCT sections with outlines of layers (b, f) and anterior (c, g) and apical (d, h) views of 3D models of enamel knots developing within upper canine (C¹) (a-d) and lower dP₃ (e-h). Colours indicate the following: Orange=enamel knots, green=enamel cords, pink=IEE layer of (C¹), blue=IEE layer of dP₃. Specimens of 7 and 14 days were segmented around their inner and outer enamel epithelium. Scanned at the XMFIG, Monash University. Scale bar = 100 μ m.

Interestingly, in our oldest specimen 6843, mature enamel appears less bright in attenuation than dentine. An area of low attenuation within the tooth germ likely represents the dental papilla, and the matrix outside the stellate reticulum; however, individual cells cannot be distinguished at this resolution. The outer enamel epithelium is visible as a thin band of high attenuation wrapping itself around the enamel organ. At the cervical loops the outer enamel epithelium is connected to its inner counterpart, which appears denser and brighter (Figure 2.6). In many tooth germs, the outer enamel epithelium still retains a faint attachment ($\sim 8 \mu\text{m}$ thick) to the primary dental lamina. At highly mineralised stages, the dental lamina connection is lost (see Figure 2.3, 82 days).

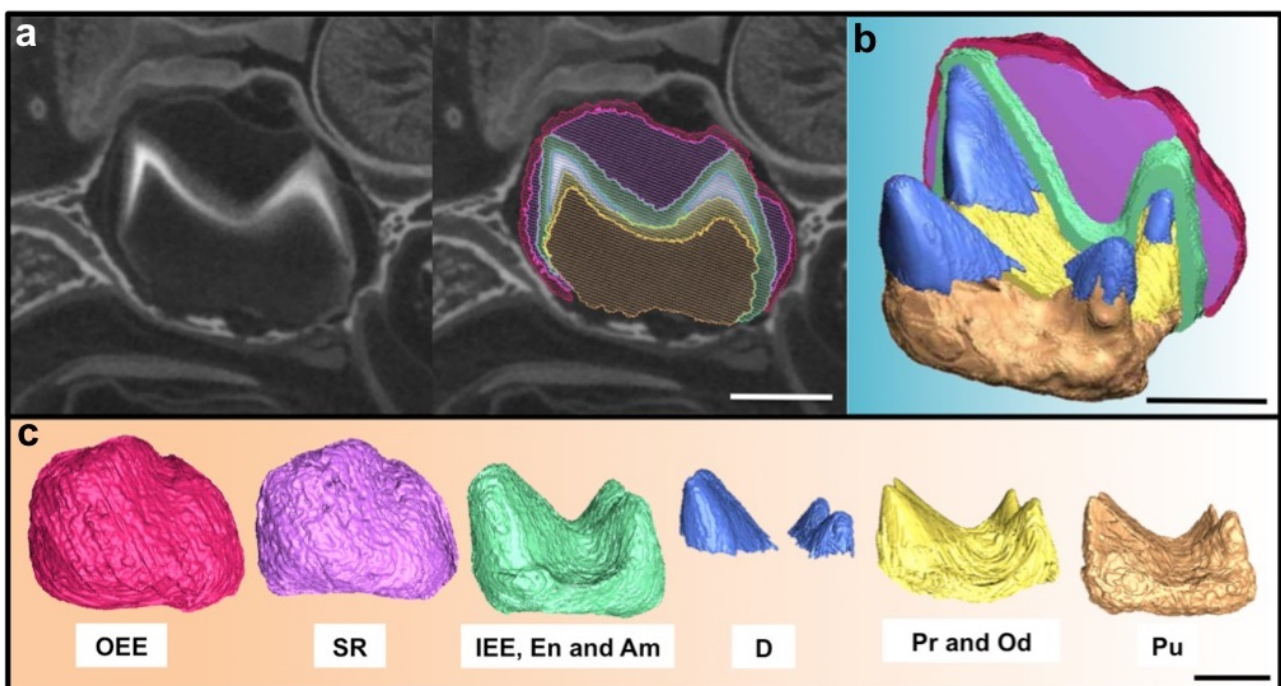


Figure 2.6 2D to 3D reconstruction of soft and mineralised tissue layers of the upper right dP3 (specimen 4946, 57 days old) at bell stage. a) 2D coronal section of diceCT scan (left) and same section with tissues labelled with colours in (right); b) 3D model revealing tissue layers *in-situ* in anterior-lateral view; c) 3D model of tissue layers in anterior view, starting from the outermost layer to innermost (left to right). Abbreviations: Am (Ameloblast), D (Dentine), En (Enamel), IEE (Inner Enamel Epithelium), Od (Odontoblasts), OEE (Outer Enamel Epithelium), Pr (Predentine), Pu (Pulp), SR (Stellate reticulum). Scanned at the XFIG, Monash University. Scale bar = 1 mm.

2.3.4. Applications Beyond Tooth Development

Using the diceCT technique, we could easily produce 3D models of complex unmineralised and mineralised structures beyond those of the developing teeth, resulting in concurrent imaging of developing craniofacial structures. For example, we could observe the cranial ossification sequence, as well as muscle groups, brain, cartilage, nasal cavities, inner ear and eye development (Figure 2.1e–f).

2.4 Discussion

2.4.1. Stain and Scan Technique

Using diceCT, we were able to enhance the contrast of soft and mineralised tissues to effectively document the development of increasingly mineralising tooth structures. Our stained tammar wallaby fetal and pouch young specimens show a vast increase in visual differentiation of tissues, which in turn results in markedly improved scans both from a qualitative and a quantitative perspective. The affinity of Lugol's solution for epithelial tissues creates graded attenuation between them and mesenchymal layers, enabling digital segmentation and the production of 3D models to trace the development of multiple tooth classes and generations *in-situ*.

Established diceCT protocols proved effective at staining our specimens. In particular, a staining concentration of 1.5% w/v, combined with staining time of 2–14 days, appeared to work for our material, as it had previously done for mice (Degenhardt *et al.*, 2010; Baverstock *et al.*, 2013). Nevertheless, we found that replenishing the solution frequently with fresh Lugol's, rather than simply extending staining time, improved penetration.

Through trialling variations in scanning parameters, we found that relatively low power, combined with higher exposure time and number of projections, produced the clearest results, but also necessitated a greater time investment per scan. This is because lower energy gives greater contrast between materials with similar electron density, but scan times are longer because fewer X-rays reach the detector. The high quality of 34 keV scans at the Australian Synchrotron demonstrates the necessity of scanning at energies high enough to dislodge K-Shell electrons (above the K-edge) from the target element – in this case, the iodine in the stain. Using energy levels just above the K-edge causes an increased and more uniform attenuation of X-rays, which produces a clearer image.

2.4.2. Histological Comparisons

Using histological sections to confirm the identity of structures proved a useful method to compare and gain greater confidence in our scans. This histological confirmation has not

previously been reported in diceCT studies. Finding no significant difference between measured tissue layer thicknesses of scans and histology sections indicates accurate representation of dental morphology via diceCT. The tissues differing most in thickness (outer and inner enamel epithelia, ameloblasts) are the single cell layers, which are below the resolution of microCT. Our whole-head scans produced voxel sizes between 4.93–42 μm . An odontoblast cell, for example, is 25–40 μm long but only 4–7 μm wide. To be able to distinguish a structure, the voxel size must be at least half its size (Nyquist frequency). Despite not being able to reach cellular resolution with this study, we still could sometimes visualize single-cell tissue layers. In the much smaller voxel sizes achieved in our sub-volume scans, the measured dimensions of these single-cell layers were not significantly different to those from histological sections, suggesting that diceCT can be an appropriate method to obtain metrics such as tissue thickness and volume. In the future, diceCT may be able to achieve cellular level resolution if parameters were refined, or, as in our case, via sub-volume scans.

2.4.3. From 2D to 3D Tooth Development

The use of diceCT to define tooth classes and generations complements studies relying purely on adult tooth morphology. For example, the ability to observe small developing structures in 3D can evince the direct link between a developing tooth to the primary or secondary dental lamina. O’Leary *et al.* (2013) and Williamson *et al.*, (2014) suggested that the M1 of modern marsupials is ancestrally a dP5, a tooth class that characteristically develops from the primary dental lamina. Our observation that the M1 of the tammar wallaby develops from a secondary posterior extension of the dental lamina (Figure 2.3) contradicts this scheme, and suggests no deciduous premolar heritage of the tooth in this position. Another use of identifying dental lamina connections is to better define the relationship between tooth generations. The successional tooth generation develops from, and is attached to, its predecessor via the successional lamina. This relationship is difficult to pinpoint when teeth are spatially complex 3D structures. The ability to segment and construct three-dimensional models overcomes the difficulty of visualising structures that seemingly overlap in 2D slices, allowing us to confirm which generation a given tooth belongs to. Additionally, the enamel knot development pattern was produced with relative

ease, allowing us to see the precursory patterning of cusp morphogenesis. Cusp development has been previously observed in mice and the South American opossum *Monodelphis domestica* (Moustakas *et al.*, 2011; Jernvall and Thesleff, 2012) using serial section reconstructions. Without the availability of fluorescent transgenic lines such as *ShhGFP* in less traditional model species, this non-destructive alternative allows us to visualise these signalling centres of tooth shape and complexity.

2.4.4. Simultaneous Studies *In-Situ*

We have demonstrated that using diceCT enables concurrent 3D imaging of complex unmineralised and mineralised craniofacial structures in developing small to moderate-sized specimens. Unlike histology, no de-mineralisation is necessary, resulting in less distortion of morphology and allowing the imaging of larger and more dense specimens. Nevertheless, application of this technique is ultimately limited by the field of view and X-ray power of the of the microCT scanner. The ability to remove Lugol's staining from specimens using sodium thiosulfate prevented excessive shrinkage, thus minimising damage and allowing further analyses using H & E staining and sectioning. Overall, diceCT therefore allowed us to maximise and even expand our use of rare specimens, and continuous improvement of this protocol may one day make it the method of choice for irreplaceable specimens, such as museum collection items.

DiceCT is a highly promising technique for further odontogenic studies. Its simplicity and rapidity make it both cost- and time-effective, with the reversibility of the stain minimising damage and maximizing the information gained from a single specimen. Furthermore, its results produce a digitised, sharable dataset that can easily be utilised by future studies. The multitude of advantages diceCT offers over destructive techniques allows for a multi-faceted investigation of rare specimens to provide a 3D mammalian model of development.

2.5 Acknowledgments

This research would not have been possible without the Renfree Lab team: we thank all the members of the wallaby research group for help in collecting and fixing the specimens. We thank Drs Anton Maksimenko and Karen Siu at the Australian Synchrotron for assistance in IMBL operations and the processing of scans. We are grateful to Lap Chieu for assistance in centering and recording scan data. We thank Asadul Haque for his insights into optimising scanning parameters, assisting with the Xradia operations and trouble shooting. Lastly, we thank the Monash Histology Platform team, especially Camilla Cohen and Jonathan Bensley for assisting in the staining and sectioning of specimens.

2.6 References

- Andl, T., Ahn, K., Kairo, A., Chu, E. Y., Wine-Lee, L., Reddy, S. T., ... Millar, S. E. (2004). Epithelial *Bmpr1a* regulates differentiation and proliferation in postnatal hair follicles and is essential for tooth development. *Development*, 131, 2257–2268.
- Baverstock, H., Jeffery, N., & Cobb, S. (2013). The morphology of the mouse masticatory musculature. *Journal of Anatomy*, 223, 46–60.
- Berkovitz, B. K. B. (1972). Tooth development in *Protemnodon eugenii*. *Journal of Dental Research*, 51(5), 1467–1473.
- Berkovitz, B. K. B. (1978). Tooth ontogeny in *Didelphis virginiana* (Marsupialia: Didelphidae). *Australian Journal of Zoology*, 26(1), 61–68.
- Celli, J., Duijf, P., Hamel, B. C., Bamshad, M., Kramer, B., Smits, A. P., ... Woods, C. G. (1999). Heterozygous germline mutations in the p53 homolog p63 are the cause of EEC syndrome. *Cell*, 99(2), 143–153.
- Correia, T., Lockwood, N., Kumar, S., Yin, J., Ramel, M. C., Andrews, N., ... Frankel, P. (2015). Accelerated optical projection tomography applied to In vivo imaging of zebrafish. *PLoS One*, 10(8), e0136213.
- D'Souza, R. N., Aberg, T., Gaikwad, J., Cavender, A., Owen, M., Karsenty, G., & Thesleff, I. (1999). *Cbfa1* is required for epithelial-mesenchymal interactions regulating tooth development in mice. *Development*, 126, 2911–2920.
- Degenhardt, K., Wright, A. C., Horng, D., Padmanabhan, A., & Epstein, J. A. (2010). Rapid 3D phenotyping of cardiovascular development in mouse embryos by micro-CT with iodine staining: Clinical perspective. *Circulation: Cardiovascular Imaging*, 3, 314–322.
- Descamps, E., Sochacka, A., De Kegel, B., Van Loo, D., Van Hoorebeke, L., & Adriaens, D. (2014). Soft tissue discrimination with contrast agents using micro-CT scanning. *The Belgian Journal of Zoology*, 144, 20–40.

- Evans, A. R., Daly, E. S., Catlett, K. K., Paul, K. S., King, S. J., Skinner, M. M., ... Jernvall, J. (2016). A simple rule governs the evolution and development of hominin tooth size. *Nature*, 530(7591), 477–480.
- Fennerty, M. B. (1999). Tissue staining (chromoscopy) of the gastrointestinal tract? *Canadian Journal of Gastroenterology and Hepatology*, 13(5), 423–429.
- Fraser, G. J., Hulseay, C. D., Bloomquist, R. F., Uyesugi, K., Manley, N. R., & Streelman, J.T. (2009). An ancient gene network is co-opted for teeth on old and new jaws. *PLoS Biology*, 7(2), e1000031.
- Gignac, P. M., & Kley, N. J. (2014). Iodine-enhanced micro-CT imaging: Methodological refinements for the study of the soft-tissue anatomy of post-embryonic vertebrates. *Journal of Experimental Zoology Part B: Molecular and Developmental Evolution*, 322(3), 166–176.
- Gignac, P. M., Kley, N. J., Clarke, J. A., Colbert, M. W., Morhardt, A. C., Cerio, D., ... Echols, M. S. (2016). Diffusible iodine-based contrast-enhanced computed tomography (diceCT): an emerging tool for rapid, high-resolution, 3-D imaging of metazoan soft tissues. *Journal of Anatomy*, 228(6), 889–909.
- Gomes Rodrigues, H., Renaud, S., Charles, C., Le Poul, Y., Solé, F., Aguilar, J. P., ... Viriot, L. (2013). Roles of dental development and adaptation in rodent evolution. *Nature Communications*, 4, 1–8.
- Goswami, A., Randau, M., Polly, P. D., Weisbecker, V., Bennett, C. V., Hautier, L., & Sánchez-Villagra, M. R. (2016). Do developmental constraints and high integration limit the evolution of the marsupial oral apparatus? *Integrative and Comparative Biology* [icw039].
- Harjunmaa, E., Kallonen, A., Voutilainen, M., Hämäläinen, K., Mikkola, M. L., & Jernvall, J. (2012). On the difficulty of increasing dental complexity? *Nature*, 483(7389), 324–327.
- Hickford, D., Frankenberg, S., & Renfree, M. B. (2009). Collection, handling, fixation, and processing of tammar wallaby (*Macropus eugenii*) embryos. *Cold Spring Harbor Protocols*, 2009(12), pdb–prot5335.
- Jernvall, J., & Thesleff, I. (2012). Tooth shape formation and tooth renewal: Evolving with the same signals. *Development*, 139(19), 3487–3497.

- Jernvall, J., Aberg, T., Kettunen, P., Keranen, S., & Thesleff, I. (1998). The life history of an embryonic signaling center: BMP-4 induces p21 and is associated with apoptosis in the mouse tooth enamel knot. *Development*, 125(2), 161–169.
- Kangas, A. T., Evans, A. R., Thesleff, I., & Jernvall, J. (2004). Nonindependence of mammalian dental characters. *Nature*, 432(7014), 211–214.
- Lesot, H., Vonesch, J. L., Peterka, M., Tureckova, J., Peterková, R., & Ruch, J. V. (1996). Mouse molar morphogenesis revisited by three-dimensional reconstruction. II. Spatial distribution of mitoses and apoptosis in cap to bell staged first and second upper molar teeth. *International Journal of Developmental Biology*, 40(5), 1017–1031.
- Lesot, H., Vonesch, J. L., Peterka, M., Turecková, J., Peterková, R., & Ruch, J. V. (1996). Mouse molar morphogenesis revisited by three-dimensional reconstruction. II. Spatial distribution of mitoses and apoptosis in cap to bell staged first and second upper molar teeth. *The International journal of developmental biology*, 40(5), 1017.
- Luckett, W. P. (1993). Ontogenetic staging of the mammalian dentition, and its value for assessment of homology and heterochrony. *Journal of Mammalian Evolution*, 1(4), 269–282.
- Metscher, B. D. (2009a). MicroCT for comparative morphology: Simple staining methods allow high-contrast 3D imaging of diverse non-mineralized tissues. *BMC Physiology*, 9(1), 1.
- Metscher, B. D. (2009b). MicroCT for developmental biology: A versatile tool for highcontrast 3D imaging at histological resolutions. *Developmental Dynamics*, 238, 632–640.
- Moustakas, J. E., Smith, K. K., & Hlusko, L. J. (2011). Evolution and development of the mammalian dentition: insights from the marsupial *Monodelphis domestica*. *Developmental Dynamics*, 240(1), 232–239.
- Neubüser, A., Peters, H., Balling, R., & Martin, G. R. (1997). Antagonistic interactions between *FGF* and *BMP* signaling pathways: A mechanism for positioning the sites of tooth formation? *Cell*, 90(2), 247–255.
- Nieminen, P., Arte, S., Tanner, D., Paulin, L., Alaluusua, S., Thesleff, I., & Pirinen, S. (2001). Identification of a nonsense mutation in the *PAX9* gene in molar oligodontia? *European Journal of Human Genetics*, 9(10), 743–746.

- O'Leary, M. A., Bloch, J. I., Flynn, J. J., Gaudin, T. J., Giallombardo, A., Giannini, N. P., ...Ni, X. (2013). The placental mammal ancestor and the post-K-Pg radiation of placentals. *Science*, 339(6120), 662–667.
- Ooë, T. (1979). Development of human first and second permanent molar, with special reference to the distal portion of the dental lamina. *Anatomy and Embryology*, 155(2), 221–240.
- Ooë, T. (1981). Human tooth and dental arch development. Incorporated Ishiyaku EuroAmerica.
- Peterková, R., Lesot, H., Vonesch, J. L., Peterka, M., & Ruch, J. V. (1996). Mouse molar morphogenesis revisited by three-dimensional reconstruction. I. Analysis of initial stages of the first upper molar development revealed two transient buds. *International Journal of Developmental Biology*, 40(5), 1009–1016.
- Peterková, R., Lesot, H., Viriot, L., & Peterka, M. (2005). The supernumerary cheek tooth in tabby/*EDA* mice—A reminiscence of the premolar in mouse ancestors. *Archives of Oral Biology*, 50(2), 219–225.
- Peterková, R., Lesot, H., & Peterka, M. (2006). Phylogenetic memory of developing mammalian dentition? *Journal of Experimental Zoology Part B: Molecular and Developmental Evolution*, 306(3), 234–250.
- Peters, H., Neubüser, A., Kratochwil, K., & Balling, R. (1998). *Pax9*-deficient mice lack pharyngeal pouch derivatives and teeth and exhibit craniofacial and limb abnormalities. *Genes & Development*, 12(17), 2735–2747.
- Poole, W. E., Simms, N. G., Wood, J. T., & Luboloa, M. (1991). Tables for age determination of the Kangaroo Island Wallaby (Tamar) *Macropus eugenii*, from body measurements. CSIRO (Division of Wildlife and Ecology) Technical Memorandum No. 32.
- Prochazka, J., Pantalacci, S., Churava, S., Rothova, M., Lambert, A., Lesot, H., ... Peterková, R. (2010). Patterning by heritage in mouse molar row development. *Proceedings of the National Academy of Sciences*, 107(35), 15497–15502.
- Radlanski, R. J., Renz, H., Tsengelsaikhan, N., Schuster, F., & Zimmermann, C. A. (2016). The remodeling pattern of human mandibular alveolar bone during prenatal formation from 19 to 270 mm CRL. *Annals of Anatomy-Anatomischer Anzeiger*, 205, 65-74.

- Raj, M. T., Prusinkiewicz, M., Cooper, D. M., George, B., Webb, M. A., & Boughner, J. C. (2014). Technique: imaging earliest tooth development in 3D using a silver-based tissue contrast agent. *The Anatomical Record*, 297(2), 222-233.
- Renfree, M. B., Holt, A. B., Green, S. W., Carr, J., & Cheek, D. B. (1982). Ontogeny of the brain in a marsupial *Macropus eugenii*, throughout pouch life. I. Brain growth and structure. *Brain Behavior and Evolution*, 20, 57–71.
- Sanson, G. D. (1989). Morphological adaptations of teeth to diets and feeding in the Macropodoidea. In G. Grigg, P. Jarman, & I. Hume (Vol. Eds.), *Kangaroos, wallabies and rat-kangaroos: 1*, (pp. 151–168). Sydney: Surrey Beatty.
- Satokata, I., & Maas, R. (1994). Msx1 deficient mice exhibit cleft palate and abnormalities of craniofacial and tooth development. *Nature Genetics*, 6(4), 348–356.
- Sharpe, J. (2003). Optical projection tomography as a new tool for studying embryo anatomy. *Journal of Anatomy*, 202(2), 175–181.
- Sharpe, J. (2003). Optical projection tomography as a new tool for studying embryo anatomy. *Journal of anatomy*, 202(2), 175-181.
- Smith, B. H. (1989). Dental development as a measure of life history in primates. *Evolution*, 43(3), 683–688.
- Sofaer, J. A., Bailit, H. L., & MacLean, C. J. (1971). A developmental basis for differential tooth reduction during hominid evolution. *Evolution*, 509–517.
- Soukup, V., Epperlein, H. H., Horáček, I., & Cerny, R. (2008). Dual epithelial origin of vertebrate oral teeth. *Nature*, 455(7214), 795–798.
- Thesleff, I. (2003). Epithelial-mesenchymal signalling regulating tooth morphogenesis? *Journal of Cell Science*, 116(9), 1647–1648.
- Tucker, A. S., Headon, D. J., Schneider, P., Ferguson, B. M., Overbeek, P., Tschopp, J., & Sharpe, P. T. (2000). *Edar/Eda* interactions regulate enamel knot formation in tooth morphogenesis. *Development*, 127(21), 4691–4700.

- Tyndale-Biscoe, H., & Renfree, M. (1987). *Reproductive physiology of marsupials*. Cambridge University Press [476pp].
- Vaahtokari, A., Åberg, T., Jernvall, J., Keränen, S., & Thesleff, I. (1996). The enamel knot as a signaling center in the developing mouse tooth. *Mechanisms of Development*, 54(1), 39–43.
- Williamson, T. E., Brusatte, S. L., & Wilson, G. P. (2014). The origin and early evolution of metatherian mammals: The Cretaceous record. *ZooKeys*, 465, 1.
- Wong, M. D., Spring, S., & Henkelman, R. M. (2013). Structural stabilization of tissue for embryo phenotyping using micro-CT with iodine staining. *PLoS One*, 8(12), e84321.

It's not that I'm so
smart; it's just that I
stay with problems
longer.

- Albert Einstein

Chapter 3

From embryo to adult: The complete development and unusual replacement of the tammar wallaby (*Macropus eugenii*) dentition.

ABSTRACT

Unlike their reptile-like ancestors, modern mammals replace their teeth only once (diphyodonty) or never (monophyodonty). While the mode of replacement has been documented in some mammals, it remains undetermined within some marsupial groups, particularly macropodids (kangaroos and wallabies). In answer to this issue, this study aims to document the complete tooth development and replacement pattern within the tammar wallaby (*Macropus eugenii*). The tammar represents an opportune model for studying mammalian odontogenesis. *Macropus eugenii* has tooth replacement, four tooth classes, and – unusually among mammals – molar progression, but only preliminary investigations in the 1960s and 1980s have been carried out on its dental development. To provide a more comprehensive documentation of the spatio-temporal pattern of tooth development, we stained heads of pouch young aged between 0-135 days in 10% Lugol's Iodine (I2KI), then microCT scanned using a Zeiss Xradia 520Versa and the micro-CT Imaging and Medical Beamline at the Australian Synchrotron. These were reconstructed and segmented in Avizo, generating 3D models. Our results reveal that the functional incisors are composed of a successional generation, where the primary dentition initiates but never erupts. Furthermore, we track the P3 development from initiation to eruption, and find it develops from the primary dental lamina, mesial to the dP3, indicating that no tooth succession occurs in the tammar wallaby. Our findings show that tooth replacement occurs differently in the tammar, suggesting that other mammals may not follow convention.

3.1 Introduction

Limited tooth replacement is one defining feature of mammals. From a reptile-like ancestor with multiple generations of teeth, most mammals now only replace teeth once at each premolar locus (Jussila and Thesleff, 2012). Marsupials have reduced replacement further, where incisors and canines represent one erupted and unreplaced generation, and replacement only happens at one locus – the third premolar (P3). The plesiomorphic condition in marsupials is considered to be three premolars (numbered P1-P3) and four molars, in contrast to that of placental mammals of four premolars (numbered P1-P4) and three molars (Kielan-Jaworowska, Cifelli and Luo, 2004). Since the distalmost premolars initiate first, the P3 of marsupials is considered homologous to the P4 of placentals, and when teeth are lost in evolution the mesialmost P1 is lost first. In an unusual situation for mammals, the P3 erupts below and pushes out the two deciduous premolars (dP2 and dP3) (Cifelli *et al.*, 1996). Tooth replacement patterns have been documented to an extent within placentals and to a lesser extent in marsupials. While most mammals seem to adhere to a conventional pattern, there seems to be controversy within marsupials whether all species follow this generalised pattern.

Tooth development transpires as interactions between the dental epithelium and underlying mesenchyme (Thesleff, 2003). Initiation begins from the primary dental lamina, which thickens at localised placodes to form the future sites of teeth. Incisors and molars initiate one locus at a time antero-posteriorly, while primary premolars initiate in the posterior-anterior direction, with the dP3 usually initiating first. Developing tooth germs pass through bud, cap and bell morphological stages, and then become increasingly mineralised before erupting (Lockett, 1993b).

However, successional teeth and molars initiate in different ways and are formed from a secondary extension of the dental lamina. This extension, known as the successional lamina, expands posteriorly from the last premolar initiation to give rise to the first molar (M1), then M1 extends posteriorly to initiate the next molar (M2) and this pattern continues for the remaining molars. This is another characteristic that distinguished molars from

premolars, where the primary generation of molars develops from successional lamina. For tooth replacement of non-molars, the successional lamina develops lingually from the predecessor and a replacement tooth is produced from it (Lockett 1993a). The successional lamina degrades after giving rise to the replacement tooth (Štembírek *et al.*, 2010). This degradation is thought to be responsible for limiting the number of tooth generations.

Most tooth development studies have been conducted with laboratory mice (*Mus musculus*), which do not have tooth replacement. However, studies on non-model species, such as the marsupial *Antechinus flavipes*, argue us that tooth replacement may not always occur via the assumptive pattern (Archer, 1974). Unlike diphyodont placentals that have two sets of each teeth at each locus, marsupials only replace one tooth at the third deciduous premolar (dP3 locus) by the permanent premolar (P3) (Lockett and Woolley, 1996).

A key study by Lockett (1993a) included 13 orders of eutherians and 4 major marsupial families to find homologies between these divergent groups. Lockett proposed two rules to determine a true successional tooth within these mammals: 1) that it develops from the successional lamina, and 2) that it develops lingually from the deciduous predecessor.

However, within marsupials, there is conflict over whether tooth succession occurs in this way or at all, especially within macropodids (kangaroos and wallabies). Some authors believe that the P3 develops mesial to the dP3 from the primary dental lamina, and thus there is no true successor to the dP3. This remains uncorroborated as there lacks a complete documentation of any macropodid tooth development and the replacement event. There are only a handful of studies on tooth development and replacement within the Macropodidae (See Figure 3.1) which provide snapshots of their tooth development patterns, but not comprehensively enough to convince Lockett (1993a) whether macropodids break the mould.

Over a century ago, Woodward (1893) looked at 7 widely-spread species of the Macropodidae family and one of the sister family Potoroidae and found that tooth succession does not occur in the same manner in all species. He found that in some species the successor in macropodids (the P3) develops mesially to the dP3 from the primary dental

lamina, rather than lingually to it (Figure 3.1a). This occurs first as a small swelling, then as a long thin stalk with a bud, projecting towards the dP3's future tooth crown (Figure 3.1b). Hopewell-Smith and Tims (1911) documented the same stalk-like structure within wallaby *Macropus billiardieri* (Figure 3.1c).

Fast-forward 60 years, where Kirkpatrick (1969, 1978) and Berkovitz (1966) looked at *Macropus giganteus* (Figure 3.1d) and *Setonix brachyurus* (quokka) respectively and both noted the same phenomenon, where the replacing tooth of dP3 develops mesially to it from the primary dental lamina, and at no time forms a development connection directly to the tooth it replaces. This pattern was found again in *Macropus eugenii* (Berkovitz 1972), including the elongated lamina stalk which appears to bear the P3 (see Figure 3.1e and f). However, Berkovitz (1972) only followed development of pouch young up until 55 days old and could not confirm that the stalk of tissue becomes the functional replacement P3.

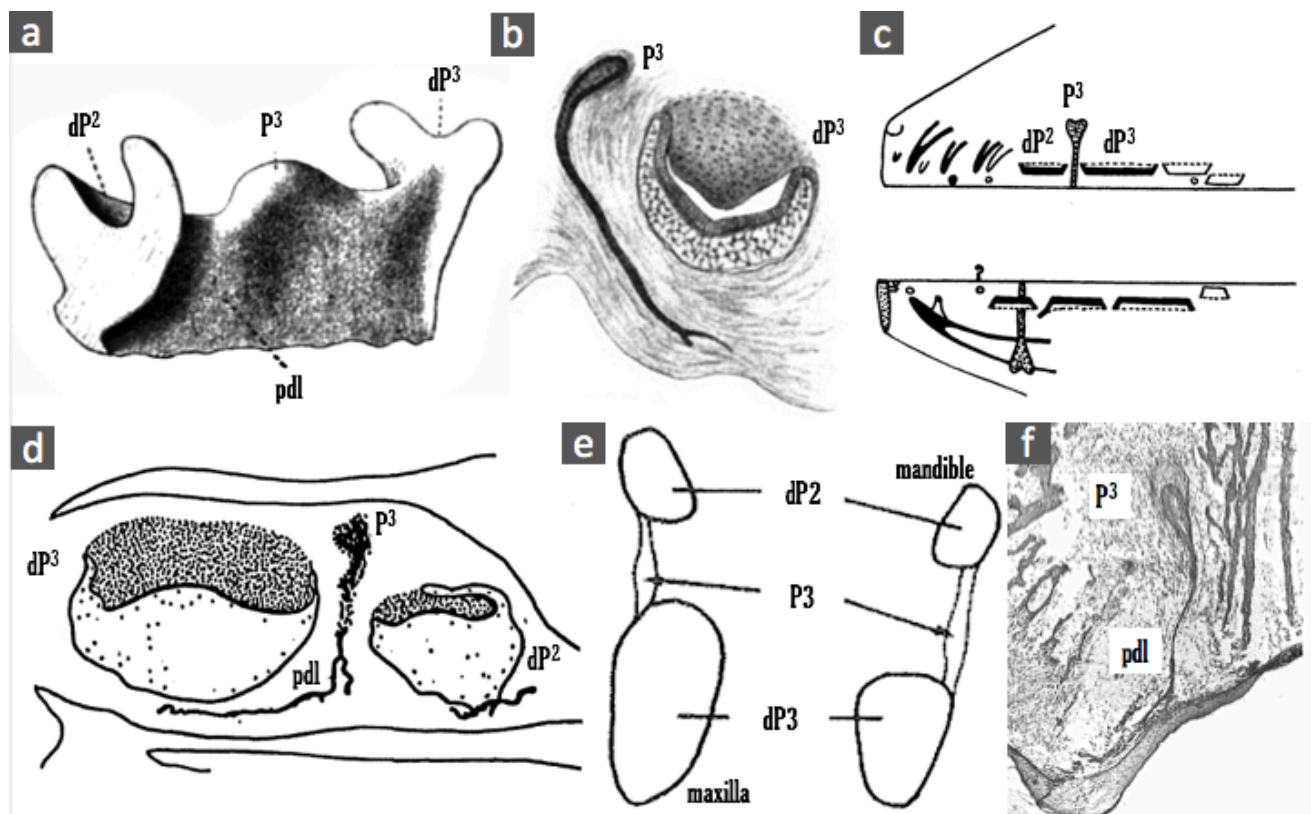


Figure 3.1 History of tooth replacement studies within Macropodidae: a) and b) from Woodward (1893), c) schematic from Hopewell-Smith and Tims (1911); d) Kirkpatrick (1969); e) and f) Berkovitz (1972). Structures were relabelled for consistency as naming conventions have changed e.g. P3 had been called "PPM" and "P4" previously, while dP2 and dP3 have been previously labelled "P2, P3, PM3" and "PM4, DM" respectively. Abbreviations: deciduous premolars two and three (dP2, dP3), permanent premolar (P3), primary dental lamina (pdl).

Despite the efforts of these studies, it is difficult to be confident whether the P3 originates from the primary dental lamina via this stalk-like structure, or whether it arises from a successional lamina that had been redirected mesially. Alternatively, it is possible that the P3 arises lingually from successional lamina later than 55 days of development, and that the stalk does not produce any tooth. Previous authors have deemed this stalk-like structure as “residual dental lamina”, a mere thickening of the free border, that exhibits no differentiation (Wilson and Hill, 1897) – though some have considered that it may have the potency to produce tooth generations (Leche, 1892). Due to the majority of these macropodid studies sampling intermittent developmental time points, and not being able to document P3 development from initiation through to eruption, the fate of this stalk remains unexplained. Lockett (1993a) acknowledges the incompleteness of these studies stating, “Although these studies show that P3 develops mesially to dP3 in macropodids, it remains unclear whether P3 originates by a separate primary dental lamina stalk from the oral epithelium” and urges for attention to be drawn to this long-understudied group of mammals. By providing a complete documentation of macropodid tooth development, this would demonstrate whether the P3 develops from the successional lamina, and is a true successor to the dP3, or whether the replacement pattern in this group is distinct from other marsupials.

Another complexity within Macropodidae is determining the number of teeth that initiate versus the number that become part of the functional adult dentition. Again, macropodids are unusual where, depending on the species, they can have 5 or 6 upper and 3 lower incisor tooth germs initiating, with only 3 and 1 of those teeth, respectively, becoming functional, (Berkovitz, 1972; Kirkpatrick, 1978). This indicates that perhaps there is no generalized pattern for macropodids, and that each species needs to be treated independently. A reason initiation may be particularly difficult to document within macropodids is because the incisors develop quite early: they are already visible at 2 days old in the tammar wallaby (Berkovitz, 1972), which indicates these teeth may initiate *in utero*. Embryo material is particularly difficult to obtain for most marsupial species.

These past studies have all used histological sectioning, with some 3D reconstruction. However, these results can be hard to corroborate. Recent technology of combining Lugol’s

Iodine with CT scanning has revolutionised the documentation of developing embryos and young. Using this method, the combination of microCT scanning with Lugol's solution is a relatively recent technique, first introduced by Metscher (2009), and termed diceCT (Diffusible Iodine-base Contrast-Enhanced Computed Tomography) by Gignac *et al.* (2016). Recently we established the utility of this method to document soft and hard tissue tooth development of the tammar wallaby (See Chapter 2). Using this method, we now can report the entire tooth development pattern of the tammar.

Here we investigate the macropodid tooth development and replacement pattern by using the tammar wallaby (*Macropus eugenii*). The tammar has functional dental formula (teeth that fully mineralise and erupt) of $I^3/1, C^0/0, dP^2/2, P^1/1, M^4/4$ (Figure 3.2). Unusually, marsupials replace two deciduous premolars (dP2 and dP3) with one premolar (P3). The tammar wallaby develops *in utero* for about 26 days, then is in the pouch until the age of 9 months. Berkovitz (1972) documented pouch young from days 2-55, up to the emergence of the M2 (second molar) buds, but did not follow the series to completion (up to the appearance of the M4s). In addition, the premolar replacement event had not occurred yet, nor was there clear evidence where the P3s are initiated. Inns (1982) looked at tooth eruption patterns in the tammar wallaby, up to the age of 14 years, capturing both the timing of eruption of molars, deciduous premolars and the P3. However, soft tissue development was not included and so the origin of the P3 remains unclear.

We aim to provide a complete documentation of the tammar wallaby tooth development and replacement pattern in answer to Lockett's (1993a) appeal to resolve macropodids' place amongst mammalian patterns. We will follow tooth development to completion, once the M4s develop and erupt, as well as the P3s development from initiation to its replacing of the deciduous premolars. In addition, using the relatively recent technique of diceCT, we will produce *in-situ* 3D models, with tissue level resolution, of the tooth development and replacement event, that can be shared and verified. This will allow us to confirm whether the P3 is a true successor or not in this species, and help us to interpret patterns of development within other macropodids and marsupials.

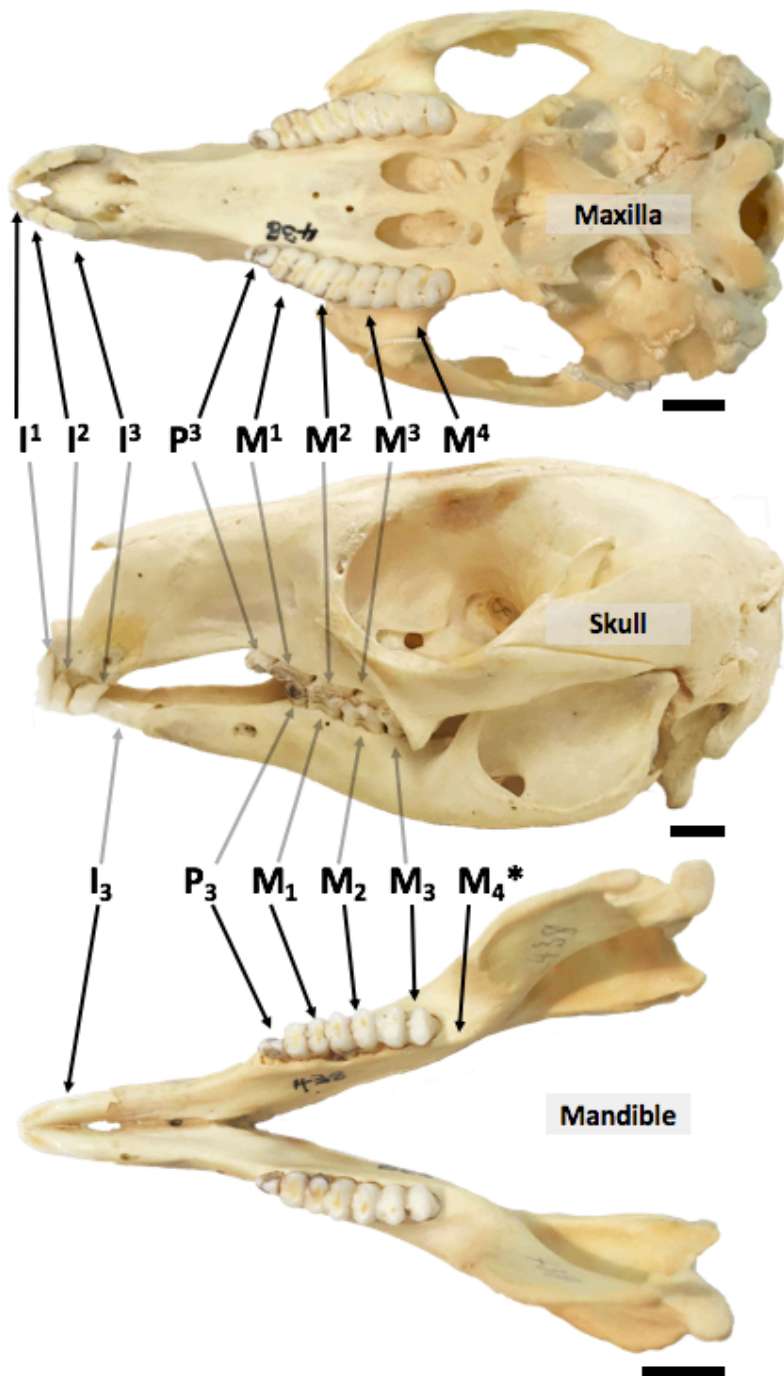


Figure 3.2 Occlusal views of Maxilla and Mandible, and lateral view of the Skull of the adult tammar wallaby (*Macropus eugenii*) (Specimen NMV 6455), showing dental pattern. The tammar has a maximum of three upper and one lower Incisor (I), one upper and lower Permanent Premolar (P) and four upper and lower Molars (M). *Note M₄ has not erupted yet in this specimen. Scale = 1cm.

3.2 Methods

3.2.1 Specimen Descriptions and Preparations

Embryonic and fetal stages are timed from the day when the former pouch young is removed from its sucking stimulus (RPY), which initiates the development of the next blastocyst. The day of birth was designated as day 0 post-partum (pp). Heads of 20 wallaby fetuses (day 23 RPY to day 26 RPY) and pouch young ranging in age from day of birth (day 0 pp) to 4 years old were collected as previously described (Renfree *et al.*, 1982; Hickford *et al.*, 2009) (see Tables A3.1 and A3.2 for full list of specimens). Ages were recorded from known day of birth, and sexes were combined as males and females do not differ significantly in growth (Poole, 1991).

Soft tissue specimens were fixed in 4% paraformaldehyde for 24 hours, washed in PBS and stored in either 100% methanol or 70% ethanol. The specimens were stained in a 1.5% w/v Lugol's solution (see Chapter 2, Methods sections 2.2.1-2.2.2) from 1-28 days, placed on a gentle 2D rocker, with intermittent replenishment of solution to assist in penetration. After being X-ray microCT scanned, specimens were de-stained in dH₂O overnight, then in 1% sodium thiosulfate for a week. Specimens were then transferred back into their original storage solution (100% methanol or 70% ethanol).

To help distinguish tissue layers of similar density, such as primary and secondary lamina, and to see cellular level resolution, we also utilised newly prepared as well as archival sets of haematoxylin & eosin stained histological sections, ranging from 1-55 days (pp) in age. The archival sections are the same ones prepared for and examined by Lockett (1993a). These sections were photographed using a Moto microscope camera, and then compared to equivalent microCT scan slices.

3.2.2 MicroCT Scanning

Specimens were prepared for scanning as per the methods in Chapter 2. Specimens were microCT scanned at the Monash University X-ray Microscope Facility for Imaging

Geomaterials (XMFIG) Zeiss Xradia 520 Versa microCT. Scans were performed using 80–130 kV, 7–24 μ A at .39x magnification (4x for sub-volume scans), 1601–3201 projections with 1–16 sec exposures. Scan times ranged from 1 to 20 hours, resulting in 4.93–42.8 μ m cubic voxel reconstructions. Greyscale values in scan images were used as a proxy for comparing attenuation levels (see Metscher, 2009), where low levels of attenuation produced darker values (approaching black), while higher attenuation approached white, indicating low to high levels of density (mineralisation or Lugol's staining) respectively.

3.2.3 3D Reconstructions and Description of Tooth Structures

MicroCT scans were reconstructed using Automatic Reconstructor (Zeiss, Oberkochen, Germany). These were then segmented in 3D using Avizo 9.0.1 (FEI, Oregon, USA). We occasionally used despeckle and Nagao filters to improve contrast and sharpen outline of tooth germs (as indicated in figures). Using a combination of magic wand with thresholding, brush with limited range, and the blow tool, unmineralised and mineralised dental tissues were segmented out and surfaces extracted to create 3D models. For unmineralised tooth germs, we segmented between the inner and outer enamel epithelium (IEE and OEE), and for mineralised teeth, between the ameloblast and outer enamel layers (as indicated in the figure captions).

Tooth identities are abbreviated as per Lockett and Woolley (1996): incisors (I), canines (C), premolars (P) and molars (M), where a superscript letter denotes upper teeth, and subscript denotes lower teeth (e.g. M¹ or M₁). When referring to both upper and lower, the number is normal case (e.g. M1). Premolars are defined as ante-molar teeth that develop posteriorly-anteriorly, while molars are unreplaced primary teeth that develop anteriorly-posteriorly (Lockett, 1993a). We defined first and second generations of teeth based on their primary or secondary lamina connections but retained traditional nomenclature of "deciduous" (indicated by "d") for the primary generation, and "permanent" for the second generation (e.g. dP³ or P³). The orientation of the successional generation was described with respect to its predecessor, either lingually (towards the tongue side) or buccally (towards the cheek side, or lips for the incisors). Finally, the teeth are numbered mesio-distally (assuming P1 is absent in macropodids). For example, dI₂ is the second deciduous

lower incisor. When describing the whole tooth germs, we used staging from Lockett (1993b) to describe the bud, cap and bell stages of their development.

3.3 Results

Here we summarise our findings of the tammar tooth development pattern. We observed in total the initiation of six upper (dI/I^{1-3}) and five lower incisor tooth germs (dI_{1-3}/I_1 and I_3), one upper canine tooth locus with two generations (dC^1/C^1), two upper and two lower deciduous premolar tooth germs ($dP2-dP3$), one upper and one lower permanent premolar ($P3$), and four upper and four lower molar tooth germs ($M1-M4$), on each side of the jaw. Only some of these progressed through stages of development to mineralisation and eruption, becoming the functional set with formula: $I^3/1$, $C^0/0$, $dP^2/2$, $M^4/4$ before replacement, with $P^1/1$ after replacement (Figures 3.3-3.4).

The deciduous incisors (upper and lower dI^{1-3}/dI_{1-3}) initiated first within the embryo (at or before 23 embryonic days) where successors for lower dI_{1-3} were already present (I_{1-3}), together with the upper dP^3 . By birth (0 days pp) primordia of the deciduous upper canine (dC^1) and both upper and lower $dP3$ s were present, with $dP2$ s appearing by 7 days pp. The upper incisors (dI^{1-3}) and two lower incisors (dI_1 and dI_3) produced successional teeth lingually, where the successor at the upper three loci (I^{1-3}) and at the third locus in the lower (I^3) developed into the final functional dentition. By 14 days RPY the upper canine (dC^1) produced a successor (C^1), whilst the lower locus (C_1) never produced a deciduous or permanent primordium. Most importantly, the upper and lower $P3$ s developed mesially to the $dP3$ s, and from the primary dental lamina. Each began as a swelling on the primary dental lamina between the two deciduous premolars, which then grew as a long thin stalk, and eventually produced a tooth bud which mineralised and erupted. While the upper and lower deciduous premolars do develop strands of successional lamina which appear briefly, it is not contiguous with the lamina the $P3$ s develop from, indicating that the $P3$ s do not develop from a successional lamina. Here we describe in detail the steps that unfold through each tooth class and generation (See Figures 3.3-3.4, Figures A3.1- A3.12, Tables A3.1-A3.2).

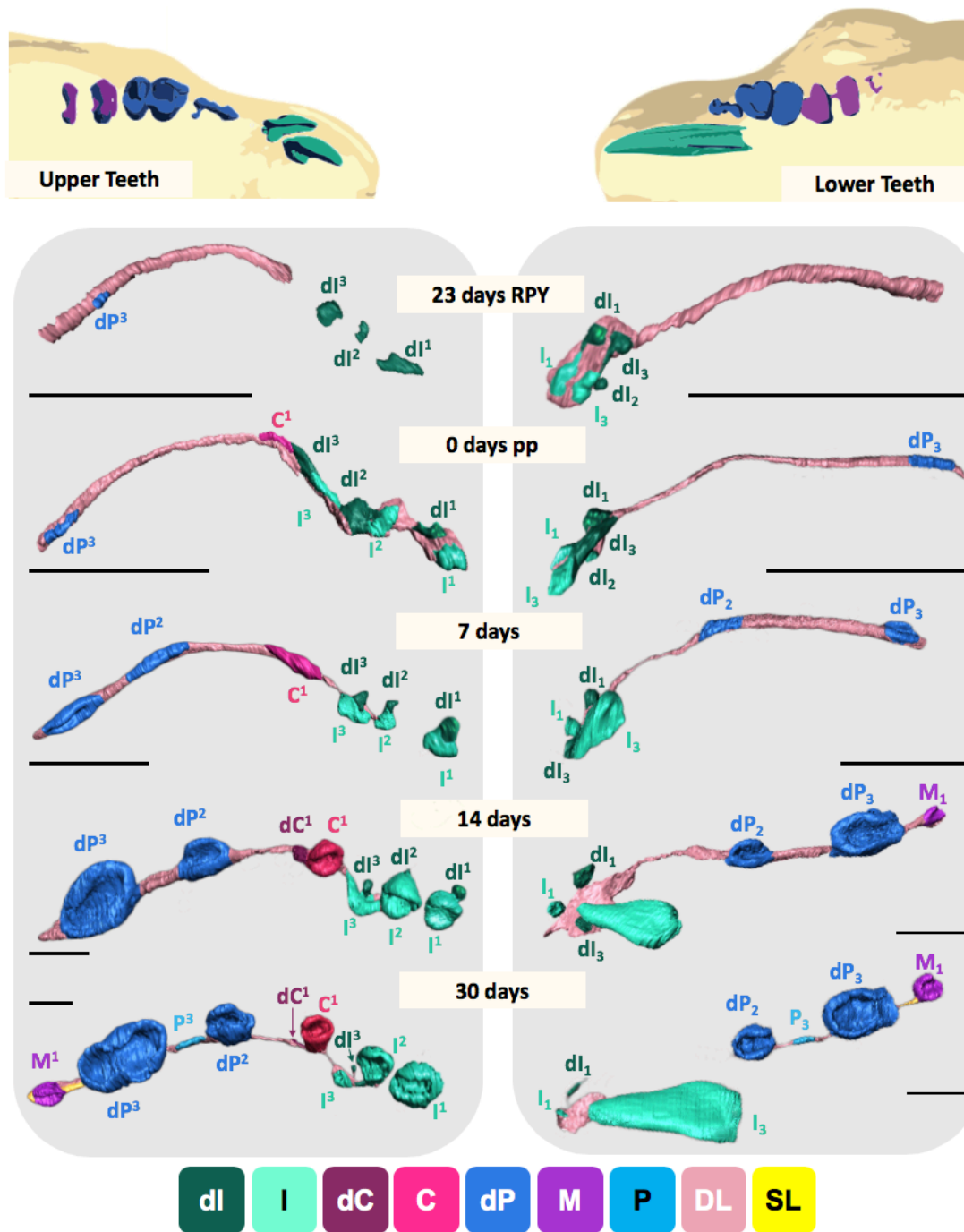


Figure 3.3 3D reconstructions of tooth development of soft and mineralised tissue using diceCT for the upper (left column) and lower (right column) jaws of the tammar wallaby, from 23 days RPY to 30 days pp. Models are in apical view (viewing the dental lamina and tooth germs from below, with the dental lamina behind the teeth) and are mirrored upper and lower right quadrants. Abbreviations: C (Canine), dC (deciduous canine), dI (deciduous incisor), DL (Dental lamina), dP (Deciduous Premolar), I (Incisor), M (Molar), P (Permanent Premolar), SL (successional lamina). Tooth loci are numbered, with superscript for uppers, and subscript for lowers. Specimens were segmented between the inner (IEE) and outer enamel epithelium (OEE). The numbers of the labelled teeth denote generation and locus (e.g. dI3 = deciduous third upper incisor). Scale bars = 1 mm.

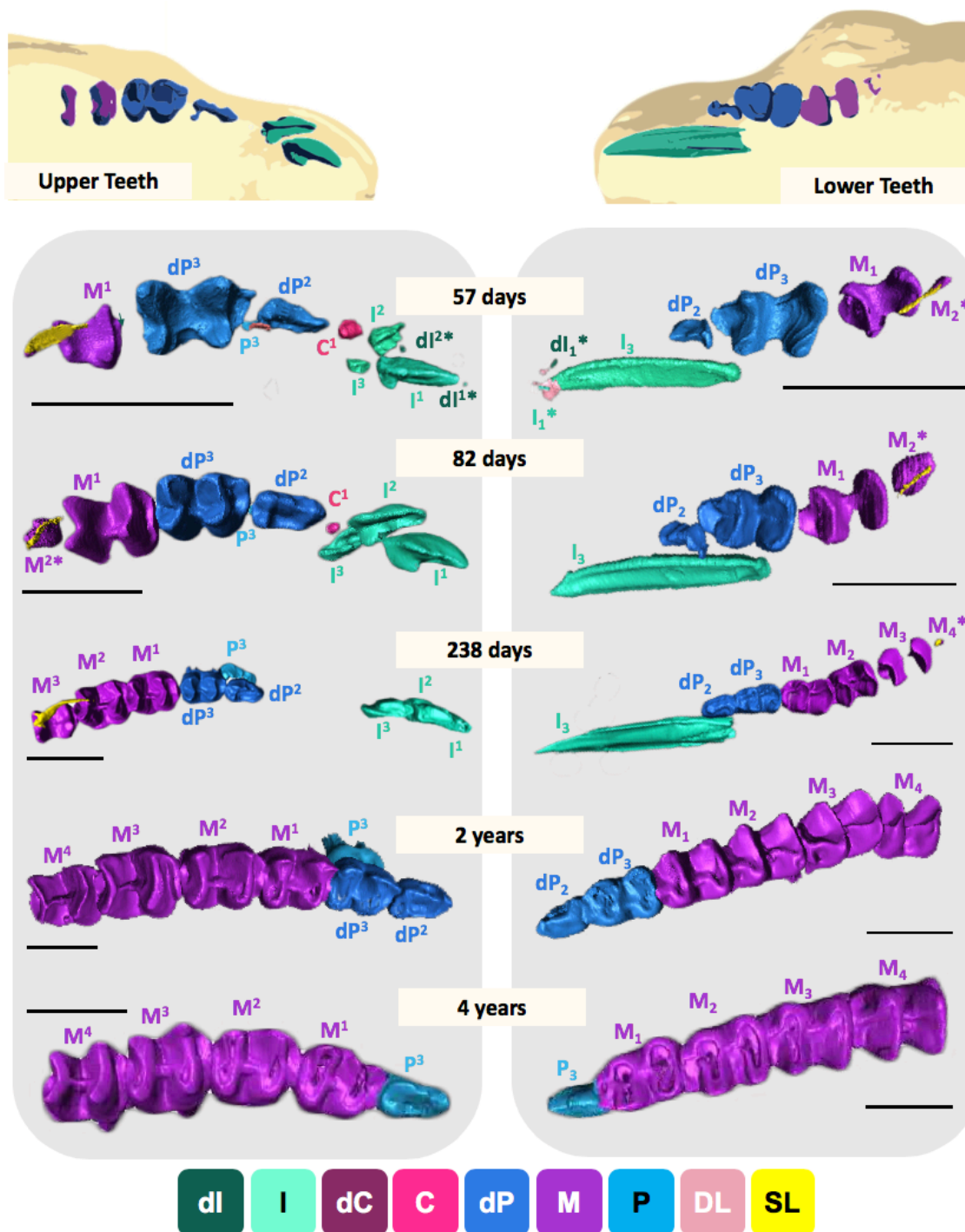


Figure 3.4 3D reconstructions of tooth development of soft and mineralised tissue using diceCT for the upper (left column) and lower (right column) jaws of the tammar wallaby, from 57 days to 4 years. Models are in occlusal view (viewing the tooth crowns from above) and are upper and lower right quadrants. Abbreviations: C (Canine), dC (deciduous canine), dI (deciduous incisor), DL (Dental lamina), dP (Deciduous Premolar), I (Incisor), M (Molar), P (Permanent Premolar), SL (successional lamina). Incisors were excluded in models 2 and 4 years to save space, as they had already erupted. Specimens with mineralisation were segmented between the ameloblast and outer enamel layers, where * denotes unmineralised teeth segmented between the inner (IEE) and outer enamel epithelium (OEE). The numbers of the labelled teeth denote generation and locus, (e.g. dI3 = deciduous third upper incisor). Scale bars = 6 mm.

3.3.1 Incisors

Upper Jaw

Six tooth germs are initiated (three deciduous and permanent pairs), with only the three successional teeth becoming the functional dentition. At 23 embryonic days RPY, there are three deciduous incisor primordia (dI^{1-3}). At birth (day 0 pp) all three primordia split into buccal primary and lingual secondary pairs (into dI^1/I^1 , dI^2/I^2 and dI^3/I^3 respectively) (Figure 3.5a-c, d-f). At 7 days, both dI^1 and I^1 are at bud stage, though I^1 is developing more quickly and is larger. Pairs of dI^2/I^2 and dI^3/I^3 are equally sized, each consisting of a buccal primary bud and lingual secondary buds.

By day 14, there is an enlarged I^1 , already at mid-cap stage, while the buccal dI^1 has remained at mid-bud. The second pair similarly shows faster development of the secondary tooth, where the lingual successor I^2 has developed to a late cap stage, while the buccal dI^2 has is only at late-bud stage. The third pair are at mid-bud (buccal dI^3) and late bud (lingual I^3) stages respectively.

By day 30, both I^1 and I^2 have reached bell stage, while their counterparts have reached a diminutive cap stage (dI^1) and late bud stage (dI^2), with dI^2 exhibiting irregular mineralisation with indistinct layers. I^3 has developed into mid-cap stage, where dI^3 has remained at mid-bud stage.

By 36 days, I^1 has begun mineralizing, I^2 is still at late bell stage and I^3 has reached late-cap stage. dI^1 and dI^2 are rudimentary in their development, and now both mineralized spheres with no distinct layers visible, while dI^3 has disappeared (Figures A3.1, A3.4). I^1 continues to increasingly mineralise, eventually with clear bands of dentine and enamel visible by 80 days and erupts between 150 and 238 days. I^2 and I^3 begin mineralizing by 74 days where distinct layers of dentine and enamel are distinguishable by 120 days for I^2 and 150 days for I^3 . Though I^2 and I^3 began mineralising later than I^1 , they rapidly catch up developmentally and erupt at a similar time between 150-238 days (Figures A3.2, A3.5). The developmentally suspended dI^1 is visible until 74 days, but disappears by 82 days, whilst dI^2 is last seen at 70 days (Table A3.1).

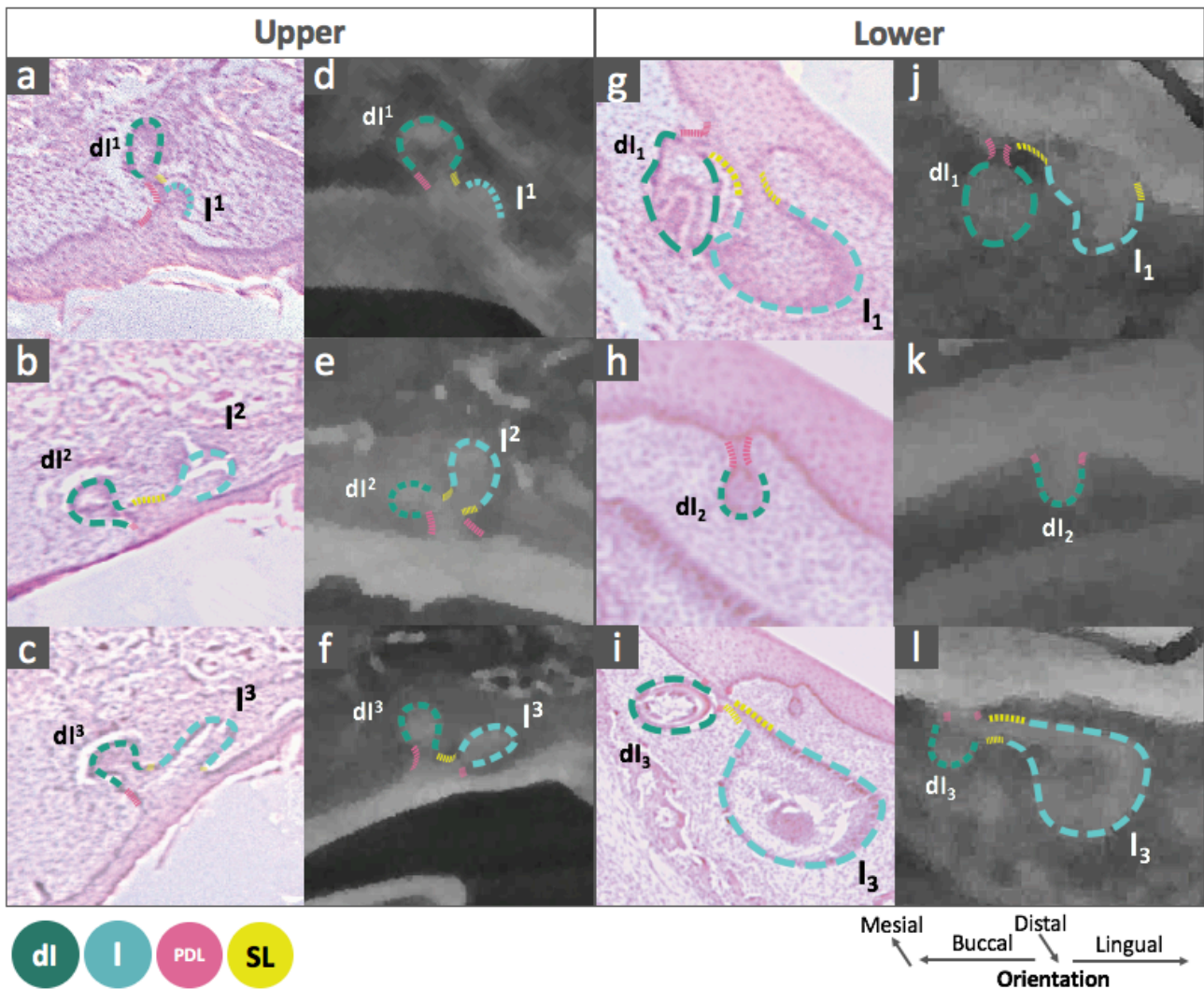


Figure 3.5 Axiobuccolingual sections from histology (a-c, g-i) and microCT scans (d-f, j-l) of the first, second and third upper (a-f) and lower (g-l) incisor loci at 7 days pp. Arrows indicate buccal (to the left) and lingual (to the right) directions. Abbreviations: dI = deciduous incisor (dark green), I = permanent incisor number (light teal), PDL= primary dental lamina (pink), SL = successional lamina (yellow).

Lower Jaw

In total, there appears to be two generations of incisors at the first and third loci, and one generation bud that initiates at the second locus which never developmentally progresses but remains present for much of incisor development. While five tooth germs are initiated in total, the successional tooth at the third locus becomes the one functional incisor (I_3). At 23 days RPY there is already one mesial pair (dI_1 and I_1), a second isolated bud (presumably dI_2) and another distal pair (dI_3 and I_3), where, similarly to the uppers, I_1/I_3 are lingual to dI_1/dI_3 (See Figure 3.5g-l).

At birth (0 days pp) dI_1 and I_1 are already at mid-bud stage, dI_2 at early bud stage, and dI_3 and I_3 at late bud stage. By day 7, dI_3 and I_3 have reached early cap and late cap stages respectively, whereas dI_1 and I_1 are at late bud stage and dI_2 is still at an early bud. By 14 days, I_3 has reached late-bell stage and has even begun partially mineralizing, whereas its counterpart dI_3 is at early cap, but its diameter is a fifth of that of the I_3 , and hasn't yet begun mineralising. dI_1 and I_1 have both reached an early-bell stage and are of similar size to the dI_3 . The dI_2 bud is still present. The I_3 continues to mature, with clear dentine and enamel bands by 36 days (Figures A3.7, A3.10), and erupting by 238 days (Figures A3.8, A3.11). dI_1 and I_1 continue to mineralise, reaching their peak size and density at 43 days, before beginning to diminish in comparative size and density, seen as two mineralised specks at 70 days, and not visible by 74 days. dI_2 also grows slightly to mid-bud stage by 43 days, becoming more elongate, before also reducing in size and disappearing by 74 days. dI_3 is seen reaching early cap by 30 days but having disappeared by day 36 (Table A3.2).

3.3.2 Canines

A primary and secondary pair of upper canine buds initiate, where the successor progresses the furthest. However, no bud erupts to become part of the functional set of an adult tammar. No lower jaw primary or secondary bud ever appear, where there is dental lamina present in the region between the last incisor and first deciduous premolar, but it never thickens to indicate canine bud initiation.

Upper Jaw

A thickening distal to the dI^3 appears at birth (0 days pp) (Figure 3.3), where a buccal primary (dC^1) and lingual secondary (C^1) buds area initiating by day 7. By 14 days, C^1 is at late-cap stage, while dC^1 is at early bud. By day 30, C^1 has reached late-bell stage, where the enamel knot and cord are visible and dC^1 has now disappeared (Figures A3.1, A3.4). From 70 days through to 120 days, C^1 begins and continues to mineralise, though mineralisation only occurs at the cusp of the canine (Figure 3.4). From 150 days onwards,

C¹ begins to demineralise, becoming less dense, and by 238 days, it is no longer visible in the scans (Figures A3.2, A3.5; Table A3.1).

3.3.3 Deciduous Premolars

Upper Jaw

The dP³ bud initiates before birth (at 23 days) and has already reached late-cap stage by 7 days. The dP² bud also appears suddenly at 7 days, when it too is already at late-cap stage. By 14 days dP³ is at late-bell while dP² at early bell. By day 30 both are at late bell stage. By 43 days, secondary enamel knots and enamel cords are visible in both premolars (Figures A3.1, A3.4). Both dP² and dP³ begin to mineralise at 57 days. Dentine is apparent at 120 days, while enamel appears at 150 days. They continue to enlarge and mineralise, before erupting between 150-238 days old (Figures A3.2-A3.3, A3.5-A3.6; Table A3.1).

Lower Jaw

The dP₃ bud is present at birth, reaching mid-cap by day 7, when the dP₂ begins to initiate. By 14 days, dP₂ is at mid-cap, whilst dP₃ is at early bell. By 30 days both are at late bell stage (Figures A3.7, A3.10). Similarly, to the uppers, dP₂ and dP₃ also start mineralizing at 57 days through to 150 days, and also erupt at after 150 but before 238 days old (Figures A3.8, A3.11; Table A3.2).

3.3.4 Permanent Premolars

Upper and Lower Jaws

At 14 days, a raised bump appears along the primary dental lamina between the dP₂ and dP₃ in both the upper and lower jaws (Figure 3.6a, e). By 30 days, this projection has grown into a long vertical stalk, with a thickening at between the apical surfaces of the deciduous premolars, similar to a tooth bud shape (Figure 3.6b, f). This stalk continues to elongate, reaching the apical margins of the upper and lower dP₃ organs (Figure 3.6c,g). A crypt within the bone is present to accommodate this structure. At 57 days, the lower

lamina stalk begins to degrade (Figure 3.4, Figure A3.2, A3.5, A3.8, A3.11). By 74 days, both the upper and lower stalks have disappeared, and now late-staged tooth buds remain within the upper and lower crypts; however, they are now situated apical to the distal part of the dp^2 in the upper jaw, and apical to the dp^3 in the lower. By 82 days, the permanent premolars are at a mid-late cap stage (Figure 3.6d, h). By 120 days they have reached late-bell stage, and enamel knots and cords are visible. At 150 days, mineralisation begins. At 238 days, these have elongated and developed multiple ridges, exhibiting blade-like plagioclacoid form. They continue to enlarge and mineralized, where enamel and dentine layers are distinct bands at 320 days. Lower premolars erupt at 3 years, where upper premolars erupt by 4 years old (Figures A3.3, A3.6, A3.9, A3.12; Tables A3.1, A3.2).

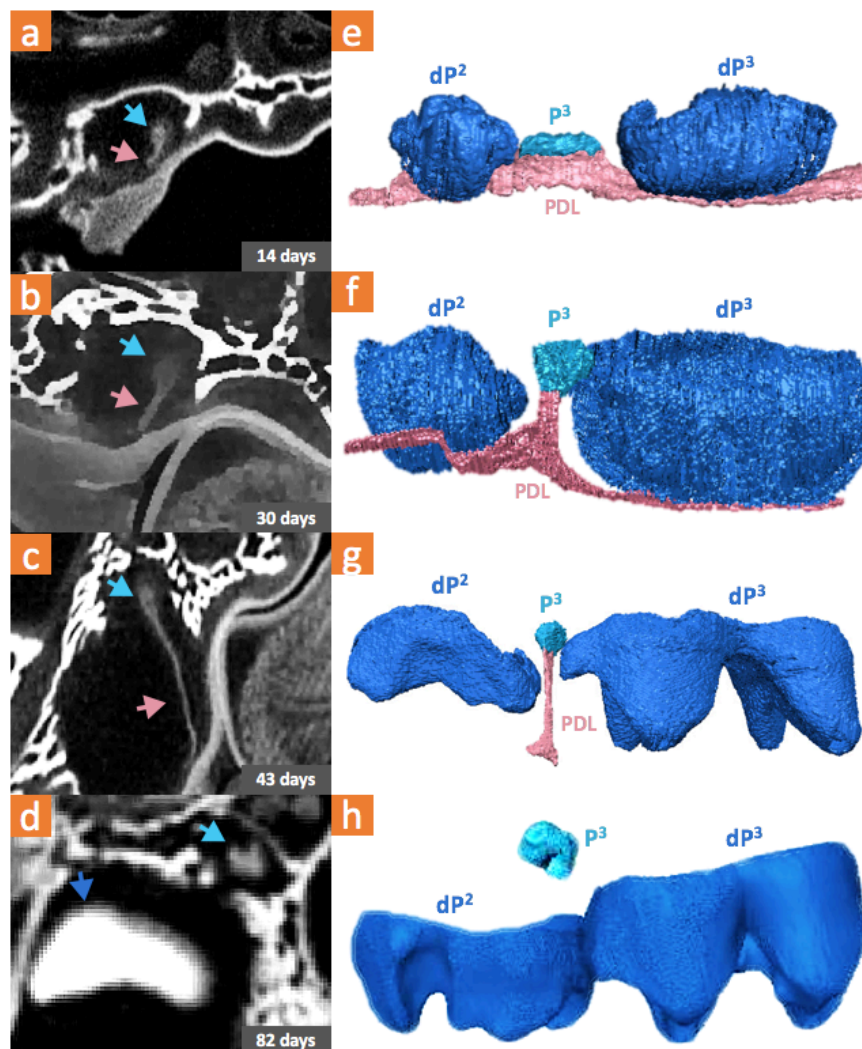


Figure 3.6 MicroCT scan sections (a-d) and 3D models (e-h) showing the development of the upper deciduous premolars (dp^2 and dp^3) and the permanent premolar (p^3) from 14 to 82 days. Light blue arrow indicates p^3 , dark blue = deciduous premolars, pink = primary dental lamina (PDL).

3.3.5 Molars

Upper Jaw

At 14 days there is no sign of the M¹, but by 30 days, it has appeared and is already at late-cap stage, indicating initiation between these time-points. At 36 days, the M¹ has reached early-bell stage and by 43 days it is at mid-bell stage (Figures A3.1, A3.4). There is also a distal extension of successional lamina originating from the apical-lingual region of the M¹. By 57 days, the M¹ is at late-bell stage, and the M² has begun to initiate, where the distal end of the successional lamina has produced a thickening. At 70 days, M¹ has begun to mineralize while the M² is now at an early-cap stage. At 82 days, distinguishable layers of enamel have appeared in the M¹, with M² at early-bell stages. At 120 days, M² has begun to mineralise. At 150 days M¹ continues to mineralise with increasing thicknesses of both dentine and enamel, and a small distal extension from the M² of successional lamina is seen. By 238 days M¹ has erupted, M² has thickened layers of enamel and dentine, and M³ has appeared at late-bell stage and has visible outer enamel epithelium and attachments to the successional lamina (Figures A3.2, A3.5). By 320 days, M² has fully erupted, the M³ has begun mineralising, and there is a successional lamina tail from the M³. By 18 months, M³ has enamel and dentine, and there is now a definitive crypt visible for the M⁴ (indicated in dry skull specimen). By 2 years old, M³ has erupted and is in occlusion, while the M⁴ has distinguishable enamel layers being deposited, but has not yet formed roots. By three years, M⁴ begins to erupt where by four years all teeth have erupted and are in occlusion (Figures A3.3, A3.6; Table A3.1).

Lower Jaw

At day 14, the M₁ is at bud stage, initiated at the free end of the distal successional lamina of the dP₃. At 30 days the M₁ has reached an early-bell stage. At 36 days, an M₂ bud has now appeared developing from a lamina extension off the M₁. By 43 days, the M₁ is at mid-bell stage, while the M₂ is still at bud stage (Figures A3.7, A3.10). By 57 days, M₁ is at late-bell stage. At 74 days, M₁ have begun to mineralize, with layers of similar density of enamel or dentine. The M₂ has now reached early-bell stage. At 82 days, dentine and enamel have distinguished layers of different densities in the M₁, while the M₂ is at late-bell stage. At 150

days, there is a knot of tissue apically to the M₂, indicating the initiation of the M₃. By 238 days, M₁ has erupted, while M₂ has begun mineralisation and M₃ is at late-bell stage (Figures A3.8, A3.11). By 320 days, M₂ has fully erupted, but no visible crypt for the M₄. By 380 days, M₃ has enamel and dentine, and there is now a crypt for the M₄ (indicated in dry skull specimen). By two years old, the M₃ has erupted and is in occlusion. By four years the lower M₄ has erupted to occlude with the upper M³ (Figures A3.9, A.12; Table A3.2).

3.4 Discussion

Using a 3D scanning and modelling approach, we could fully document tooth development in the tammar wallaby, including the eruption of all four molars, as well as the replacement event of the P3s. This has long been overdue in order to complete Lockett's (1993a) assessment of mammalian dental homologies. Here we discuss the significance of the tammar pattern, how it compares to other marsupial species, and the broader implications for how we define and categorise tooth generations in mammals.

We find that in the tammar the number of teeth that initiate differs substantially to its functional adult set. Incisors exhibit a suppressed vestigial primary generation, where only the successor at each loci (except for I_1 and I_2) comprise the final functional dentition. We see a pair of upper canines but no sign of a lower canine primordium. The upper and lower primary premolars are highly correlated in timing of development (within seven days of each other), and also erupt in synchrony with the incisors. The permanent premolar exhibits unusual development from the generalised mammalian pattern: initiating mesial to the dP3s, and from the primary dental lamina. Finally, we see four molars develop, where the fourth molars erupt after the permanent premolar.

3.4.1 Incisors

A notable new finding is how early the incisor buds appear; they are already at bud stage at 23 days RPY, indicating initiation occurs earlier than expected. In the current study we found six upper incisor primordia as three pairs of primary and secondary tooth germs. In contrast, Berkovitz (1972) described five, where no successor was recorded for the dI^3 . This number seen in the tammar is comparable to macropodids *Macropus billardieri* and *Aepyprymnus rufescens* (Berkovitz, 1968b). The successor in all pairs of incisors becomes the functional tooth, a pattern also seen in several marsupials, such as *Monodelphis* (Kozawa *et al.*, 1998) that have vestigial first-generation incisors. This suppression of the first generation of teeth has been proposed to be due to the "fixation" period of suckling,

but was refuted by van Nievelt and Smith (2005), leaving reasons for this unusual development pattern unknown.

In addition, we observed five lower incisor buds as opposed to the three previously recorded by Berkovitz (1972). We saw pairs of primary and successional teeth at both the first (dI_1 and I_1) and third loci (dI_3 and I_3), with a fifth primary bud at the second locus (dI_2) (Figure 3.4g and j). Within Macropodidae, five buds were recorded in *Aepyprymnus rufescens* (Dependorf, 1898), and in several phalangerids (possums) (Berkovitz 1968a). Interestingly, the mesial pair (dI_1 and I_1) and dI_3 do develop and partially mineralise, while dI_2 never progresses through the traditional tooth stages, but does elongate. These non-functional teeth are present until 74 days before being reabsorbed, which coincides with the time that the young leave the pouch and the nutrition it receives is altered.

Similarly, to I^1 - I^3 of the upper dentition, the main functional tooth in the lower dentition is the second generation of the pair (I_3). This is not an uncommon feature, where incisors have a vestigial first tooth generation, with a functional second generation (Luckett 1993a). Berkovitz (1972) never provides evidence of which locus or generation the I_3 belongs to, simply calling it "I". This is the only functional lower incisor in the adult dentition. Berkovitz (1968b) had recorded the third tooth locus becoming the functional lower incisor in the quokka (*Setonix brachyurus*), and postulated that it belonged to a second generation. The defining characteristic of the largest order of marsupials Diprotodontia is the enlarged single lower incisor in each jaw, giving 'two front teeth' (diprotodont) (Aplin and Archer, 1987). This group diverged ~57 million years ago and includes at least 125 living species (Meredith *et al.*, 2009). Given the long divergence and large diversification of this order, it would be interesting to find whether this uniting trait has diverged among diprotodontians in terms of its development.

3.4.2 Canines

Kirkpatrick (1969) and Berkovitz (1972) only reported one tooth primordium for the upper canine in macropodids, and did not identify its generation (presumably primary dentition). We reveal that the upper canine in the tammar develops similarly to incisors, where a

primary and secondary bud develop (dC^1 and C^1), and the successor develops the furthest, even depositing dentine before disappearing after 150 days. The reduction or often absence of functional canines is a common feature within Diprotodontia (Cifelli *et al.*, 1996; Goodrich, 1935).

3.4.3 Deciduous Premolars

The dP3s are the first post-canine teeth to initiate, which is consistent with most marsupials (Luckett, 1993a). Interestingly, although they initiate later, the dP2s development is accelerated so that they catch up with the dP3s. Both upper and lower dP2s and dP3s are roughly equal-sized by 43 days and mineralise at the same time, indicating the well-tuned developmental timing. Both upper and lower deciduous premolars develop projections of lingual successional lamina, which are visible up until 57 days, but these never produce successor tooth germs.

3.4.4 Molars

The molar development and eruption pattern was consistent with that described in Inns (1982). Inns (1982) measured the timing of captured wallabies as the following: M1s to begin to erupt 200-300 days, M2s 300-450 days, M3s 450-1000 days, M4s 3.5-6 years. All our observations fall within these timeframes, although occur at the earlier ends of these ranges. Interestingly, it has been observed previously in some marsupials that the eruption of both the upper and lower fourth molars is synchronous with the permanent premolars (Ride, 1956). However, we find that in the lower jaw, the P_3 erupts before the M_4 does (at three years), where by four years M^4/M_4 and P^3 erupt. This indicates heterochrony of permanent premolar eruption between the upper and lower jaw, and that also M_4 and P_3 eruption is not necessarily in synchrony.

3.4.4 Permanent Premolar

We observe the initial development of the P3s to be as noted by Berkovitz (1972), but with differences to the generalized pattern proposed by Luckett (1993a). First, the P3 buds

initiate earlier than usual, at 14 days, whereas in other successional teeth they generally begin when the deciduous premolars are at late-bell (mineralisation) stages (Lockett, 1993), which does not occur until 57 days in the tammar.

Second, the P3s develop mesially to the dP3s, instead of lingually as expected by Lockett (1993a). This pattern been observed in several macropodids (Figure 3.1), but Lockett (1993a) had suspected in these cases that the P3 developed from a mesially-deviated successional lamina, as he demonstrated in *Dasyurus viverrinus*. In the tammar, we saw the dental lamina stalk of the upper P³ extend towards the dP³, making it seem lingual to these predecessors. However, tracing it from initiation, we can confirm it originally initiated mesially to the dP³. We suggest in some studies flagged by Lockett (1993a) that appear to have a mesially deviated successional lamina, may have a mesially originated primary lamina, like we see in the tammar. A different situation is seen in the lowers, where the P₃ is in closer association with the dP₂, which is also seen in species like *Macropus billardieri* (Hopewell-Smith and Tims, 1911). This may be another source of confusion when interpreting later-staged specimens as to where P3s originate and is why it is pertinent to include earlier stages in studies to find the true origin of P3s.

The final line of evidence that demonstrates a different mode of replacement in the tammar wallaby is that the P3s do not develop from a successional lamina, but rather the primary dental lamina between the dP2s and dP3s. This indicates that the P3s appears to be delayed members of the primary (or deciduous) generation, akin to the dP2s and dP3s. Again, this pattern was noted, in combination with the mesial origin, in several other macropodids (Woodward 1893, Hopewell-Smith and Tims, 1911, Berkovitz 1968b, 1972, Kirkpatrick, 1969).

3.4.5 Tooth Replacement Modes in Macropodidae

Elucidating the true origin of the permanent premolar of the tammar wallaby opens up several questions of the true identity of the P3s. As the P3s initiate from the primary dental lamina in a similar manner to the deciduous premolars, it could be argued that they therefore represent a deciduous premolar between the dP2s and dP3s. However as the

dP3s are the first tooth to initiate, and as the P3s initiated anteriorly to the dP3s, therefore the dP2s may be "dP1s", and the P3s, delayed "dP2s". The typical unreduced dental formula for marsupials includes four premolars (Ziegler 1971) so it is plausible that the tammar could have three deciduous premolars, if including the P3s now as one of the same generation. This definition is based on considering the lamina connection as the most important characteristic to define which generation a tooth belongs to.

The current reigning hypothesis to explain how these delayed generations of teeth are produced is the "Zone of Inhibition" theory (Whitlock and Richman, 2013). This hypothesis suggests that developing teeth emit a signal of inhibition into the surrounding tissue, which may delay the development of adjacent teeth. As the wallaby skull and jaw lengthen, this may have released potential P3s buds from the zone of inhibition, and allowed them to develop. This hypothesis would explain why it developed from the primary dental lamina but its initiation was delayed so that it appeared after the dP2s and dP3s. Furthermore, in comparison to molars, the delayed development of the P3 is short. Between the first molars (M1s) and last molars (M4s) to initiate is up to 17 months, where the initiation of the P3s are only 7 days after the dP2s.

Ultimately, the answer to Lockett's long-unanswered question is that it appears that some macropodids may be doing things differently. We see the replacement generation in the tammar wallaby developing mesially to its predecessor. Furthermore, it appears that alternative modes of succession are present in a multitude of macropodids. An in-depth review of past studies, in combination with more 3D modelling, could answer whether replacement within Macropodidae is phylogenetically, functionally or randomly associated.

3.5 Conclusions and Future Directions

By using 3D imaging and models, we are able to provide more comprehensive and less ambiguous data on the development of mammal teeth, which can easily be shared and verified. We were able to complete the documentation of the tammar wallaby tooth development pattern, including vestigial and functional generations of incisors, the novel observation of two generations of canines, deciduous premolars, molars one to four (which take up to four years to erupt). Most importantly we were able to view the initiation of the only replacement tooth, the P3, which develops mesially to the dP3 and from the primary dental lamina, demonstrating the first major exception to Lockett's definitions of tooth replacement and successional generations in mammals. These findings complete the series started by Berkovitz (1972), and in response to Lockett (1993a) show that the P3s do indeed develop from a stalk of primary dental lamina, and not from successional lamina lingually from the dP3s.

An investigation into tooth replacement using a 3D modelling approach could help better document and define dental patterns in other marsupials and mammals more generally, which could also help with interpretations of tooth generations in the therian fossil record. Looking at fetal specimens allowed us to observe the initiation of vestigial tooth buds and their successors, while using specimens of several years of age allowed us to witness the eruption of the permanent premolars and final molars, demonstrating the need for a temporally-broad developmental series to study. Furthermore, using techniques such as cellular fate-mapping could help us to better understand and define what the successional lamina is, how it may be redirected and its connectivity to successional tooth generations.

3.6 References

- Aplin K. P., Archer M. (1987). Recent advances in marsupial systematics with a new syncretic classification. In: Archer M (ed) Possums and opossums: studies in evolution. Surrey Beatty and Sons, Chipping Norton, New South Wales, pp xv–xxii
- Archer, M. (1974). The development of cheek teeth in *Antechinus flavipes* (Marsupialia, Dasyuridae). *Journal of the Royal Society of Western Australia*, 57, 54-63.
- Berkovitz, B. K. B. (1966). The homology of the premolar teeth in *Setonix brachyurus* (Macropodidae: Marsupialia). *Archives of oral biology*, 11(12), 1371-IN39.
- Berkovitz, B. K. B. (1968a). Some stages in the early development of the post-incisor dentition of *Trichosurus vulpecula* (Phalangeroidea: Marsupialia). *Journal of Zoology*, 154(4), 403-414.
- Berkovitz, B. K. B. (1968b). The early development of the incisor teeth of *Setonix brachyurus* (Macropodidae: Marsupialia) with special reference to the prelacteal teeth. *Archives of oral biology*, 13(2), 171-IN10.
- Berkovitz, B. K. B. (1972). Tooth development in *Protemnodon eugenii*. *Journal of dental research*, 51(5), 1467-1473.
- Cifelli, R. L., Rowe, T. B., Luckett, W. P., Banta, J., Reyes, R., & Howes, R. I. (1996). Fossil evidence for the origin of the marsupial pattern of tooth replacement. *Nature*, 379(6567), 715.
- Dependorf H. 1898. Zur Entwicklungsgeschichte des Zahnsystems der Marsupialier. *Denkschr. med.- naturw. Ges. Jena.*, 6 (1898), pp. 243-402
- Edmund, A. G. (1960). Tooth replacement phenomena in the lower vertebrates. *R. Ont. Mus., Life Sci. Div., Contr.*, 52, 1-190.
- Gignac, P. M., Kley, N. J., Clarke, J. A., Colbert, M. W., Morhardt, A. C., Cerio, D., Cost, I. N., Cox, P. G., Daza, J. D., Early, C.M. & Echols, M. S. (2016). Diffusible iodine-based contrast-enhanced computed tomography (diceCT): an emerging tool for rapid, high-resolution, 3-D imaging of metazoan soft tissues. *Journal of anatomy*, 228(6), 889-909.

- Goodrich, E. S. (1935). Syndactyly in Marsupials. In *Proceedings of the Zoological Society of London* (Vol. 105, No. 1, pp. 175-178). Oxford, UK: Blackwell Publishing Ltd.
- Hickford, D., Frankenberg, S., & Renfree, M. B. (2009). Collection, handling, fixation, and processing of tammar wallaby (*Macropus eugenii*) embryos. *Cold Spring Harbor Protocols*, 2009(12), pdb-prot5335.
- Hopewell-Smith, A., & Tims, H. W. (1911). Tooth-germs in the Wallaby *Macropus billardieri*. *Journal of Zoology*, 81(4), 926-942.
- Inns, R. W. (1982). Age determination in the Kangaroo Island wallaby, *Macropus eugenii* (Desmarest). *Wildlife Research*, 9(2), 213-220.
- Jussila, M., & Thesleff, I. (2012). Signaling networks regulating tooth organogenesis and regeneration, and the specification of dental mesenchymal and epithelial cell lineages. *Cold Spring Harbor perspectives in biology*, a008425.
- Kielan-Jaworowska, Z., Cifelli, R. L., & Luo, Z. X. (2004). Mammals from the age of dinosaurs: origins, evolution, and structure. Columbia University Press.
- Kirkpatrick, T. H. (1969). The dentition of the marsupial family Macropodidae: with particular reference to tooth development in the grey kangaroo *Macropus giganteus* Shaw.
- Kirkpatrick, T. H. (1978). The development of the dentition of *Macropus giganteus* (Shaw): an attempt to interpret the marsupial dentition. *Australian Mammalogy*, 2, 29-35.
- Kozawa, Y., Iwasa, Y., & Mishima, H. (1998). Degeneration of tooth germ in the developing dentition of the gray short-tailed opossum (*Monodelphis domestica*). *European Journal of Oral Sciences*, 106(S1), 509-512.
- Leche, W. (1892). Studien über die Entwicklung des Zahnsystems bei den Säugethieren. Engelmann.
- Luckett, W. P. (1993a). An ontogenetic assessment of dental homologies in therian mammals. In *Mammal phylogeny* (pp. 182-204). Springer, New York, NY.
- Luckett, W. P. (1993b). Ontogenetic staging of the mammalian dentition, and its value for assessment of homology and heterochrony. *Journal of Mammalian Evolution*, 1(4), 269-282.

- Lockett, W. P., & Woolley, P. A. (1996). Ontogeny and homology of the dentition in dasyurid marsupials: Development in *Sminthopsis virginiae*. *Journal of Mammalian Evolution*, 3(4), 327-364.
- Meredith, R. W., Westerman, M., & Springer, M. S. (2009). A phylogeny of Diprotodontia (Marsupialia) based on sequences for five nuclear genes. *Molecular Phylogenetics and Evolution*, 51(3), 554-571.
- Metscher, B. D. (2009). MicroCT for developmental biology: A versatile tool for high-contrast 3D imaging at histological resolutions. *Developmental dynamics*, 238(3), 632-640.
- van Nievelt, A. F., & Smith, K. K. (2005). To replace or not to replace: the significance of reduced functional tooth replacement in marsupial and placental mammals. *Paleobiology*, 31(2), 324-346.
- Poole, W. E., Simms, N. G., Wood, J. T., & Luboloa, M. (1991). *Tables for age determination of the Kangaroo Island tammar wallaby (Macropus eugenii), from body measurements* (No. 32). Technical Memorandum.
- Renfree, M. B., Holt, A. B., Green, S. W., Carr, J. P., & Cheek, D. B. (1982). Ontogeny of the brain in a marsupial (*Macropus eugenii*) throughout pouch life. *Brain, behavior and evolution*, 20(1-2), 57-71.
- Ride, W. D. L. (1956). The affinities of *Burramys parvus* Broom a fossil phalangeroid marsupial. *Journal of Zoology*, 127(3), 413-429.
- Štembírek, J., Buchtová, M., Král, T., Matalová, E., Lozanoff, S., & Míšek, I. (2010). Early morphogenesis of heterodont dentition in minipigs. *European journal of oral sciences*, 118(6), 547-558.
- Thesleff, I. (2003). Epithelial-mesenchymal signalling regulating tooth morphogenesis. *Journal of cell science*, 116(9), 1647-1648.
- Whitlock, J. A., & Richman, J. M. (2013). Biology of tooth replacement in amniotes. *International Journal of Oral Science*, 5(2), 66.
- Wilson, J. T., & Hill, J. P. (1897). *Memoirs: Observations upon the Development and Succession of the Teeth in Perameles; together with a Contribution to the Discussion of the Homologies of the Teeth in Marsupial Animals*. *Journal of Cell Science*, 2(156), 427-588.

Woodward, M. F. (1893). Contributions to the study of mammalian dentition.-Part I. On the development of the teeth of the Macropodidae. In Proc. Zool. Soc. London (pp. 450-473).

Ziegler, A. C. (1971). A theory of the evolution of therian dental formulas and replacement patterns. *The Quarterly Review of Biology*, 46(3), 226-249.

Nothing will work
unless you do.
- Maya Angelou

Chapter 4

Developmental patterns of continuous tooth generation in the nabarlek (*Petrogale concinna*)

ABSTRACT

The nabarlek (*Petrogale concinna*) is a species of rock-wallaby and one of 5 mammalian species in the world that has the ability to continuously replace its molars. We hypothesise that one key to its ability may be an activation/inhibition balance of signalling molecules during tooth development causing newly-produced posterior molars to grow to a consistent size and shape. Combined with its molar progression ability, this would allow for a seamless production line of molars to be produced to replace worn teeth. To test our tooth-size pattern hypothesis, we measured the size of teeth in nabarleks and compared their tooth row patterns to those of other *Petrogale* species. We found that in young nabarleks and *Petrogale* spp. of all ages that teeth increased in size from anterior to posterior. However, in adult nabarleks, the teeth were essentially equal in size. We propose that there is a change in developmental signalling toward adulthood, creating a change from an increasing tooth row size, to equal size, facilitating this continuous tooth replacement ability. This discovery represents the precursory steps towards a better understanding of genetic pathways that are responsible for tooth replacement limitations within humans and other mammals.

4.1 Introduction

One trait that separates mammals from other vertebrates is the limited ability for tooth replacement. Surprisingly, there are a few exceptional species that have unlimited tooth generation, with a continuous production of molars that erupt and are replaced. The nabarlek rock-wallaby (*Petrogale concinna*) is one of 5 mammal species (Gomes Rodrigues *et al.*, 2011), and the only marsupial, to have continuous tooth generation. The nabarlek is only found in the top end of Northern Territory, and the Kimberley region of Western Australia (Churchill, 1997), comprises three subspecies and consumes predominantly grasses, sedges and ferns (Sanson *et al.*, 1985). A colony was started and maintained from 1977 to 1986 at Monash University (Melbourne), where observations about reproduction and behaviour were collected (Goldstone and Nelson, 1986; Nelson and Goldstone, 1986). Despite this work, there still remain unanswered aspects of the nabarlek's biology, especially how it gained continuous molar replacement while other *Petrogale* species and most other mammals have not.

In mammals, tooth buds are produced from thickened epithelial-mesenchymal tissues in the jaw called the primary and secondary dental lamina. The primary dental lamina, a band that appears in a horseshoe shape around the jaws, produces the first generation of teeth, which are initiated at localized placodes (Jernvall and Thesleff, 2000). The successional generation of teeth develop from a thread of secondary lamina that originates as an offshoot (usually lingually) from the primary dental lamina of the tooth it replaces. The primary tooth is replaced by this successional in a vertical fashion where the successional tooth pushes from beneath, for lower teeth, or above, for upper teeth, and (usually) ejects the tooth out of the jaw. In non-mammalian vertebrates successive generations continue to bud off successional lamina from the previous tooth leading to multiple replacements (Juuri *et al.*, 2013). Most mammals only can replace their incisors, canines and premolars once by this process (Lockett, 1993). This limits them to a maximum of two tooth generations at any one locus and are considered 'diphyodont'.

Although mammalian molars are generally termed 'monophyodont' because only one tooth erupts at each molar locus, molar development is more similar to successional tooth

replacement in the mesial teeth. The first molar buds off posteriorly from successional lamina coming from the posterior-most deciduous premolar (dP3 in marsupials, dP4 in placental mammals). Molars are then generated serially, similar to the replacement generations produced in non-mammalian vertebrates, except that molars are added horizontally, and all remain in the jaw at the same time (Juuri *et al.*, 2013).

Because sequential teeth are generated from the successional lamina, tooth production ceases when the successional lamina degrades (Štembírek *et al.*, 2010). This degradation appears to be why a maximum of two generations of teeth are produced in the mesial teeth, and presumably occurs to limit the number of molars produced: the maximum number of molars in marsupials is generally four, while in placentals it is three. Although humans and other mammals produce a limited number of sequential molars in this way, the nabarlek is able to maintain this process, making molars perpetually in its lifetime. This suggests that its successional lamina does not degrade or does so only towards the end of its life.

Another characteristic that would allow for continuous molar replacement is molar progression, a relatively common trait amongst kangaroos and wallabies (Sanson, 1980). In addition to vertical replacement of deciduous premolars, some macropodids can replace teeth horizontally through molar progression. This is the anterior movement of the entire tooth row, resulting in the ejection of an often-worn front tooth (either the P3 or anterior molar) and the eruption of a new back tooth (such as the fourth molar). It has been noted that species with prominent premolars do not have molar progression, where the P3 is thought to act as an anchor to the tooth row to prevent anterior movement of the teeth (Sanson, 1989). Those macropodid species with this ability only replace one tooth via horizontal molar progression, while the nabarlek repeats this process creating a perpetual “conveyor belt” of molars. With continuous molar generation in the nabarlek, a consistent tooth size pattern would be required for the molars to continue to fit.

Mammalian cheek-teeth typically follow distinct size patterns, where sequential deciduous premolars and molars grow in an increasing, decreasing or uniform size. These patterns of tooth size are proposed to be controlled via an Inhibitory Cascade (IC), an interplay of activation and inhibitory growth molecules, where the growth of one tooth dictates the size

of the adjacent teeth (Kavanagh *et al.*, 2007). Kavanagh *et al.* (2007) demonstrated the IC model by separating the second mouse molar (M2) bud from the first molar (M1) and culturing them in-vitro. They found that the M2 was able to grow larger and more quickly, suggesting it had been freed from inhibitory molecules being released by the M1.

A key element of the nabarlek's continuous molar replacement ability may be the achievement of an activation/inhibition balance in growth molecules during tooth development causing the newly grown posterior molars to grow a similar size, a pattern previously observed by Tate (1948). This would be conducive to continuous tooth production.

We propose three elements are required for continuous tooth replacement:

1. Prolonged maintenance of molar successional dental lamina
2. Continuous molar progression to create for room for new teeth.
3. Tooth size growth patterns that do not lead to teeth too small/large for the jaw.

We aim to investigate one of these elements, the tooth size growth patterns, by quantifying it within the nabarlek. Currently it is unclear whether this pattern changes between juvenile and adult nabarleks, which we aim to clarify by comparing tooth size patterns of different aged nabarleks.

A common method of aging mammals uses the eruption pattern of the teeth (Inns, 1982), but this is not applicable to the nabarlek as once their premolars are shed, it may be difficult to distinguish their fourth from their fortieth molar. Therefore, in addition to tooth eruption, we will also employ skull suture closure patterns, which have been used to categorize *Macropus* species (Rager *et al.*, 2014). To more completely document nabarlek ages, we will also measure skull length, an additional and widely-used age proxy (Murphy and Smith, 1970). By using multiple indicators of age, we will provide a more detailed categorisation of this unusual species.

We will also conduct a comparison of tooth size patterns between closely related *Petrogale* species that do not have continuous tooth replacement to determine whether this pattern is

likely to be an adaptation unique to the nabarlek among its kin. We will compare it to *Petrogale burbidgei* the nabarlek's sister species (Potter *et al.*, 2017) but because it is poorly represented in museum collections we will also use *Petrogale brachyotis*, the next closest species.

4.2 Methods

4.2.1 Specimens

We assessed and measured dry skeletal specimens of *Petrogale concinna*, *P. brachyotis* and *P. burbidgei* specimens from Australian National Wildlife Collection (ANWC) (37), Western Australian Museum (WAM) (74), Museums Victoria (MV) (16), Monash University Zoology Research Collection (MZRC) (25), South Australian Museum (SAM) (7), Australian Museum (AM) (5) and Museum and Art Gallery of Northern Territory (MAGNT) (29), giving a total of 193 specimens comprising of 61 *P. concinna*, 116 *P. brachyotis* and 16 *P. burbidgei* (see Table A4.1 for complete specimen list).

4.2.2 Aging

The suture closure pattern we used was modified from Rager *et al.* (2014) based on *Macropus eugenii*, *M. parryi* and *M. rufus* species. Taking the first four sutures (the only ones to close for *Macropus* spp.) we made five age categories in order of their fusion: A) none, B) basioccipito-exoccipital, C) supraoccipito-exoccipital, D) basioccipito-basisphenoid, E) parieto-supraoccipital (Figure A4.1). Fusion was considered achieved when less than half of the suture was open or visible.

We also assessed tooth eruption patterns and measured skull length. Eruption patterns were scored as Juvenile: deciduous premolars present; Intermediate: premolars present; Adult; premolars worn or lost (only molars present) (Figure 4.1). The P3 served as an anchor point for aging our specimens – if the P3 is present, we know that the following molars will be M1 onwards. For our results, known teeth are labelled, while unknown molars (after the P3 is lost) are labelled as Mx1, meaning the first molar present in the row but at an unknown molar position compared to the M1. When recording tooth eruption data, upper teeth were denoted with a superscript numbers: e.g. dP², P³, M¹, Mx¹, while lower teeth were given a subscript number: dP₂, P₃, M₁, Mx₁. Skull length was measured from the posterior-most point of the occipital to the anterior-most point of the premaxilla

(roughly between its two front incisors), using Mitutoyo digital callipers (± 0.01 mm) (Figure 4.2).

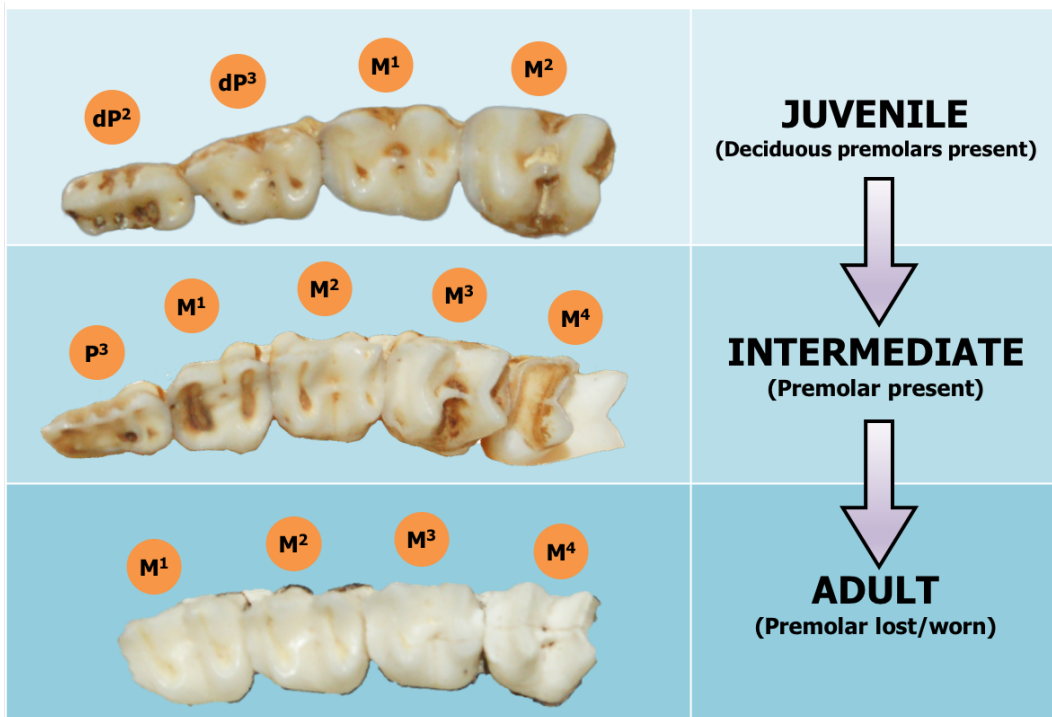


Figure 4.1 Tooth eruption patterns in *Petrogale* spp. from juvenile (deciduous premolars present), intermediate (deciduous premolars lost, P3 erupted), and adult (P3 lost or worn). In the adult nabarleks, M1-M4 is instead Mx1-Mx4 where after the P3 is lost, it is uncertain which molar is at the first tooth position. Photographs show *P. concinna* specimens.

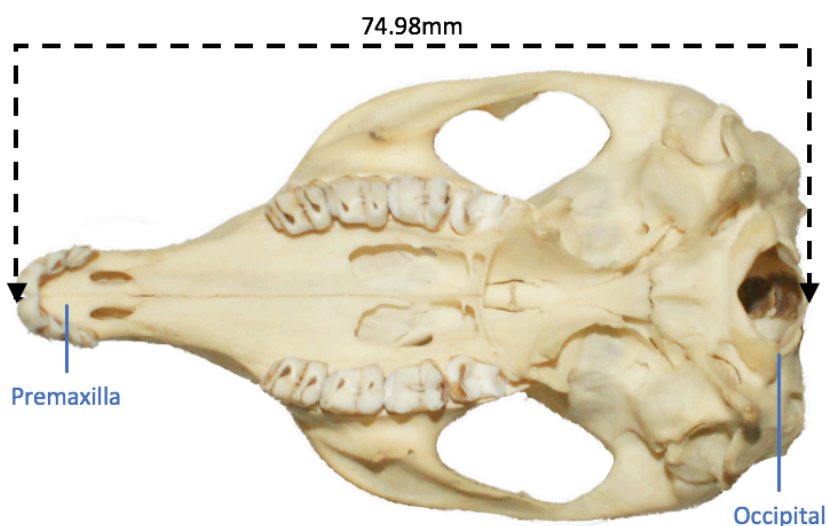


Figure 4.2 *Petrogale* spp. skull showing points where skull length were measured from: between the anterior-most point of the premaxilla bone to the posterior-most point of the occipital bone.

The combination of both tooth eruption pattern and suture closure pattern has allowed us to develop six staging categories (Figure 4.3), where suture category C was split into C1 and C2, as both *P. concinna* and *P. brachyotis* had different tooth eruption stages coinciding with the same suture category.

Skull length was compared to both tooth eruption patterns and skull suture closure patterns to determine whether there was a correlated for skull length with any of the other age categories.

Age Categories		A	B	C1	C2	D	E
Tooth Eruption Pattern	<i>Petrogale concinna</i> (nabarlek)	dP2 and dP3		P3	molars only		
	<i>Petrogale burbidgei</i>	dP2 and dP3			P3		
	<i>Petrogale brachyotis</i>	dP2 and dP3			P3	P3 worn	
	Suture Closure Stage	A	B	C		D	E

Figure 4.3 Age categories (A, B, C1, C2, D, E) based on both suture closure order and tooth eruption pattern for *Petrogale* spp. Tooth eruption stages: dP2 and dP3 are present (Juvenile); P3 have erupted (Intermediate); P3 is worn or lost, only molars present (Adult) (See Figure 4.1). Suture closure order consisted of five categories (A-E): A) none closed; B-E) each suture closure in order, where the basioccipito-exoccipital is the first, parieto-supraoccipital the last (Figure A4.1).

In addition, we also examined the five only nabarlek specimens of recorded ages from the Monash University breeding colony (Nelson and Goldstone, 1986): 5 months, 6 months (n=2), 1.5 years and 2 years old, which we could use to determine the chronological age that key tooth development and replacement events occur within this species.

4.2.3 Tooth Measurements

Evans *et al.* (2016) demonstrated that a 2D occlusal outline of hominin teeth correlated highly with the 3D volume obtained from CT scans, when comparing tooth sizes along a tooth row. Therefore, to increase sample size and reduce costs, we opted to obtain photographs and measure the 2D outline of the teeth. Photographs were taken of each occlusal surface of left and right tooth rows of upper and lower jaws of the specimens. Using the polygonal tool within Fiji image processing package (Schindelin *et al.* 2012), we created outlines of the maximum occlusal perimeter of each tooth. A scale was set for each photo and then the area was calculated (in mm²) (Figure 4.4).

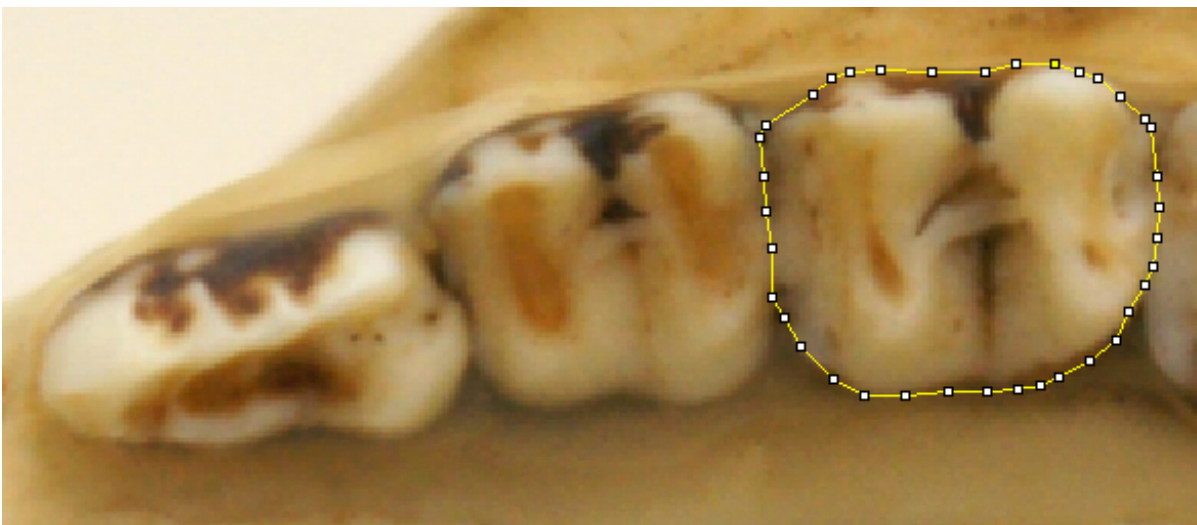


Figure 4.4 Upper right tooth row of *P. concinna* specimen, demonstrating maximum occlusal outline perimeter of the M¹, created using the polygonal tool in Fiji.

4.2.4 Tooth Size Pattern Analyses

To avoid pseudo-replication of individual-level data, we averaged the left and right sides of each individual for both upper and lowers to obtain an individual average. We plotted raw measurements of the occlusal area to show tooth size patterns along rows of *Petrogale* spp. teeth, including species averages and minimum and maximum values. To look at the proportional size differences along the tooth row, we divided each tooth occlusal area by the M1 (or Mx1 for specimens that had shed their premolars) and reported as a proportion (e.g. 1.5 times the size of an M1). The P3 was not measured as part of the tooth size patterning, as this tooth is the only one from the second generation, and thus may not be expected to follow the same size patterning as the primary generation. Tooth size

proportions for species averages, minima and maxima were also plotted. These graphical analyses were all carried out in Prism version 7.0d (for Mac OS X. GraphPad Software, La Jolla California USA, www.graphpad.com).

4.3 Results

4.3.1 Aging

Using tooth suture closure patterns, we could separate *Petrogale* specimens that had the same tooth eruption pattern, but a different suture pattern, including specimens with deciduous premolars present (which ranged over two or three suture categories) and those that had worn or lost their P3 (which ranged over two to three suture categories). Based on our aging categories, we found that the nabarlek has relatively more rapid tooth development and replacement, where it loses its deciduous premolars, gains its permanent premolar, then loses its permanent premolar in the same time that *P. burbidgei* and *P. brachyotis* have only begun to shed its deciduous premolars (Figure 4.3).

Out of the 16 *P. burbidgei* individuals measured, there were no specimens with the suture closure stage B, but there were some at A and C. Due to the small sample size, it is possible that this stage just wasn't sampled, especially as the basioccipital-basisphenoid suture was fused in the specimens staged C. Of the 107 *P. brachyotis* measured, there were no specimens in the Stage A, with no sutures fused. It is possible that these may fuse very early and no specimens younger than Stage B were sampled.

As expected, we find that the skull length of the nabarleks generally increases through the suture closure and tooth eruption patterns (Figure 4.5a-b). For the suture closure stages, average skull size increases from under 60 mm to ~74 mm from A-C1, then begins to plateau from stage C2 at 74-76 mm (Figure 4.5a), indicating that the skull ceases to elongate. There is overlap in skull length between suture stages B-E, indicating that from skull size alone it is not possible to denote the suture closure stage, and thus categorise age. When comparing skull size to the tooth eruption pattern, skull size increases from ~62 mm to ~76 mm from Juvenile through to Adult (Figure 4.5b). Again, there is overlap between all three stages, indicating that skull size alone is not a reliable indicator of eruption stage.

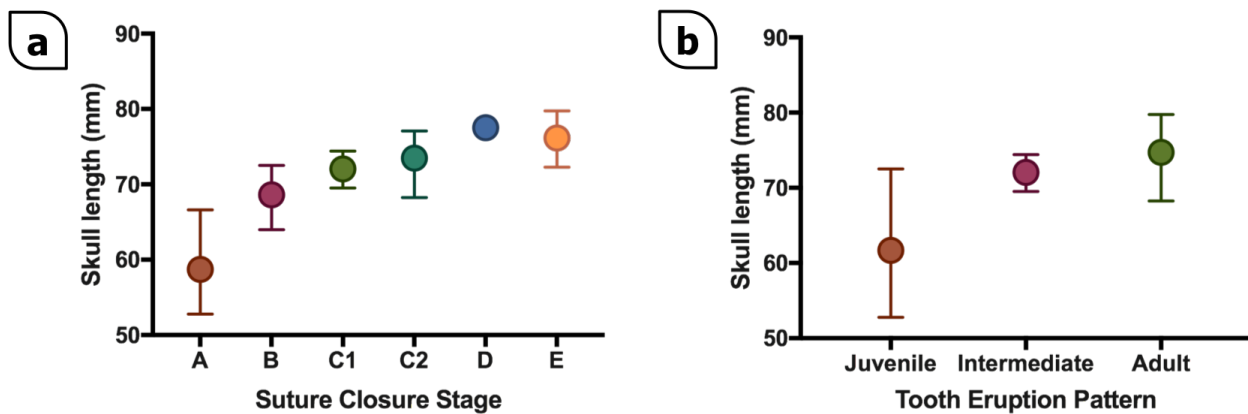


Figure 4.5 Nabarlek skull length vs a) suture closure category and b) tooth eruption pattern. Tooth eruption stages are Juvenile= deciduous premolars present; Intermediate = premolars present; Adult = molars only. See Figures 4.1, 4.3, A4.1.

From the captive colony specimens with known ages we were able to see the following: at five months (MZRC 6465), both deciduous premolars have erupted and the P3 is in the crypt. At six months both specimens (MZRC6410 and 6398) retain their deciduous premolars. In the 18-month-old specimen (MZRC6399), both upper and lower P3s have been lost, while in the 24-month-old specimen (MZRC6397), the lower P3s have been lost, but the upper P3s are retained. This indicates that the P3 erupts between 6-18 months and can be lost between 18 to 24 months of age, or possibly later.

4.3.2 Tooth Size Patterns

In the younger nabarlek specimens (Stages A-C1) upper tooth size (as indicated by occlusal outline area) increases from dP^2-M^3 , where M^3 and M^4 are more similar in size for Stage C1 (Figure 4.6a). Interestingly, M^1-M^3 in C1 matched sizes almost exactly as those of dP^3-M^2 at stages A and B. In adult nabarleks with all molars (Stages C2-E) the molars are approximately uniform in size. From dP^2 to M^1 , teeth are between 10-20 mm^2 (Stage A). M^1-M^3 s are between 13-20 mm^2 . After the P^3 is shed, the additional molars (greater than M^5) continue to oscillate between 14-18 mm^2 in average size (Stages C2-E). M^2-M^4 at stage C1 appeared uniform in size. At Stage C2 some rows are still increasing in size, while others have plateaued, indicating a mix of tooth positions at this suture closure stage. These patterns were similar in the lower teeth, but sizes were 5 mm^2 smaller on average (Figure A4.2a). To summarise, the nabarlek tooth size pattern for both upper and teeth changed

with age, increasing in average size along the row (Stage A) to a relatively uniform size (Stage E) (Figures 4.6a, A4.2a).

The nabarlek tooth ratios (tooth size divided by M1/Mx1 size) for the upper teeth revealed similar patterns (Figure 4.6b). For stages A-C1, there was an increase in tooth size ratio along the row, where dP²s were from 0.6 times the size of an M¹, until M³s that were around 1.4 times bigger than M¹s on average. In C2-E the tooth size ratio flattened, to an average of 0.8-1.1 times the size of the Mx¹, although C2 still exhibits a greater variation of patterns. Again, this pattern was reflected in the lower teeth, with ratios from first to last tooth along the row between A-C1 at 0.5-1.7 times and 0.9-1.4 times the size between C2-E. Again notably, M₄-M₅ appear to be of similar size in C1 (Figure A4.2b).

For both *P. burbidgei* and *P. brachyotis*, there was an increase in tooth size along the upper rows (Figures 4.6c and e, A4.2c and e). At Stage A *P. burbidgei* dP²s were 11 mm², increasing up to 12 mm² M¹s. For stages C-E, from M¹ to M⁴ there was an increase from 10 to 20 mm² (Figure 4.6c), similar to the size ranges seen in the nabarlek. *Petrogale burbidgei* lower teeth shared a similar size pattern, with a range of 5 mm² dP₂s to 15 mm² M₄s from Stage A-E (Figure A4.2c). *Petrogale brachyotis* exhibits similar size patterns, but with much larger tooth sizes (Figure 4.6e). At stage B in the uppers, size increases from 15 mm² at dP² to 20 mm² at M¹. From stage C-E, size increases from ~20 to 45 mm² on average between M¹ and M⁴. *Petrogale brachyotis* lower teeth were of similar sizes, with ranges from 8 to 15 mm² from the dP₂ to M₁ at Stage B, and ~15 to 40 mm² from M₁ to M₄ from stage C-E (Figure A4.2e).

For tooth size ratios, *P. burbidgei* exhibited a similar pattern between all Stages (A-E), where size increased from 0.9 for dP²s, to 1.8 for M⁴s (Figure 4.6d). This differs from the nabarlek ratio pattern, in which the dP² is a much smaller size than that of the M¹s (almost half the size 0.5) (Figure 4.6b). The lower teeth of *P. burbidgei* reflect a similar pattern to the uppers, with slightly lower ratios of 0.5 for dP₂s, to 1.7 for M₄s (Figure A4.2d). These ratios overlap more closely with those of the nabarlek lower teeth (Figure A4.2b).

The tooth size ratios of *P. brachyotis* are noticeably different from both the nabarlek and *P. burbidgei* where between the upper dP² and M⁴, ratios increase from 0.7-2.4 times the size

of M¹s (Figure 4.6f). The lowers exhibit an even larger increase in size along the tooth row, where from the dp₂ to M₄, it increases from 0.5 to almost 3.0 times the size of the M₁ (Figure A4.2f).

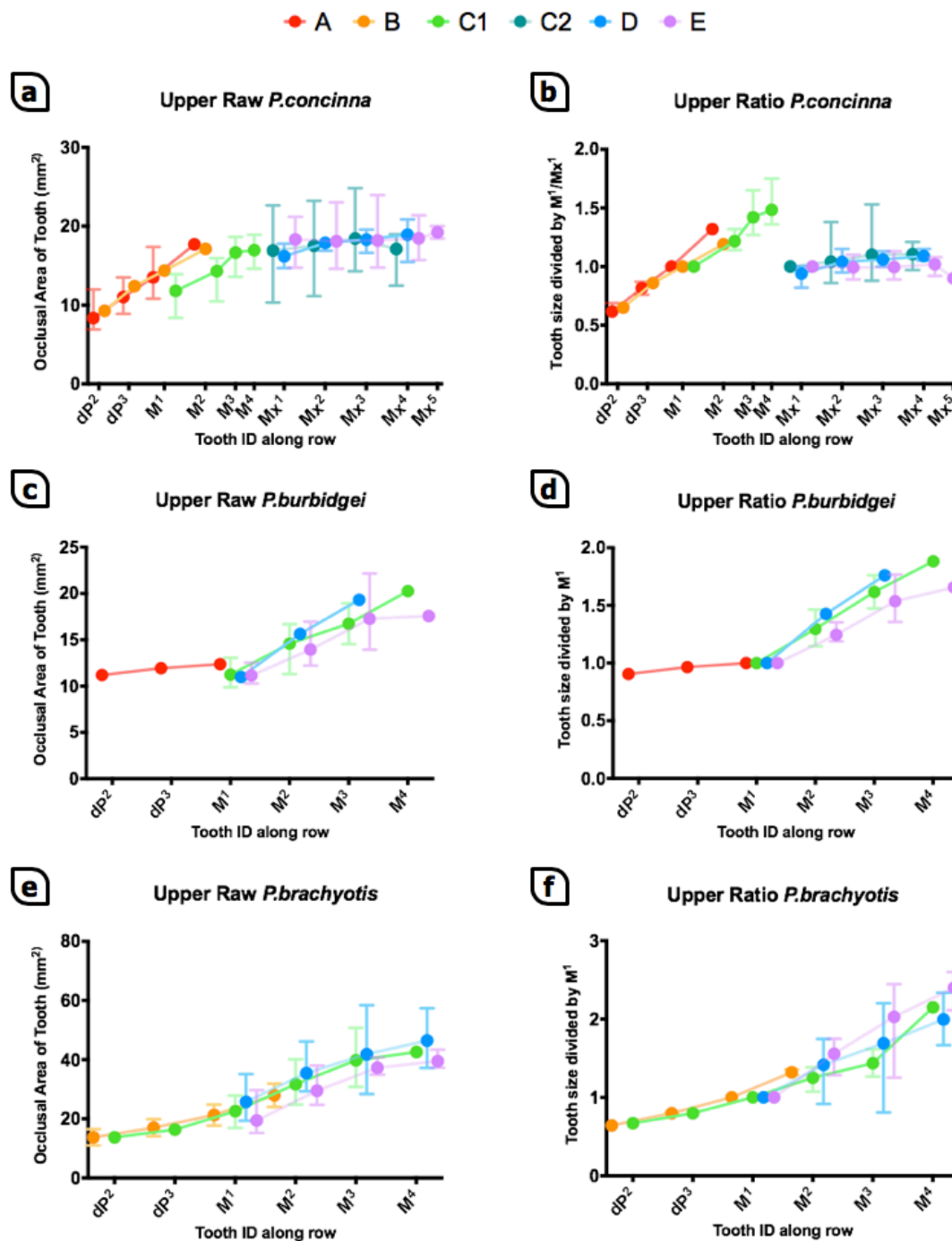


Figure 4.6 *Petrogale* spp. upper tooth size (occlusal area in mm²) (a, c and e) and tooth ratios (tooth size divided by M¹ or Mx¹ size, shown as proportions) (b, d and f) patterns according to age as indicated by the suture closure stage (A-E). Whiskers represent range (min-max). Suture stages are colour coded, located above the graphs.

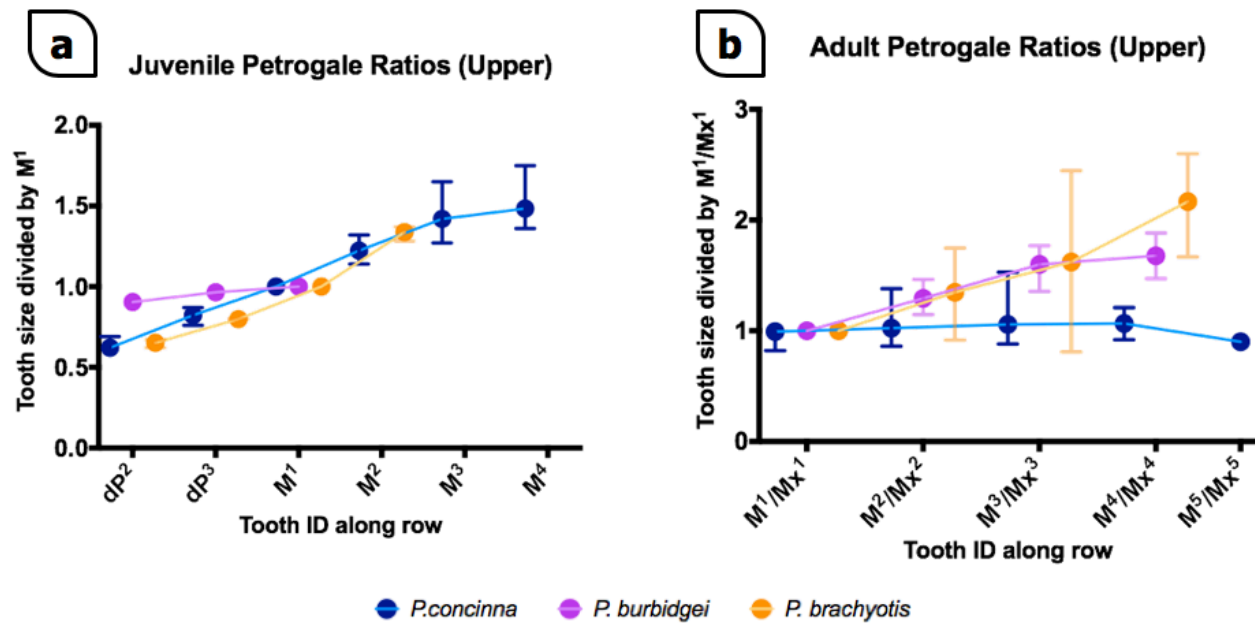


Figure 4.7 *Petrogale* spp. upper tooth ratios (tooth size divided by M^1/Mx^1 size) for a) juveniles (premolars present) and b) adults (molars only). Whiskers represent range (min-max).

When comparing tooth size patterns between juvenile (Stages A-C1) *Petrogale* spp., all three species exhibited similar tooth sizes, and a linear increase in size along the tooth row (Figure 4.7a). This increase was less sharp within *P. burbidgei*, and there also appeared to be less of a size difference between the M^3 and M^4 in the nabarlek. Among the adults (Stages C2-E), *P. burbidgei* and *P. brachyotis* still exhibit an increase along the tooth row, while *P. concinna* shows a plateauing of tooth size, oscillating around 1.0 times (same size along the row) (Figure 4.7b). We also see that *P. brachyotis* has a much greater increase in size along the row, where at the M^4 position this tooth is 2.2 times the size of the M^1 , as opposed to 1.7 times within *P. burbidgei*. These patterns were similar in the lowers (Figure A4.3) where juveniles of all *Petrogale* spp. had an increase in tooth size, where *P. burbidgei* incline was greater in the lowers (0.5-1.0 times from dp_2 - M_1 , versus 0.8-1.0 in the uppers, See Figure 4.7a, Figure A4.3a). In the adults, the nabarlek exhibited a more uniform pattern, where Mx_1 - Mx_5 had an average of 1.0 times, compared to the other *Petrogale* spp. that had 1.0-1.6 times (*P. burbidgei*) and 1.0-2.2. (*P. brachyotis*) (Figure A4.3b).

4.4 Discussion

4.4.1 Nabarlek Developmental Timing

From skull suture closure, we identified specimens that had lost their deciduous and replacement premolars, but that were still considered juvenile or sub-adult, where tooth eruption patterns alone would not have indicated this. The suture closure timing also provided more detailed information about relative ages than just the skull length or tooth eruption. The skull ceased to grow in length around when the P3 is lost, which we estimate to be between 18-24 months of age, or when the supraoccipito-exoccipital suture is starting to fuse, indicating that skull fusion continues after the permanent premolar has erupted and the skull has completed elongation.

Sutures have been used to refine ages of other mammals such as racoons (Grau *et al.*, 1970), as well as grey wolves (Landon *et al.*, 1998) beyond that of tooth eruption. However, tooth eruption (including molar progression) and head length still are the most commonly used age proxies within macropodid studies (Inns, 1982; Poole *et al.*, 1985, 1991; Johnson and Delean, 1999; Jones *et al.*, 2004; Death and Coulson, 2016). Suture closure would especially be useful for looking at macropodids without molar progression, as age information based on dentition is more limited. A combination of these age proxies would be useful for analysing other species with continuous tooth generation, to see whether their tooth development rates are also accelerated with respect to their ossification when compared to closely related species.

From the captive colony specimens, we determine that the P3 can be lost between 18-24 months (550-730 days), possibly even later. This indicates a large window for the deciduous premolars to be lost and replaced. Large ranges have also been noted in the yellow-footed rock-wallaby (*Petrogale xanthopus*) and the allied rock-wallaby (*Petrogale assimilis*) (Delaney and Marsh, 1995) with age ranges of 480-680 days and 255-550 days, respectively for P3 eruptions. Large age ranges for P3 eruption thus appears to be not uncommon among rock-wallabies, where the nabarlek range seems to be comparable to other species.

We see that the nabarlek has a more rapid tooth development and replacement process when comparing it to other *Petrogale* spp. at the same suture stage (Figure 4.3). The rapid loss of the P3 has been noted before, so much so that previous authors have thought it never to exist (Collett, 1897). This may allow for a higher turnover of molars if the premolars are lost sooner, which has been attributed to blocking molar progression (Sanson 1989). Sanson (1989) also suggested nabarleks have a more rapid rate of molar progression because of the inefficiency of its teeth and greater chewing demand.

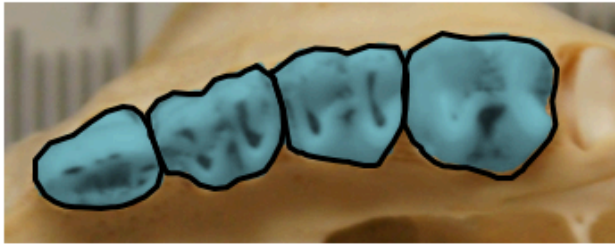
Another possibility is that the suture closure rate in the nabarlek is slower, as the nabarlek has also been shown to have paedomorphic characteristics (Gomes Rodrigues *et al.*, 2017) and perhaps has a delayed maturation rate. The nabarlek has been shown to have the shortest gestation period of other rock-wallabies, with a period of 14-18 days, compared to ~30 days for other species (Taggart *et al.*, 2005). Weaning is also shorter in the nabarlek than other rock-wallabies, with only a 15 day window from when the joey first leaves its pouch to when it is permanently expelled, apparently quickly and sometimes violently (Nelson and Goldstone, 1986). This may be because accelerated tooth development means teeth erupt more quickly, which irritate the mother. In our 5-month old specimen, the deciduous premolars had begun to erupt, which is approximately 150 days, and coincides almost exactly when the young have been recorded to leave the pouch (160-175 days).

4.4.2 Developmental Controls of Tooth Size

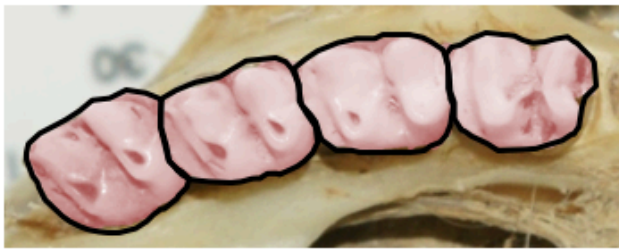
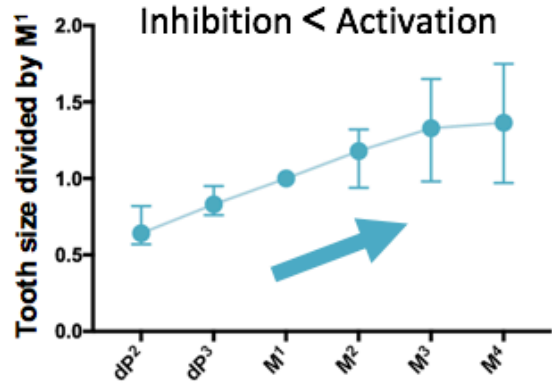
In addition to accelerated tooth development, we have also demonstrated that the nabarlek changes its tooth size pattern from an increase in size along the row, common in those species without tooth replacement, to a uniform tooth size. We propose that the patterns in juvenile nabarleks, and both juveniles and adults in *P. brachyotis* and *P. burbidgei*, are a result of a greater relative level of activation signalling molecules, which encourages the next developing tooth to grow bigger. This would result in an increasing size pattern (Figure 4.8). However, when the nabarlek loses its P3 (from 18-24 months, or at stage C2), the tooth size pattern changes to a uniform size (seemingly between tooth positions M3-M5), which we propose is achieved through a balance of inhibition and activation growth molecules (Figure 4.8).

Interestingly, the sizes of the upper and lower M1s-M3s at Stage C1 for the nabarlek seemed to match almost exactly with the sizes along the row of dP3s-M2s for Stages A and B. All specimens at stage C1 had a P3 present, which is morphologically distinct from the dP3 (See Figure 4.1). However, it seems as if the tooth row sizes for C1 should be shifted one position anteriorly, matching up the dP3 (Stage A/B) with M1 (Stage C). This suggests that the P3 may only replace the dP2 in nabarleks, indicating the tooth at the M1 position in Stage C1 specimens is a dP3, which would explain why these tooth rows match so closely in size. Although macropodids usually replaced both dP2 and dP3 with the P3 (Sanson, 1980), relatives within order Diprotodontia only replace one position (dP3 with P3) such as possums and carnivorous marsupials (Ride, 1956; Archer, 1978; Lockett, 1993).

Another finding of note is that the tooth sizes in *P. brachyotis* begin similarly to the nabarlek and *P. burbidgei*, where its deciduous premolars were within the same ranges. However, the rate of molar growth along the row was much steeper, where the M4 was double the size of those of other species. This may indicate a more extreme version of the growth pattern, where there is a much greater level of activation than inhibition, producing a steeper growth curve, and much larger posterior teeth compared to the anterior teeth. Another possibility is that the tooth buds initiate at a greater distance between each other, which may reduce tooth-tooth inhibition (Kavanagh *et al.*, 2007).



Juvenile teeth



Adult teeth

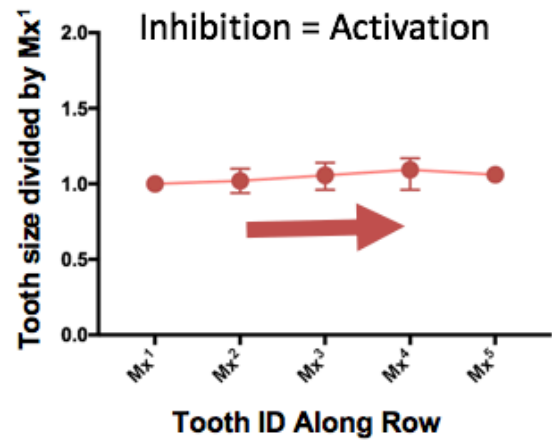


Figure 4.8 The inhibitory cascade model as an explanation for nabarlek tooth size patterns. The juvenile teeth (blue) show a pattern of increasing size, suggesting a greater level of activating over inhibiting growth molecules. In adult teeth (red) of similar size, the activation/inhibition growth molecules may be balanced.

4.5 Conclusions and Future Directions

We propose that the inhibitory cascade model can explain how the nabarlek can change its tooth size pattern, where if activation is greater (or inhibition is reduced), we see an increase in size along the tooth row. Where a balance of activation/inhibition is achieved, the nabarlek can produce teeth of uniform size, as seen in the adults. In addition, molar progression seems to be more rapid in the nabarlek, or possibly skull suture fusion rates are comparatively slower.

While we were able to use a combination of age proxies to look at tooth size patterns through maturation, known ages would provide the most accurate data. While breeding colonies are expensive to establish and run, it could be possible to capture, tag and release nabarleks in the wild. One thing that could also be measured is the number of teeth a nabarlek produces. This could be done by marking a molar with a non-toxic permanent stain, and rechecking the same individual over time to see how quickly the molars are replaced. A capture and release program would not only help build a database with known ages, but also help monitor populations of this rare species (REF).

Another future study to improve our understanding of continuous molar production could be quantifying molar progression rates, which have been done previously in *Macropus eugenii*, *Macropus parma* and *Petrogale penicillata* by measuring the distance of molars from reference points on the skull (Lentle *et al.*, 2003a,b). This could be done on museum skull specimens of nabarleks, or possibly on live individuals, especially if ages are known.

One line of examination that we were not able to achieve but would be highly informative is to visualise nabarlek development in 3D. This data would provide documentation of the replacement pattern, especially whether the P3 replaces only the dP2 and not the dP3. Additionally, molar progression patterns could be visualised, especially the bone remodelling process. Gomes Rodrigues and Šumbera (2015) used microCT to look inside the mandible at bone deposition and resorption of the silvery mole-rat, another species with continuous tooth replacement. They also looked at the mandibular alveolar dental wall

of a pygmy rock-wallaby, but only with photographs of the surface. Therefore, the nabarlek molar production and progression has yet to be studied in three-dimensions.

In addition to morphological-based studies, another avenue to explore would be gene expression patterns within the nabarlek and the species with continuous tooth replacement. At the crucial time points when the nabarlek tooth size patterns seem to change from an increase in size to a uniform size, this would be when genes are expected to be up or down regulated. There is a suite of more than 50 genes that are associated with tooth development, and several have been considered as candidates for the regulation of tooth size, including *Sostdc1*, *Wise*, *BMPs*, *Follistatin* and *Activin A*. Both BMP4 and Activin A have been tested in *in-vitro* tissue cultures, where both were shown to accelerate molar growth (Kavanagh *et al.*, 2007). However, it is still unknown how tooth size is controlled, and how tooth size is scaled for body size.

Another key feature of continuous tooth generation is the delayed degradation of the successional dental lamina, which usually happens after the third molar in placentals (fourth molar in marsupials) is produced in mammals of limited molar replacement (Štembírek *et al.*, 2012). If the additional molars in the nabarlek are produced by the same successional lamina, then there are genes maintaining the successional dental lamina with the ability to produce new teeth, or preventing its apoptosis. *Sox2* is a strong candidate, where it has been shown to be active at successional lamina of both vertically replaced teeth, and the posteriorly added molars (Juuri *et al.* 2013). These genes would be crucial in the enabling the ability of continuous tooth generations.

An obstacle for genetic study of the nabarlek is that material is extremely rare. An alternative could be to experiment with candidate tooth size genes in other marsupial models, such as the tammar wallaby (*Macropus eugenii*) or the fat-tailed dunnart (*Sminthopsis crassicaudata*). While these species do not have continuous molar production, they may have the inherent potential for it, where molar progression and successional lamina degradation could be studied. The regenerative medical potential linked to understanding continuous tooth replacement is vast, including the possibility of one day regrowing human teeth for a more natural replacement, instead of tooth implants or dentures.

4.6 References

- Archer, M. (1978). The nature of the molar-premolar boundary in marsupials and a reinterpretation of the homology of marsupial cheekteeth. *Memoirs of the Queensland Museum*, 18(2), 157-164.
- Churchill, S. (1997). Habitat use, distribution and conservation status of the nabarlek, *Petrogale concinna*, and sympatric rock-dwelling mammals, in the Northern Territory. *Australian Mammalogy*, 19, 297-308.
- Collett, R. (1897). 2. On a Collection of Mammals from North and North-west Australia. *Journal of Zoology*, 65(2), 317-336.
- Death, C., & Coulson, G. (2016). A method for age estimation in the swamp wallaby (*Wallabia bicolor*). *Australian mammalogy*, 38(2), 246-248.
- Delaney, R., & Marsh, H. (1995). Estimating the age of wild rock-wallabies by dental radiography: a basis for quantifying the age structure of a discrete colony of *Petrogale assimilis*. *Wildlife Research*, 22(5), 547-559.
- Evans, A. R., Daly, E. S., Catlett, K. K., Paul, K. S., King, S. J., Skinner, M. M., ... & Jernvall, J. (2016). A simple rule governs the evolution and development of hominin tooth size. *Nature*, 530(7591), 477.
- Goldstone, A. D., & Nelson, J. E. (1986). Aggressive-Behavior in 2 Female *Peradorcas-Concinna* (Macropodidae) and Its Relation to Estrus. *Wildlife Research*, 13(3), 375-385.
- Gomes Rodrigues, H., Marangoni, P., Šumbera, R., Tafforeau, P., Wendelen, W., & Viriot, L. (2011). Continuous dental replacement in a hyper-chisel tooth digging rodent. *Proceedings of the National Academy of Sciences*, 108(42), 17355-17359.
- Gomes Rodrigues, H., Hautier, L., & Evans, A. R. (2017). Convergent Traits in Mammals Associated with Divergent Behaviors: the Case of the Continuous Dental Replacement in Rock-Wallabies and African Mole-Rats. *Journal of Mammalian Evolution*, 24(3), 261-274.
- Gomes Rodrigues, H., & Šumbera, R. (2015). Dental peculiarities in the silvery mole-rat: an original model for studying the evolutionary and biological origins of continuous dental generation in mammals. *PeerJ*, 3, e1233.

- Grau, G. A., Sanderson, G. C., & Rogers, J. P. (1970). Age determination of raccoons. *The Journal of Wildlife Management*, 364-372.
- Inns, R. W. (1982). Age determination in the Kangaroo Island wallaby, *Macropus eugenii* (Desmarest). *Wildlife Research*, 9(2), 213-220.
- Jernvall, J., & Thesleff, I. (2000). Reiterative signaling and patterning during mammalian tooth morphogenesis. *Mechanisms of development*, 92(1), 19-29.
- Johnson, P. M., & Delean, J. S. C. (1999). Reproduction in the Proserpine rock-wallaby, *Petrogale persephone* Maynes (Marsupialia: Macropodidae), in captivity, with age estimation and development of pouch young. *Wildlife Research*, 26(5), 631-639.
- Jones, M., Taggart, D., & Temple-Smith, P. (2004). Age determination and growth in wild *Petrogale lateralis pearsoni* and captive *Petrogale lateralis* 'MacDonnell Ranges race'. *Australian Journal of Zoology*, 52(4), 447-461.
- Juuri, E., Jussila, M., Seidel, K., Holmes, S., Wu, P., Richman, J., ... & Klein, O. (2013). *Sox2* marks epithelial competence to generate teeth in mammals and reptiles. *Development*, 140(7), 1424-1432.
- Kavanagh, K. D., Evans, A. R., & Jernvall, J. (2007). Predicting evolutionary patterns of mammalian teeth from development. *Nature*, 449(7161), 427.
- Landon, D. B., Waite, C. A., Peterson, R. O., & Mech, L. D. (1998). Evaluation of age determination techniques for gray wolves. *The Journal of wildlife management*, 674-682.
- Luckett, W. P. (1993). An ontogenetic assessment of dental homologies in therian mammals. In *Mammal phylogeny* (pp. 182-204). Springer, New York, NY.
- Murphy, C. R., & Smith, J. R. (1970). Age determination of pouch young and juvenile Kangaroo Island wallabies. *Trans. R. Soc. S. Aust*, 94, 15-20.
- Nelson, J. E., & Goldstone, A. (1986). Reproduction in *Peradorcas-Concinna* (Marsupialia, Macropodidae). *Wildlife Research*, 13(4), 501-505.
- Poole, W. E., Merchant, J. C., Carpenter, S. M., & Calaby, J. H. (1985). Reproduction, Growth and Age Determination in the Yellow Footed Rock Wallaby *Petrogale xanthopus* Gray, in Captivity. *Wildlife Research*, 12(2), 127-136.

- Poole, W. E., Simms, N. G., Wood, J. T., & Luboloa, M. (1991). Tables for age determination of the Kangaroo Island tammar wallaby (*Macropus eugenii*), from body measurements (No. 32). Technical Memorandum.
- Potter, S., Bragg, J. G., Blom, M. P., Deakin, J. E., Kirkpatrick, M., Eldridge, M. D., & Moritz, C. (2017). Chromosomal speciation in the genomics era: Disentangling phylogenetic evolution of rock-wallabies. *Frontiers in genetics*, 8, 10.
- Rager, L., Hautier, L., Forasiepi, A., Goswami, A., & Sánchez-Villagra, M. R. (2014). Timing of cranial suture closure in placental mammals: phylogenetic patterns, intraspecific variation, and comparison with marsupials. *Journal of Morphology*, 275(2), 125-140.
- Ride, W. D. L. (1956). The affinities of *Burramys parvus* Broom a fossil phalangeroid marsupial. *Journal of Zoology*, 127(3), 413-429.
- Sanson, G. (1980). The morphology and occlusion of the molariform cheek teeth in some Macropodinae (Marsupialia: Macropodidae). *Australian Journal of Zoology*, 28(3), 341-365.
- Sanson, G. D. (1989). Morphological adaptations of teeth to diets and feeding in the
- Sanson, G. D., Nelson, J. E., & Fell, P. (1985). Ecology of *Peradorcas concinna* in Arnhemland in a wet and a dry season. In *Proceedings of the Ecological Society of Australia* (Vol. 13, pp. 69-72).
- Schindelin, J., Arganda-Carreras, I., Frise, E., Kaynig, V., Longair, M., Pietzsch, T., ... & Tinevez, J. Y. (2012). Fiji: an open-source platform for biological-image analysis. *Nature methods*, 9(7), 676.
- Štembírek, J., Buchtová, M., Král, T., Matalová, E., Lozanoff, S., & Míšek, I. (2010). Early morphogenesis of heterodont dentition in minipigs. *European journal of oral sciences*, 118(6), 547-558.
- Taggart, D. A., Schultz, D., White, C., Whitehead, P., Underwood, G., & Phillips, K. (2005). Cross-fostering, growth and reproductive studies in the brush-tailed rock-wallaby, *Petrogale penicillata* (Marsupialia: Macropodidae): efforts to accelerate breeding in a threatened marsupial species. *Australian Journal of Zoology*, 53(5), 313-323.
- Tate, G. H. H. (1948). Studies on the anatomy and phylogeny of the Macropodidae (Marsupialia) (No. 59). American Museum of Natural History.

Fall seven times and
stand up eight.

七転び八起き

- Japanese proverb

Chapter 5

Patterns of tooth shape development and the evolution of the anteroconid in murid rodents.

ABSTRACT

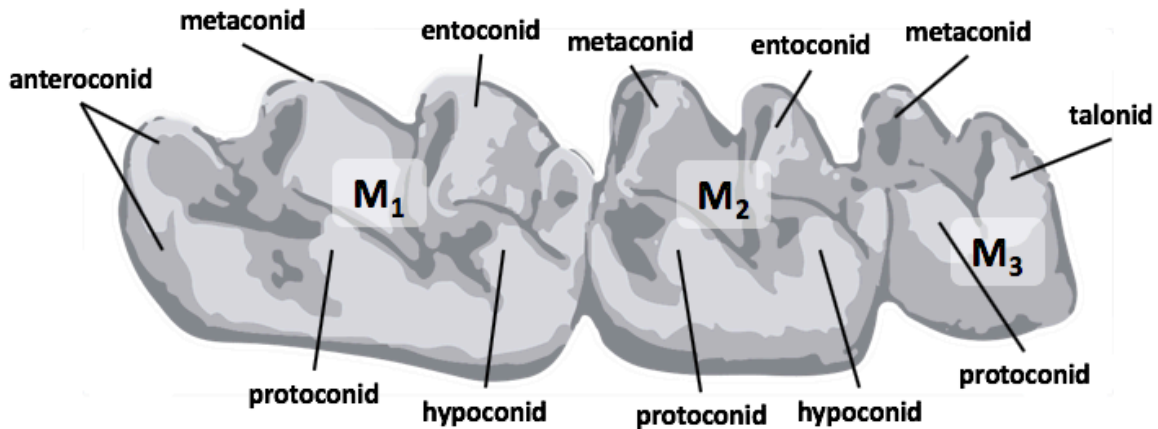
The anteroconid (an anterior cusp on the first molar) first appeared in the murid rodent fossil record around 55 million years ago, at the same time when the sole premolar was lost. One hypothesis has been that the premolar bud merged with the M1 bud to form an additional cusp; this concept is known as concrescence. However, to date, there has been no evidence of the concrescence of two tooth buds. Here we propose an alternative, that the inhibitory cascade model can explain the appearance of the anteroconid. Preliminary data have shown that tooth shape in mice may be influenced by the balance of inhibition/activation signals. This implies that there is a disparity between the potential and final shape of a tooth. Our aim was to experiment with inhibition on cultured tooth samples to unlock the potential of tooth shape. We experimented with cultures of transplanted molars of differing developmental stages to pinpoint key times of shape determination. We found that tooth shape complexity increased when inhibition was reduced. This supports our hypothesis that the loss of the premolar reduced inhibitory pressures on the M1, allowing it to grow larger and more complex. This has significant implications for tooth shape diversification and evolution in all vertebrates.

5.1 Introduction

The dentition of modern mammals not only exemplifies a reduction in the number of teeth and tooth generations from their evolutionary ancestors, but an increase in tooth complexity in the form of multi-cusped teeth (Jernvall, 1995). Where most modern placentals and marsupials now have a maximum number of 4 or 3 premolars and 3 or 4 molars in each dental quadrat respectively (Ziegler, 1997), the dentition of rodents and other Glires are further reduced: lagomorphs (e.g. rabbits) have only two premolars left, while squirrels have only one (Luckett and Hartenberger, 1993). Mice have lost all teeth but one incisor and three molars, with a large diastema (gap) in between the two tooth classes (Peterková *et al.*, 1993). Functional premolars were recorded lost in murid rodents, such as the mouse, 55 million years ago (Viriot *et al.*, 2002). However, in developmental studies, it has been reported that there are still vestigial tooth buds (named MS and R2) that initiate anterior to the front-most molar (M1). These potential tooth germs are possibly remnants of these premolars once lost (Prochazka *et al.* 2010).

In the same palaeontological timeframe that we see the premolars disappear and the diastema enlarge in the murid rodent fossil record (the Eocene), we also see the M1 develop an additional anterior eminence (Viriot *et al.*, 2002) (Figure 5.1). Known as the anteroconid, this structure is thought to be homologous in two rodent superfamilies, Muroidea and Dipodoidea, and is used as a phylogenetically informative trait in rodent evolution studies (Lazzari *et al.*, 2008; Gomes Rodrigues *et al.*, 2011). The development of this and other cusps is also of importance to developmental biologists for identifying molecular pathways behind the evolutionary transitions of ancestral to modern states (Jernvall *et al.*, 2000; Harjunmaa *et al.* 2014).

Mus musculus (wildtype)



Tribosphenomys minutus

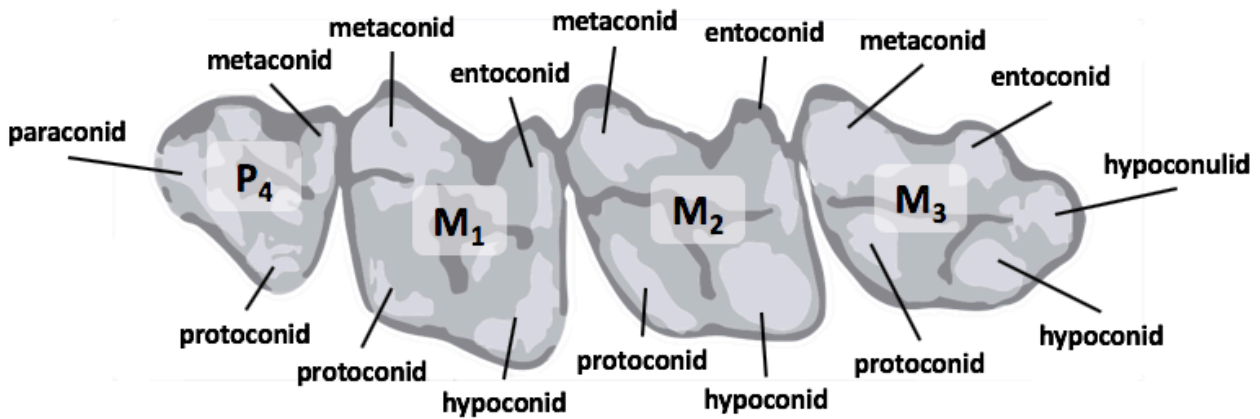


Figure 5.1 Cusp patterning in the modern-day mouse *Mus musculus* (wildtype) and 55 myo (million year old) fossil murid *Tribosphenomys minutus*. M1 in *Mus musculus* has developed an additional cusp, the anteroconid, and has lost the P4 entirely. Viewed from buccal side, where left is anterior, and right is posterior. Modified from Harjunmaa *et al.* 2012.

Several hypotheses of how the anteroconid appeared have been proposed, each relating to theories on the evolution of multi-cusped teeth in mammals from a single-cusped ancestor. The Cope-Osborn theory (Osborn, 1907) suggests multi-cusped teeth were gained via the differentiation of a single primitive cone (major cusp), which formed additional cusps arising as surrounding buds. Evidence of this concept has been well-documented, where single cusped teeth only have one tooth signalling centre, known as the primary enamel knot, while in multi-cusped teeth, secondary enamel knots appear at the location of each future cusp (Jernvall *et al.*, 1994). *Bmps*, *Fgfs* and *Shh* are genes that associate with the

positioning and timing of the secondary enamel knots (Jernvall and Thesleff, 2000), where gene expression patterns have been shown using both *in-situ* hybridisation studies and fluorescence (in *ShhGFP* mice) (Jernvall and Thesleff, 2012). These studies suggest cusp morphogenesis occurs in line with the Cope-Osborn theory.

An alternative theory is of concrescence, developed by Kukenthal (1891) and Rose (1892). It was proposed that multi-cusped teeth such as molars are the result of the union or “concrescence” of many single cusped teeth, such as those in reptiles and fish. While the Cope-Osborn theory suggests one tooth produces many cusps, the concrescence theory suggests each cusp on a molar represents a single, once-independent, tooth. The concrescence theory lacks empirical support, where the only cases of concrescence have been seen in dentistry, where the cementum of adjacent teeth can fuse, after the tooth roots have formed (Venugopal *et al.*, 2013). Despite the lack of evidence for this theory, concrescence remains a favourable explanation to some for the evolution of the anteroconid.

Viriot *et al.* (2000), Peterková *et al.* (2005), Peterková, Lesot and Peterka (2006) and Prochazka *et al.* (2010) have undertaken several studies on the supposed rudimentary premolar tooth buds and their fates. They have shown that *Shh* signalling centres appear at embryonic day 12.7 (e12.7) and e13.5 until the M1 primary enamel knot signal appears at e14.3 (Prochazka *et al.*, 2010). They identified the earlier two *Shh* signals as representing vestigial tooth buds (named R2 and MS) that belong to premolars once lost in murid rodents. However, they further suggest that the R2 bud (the bud anterior to the M1) is integrated into the M1, attributing its enamel knot to the formation of the M1’s anteroconid, which explains the simultaneous loss of the premolar. Although there is evidence that the proposed buds of R2 and M1 coincide in time and may even be physically close to one another, there is still no evidence for the concrescence of two buds. This also conflicts with the enamel knot patterning shown by Jernvall and Thesleff (2000), particularly because the secondary enamel knots that signal multi-cusped patterning do not appear until after the apoptosis of the primary enamel knot.

An alternative model that could explain the gain of the anteroconid is the Inhibitory Cascade (IC). Mammalian molars have been demonstrated to inhibit the growth of one

another through an interplay of activating and inhibitory molecules. Tissue culture experiments removing the developing M2 tail from the M1 resulted in molars that grew larger and faster than the control (Kavanagh *et al.* 2007). This pattern has already been suggested to explain the case of the anteroconid, where in rodent evolution the gradual reduction and loss of the anterior premolar saw an increase in the size of the M1 (Gomes Rodrigues, *et al.*, 2011; Labonne *et al.* 2012). Labonne *et al.* (2012) noted that the anteroconid develops regardless of the gain or loss of an anterior premolar, where the cusps were still present on the M1 in the company of a reduced premolar (P4). Furthermore, developmental studies show there are multiple mouse mutant or transgenic lines that have both an additional anterior tooth (similar to a primitive premolar) and the anteroconid on the M1 present simultaneously (Kangas *et al.*, 2004; Haara *et al.*, 2012; Harjunmaa *et al.*, 2012). We therefore propose that inhibitory pressure from the premolar affects the shape of the M1, as well as size. We postulate that when the premolar began to be reduced and was eventually lost, that the M1 was released from inhibition and grew larger as well as produced an additional cusp. The P4 may have been lost due to the expansion of the diastema region, which is shown to express signals that repress tooth development (Klein *et al.*, 2006).

To test this hypothesis, we sought to replicate the conditions of a premolar anteriorly to the M1 to see if the growth of the M1 would be inhibited. As wild-type mice do not typically develop premolars, we used a similar-sized molar to mimic the effect of an anterior premolar. In addition to testing our model of the anteroconid development, we wanted to explore additional parameters not tested in the Kavanagh *et al.* (2007) Inhibitory Cascade experiment. We wanted to know whether the inhibitory effect is impacted by tooth orientation, initial tooth size and tooth identity. To answer these questions, we chose to culture an embryonic day 16 (e16) lower M₂ anteriorly to an embryonic day 14 (e14) lower M₁. An e16 M₂ is roughly the same size as an e14 M₁, and of a similar developmental (cap) stage. This would indicate whether: a) the starting size (an M₂ the same size as an M₁), b) orientation (if the M₂ was anterior to the M₁), and c) tooth identity (an M₁ versus an M₂) exhibited differing developmental patterns, and thus contribute towards more detailed framework for the inhibitory cascade model. In addition, this experimental setup would

mimic the ancestral scenario where a tooth develops anteriorly to the M_1 and allow us to test developmental patterns of the anteroconid.

5.2 Materials And Methods

5.2.1. Methods Summary

A pilot study was conducted first at the Institute of Biotechnology, University of Helsinki, Finland, where we dissected lower molar tooth germs from embryos at day 14.5 and 16.5 from mice (See Figure 5.2, Table A5.1) and cultured them *in vitro*. We placed the e16.5 M₂ anteriorly to e14.5 M₁ (using the M₂ tail of the M₁, and M₃ tail of the M₂, as indicators of the distal pole). These were wildtype strain NMRI sourced from the Laboratory Animal Centre, University of Helsinki. Main experiments were then modified from the pilot and conducted at Monash University, Australia, where we used e14 M₁s, and both e16 and e17 mouse embryos (as we were not sure how comparable the mice strains were in developmental timing). These were from the black wildtype mice strain C57BL/6JAsmu (Black 6) sourced from MARP (Monash Animal Research Platform). The tooth germs were excised and cultured in different control and experimental combinations (See Figure 5.2, Tables A5.2-A5.4). Experimental controls were: e14 M₁ cultured alone, e16 M₂ cultured alone (we were unable to culture e17 M₂ alone), and e17 M₂ cultured posteriorly to e17 M₁. Experimental treatments were: e16 or e17 M₂s placed anteriorly (distal end M₂ facing mesial end of M₁) to e14 M₁s; e16 M₂s or e17 M₂ placed posteriorly to an e14 M₁. We used the Trowell method as in Kavanagh *et al.* (2007) and described by Närhi and Thesleff (2010). Tissue was cultured for a minimum of 5 days and up to 2 weeks. Photos were taken daily, and culture media was changed every second day. Final number of cusps were tabulated. The maximum outline areas of the developing tooth buds were measured using Fiji version 2.0.0. (Schindelin *et al.* 2012) in μm^2 . Results were plotted using Graphpad Prism 7. For full details see Supplementary Materials and Methods (Appendix D).

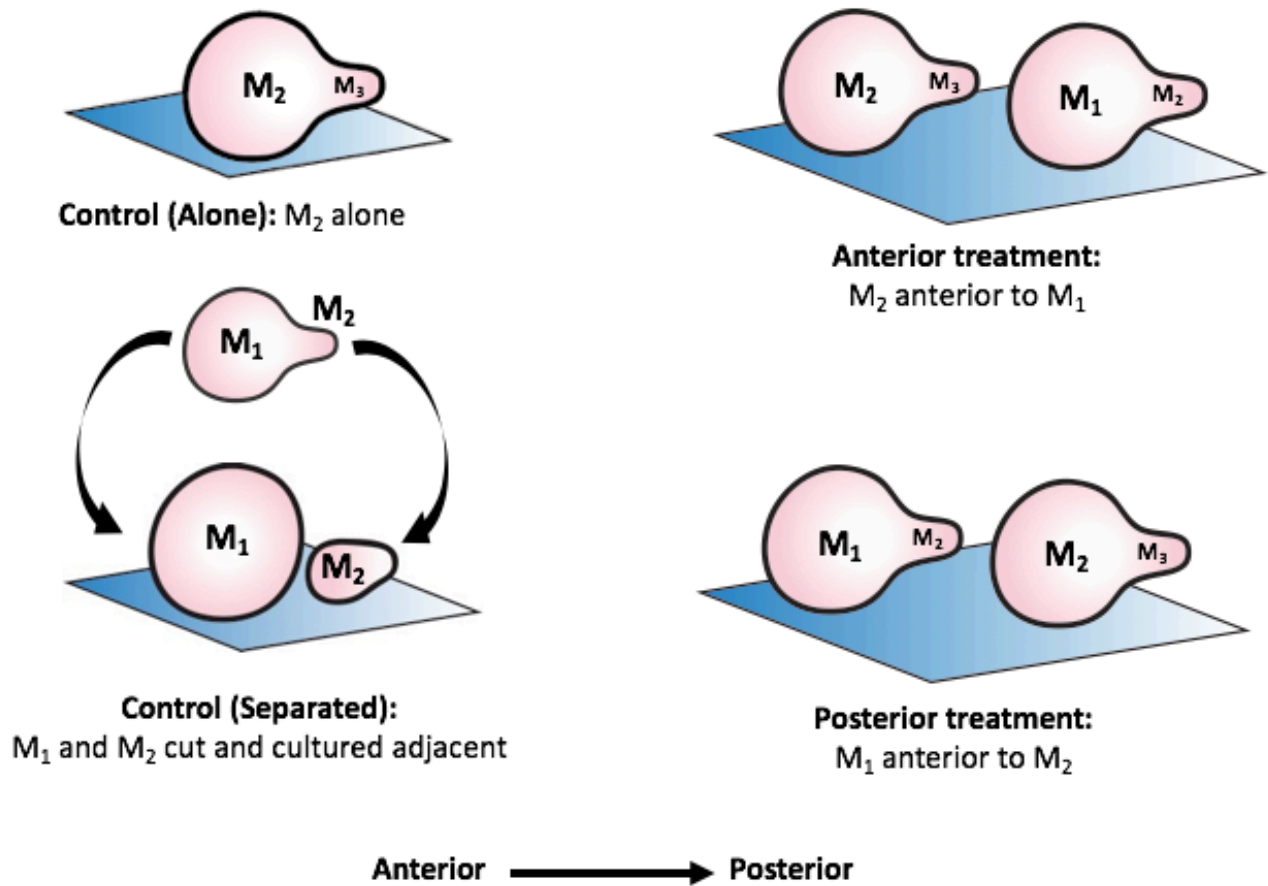


Figure 5.2 Experimental conditions for cut, transplant and culturing of e14 M₁s and e16/e17 M₂s. Control (Alone) e16 M₂ alone; Control (Separated) e17 M₁ and M₂ cut and separated; Anterior treatment, e16/17 M₂ cultured anteriorly to e14 M₁; Posterior treatment, e14 M₁ anterior to e16/e17 M₂. In Anterior treatments the M₂ tail was cut off the M₁ bud.

5.3 Results

5.3.1 Morphology

From the pilot study, we found that all e16.5 M₂s developed an additional cusp (compared to *in vivo*) on the anterior portion of the tooth germ (n = 4), totalling five instead of four, while e14.5 M₁s developed as per *in vivo* (with five cusps also; n = 4) (Figure 5.3, Figure A5.1a, Table A5.1).

From the main set experiments, e16 M₂s cultured posteriorly to e14 M₁s did not develop an additional cusp and exhibited wildtype morphology (four cusps; n = 11) (Figure A5.1b, Table A5.2), nor did the e16 M₂s cultured alone (n = 3; Figure A5.1c, Table A5.3).

The e16 M₂s cultured anteriorly to e14 M₁s also exhibited wildtype morphology (n = 5; Figure A5.1d, Table A5.3).

However, some of the Australian e17 M₂s cultured in front of e14 M₁s did develop an additional anterior cusp (n = 4 out of 15; Figure A5.1e, Table A5.4), as well one M₂ cultured posteriorly to an e17 M₁ (n = 1 out of 16; Figure A5.1f, Table A5.4).

All experimental M₁s that were cultured next to the e16/e17 M₂s developed a typical number of cusps (five) (n = 31; Figures A5.1a-b, d-f, Tables A5.1-A5.4).

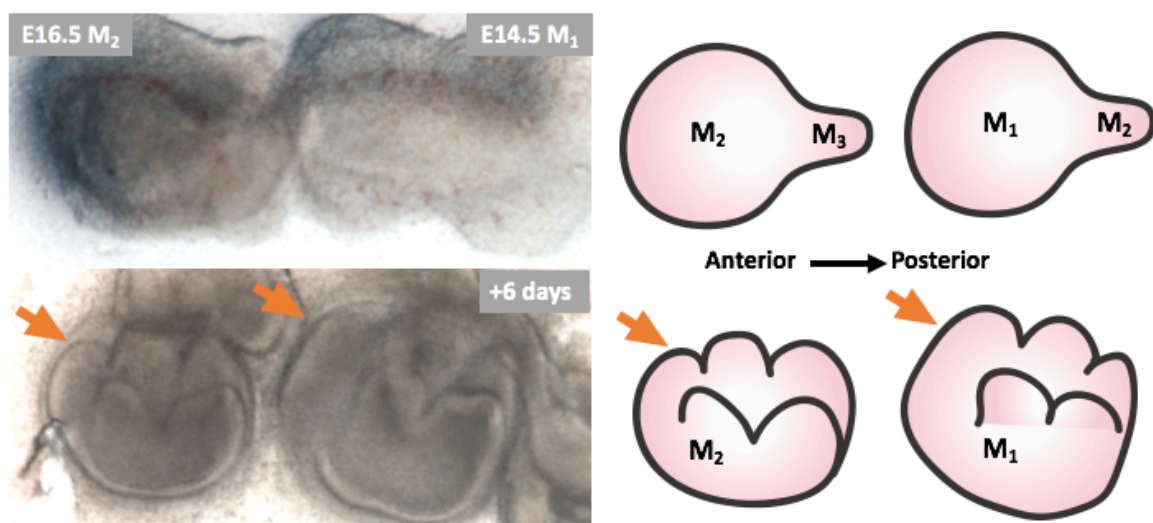


Figure 5.3 Transplant tissue culture photos and schematics of e16.5 M₂ (left) and e14.5 M₂ (right) cultured *in vitro* for 6 days. Arrows indicates fifth anterior cusp on both the e16 M₂ and e14 M₁.

5.3.2 Initial and Final Size

Tooth germs from the pilot study exhibited overlap in size from Day 1 of the culture, but by Day 7 showed slight differences in size, where the e14.5 M₁ was larger, but still overlapped in range of the e16.5 M₂s (Figure A5.2).

From the main body of experimental cultures, where the e16 M₂ was placed anteriorly to the e14 M₁, the M₂s grew smaller on average in size (M=217966 μm², SD=61890) than the control e16 M₂s which were cultured alone (M=254331 μm², SD=91296), though not significantly so (t[4] =2.21, p=0.09). The e14 M₁s cultured in the transplants grew larger on average than the e16 M₂s anterior, but smaller than the e16 M₂s that grew alone. All three conditions began culturing at similar sizes (Figure A5.3).

Cultures of e17 M₂s placed anteriorly to the e14 M₁s began at a similar size to each other and remained close in size by culture day 10. Those e17 M₂s that developed an anteroconid began slightly smaller than the e14 M₁s and ended up at similar sizes. The e17 M₁s cultured anteriorly to e17 M₂s began larger than tooth buds in the other conditions but ended up within the same range at culture day 10. The e17 M₂s cultured posteriorly to its e17 M₁ counterpart began smallest on average of all the tooth germs, and ended up the smallest, more than half the average size of the tooth germs in all other conditions (M=206201 μm², SD=54776 versus M=291833 μm², SD=110084), though not significantly different (t[4] =2.70, p=0.06) (Figure A5.4).

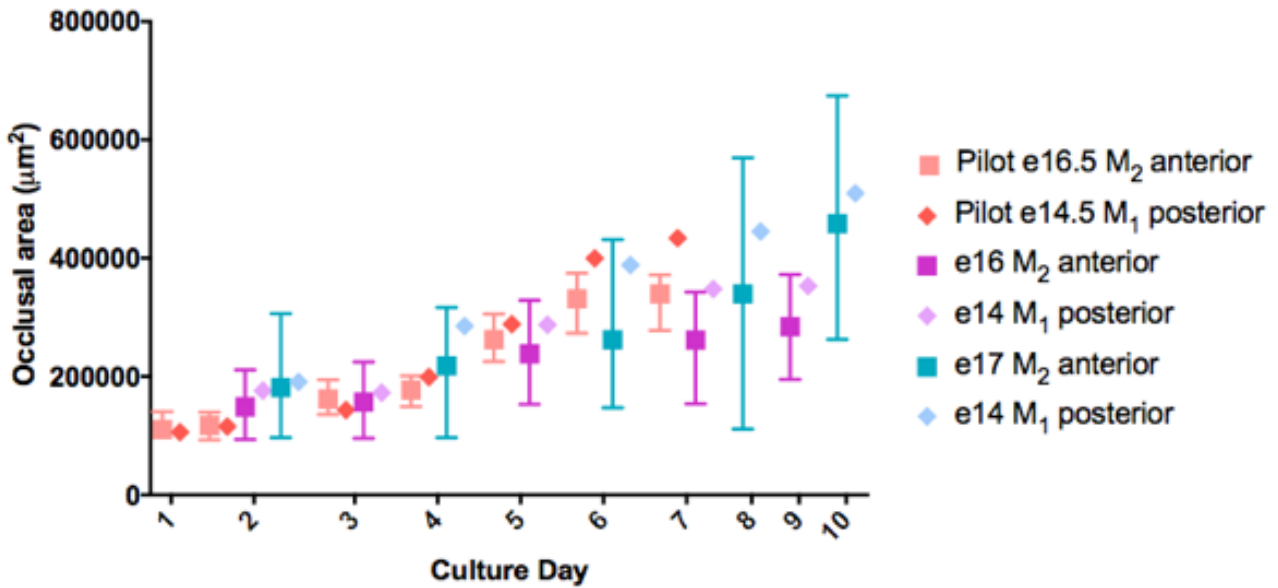


Figure 5.4 Mean maximum outline area (in μm^2) of pilot study cultures e14.5 M₁s and e16.5 M₂s (conducted in December 2013), and e14 M₁s and e16/e17 M₂s (conducted in November 2017). Squares=M₂s, diamonds=M₁s, experimental pairs are colour coded to match. Anterior/posterior indicates orientation during culturing. Whiskers give ranges of measurements (min-max).

When comparing the cultures from all conditions where an M₂ was placed anteriorly to an M₁, we saw that the e16.5 M₂s (strain NMRI) begin smaller than both the e16 and e17 M₂s (strain C57BL6). However, the e16.5 M₂s (strain NMRI) eventually outgrew the e16 M₂s (strain C57BL6). The e17 M₂s remained the largest, especially those teeth that developed an additional cusp. Interestingly, the e14 M₁s that are cultured alongside with the various M₂s remained a similar size and tracked the growth patterns of the M₂ adjacent. In all pairs, the e14 M₁s were always bigger, both initially and finally (Figure 5.4).

5.4 Discussion

5.4.1 Inhibition May Control Tooth Shape

We were able to grow additional anterior cusps on e16.5 and e17 M₂s by culturing them anterior to e14 M₁s (molar buds of similar size). Furthermore, we produced additional cusps on one e17 M₂ separated but cultured posteriorly to its e17 M₁ counterpart. This suggests that the M₂s were released from the inhibition of the M₁ and were able to develop greater tooth complexity and produce an additional cusp. Harjunmaa *et al.* (2012) shows that EDA and Activin A can promote cusp formation, where cusp sizes are regulated by FGF20 (Häärä *et al.* 2012), and SHH seems to inhibit cusp number. Klein *et al.* (2006) showed that Sprouty genes, *Spry2* and *Spry4*, seem responsible for producing the diastema region within mouse jaws, and loss of its function of these genes also produce an additional anterior tooth. These are candidate activator and inhibitor molecules that together affect the number and size of teeth and cusps. We propose that the simple removal of the e16/e17 M₂s away from the M₁ that may be releasing inhibitory molecules, such as SHH, perhaps changes the net amount of activating molecules expressed in the M₂s, such as EDA and FGF20, which could lead to the promotion of cusp formation.

5.4.2 Size not Location Influences Inhibitory Effects

We found that e17 M₂s that were cultured either anteriorly or posteriorly to M₁s could develop additional cusps. However, those M₂s that were cultured posteriorly to e17 M₁s (rather than e14 M₁s) grew a lot smaller. We cannot be certain whether it is the stage of the M₁ (being e17 rather than e14) or being placed anteriorly to it that resulted in a smaller size, as we did not culture an e17 M₁ posteriorly to the e17 M₂. However, the e16 M₂s cultured alone grew larger than those cultured anteriorly to the e14 M₁s. This suggests that location may not be as important, but rather the size of the M₁ and being adjacent (whether anteriorly or posteriorly) to the M₁ that can cause an inhibitory effect.

While we were able to somewhat “free” the e16.5/e17 M₂s from inhibition from the e14 M₁s, we were not able to inhibit the e14 M₁s when attempting to mimic the effect of an

anterior tooth. All M₁s remained larger than their M₂ counterparts, and also all developed the expected “wildtype” number of cusps. It is possible that the M₂s were just not large enough to inhibit the M₁s. Alternatively, it may be that the M₁s possess unique signals that the sequentially produced molars (M₂s and M₃s) may not.

Something that we did not test is whether the distance between cultured e14 M₁s and e16/17 M₂s effected the final size and also number of cusps of the M₂s. This is something that could be tested in the future by conducting experiments of varying but maintained distances. Orientation may have also played a part in the variability of our results, where e14 M₁s and e16/17 M₂s cultured together may not have always been exactly antero-posteriorly oriented. While we used the position of the tail of subsequent teeth (M₂ tail for M₁, M₃ tail for M₂) as the indicator for the posterior region of the developing tooth, more accurate techniques, such as fluorescent markers, could be used to help indicate exactly where the anterior pole of a developing tooth germ would be.

When looking at the results of the main study alone, it seems that size is important if wanting to reduce inhibitory effect of the M₁s, as some e17 M₂s grew additional cusps, while no e16 M₂s did. However, the pilot study using e16.5 M₂s were smaller initially than both the e16/e17 M₂s of the main study, but the e16.5 M₂s produced an additional cusp in all samples. This indicates that although the absolute size of molars may be smaller between the pilot strain (NMRI) and the main study strain (C57BL), the developmental stages may be similar, or even more advanced in the pilot strain. This suggests that timing of the dissection and transplanting of the M₁ and M₂s buds may be crucial to reduce the inhibitory effects during culturing, where e16.5 or older produces additional cusps, but e16 or younger do not. Both e13 and e14 M₂ tails were separated from M₁s and cultured in the Kavanagh *et al.* (2007) experiment, but again no additional cusps were reported to be produced. This result supports our notion that the inhibitory effect may be greater on younger M₂s.

We show that when an M₂ is removed from the inhibitory effects of the M₁, it can develop an additional anterior cusp analogous to the anteroconid unique to the M₁s. We propose this is the same process that happened 55 million years ago, where the loss of the P₄ led to the M₁s being freed from the premolar inhibition and could develop the additional bi-cuspid

structure (the anteroconid). Whereas Prochazka *et al.* (2010) suggests that the anteroconid of the M1 is the result of concrescence of the premolar and M₁ bud, we show that the M₂ can also develop a similar cusp, without the presence of an additional bud, such as a rudimentary premolar, to fuse with. We propose that the inhibitory cascade model provides a more plausible explanation as to how the anteroconid evolved (Figure 5.5).

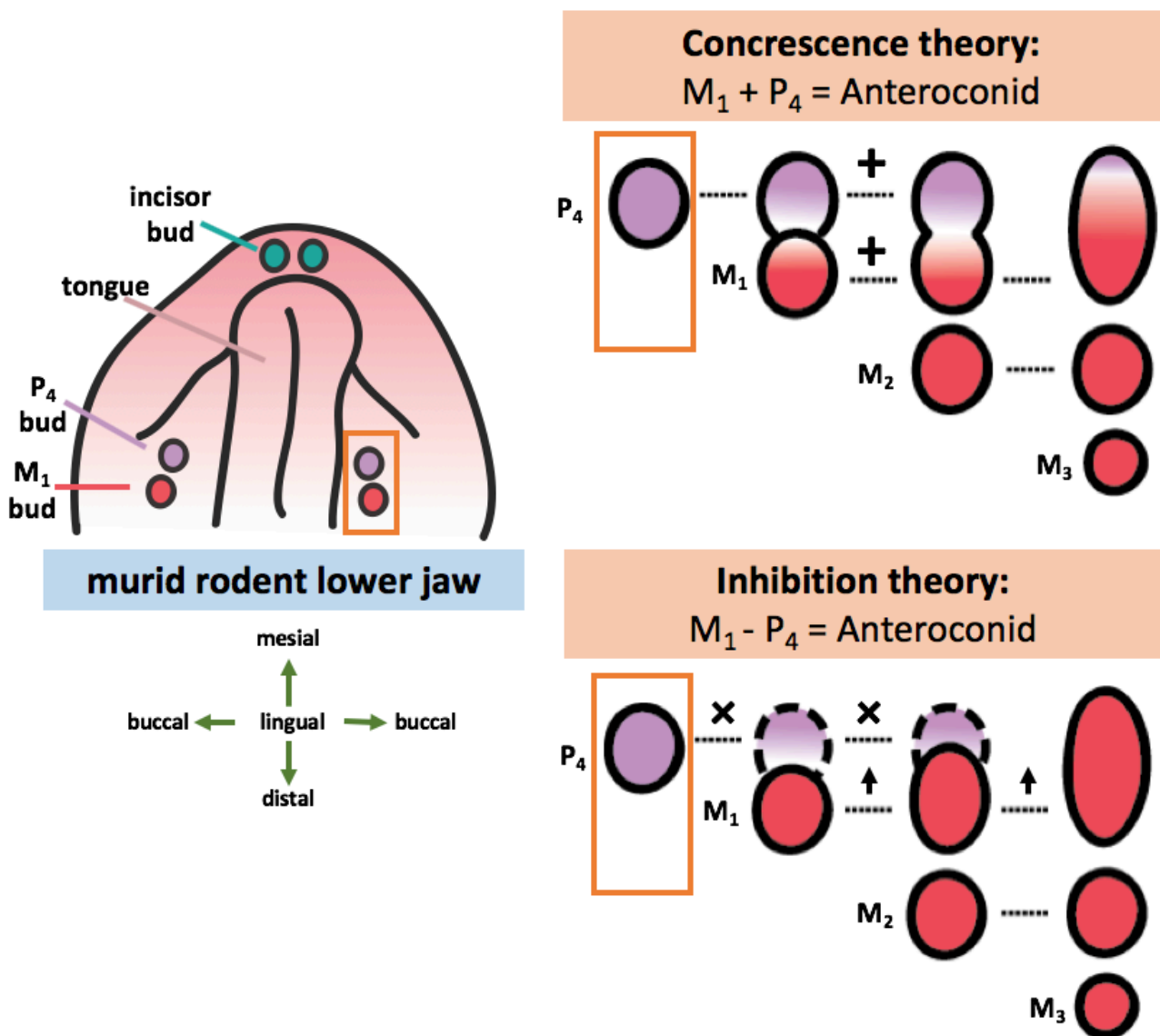


Figure 5.5 Concrescence theory versus our proposed inhibition theory of the evolution of the anteroconid within the murid rodent. The concrescence theory suggests that 55 mya the P₄ bud is integrated into the anterior portion of the M₁, providing the additional cusp. We suggest that the loss of the premolar reduces inhibition on the M₁, allowing it to expand into the region formerly occupied by the premolar bud. Symbols: X = apoptosis; + = integration/concrescence, → = expansion of tooth buds.

Our findings provide continuing support for the Cope-Obsorn theory (1907), where cusps are produced from within the bud, rather than the Kukenthal (1981) and Rose (1892) concrescence theory, which requires another bud to gain the extra cusp. Furthermore, *Fgf4* signalling has been shown in the anteroconid region, as well as the other cusp regions (Cai *et al.*, 2007), indicating it develops in a similar manner and timing to other murid rodent tooth cusps. The MS and R2 *Shh* signalling centres, that Prochazka *et al.* (2010) had identified as vestigial premolar buds, may be signalling centres belonging to the M₁. *Bmp2*, *Bmp4* and *Shh* have been noted to be expressed in the M₁ region at e13 (an early signalling centre) and e14 (the primary enamel knot; Jernvall *et al.*, 1998), suggesting these are the same signalling centres possibly mistaken for vestigial premolar buds. Finally, both developmental (Haara *et al.*, 2012; Harjunmaa *et al.*, 2012) and fossil studies (Gomes Rodrigues *et al.*, 2011; Labonne *et al.*, 2012) show the co-existence of an anterior tooth and the anteroconid cusp on the M₁. These studies alone refute the suggestion of concrescence: if the premolar developed as a separate tooth, then it cannot also be part of the M₁.

5.5 Conclusions

After transplanting molar buds of similar sizes (e14 M₁ and e16/e17 M_{2s}) adjacent, and culturing them *in vitro*, we produced additional cusps in some of the M_{2s}. The appearance of this cusp in our M₂ cultures, with morphology akin to the M₁ anteroconid, suggests that inhibition not only has influence over tooth size (Kavanagh *et al.*, 2007) but also shape. By reducing inhibition placed on the M_{2s}, tooth complexity increases. We suggest this same process is responsible for the evolution of the anteroconid in the M₁ of murid rodents. This has been supported in the fossil record studies by both Gomes Rodrigues *et al.* (2011) and Labonne *et al.* (2012), where they see the gradual loss of the premolar coincide with the gain of the anteroconid.

Our results are also significant in terms of tooth differentiation as it implies that perhaps, at least in the mouse and possibly other mammals, that all molars appear to have a similar shape potential, rather than each individual tooth having a pre-determined shape, and it is merely timing and inhibition that determines how far it fulfils its potential. To confirm this result, further tissue culture experiments should be conducted, with the aim of developing additional cusps in the M₃; such a result will provide strong evidence that all molars may have the potential to reach the same shape. *ShhGFP* mice would provide compelling evidence of the cusp development of these M_{2s} and M_{3s} that could reach the same shape as an M₁, to provide us with a deeper understanding of cusp generation patterns and controlling mechanisms.

5.6 References

- Cai, J., Cho, S. W., Kim, J. Y., Lee, M. J., Cha, Y. G., & Jung, H. S. (2007). Patterning the size and number of tooth and its cusps. *Developmental biology*, 304(2), 499-507.
- Gomes Rodrigues, H., Marangoni, P., Šumbera, R., Tafforeau, P., Wendelen, W., & Viriot, L. (2011). Continuous dental replacement in a hyper-chisel tooth digging rodent. *Proceedings of the National Academy of Sciences*, 108(42), 17355-17359.
- Häärä, O., Harjunmaa, E., Lindfors, P. H., Huh, S. H., Fliniaux, I., Åberg, T., ... & Thesleff, I. (2012). Ectodysplasin regulates activator-inhibitor balance in murine tooth development through Fgf20 signaling. *Development*, 139(17), 3189-3199.
- Harjunmaa, E., Kallonen, A., Voutilainen, M., Hämäläinen, K., Mikkola, M. L., & Jernvall, J. (2012). On the difficulty of increasing dental complexity. *Nature*, 483(7389), 324.
- Harjunmaa, E., Seidel, K., Häkkinen, T., Renvoisé, E., Corfe, I. J., Kallonen, A., ... & Jernvall, J. (2014). Replaying evolutionary transitions from the dental fossil record. *Nature*, 512(7512), 44.
- Jernvall, J., Kettunen, P., Karavanova, I., Martin, L.B., & Thesleff, I. (1994). Evidence for the role of the enamel knot as a control center in mammalian tooth cusp formation: non-dividing cells express growth stimulating *Fgf-4* gene. *International Journal of Developmental Biology*, 38: 463-469.
- Jernvall, J. (1995). Mammalian molar cusp patterns: Developmental mechanisms of diversity. *Acta Zoologica Fennica* 198: 1-61.
- Jernvall, J., Åberg, T., Kettunen, P., Keränen, S., & Thesleff, I. (1998). The life history of an embryonic signaling center: BMP-4 induces p21 and is associated with apoptosis in the mouse tooth enamel knot. *Development* 125: 161-169.
- Jernvall, J., Keränen, S. V., & Thesleff, I. (2000). Evolutionary modification of development in mammalian teeth: quantifying gene expression patterns and topography. *Proceedings of the National Academy of Sciences*, 97(26), 14444-14448.

- Jernvall, J., & Thesleff, I. (2000). Reiterative signaling and patterning during mammalian tooth morphogenesis. *Mechanisms of development*, 92(1), 19-29.
- Jernvall, J., & Thesleff, I. (2012). Tooth shape formation and tooth renewal: evolving with the same signals. *Development*, 139(19), 3487-3497.
- Kangas, A. T., Evans, A. R., Thesleff, I., & Jernvall, J. (2004). Nonindependence of mammalian dental characters. *Nature*, 432(7014), 211.
- Kavanagh, K. D., Evans, A. R., & Jernvall, J. (2007). Predicting evolutionary patterns of mammalian teeth from development. *Nature*, 449(7161), 427.
- Kukenthal, W. (1891). Das Gebiß von Didelphys. *Anat. Anz.*, 6, 658-668.
- Klein, O. D., Minowada, G., Peterková, R., Kangas, A., Benjamin, D. Y., Lesot, H., ... & Martin, G. R. (2006). Sprouty genes control diastema tooth development via bidirectional antagonism of epithelial-mesenchymal FGF signaling. *Developmental cell*, 11(2), 181-190.
- Labonne, G., Laffont, R., Renvoisé, E., Jebrane, A., Labrière, C., Chateau-Smith, C., ... & Montuire, S. (2012). When less means more: evolutionary and developmental hypotheses in rodent molars. *Journal of evolutionary biology*, 25(10), 2102-2111.
- Lazzari, V., Charles, C., Tafforeau, P., Vianey-Liaud, M., Aguilar, J. P., Jaeger, J. J., ... & Viriot, L. (2008). Mosaic convergence of rodent dentitions. *PLoS One*, 3(10), e3607.
- Lockett, W. P., & Hartenberger, J. L. (1993). Monophyly or polyphyly of the order Rodentia: possible conflict between morphological and molecular interpretations. *Journal of Mammalian Evolution*, 1(2), 127-147.
- Närhi, K., & Thesleff, I. (2010). Explant culture of embryonic craniofacial tissues: analyzing effects of signaling molecules on gene expression. In *Oral Biology* (pp. 253-267). Humana Press, Totowa, NJ.
- Osborn, H. F. (1907). *Evolution of mammalian molar teeth* (Vol. 1). Macmillan.
- Peterková, R., Peterka, M., & Ruch, J. V. (1993). Morphometric analysis of potential maxillary diastemal dental anlagen in three strains of mice. *Journal of craniofacial genetics and developmental biology*, 13(3), 213-222.

- Peterková, R., Lesot, H., Viriot, L., & Peterka, M. (2005). The supernumerary cheek tooth in tabby/EDA mice—a reminiscence of the premolar in mouse ancestors. *Archives of oral biology*, 50(2), 219-225.
- Peterková, R., Lesot, H., & Peterka, M. (2006). Phylogenetic memory of developing mammalian dentition. *Journal of Experimental Zoology Part B: Molecular and Developmental Evolution*, 306(3), 234-250.
- Prochazka, J., Pantalacci, S., Churava, S., Rothova, M., Lambert, A., Lesot, H., ... & Peterková, R. (2010). Patterning by heritage in mouse molar row development. *Proceedings of the National Academy of Sciences*, 107(35), 15497-15502.
- Rose, C. (1892). Über die Zahnentwicklung der Beuteltiere. *Anat. Anz.*, 7, 639-650.
- Schindelin, J., Arganda-Carreras, I., Frise, E., Kaynig, V., Longair, M., Pietzsch, T., ... & Tinevez, J. Y. (2012). Fiji: an open-source platform for biological-image analysis. *Nature methods*, 9(7), 676.
- Venugopal, S., Smitha, B. V., & Saurabh, S. P. (2013). Paramolar concrescence and periodontitis. *Journal of Indian Society of Periodontology*, 17(3), 383.
- Viriot, L., Lesot, H., Vonesch, J. L., Ruch, J. V., Peterka, M., & Peterková, R. (2000). The presence of rudimentary odontogenic structures in the mouse embryonic mandible requires reinterpretation of developmental control of first lower molar histomorphogenesis. *The International journal of developmental biology*, 44(2), 233.
- Viriot, L., Peterková, R., Peterka, M., & Lesot, H. (2002). Evolutionary implications of the occurrence of two vestigial tooth germs during early odontogenesis in the mouse lower jaw. *Connective tissue research*, 43(2-3), 129-133.
- Ziegler, A. C. (1971). A theory of the evolution of therian dental formulas and replacement patterns. *The Quarterly Review of Biology*, 46(3), 226-249.

You cannot get through a single day without having an impact on the world around you. What you do makes a difference, and you have to decide what kind of difference you want to make.

- Jane Goodall

Chapter 6

Discussion

6.1 Discussion of Thesis Findings

This thesis has examined developmental patterns which infer controlling mechanisms of tooth size, shape and number of generations, using multiple mammalian model species. Using a three-dimensional diceCT approach, I was able to visualize tooth development at a tissue-level resolution. With this technique, I documented the complete development pattern of the tammar wallaby. I found that tooth replacement is unusual within this macropodid and may be different in other mammals. Using another wallaby, the nabarlek, I measured its tooth size pattern to find that its ability to control its tooth size to create similar sized teeth may allow for continuous tooth generation. Finally, using the laboratory mouse for tissue culture experiments, I found that M_2 s can, on occasion, be freed from inhibitory effects of the M_1 s, so much that they grow more complex, and produce an additional cusp. This has implications for how tooth shape is determined, which may be a combination of inherent potential, and environmental inhibition.

6.1.1 Using Three-Dimensional Modelling Techniques

Traditional techniques of tooth development studies have been 2D histological sections or hand drawn interpretations (Berkovitz 1972b; Archer 1974; Ooë, 1979; van Nievelt and Smith, 2005). Though these provide other investigators a snapshot of developmental processes and have been valuable in contributing to our understanding of tooth development, they are somewhat limited in the information they can provide. These techniques only give a partial view of a three-dimensional picture and can be open to interpretation. When contentious arguments are being presented (Archer, 1978; Lockett, 1993; van Nievelt and Smith, 2005), these types of data (histological sections) cannot be easily shared or verified. For example, Archer (1974) proposes that the marsupial family Dasyuridae may replace their teeth in an unusual way, but only provides hand-drawn reconstructions and single histological section images (rather than a series of sections through the structures). Lockett (1993) rejects Archer's (1974) observations, arguing that Archer simply misinterpreted how the dental lamina develops and is connected to generations of teeth. Without three-dimensional evidence, the reader can argue structures

are hidden or misinterpreted from the images presented. Fortunately, technology has rapidly improved, making 3D-imaging now easy to achieve.

Lugol's Iodine has traditionally been used as a cell-staining agent, but it wasn't until Metcher (2009) combined this stain with microCT scanning that diceCT was born. Metscher (2009) also compared three other common histological stains/fixatives to Lugol's: gallocyenin-chromalum (lower contrast levels), phosphotungstic acid (slower penetration), and osmium tetroxide (superior stain but toxic and ineffective in alcohol-stored tissues). Since Metscher's (2009) application, there has been a surge of studies using this technique to image diverse tissues including mouse hearts (Degenhardt *et al.*, 2010), alligator cartilage (Tsai and Holliday, 2011), bat penises (Herdina *et al.*, 2015), frog tongues (Kleinteich and Gorb, 2015), millipedes (Akkari, Enghoff and Metscher, 2015) and bird brains (Balanoff *et al.*, 2016), just to name a few. The rising popularity of this technique has allowed multiple variables to be trialled, enabling this new community of scientists to collectively optimise this technique.

In **Chapter 2**, I applied diceCT to imaging tooth development, and trialled out several scanning parameters. I was able to visualise single-cell tissue thicknesses but fell short being able to image single cells. Some studies have already used X-ray tomography for sub-cellular imaging (Larabell and Le Gros, 2004; Parkinson *et al.*, 2008), reaching 10s to 100s of nanometres in resolution. However, the field of view for these studies is extremely small, such that the gap between these sub-cellular studies and current diceCT tissue-level studies needs to be bridged. Possibly with the combination of high energy scanners – such as synchrotron sources, and sub-volume scans, such as those that I trialled – cellular resolution may be achieved one day. This would enable details from cellular microscopy, MRI and microCT to be gained all from a single non-destructive scan.

The diceCT technique provides solutions to these problems of ambiguity in tooth development studies. It provides a detailed 3D view of developing structures. The diceCT technique is also useful for simultaneously imaging both unmineralised and mineralised tissues, making it ideal for imaging tooth development. This technology allows us to produce 3D models, essentially digitising a species' morphology, which can be digitally shared to other researchers around the world. This enables the evidence that one author

uses, to be confirmed or challenged by others, strengthening the scientific rigour of these studies. This process of sharing can be viewed as having the same advantages that publishing a DNA sequence on GenBank can have, which can be confirmed by others, and also analysed in alternative ways, maximising the potential of the data. In fact, this open-access of knowledge has recently been proposed to be made mandatory for morphological data – in the form of publishing three-dimensional digital data, to be verified, reproduced and reused (Davies *et al.*, 2017).

Furthermore, if the effects of Lugol's Iodine staining are tested and found to have negligible damaging effects, this technique could be used to scan rare museum specimens, such as the recently-extinct Tasmanian tiger (*Thylacinus cynocephalus*), to provide a 3D morphological encyclopedia to share digitally for countless studies, making the most of these specimens. As the genotype of a species is shared via GenBank, diceCT will allow the phenotype, in the form of 3D digital data, to be collectively analysed and appreciated.

6.1.2. Tooth Replacement in Mammals

Using the diceCT technique described above, I sought to document macropodid tooth development in three-dimensions and shed light on replacement patterns within mammals. In a comprehensive review of mammalian tooth replacement by Lockett (1993), he concluded that the mammal species in his study conformed to a pattern of producing replacement teeth from successional lamina that developed lingually from the tooth to be replaced. He proposed other mammals also follow this generalised pattern. However, my thesis shows several exceptions this.

In **Chapter 3** I found that in the tammar wallaby, permanent teeth develop in a variety of ways, where the successor is lingually from the successional dental lamina, or directly from the primary dental lamina. I find that the functional adult dentition is a composite of unreplaced first generation teeth and second-generation teeth that develop from the successional dental lamina, usually lingual to the predecessor. Marsupials are exceptional compared to other mammals, where they only replace their deciduous premolars (dP2 and dP3) with one adult premolar (P3). When I began to compare my results to other species, I

found that not only do other marsupials seem to deviate from Lockett's (1993) convention, but some placentals do also.

Mammalian Incisor Generations

I found that the upper tammar incisors were made of successional teeth (I^1 - I^3) with an unerupted vestigial first generation (dI^1 - dI^3). This development is considered typical for marsupials, where the first-generation incisors and canines undergo limited developmental progress and never erupt while the functional dentition consist of erupted second-generation teeth (Lockett 1993).

In the lower teeth, I saw a pair at the first locus (dI_1 and I_1), which both develop and mineralise to an extent, but neither erupt. I also saw a potential incisor bud at the second locus (dI_2). Kirkpatrick (1978) saw this same structure in a study on *Macropus giganteus* and denoted it as accessory lamina rather than a tooth bud. However, I saw in our histological sections that there was a separate strand of primary dental lamina, and clear cellular arrangement of a distinct tooth bud (Figure 3.5).

The only functional lower incisor (I call I_3) was also the successor to a vestigial primary tooth (dI_3), which appeared briefly. The lower functional incisor is of particular interest as it is the defining characteristic for the largest marsupial Order, Diprotodontia, comprising of 125 living species (Meredith *et al.*, 2009), including the iconic Australian kangaroos, possums, koalas and wombats. Both Kirkpatrick (1978) and Berkovitz (1968) concur that the only functional lower incisor belongs to the second generation in *Macropus giganteus* and *Setonix brachyurus*, respectively. Neither authors, though, have identified which loci it belonged to. It would be interesting to find whether the generation and locus is consistent for this shared trait.

Herskovitz (1982) stated that the functional incisors and canines in marsupials are unreplaced first generation teeth, which is contrary to Lockett's (1993) proposal. I showed that the tammar wallaby does develop both generations but only the successional generation erupt. However, other mammals do show derivations from the generalised pattern. Popa *et al.*, (2016) showed that the fruitbat (*Eidolon helvum*) incisors (I_1 and I_2) are made up of an unreplaced first generation, indicating no replacement occurs at these

loci. Our study and these examples show that incisor development and replacement in mammals can vary greatly.

Mammalian Premolar Development and Replacement

Another unconventional pattern of the tammar wallaby is that the P3 appears to develop from the primary dental lamina, mesially to the dP3, rather than lingually from it. The orientation is not so surprising, as it has been shown in other mammals that the successional teeth do not always develop lingually. What is more surprising is the origin of the P3 from the primary dental lamina. This is inconsistent with the generalised pattern proposed by Lockett (1993). Furthermore, it indicates that our current definition of replacement teeth is not inclusive of this type of pattern.

With our finding of the unusual tammar wallaby tooth replacement process, I have surveyed the literature to find out the extent unusual patterns in other marsupial species. Looking at *M. eugenii* alone, several other authors have noted the same pattern (Woodward, 1893; Kirkpatrick, 1969; Berkovitz, 1972). Within Macropodidae (kangaroos and wallabies), *Macropus giganteus* (Woodward, 1893), *Lagorchestes conspicillatus*, *Macropus robustus* (Kirkpatrick, 1969), *Petrogale pennicillata* (Woodward, 1893) and *Setonix brachyurus* (Woodward, 1893; Berkovitz, 1966) are just some examples of macropodids that seemed to produce a P3 mesially, and from the primary dental lamina based on camera lucida drawings of sections. However, I found that this was not a Macropodidae-wide trait. I also found several species that followed the conventional pattern, including *Aepyprymnus rufescens*, *Macropus rufogriseus* and *Macropus rufus* (Kirkpatrick, 1969) which developed a P3 from successional lamina, developing lingually from the dP3. Interestingly this does not seem to be a phylogenetically linked trait, because within the same genus there are species following Lockett's or the tammar wallaby' pattern.

Lockett (1993) also concluded that based on the species *Dasyurus viverrinus* that the marsupial family Dasyuridae replace their teeth by his convention and argued that Archer (1974) misinterpreted the dasyurid *Antechinus flavipes*. Archer (1974) had proposed that the P3 develops from the primary dental lamina mesially from the predecessor but Lockett (1993) suggested that what was really observed was the mesially deflected successional

lamina and that the P3 in this dasyurid followed Lockett's (1993) pattern. Looking at Dasyuridae species in the literature I fail to find much clarity on this group: Woodward (1896) report on several species including a *Phascogale* sp., *Dasyurus maculatus* and *Dasyurus viverrinus*, and it appears that the P3 also develops mesially to the dP3. Lockett and Woolley (1996) provide strong evidence of "normal" replacement in *Sminthopsis virginiae*, showing a clear connection between the P3 and the dP3 via successional lamina. However, considering the degree of variation within Macropodidae, even within the same genus, it seems possible that Archer (1974) was correct in his observations of *Antechinus flavipes* exhibiting an alternative developmental pattern.

Peramelidae is another marsupial family that Lockett (1993) had deemed to conform to convention; yet he only looked at *Perameles nasuta* and generalised about the rest of the family. Looking at other peramelid studies it is again unclear, like in the dasyurids, what is happening within the species let alone within the group. Woodward (1893) describes one *Perameles* sp. as replacing its teeth like the tammar but does not name the species. Similarly, Lockett and Hong (1989) studied another *Perameles* sp., concluding they produce a P3 lingually to the dP3 and from successional lamina, but do not name the species. These few examples leave the categorisation of patterns within this group mostly indeterminate.

Looking beyond Australian marsupials, I find a similar lack of conformity within Didelphidae (American opossums). While in *Didelphis marsupialis* Lockett (1993) observes the generalised pattern, *Didelphis virginiana* is shown to produce the P3 mesially from the dP3 (Berkovitz, 1967; 1978). van Nievelt and Smith (2005) report the *Monodelphis domestica* to conform to Lockett's convention, but they also describe the P3 first appearing "As a thickening of the free edge of dental lamina between the dP2 and dP3", which seems to fall more in line with the tammar pattern. This suggests that *Monodelphis* and other didelphids may also replace dentition differently.

These examples are not exhaustive and there is a wealth of literature on tooth development studies in the late 1800s, early 1900s and between the 1950s and 1990s. However, terminology is not consistent, nor is the evidence that is provided sufficient or verifiable. Furthermore, many studies use one token species to represent a group. Lockett (1993) was perhaps justified in proposing this generalised pattern in all marsupial groups,

as, coincidentally, the limited number of species that he used in his review all happened to follow the same pattern. However, I show this can vary between sister taxa and greatly within each marsupial group. Therefore, tooth development studies need to be conducted on a species-based level, with evidence that documents the tooth series through multiple sections, if not in three-dimensions.

Additionally, if I consider outside marsupials, there is a potential for the same assumptions to be made of placental species. Popa *et al.*, (2016) showed that the fruitbat (*Eidolon helvum*) can produce successional premolars mesially and lingually. In addition, Berkovitz (1972a; 1973) proposed that the guinea pig (*Cavia cobaya*) and the ferret (*Mustela putorius*) also produce replacement premolars from the primary dental lamina, as found in the tammar wallaby.

The take-home message is that the currently accepted pattern is not generalisable for all species, and not even for closely related taxonomic groups. Furthermore, these examples highlight that our current definition of a replacement generation is not appropriate for many mammalian species. Lockett (1993) emphasises the epithelial connections between primary dentition and the teeth that replace them is the most important evidence for assessing occurrences of tooth succession and number of generations produced at each locus. Using this same line of evidence, I show that replacement teeth (P3) in the tammar are not true successors of the dP3s. Furthermore, as the unreduced dental formula for marsupials is four premolars (Ziegler, 1971), it could be argued that the P3 occupies the dP3 locus, where we could rename the dP3 to dP4, while dP2 remains unchanged.

A possibility is that the P3 could be the first member of its own tooth family, at a locus between the dP2s and dP3s. Tooth families consist of teeth succeeding each other at a particular locus, where reptiles have multiple teeth at each locus, but mammals have a limited number (usually one or two) (Van der Heyden and Huysseune, 2000). *Zahnreihen*, a successive wave-like patterning, characteristic of reptilian dentition, has been used to also describe the initiation of family members at alternating loci in mammals (Edmund, 1960). Indeed, the tammar premolars appear in an alternating pattern, where the distal dP3 appears first, then the mesial dP2, and finally the P3 in between the two loci. However,

there is no biological explanation for this wave-like patterning and has even been deemed an improbable model, mathematically (Osborn, 1972).

An alternative explanation could be the “Zone of Inhibition” (ZOI) theory (Osborn, 1971), which proposes that new tooth germs emit a sphere of inhibitory “substances”, which create zones of inhibition and prevents new teeth from being initiated in close proximity. As the tooth matures, or if new space is created (such as with jaw lengthening), the inhibitory effect is reduced, and a new tooth can initiate. This model has been used to mathematically test and predict the alternating initiation of tooth germs in the crocodilian *Alligator mississippiensis* (Kulesa *et al.*, 1996). This model also effectively explains the delayed P3 (dP3) development within the tammar wallaby.

This finding suggests that inhibition not only plays a role in size (Kavanagh *et al.* 2007) but may control the timing of tooth initiation, and thus the number of generations that can be produced at each locus. With a combination of testable models, such as the inhibitory cascade and techniques such as diceCT, more comprehensive and verifiable studies of mammal tooth development can be undertaken. We may one day be able to uncover the controlling factors of the development of replacement dentition and potentially resolve tooth homologies between divergent mammalian groups, both living and in the fossil record.

6.1.3 Continuous Tooth Generation

From describing the limited tooth replacement in the tammar, I then explored continuous tooth production in the nabarlek, and how tooth size patterning may allow this ability. Mammals have been shown to follow linear tooth size patterns, where teeth along the row either increase, decrease or remain the same size (Kavanagh *et al.*, 2007; Evans *et al.*, 2016). Interestingly, non-mammals with multiple tooth generations, such as fish, may change their tooth size pattern over time (Streelman *et al.*, 2003). However, most mammals have limited tooth generations which poses an evolutionary and developmental gap between living species and ancestral species that had continuous tooth replacement. The nabarlek wallaby, with its continuous molar generation, allows us the opportunity to

learn more about mammalian tooth generation patterns during development, how this trait may have been lost in the past, and how it was regained.

In **Chapter 4** I measured the tooth sizes of nabarleks to determine whether tooth size patterns change through age, and whether it is conducive to continuous tooth generation. I found that the teeth of juvenile nabarleks show an increase in tooth size pattern, while tooth replacement in adults leads to pattern of similar size. This suggests that tooth size signalling in the nabarlek changes to produce similar sized teeth, enabling additional molars to fit, which wouldn't be possible if its teeth continued to increase in size.

There are only four other mammalian species that can continuously replace their molars: the silvery mole rat (*Heliophobius argenteocinereus*) and three species of manatee (*Tricheschus inunguis*, *Tricheschus manatus* and *Tricheschus senegalensis*). Gomes Rodrigues and Šumbera (2015) looked at *Heliophobius* from embryo to 9 years old. It appears from their study (indicated by figure scalebars) that the 2-month old *Heliophobius* had an decreasing tooth size pattern (anteriorly-posteriorly), which is the opposite to the tammar. The 2-year old specimen appears to exhibit an increase in size along the tooth row, while the scan of the 9-year old specimen appears to have molars of the same size. This suggests that perhaps the silvery-mole rat tooth shifts its tooth size patterns from juvenile to adult, from a changing tooth size to a stabilised size pattern. As for the *Tricheschus* spp., observations have been that they begin with smaller premolar and molar teeth, which appear to increase in size (Domning, 1982), where molar sizes seem to plateau after the fourth or fifth tooth position along the row (Domning and Hayek, 1984). This suggests that a uniform adult tooth size pattern is a common adaptation between the phylogenetically disparate nabarlek, mole rat and manatees, that have continuous tooth generation.

Some likely tooth size patterning genes include *Sostdc1*, *Wise*, *BMPs*, *Follistatin* and *Activin A*. Both BMP4 and Activin A have been tested in *in-vitro* tissue cultures, where both were shown to increase posterior molar size (Kavanagh *et al.* 2007). This technique involves using protein-soaked beads, which were placed adjacent to developing tooth buds in culture conditions (*in-vitro*). Häärä *et al.*, (2012) used the same technique to show that Fgf20 is a downstream effector of Eda, where Eda seems to regulate tooth size.

Microarrays are another tool which can be used to show differences in gene expression at different times or in different structures during tooth development (Heikinheimo *et al.*, 2002; James *et al.*, 2006; Pemberton *et al.*, 2007; Oommen *et al.*, 2013). Using techniques such as these, future studies may be able to isolate the genes responsible for regulating tooth size patterns.

Another adaptation that appears common among these special mammals is molar progression, where the teeth move along the jaw like a conveyor belt, and the front most teeth are ejected, while new teeth erupt at the back. Gomes Rodrigues and Šumbera (2015) demonstrate this occurs through mesial drift, where anterior jaw bone is reabsorbed, and posterior bone is deposited, allowing molars to move through the jaw. Without this adaptation, additional replacement teeth would not be able to be made and replaced. An abrasive diet/terrigenous matter may have been the common driving pressure for molar progression to be independently evolved (Domning, 1982; Sanson *et al.*, 1985; Gomes Rodrigues *et al.*, 2011b).

In terms of molecular controls of molar progression, RANKL and OPG (Krane 2005; Boyce and Xing, 2007) are potential proteins that may regulate osteoclast activity (bone resorption), while members of the *TGF- β* superfamily, such as *Bmps*, as well as *Runx2* (Valcourt and Moustakas, 2005) are just a few candidates that may regulate osteoblast activity (bone formation). Further investigation of these genetic pathways may show how molar progression has been acquired in some mammals, particularly those with continuous molar production.

A final key trait that is likely to be shared between these mammals with continuous tooth generation is sustained successional lamina formation. Successional generations develop from this tissue, and in most mammals with limited tooth generation, this degrades after one or two generations. In vertebrates with continuous tooth generation, such as lizards, this successional lamina continues to form and produce new generations of teeth (Handrigan, Leung and Richman, 2010; Juuri *et al.*, 2013). The cycle of successional lamina formation, the balanced tooth size pattern and mechanism of molar progression appears to be the formula the narbelek uses to attain perpetual tooth generation. *Sox2* has been shown to be expressed in active successional lamina formation (Juuri *et al.* 2012). This

gene may be one of many responsible in maintaining the successional lamina in the nabarlek, and fellow mammals with continuous molar generation. It would also be interesting to show whether the same networks that are responsible for molar generation also control lingual tooth replacement in the incisor-premolar loci.

To discover the mechanisms that control this trio of adaptations, comparative studies of these unique species need to be conducted. This includes looking at the developmental patterns of these species, including tissue morphology such as the successional lamina formation, and tooth size patterns, such as those that I conducted on the nabarlek. Analysing the genetic makeup and gene expression patterns may also reveal similarities or differences between these species. These studies could reveal whether these adaptations are convergent and produced through multiple pathways, or whether there are shared ancestral pathways present in all mammals but only reactivated in these few species.

6.1.4 Tooth Shape and Controls of Morphogenesis

From tooth size in the nabarlek, I then investigated controls of tooth shape in the mouse. The evolution of the anteroconid cusp of the mouse M_1 had been proposed to be the result of the concrescence (fusion) of a vestigial premolar bud and the M_1 bud, to create a larger more complex tooth (Prochazka *et al.*, 2010). In **Chapter 5** I tested an alternative hypothesis, that tooth-tooth inhibition was the cause of this additional cusp. I showed that when lower e16.5 and e17 M_2 s were separated from their M_1 counterparts, they could develop an additional cusp similar to the anteroconid. I proposed the separation of the M_2 from the M_1 released inhibitory influences, allowing it to grow more complex. This provides support for our hypothesis that the loss of the premolar had a similar effect, freeing the M_1 to develop the anteroconid, meaning that tooth-tooth signalling not only modulates size, but also shape. Furthermore, this reveals that M_2 s and possibly M_3 s could become more complex, and it is the degree of inhibition which dictates the final morphology.

The reiterative works of Viriot *et al.* (2000), Viriot *et al.* (2002) Peterková *et al.* (2005), Peterková, Lesot and Peterka (2006) and Prochazka *et al.* (2010) that champion the idea of concrescence to explain the appearance of the anteroconid have not yet provided evidence of the two tooth buds fusing together. Furthermore, other authors have cited that the same

signalling centres that Prochazka *et al.*, (2010) labelled as vestigial premolars (MS and R2), are all temporally spaced signals within the M₁ placode (Jernvall *et al.*, 1998). Jernvall *et al.* (1998) noted three pulses of *Bmp4* that signify the induction of the mesenchyme, the induction of the primary enamel knot, and the apoptosis of the enamel knot. This suggest there may no vestigial premolar buds present, at least in the lower jaw of modern mice, casting further doubt on the concrescence model for anteroconid evolution. In addition to developmental studies, examination of the rodent fossil record show that a reduced premolar (P₄) has co-existed with the anteroconid cups on the M₁ (Gomes Rodrigues *et al.*, 2011a; Labonne *et al.*, 2012), demonstrating that the anteroconid forms independently of the P₄ bud.

Our findings also demonstrate that M₂ molars in the mouse appear to have the potential to reach the same size and shape as M₁s, and it may just be the degree of inhibition along a gradient that dictates how much of this potential is fulfilled in the final product. A way to confirm this would be to try and produce a greater cusp number on the M₃s by separating them from M₂s and growing them in cultures. If they too can grow as many cusps as the M₁s, this is strong evidence that all molars in the mouse at least, have the same shape potential.

Tooth-tooth inhibition had been proposed to determine tooth number and tooth shape (number of cusps) in cichlids (Streelman *et al.*, 2003). While the inhibitory cascade pattern has been demonstrated to explain the size patterning of many mammal dentitions (Kavanagh *et al.*, 2007; Polly, 2007; Halliday and Goswami, 2013; Asahara, 2013; Schroer and Wood, 2015; Evans *et al.*, 2016), it has only been considered in part to explain morphological variation, such as the gain of the anteroconid in murid rodents (Labonne *et al.*, 2012).

The idea of a morphological cascade or gradient has been proposed as early as Butler (1939), where he proposed that tooth shape was governed based on morphogenetic fields, each with a unique combination of signals, which produced either incisor, canine or molar-like morphology. This theory suggests that the environment regulates tooth shape. However, molar buds (Glasstone, 1963; Lumsden, 1979) or even cheek tissues without molars initiated yet (e10-e11) (Miller, 1969) can be dissected and cultured in isolation, and

still develop tooth buds with molar-like morphology. This lends support to another theory, the clone model (Osborn, 1978) which proposes that shape signals are intrinsic to each tooth bud and the final shape is predetermined from the moment tooth initiation begins. However, this does not explain how our mouse M₂ was able to gain an additional cusp after initiation, as it appears to break its predetermined design.

A family of genes known as the Odontogenic Homeobox Code are recognised as the main contenders for producing morphological variation between tooth classes (premolars versus molars). Unlike the original three morphological fields proposed by Butler (1939) (incisor, canine and molar), models of Homeobox morphogen fields include at least 12 genes in combination to produce as few as eight overlapping fields (Catón and Tucker, 2009) across the four tooth classes. *Bmp4*, *Msx1-2* may direct incisor formation (Koussoulakou *et al.*, 2009). *BARX1* is shown to be expressed in the premolar region, while *DLX-1* and *-2* (McCollum and Sharpe, 2001), *PITX2* (Tucker and Sharpe, 2004), *PAX9* (Koussoulakou *et al.*, 2009) and *FGFs* (Mitsiadis and Smith, 2006) in the molar region. While these patterns correlate with different tooth morphologies, there have been no genes that have been confirmed as explicit morphogens (Zhao *et al.*, 2007). Some promise is shown, where incisors have been transformed to become molar-like with the addition of *NOGGIN* (Tucker *et al.*, 1998) though others argue this produces a split incisor rather than a multicusped molar (Munne *et al.*, 2010).

In agreement with the authors above, I propose that there are elements of each model which can be used to explain developmental patterns and experimental results that have been observed. I suggest that the future shapes of tooth buds are programmed by morphogens, depending on the location along the jaw they initiate, an element consistent with the Field Theory (Butler, 1939). These morphogens are likely to be in the form of the Homeobox gene fields (Catón and Tucker, 2009) which correlate with different tooth classes. This programming occurs early though, before e12. Once these early morphogens impart instructional signals, the tooth bud then becomes self-regulating for a window of time, where we know that tooth buds (aged e10 - e16) (Osborn and Lumsden, 1978), or even tissues containing future molar sites not yet initiated (Miller, 1969), can be cultured and produced fully realised molars, but do lose this ability after some time (Glasstone,

1952). This is consistent with elements of the Clone model (Osborn, 1978), where tooth buds appear to be prepatterned. The final component, which again contains elements of both the Field and Clone models, is that the final shape and size of the teeth are determined by an inhibitory gradient, such as the inhibitory cascade model suggest. Where the Field model proposes a morphogenetic gradient, and the Clone model suggests tooth-tooth inhibition (Lumsden 1979), the inhibitory cascade embodies elements of both.

Timing is crucial in determining controlling mechanisms of tooth morphogenesis, especially looking at earlier stages to determine any morphogenetic signals are emitted before tooth initiation. Butler (1978) himself states, "We need to know more about processes that precede tooth initiation in the mouse between 8th and 11th days". Lumsden (1979) too emphasise the importance of looking at mouse tooth development 12 days or earlier, such as when crest cells first emerge from neural folds (e8) to e11 when definitive tooth buds begin to appear (Lumsden, 1988).

As much as the mouse is a useful model for determining morphogenetic controls of teeth, they have limited number of tooth classes and no tooth replacement. It would be beneficial for future tooth morphogenesis studies to include non-traditional model organisms such as marsupials like the tammar wallaby (*Macropus eugenii*), fat tailed dunnart (*Sminthopsis crassicaudata*) and gray short-tailed opossum (*Monodelphis domestica*) which are becoming increasingly popular and easier to obtain material for. In addition, using non-mammalian models, such as amphibians (Wake 1980), reptiles (Handrigan and Richman, 2010) and fish (Streelman *et al.*, 2003), that have many more tooth loci, simplified tooth classes and multiple tooth generations can contribute greatly to our understanding of mammalian tooth development.

The inhibitory cascade can explain elements of the two major morphogenetic models, the Clone and the Field, where the final tooth size and shape may be determined by the degree of tooth-tooth inhibition. Using multiple model organisms, and examining pre-initiation genetic signalling, the truths within each of these models may be teased out, to ultimately elucidate how tooth shape is determined.

While it is unclear how tooth morphogenesis is initially programmed in tooth buds, I propose that the inhibitory cascade plays a crucial role in determining the final shape of these organs. Phalanges (Kavanagh *et al.* 2013), limbs and vertebrae (Young *et al.* 2015) have also been shown to follow the IC size patterns. If size is influenced by the IC, then shape may be also. It is therefore possible that morphological patterning of vertebrate anatomy may be controlled partly through inhibition/activation signalling, a process which could also constrain evolutionary trajectories of these structures. From the simple cusp of a mouse molar, to the highly derived wing of a bat, the inhibitory cascade appears to play a significant role in directing element size and shape, and provides a testable framework to study morphological patterning, variation and evolution within modern and fossil vertebrates.

6.2 Conclusions

6.2.1 Inhibitory Cascade Model for Tooth Shape, Size and Number

The inhibitory cascade model represents an integral theme throughout this thesis. It is an elegantly simple model and allowed us a testable framework to identify possible mechanisms behind the diversity of patterns we see within vertebrate dentitions. While patterns of tooth size in mammals has been extensively documented to follow the IC model, I explore and present other elements of tooth development and replacement which are also potentially shaped by tooth-tooth inhibition/activation.

Firstly, tooth-tooth inhibition may delay the initiation of adjacent teeth. This provides an explanation for the delayed initiation of the P3 in the tammar wallaby, which appears between the deciduous premolars at later stages. Tooth initiation in non-mammal vertebrates, such as reptiles, follow an alternating pattern, suggesting this may be a shared ancestral trait. Mammals might have retained aspects of this process, where tooth generation is limited, but we still see delayed initiation, or suppression of growth, for some teeth.

Secondly, a balance of inhibition/activation molecules may also allow for mammals with continuous molar generations to produce teeth of similar size. This would enable subsequent teeth to fit and allow this ability to be maintained. This appears to be a common pattern among the five mammal species that continuously replace molars. Identifying the molecules that regulate tooth size may reveal whether this trait is ancestrally shared, and possibly dormant in other mammals, or whether it has been independently evolved.

Finally, I propose that the inhibitory cascade may also govern the final shape a tooth can reach. I found that by reducing inhibition between teeth (or possibly increasing activation), this allowed for additional cusps to be grown, increasing tooth complexity. This process may also extend beyond tooth morphology, such as limbs and vertebrae shape patterning.

To conclude, I have shown that the IC is likely to play a greater role in tooth patterning than size alone, extending its influence on tooth shape and replacement; actively shaping the formation and evolution of functional dentition within vertebrates.

6.3 References

- Akkari, N., Enghoff, H., & Metscher, B. D. (2015). A new dimension in documenting new species: high-detail imaging for myriapod taxonomy and first 3D cybertype of a new millipede species (Diplopoda, Julida, Julidae). *PloS one*, *10*(8), e0135243.
- Archer, M. (1974). The development of cheek teeth in *Antechinus flavipes* (Marsupialia, Dasyuridae). *Journal of the Royal Society of Western Australia*, *57*, 54-63.
- Archer, M. (1978). The nature of the molar-premolar boundary in marsupials and a reinterpretation of the homology of marsupial cheekteeth. *Memoirs of the Queensland Museum*, *18*(2), 157-164.
- Asahara, M. (2013). Unique inhibitory cascade pattern of molars in canids contributing to their potential to evolutionary plasticity
- Balanoff, A. M., Bever, G. S., Colbert, M. W., Clarke, J. A., Field, D. J., Gignac, P. M., ... & Walsh, S. (2016). Best practices for digitally constructing endocranial casts: examples from birds and their dinosaurian relatives. *Journal of anatomy*, *229*(2), 173-190.
- Berkovitz, B. K. B. (1966). The homology of the premolar teeth in *Setonix brachyurus* (Macropodidae: Marsupialia). *Archives of oral biology*, *11*(12), 1371-IN39.
- Berkovitz, B. K. B. (1967). The dentition of a 25-day pouch-young specimen of *Didelphis virginiana* (Didelphidae: Marsupialia). *Archives of oral biology*, *12*(10), 1211-IN29.
- Berkovitz, B. K. B. (1968). The early development of the incisor teeth of *Setonix brachyurus* (Macropodidae: Marsupialia) with special reference to the prelacteal teeth. *Archives of oral biology*, *13*(2), 171-IN10.
- Berkovitz, B. K. B. (1972a). Ontogeny of tooth replacement in the guinea pig (*Cavia cobaya*). *Archives of oral biology*, *17*(4), 711-IN19.
- Berkovitz, B. K. B. (1972b). Tooth development in *Protemnodon eugenii*. *Journal of dental research*, *51*(5), 1467-1473.
- Berkovitz, B. K. B. (1973). Tooth development in the albino ferret (*Mustela putorius*) with special reference to the permanent carnassial. *Archives of Oral Biology*, *18*(4), 465-471.

- Berkovitz, B. K. B. (1978). Tooth ontogeny in *Didelphis virginiana* (Marsupialia: Didelphidae). *Australian Journal of Zoology*, 26(1), 61-68.
- Boyce, B. F., & Xing, L. (2007). The Rankl/Rank/Opg Pathway. *Current osteoporosis reports*, 5(3), 98-104.
- Butler, P. M. (1939). Studies of the Mammalian Dentition.—Differentiation of the Post-canine Dentition. *Journal of Zoology*, 109(1), 1-36.
- Butler, P. M. (1978). The ontogeny of mammalian heterodonty. *Journal de Biologie buccale*, 6(3), 217.
- Catón, J., & Tucker, A. S. (2009). Current knowledge of tooth development: patterning and mineralization of the murine dentition. *Journal of Anatomy*, 214(4), 502-515.
- Davies, T. G., Rahman, I. A., Lautenschlager, S., Cunningham, J. A., Asher, R. J., Barrett, P. M., ... & Braga, J. (2017). Open data and digital morphology. *Proc. R. Soc. B*, 284(1852), 20170194.
- Degenhardt, K., Wright, A. C., Horng, D., Padmanabhan, A., & Epstein, J. A. (2010). Rapid three-dimensional phenotyping of cardiovascular development in mouse embryos by micro-CT with iodine staining. *Circulation: Cardiovascular Imaging, CIRCIMAGING*-109.
- Domning, D. P. (1982). Evolution of manatees: a speculative history. *Journal of Paleontology*, 599-619.
- Domning, D. P., & Hayek, L. A. (1984). Horizontal tooth replacement in the Amazonian manatee (*Trichechus inunguis*). *Mammalia*, 48(1), 105-128.
- Edmund, A. G. (1960). Tooth replacement phenomena in the lower vertebrates. *R. Ont. Mus., Life Sci. Div., Contr.*, 52, 1-190.
- Evans, A. R., Daly, E. S., Catlett, K. K., Paul, K. S., King, S. J., Skinner, M. M., ... & Jernvall, J. (2016). A simple rule governs the evolution and development of hominin tooth size. *Nature*, 530(7591), 477.
- Glasstone, S. (1952). The development of halved tooth germs. A study in experimental embryology. *Journal of anatomy*, 86(Pt 1), 12.

- Glasstone, S. (1963). Regulative changes in tooth germs grown in tissue culture. *Journal of dental research*, 42(6), 1364-1368.
- Gomes Rodrigues, H., Charles, C., Marivaux, L., Vianey-Liaud, M., & Viriot, L. (2011a). Evolutionary and developmental dynamics of the dentition in Muroidea and Dipodoidea (Rodentia, Mammalia). *Evolution & development*, 13(4), 361-369.
- Gomes Rodrigues, H., Marangoni, P., Šumbera, R., Tafforeau, P., Wendelen, W., & Viriot, L. (2011b). Continuous dental replacement in a hyper-chisel tooth digging rodent. *Proceedings of the National Academy of Sciences*, 108(42), 17355-17359.
- Gomes Rodrigues, H., & Šumbera, R. (2015). Dental peculiarities in the silvery mole-rat: an original model for studying the evolutionary and biological origins of continuous dental generation in mammals. *PeerJ*, 3, e1233.
- Häärä, O., Harjunmaa, E., Lindfors, P. H., Huh, S. H., Fliniaux, I., Åberg, T., ... & Thesleff, I. (2012). Ectodysplasin regulates activator-inhibitor balance in murine tooth development through Fgf20 signaling. *Development*, dev-079558.
- Halliday, T. J., & Goswami, A. (2013). Testing the inhibitory cascade model in Mesozoic and Cenozoic mammaliaforms. *BMC evolutionary biology*, 13(1), 79.
- Handrigan, G. R., Leung, K. J., & Richman, J. M. (2010). Identification of putative dental epithelial stem cells in a lizard with life-long tooth replacement. *Development*, 137(21), 3545-3549.
- Handrigan, G. R., & Richman, J. M. (2010). Autocrine and paracrine Shh signaling are necessary for tooth morphogenesis, but not tooth replacement in snakes and lizards (Squamata). *Developmental biology*, 337(1), 171-186.
- Herdina, A. N., Kelly, D. A., Jahelková, H., Lina, P. H., Horáček, I., & Metscher, B. D. (2015). Testing hypotheses of bat baculum function with 3D models derived from microCT. *Journal of anatomy*, 226(3), 229-235.
- Heikinheimo, K., Jee, K. J., Niini, T., Aalto, Y., Happonen, R. P., Leivo, I., & Knuutila, S. (2002). Gene expression profiling of ameloblastoma and human tooth germ by means of a cDNA microarray. *Journal of dental research*, 81(8), 525-530.
- Herskovitz, P. (1982). The staggered marsupial lower third incisor (I3). *Geobios*, 15, 191-200.

- James, M. J., Järvinen, E., Wang, X. P., & Thesleff, I. (2006). Different roles of runx2 during early neural crest-derived bone and tooth development. *Journal of Bone and Mineral Research*, 21(7), 1034-1044.
- Jernvall, J., Aberg, T., Kettunen, P., Keranen, S., & Thesleff, I. (1998). The life history of an embryonic signaling center: BMP-4 induces p21 and is associated with apoptosis in the mouse tooth enamel knot. *Development*, 125(2), 161-169.
- Juuri, E., Saito, K., Ahtiainen, L., Seidel, K., Tummers, M., Hochedlinger, K., ... & Michon, F. (2012). Sox2+ stem cells contribute to all epithelial lineages of the tooth via Sfrp5+ progenitors. *Developmental cell*, 23(2), 317-328.
- Juuri, E., Jussila, M., Seidel, K., Holmes, S., Wu, P., Richman, J., ... & Klein, O. (2013). Sox2 marks epithelial competence to generate teeth in mammals and reptiles. *Development*, 140(7), 1424-1432.
- Kavanagh, K. D., Evans, A. R., & Jernvall, J. (2007). Predicting evolutionary patterns of mammalian teeth from development. *Nature*, 449(7161), 427-432.
- Kavanagh, K. D., Shoval, O., Winslow, B. B., Alon, U., Leary, B. P., Kan, A., & Tabin, C. J. (2013). Developmental bias in the evolution of phalanges. *Proceedings of the National Academy of Sciences*, 110(45), 18190-18195.
- Kirkpatrick, T. H. (1969). The dentition of the marsupial family Macropodidae: with particular reference to tooth development in the grey kangaroo *Macropus giganteus* Shaw.
- Kirkpatrick, T. H. (1978). The development of the dentition of *Macropus giganteus* (Shaw): an attempt to interpret the marsupial dentition. *Australian Mammalogy*, 2, 29-35.
- Kleinteich, T., & Gorb, S. N. (2015). Frog tongue acts as muscle-powered adhesive tape. *Royal Society open science*, 2(9), 150333.
- Koussoulakou, D. S., Margaritis, L. H., & Koussoulakos, S. L. (2009). A curriculum vitae of teeth: evolution, generation, regeneration. *International journal of biological sciences*, 5(3), 226.
- Krane, S. M. (2005). Identifying genes that regulate bone remodeling as potential therapeutic targets. *Journal of Experimental Medicine*, 201(6), 841-843.

- Kulesa, P. M., Cruywagen, G. C., Lubkin, S. R., Main, P. K., Sneyd, J., Ferguson, M. W. J., & Murray, J. D. (1996). On a model mechanism for the spatial patterning of teeth primordia in the alligator. *Journal of theoretical biology*, 180(4), 287-296.
- Labonne, G., Laffont, R., Renvoisé, E., Jebrane, A., Labruère, C., Chateau-Smith, C., ... & Montuire, S. (2012). When less means more: evolutionary and developmental hypotheses in rodent molars. *Journal of evolutionary biology*, 25(10), 2102-2111.
- Larabell, C. A., & Le Gros, M. A. (2004). X-ray tomography generates 3-D reconstructions of the yeast, *Saccharomyces cerevisiae*, at 60-nm resolution. *Molecular biology of the cell*, 15(3), 957-962.
- Luckett, W. P. (1993). An ontogenetic assessment of dental homologies in therian mammals. In *Mammal phylogeny* (pp. 182-204). Springer, New York, NY.
- Luckett, W. P., & Hong, N. (1989). Ontogenetic evidence for both replacement in marsupials (Mammalia). *Cell Differentiation and Development*, 27, 45.
- Luckett, W. P., & Woolley, P. A. (1996). Ontogeny and homology of the dentition in dasyurid marsupials: Development in *Sminthopsis virginiae*. *Journal of Mammalian Evolution*, 3(4), 327-364.
- Lumsden, A. G. (1979). Pattern formation in the molar dentition of the mouse. *Journal de biologie buccale*, 7(1), 77-103.
- Lumsden, A. G. S. (1988). Spatial organization of the epithelium and the role of neural crest cells in the initiation of the mammalian tooth germ. *Development*, 103(Supplement), 155-169.
- McCollum, M., & Sharpe, P. T. (2001). Evolution and development of teeth. *The Journal of Anatomy*, 199(1-2), 153-159.
- Meredith, R. W., Westerman, M., & Springer, M. S. (2009). A phylogeny of Diprotodontia (Marsupialia) based on sequences for five nuclear genes. *Molecular Phylogenetics and Evolution*, 51(3), 554-571.
- Metscher, B. D. (2009). MicroCT for developmental biology: A versatile tool for high-contrast 3D imaging at histological resolutions. *Developmental dynamics*, 238(3), 632-640.

- Miller, W. A. (1969). Inductive changes in early tooth development: I. A study of mouse tooth development on the chick chorioallantois. *Journal of dental research*, 48(5), 719-725.
- Mitsiadis, T. A., & Smith, M. M. (2006). How do genes make teeth to order through development?. *Journal of Experimental Zoology Part B: Molecular and Developmental Evolution*, 306(3), 177-182.
- Munne, P. M., Felszeghy, S., Jussila, M., Suomalainen, M., Thesleff, I., & Jernvall, J. (2010). Splitting placodes: effects of bone morphogenetic protein and ACTIVIN on the patterning and identity of mouse incisors. *Evolution & development*, 12(4), 383-392.
- van Nievelt, A. F., & Smith, K. K. (2005). To replace or not to replace: the significance of reduced functional tooth replacement in marsupial and placental mammals. *Paleobiology*, 31(2), 324-346.
- Ooë, T. (1979). Development of human first and second permanent molar, with special reference to the distal portion of the dental lamina. *Anatomy and embryology*, 155(2), 221-240.
- Oommen, S., Otsuka-Tanaka, Y., Imam, N., Kawasaki, M., Kawasaki, K., Jalani-Ghazani, F., ... & Ohazama, A. (2012). Distinct roles of microRNAs in epithelium and mesenchyme during tooth development. *Developmental Dynamics*, 241(9), 1465-1472.
- Osborn, J. W. (1971). The ontogeny of tooth succession in *Lacerta vivipara* Jacquin (1787). *Proc. R. Soc. Lond. B*, 179(1056), 261-289.
- Osborn, J. W. (1972). On the biological improbability of Zahnreihen as embryological units. *Evolution*, 26(4), 601-607.
- Osborn, J. W. (1978). Morphogenetic gradients: fields versus clones. *Development, function and evolution of teeth*, 171-201.
- Osborn, J. W., & Lumsden, A. G. S. (1978). An alternative to "thegosis" and a re-examination of the ways in which mammalian molars work. *N Jb Geol Paleont Abh*, 156, 371-392.
- Patterson, B. (1956). Early Cretaceous mammals and the evolution of mammalian molar teeth. *Fieldiana-Geology*, 13, 1-105.

- Parkinson, D. Y., McDermott, G., Etkin, L. D., Le Gros, M. A., & Larabell, C. A. (2008). Quantitative 3-D imaging of eukaryotic cells using soft X-ray tomography. *Journal of structural biology*, 162(3), 380-386.
- Pemberton, T. J., Li, F. Y., Oka, S., Mendoza-Fandino, G. A., Hsu, Y. H., Bringas Jr, P., ... & Patel, P. I. (2007). Identification of novel genes expressed during mouse tooth development by microarray gene expression analysis. *Developmental dynamics: an official publication of the American Association of Anatomists*, 236(8), 2245-2257.
- Peterková, R., Lesot, H., Viriot, L., & Peterka, M. (2005). The supernumerary cheek tooth in tabby/EDA mice—a reminiscence of the premolar in mouse ancestors. *Archives of oral biology*, 50(2), 219-225.
- Peterková, R., Lesot, H., & Peterka, M. (2006). Phylogenetic memory of developing mammalian dentition. *Journal of Experimental Zoology Part B: Molecular and Developmental Evolution*, 306(3), 234-250.
- Polly, P. D. (2007). Evolutionary biology: development with a bite. *Nature*, 449(7161), 413.
- Popa, E. M., Anthwal, N., & Tucker, A. S. (2016). Complex patterns of tooth replacement revealed in the fruit bat (*Eidolon helvum*). *Journal of anatomy*, 229(6), 847-856.
- Prochazka, J., Pantalacci, S., Churava, S., Rothova, M., Lambert, A., Lesot, H., ... & Peterková, R. (2010). Patterning by heritage in mouse molar row development. *Proceedings of the National Academy of Sciences*, 107(35), 15497-15502.
- Richman, J. M., & Handrigan, G. R. (2011). Reptilian tooth development. *Genesis*, 49(4), 247-260.
- Sanson, G. D., Nelson, J. E., & Fell, P. (1985). Ecology of *Peradorcas concinna* in Arnhemland in a wet and a dry season. In *Proceedings of the Ecological Society of Australia*(Vol. 13, pp. 69-72).
- Saunders, S. R., & Mayhall, J. T. (1982). Developmental patterns of human dental morphological traits. *Archives of Oral Biology*, 27(1), 45-49.
- Schroer, K., & Wood, B. (2015). Modeling the dental development of fossil hominins through the inhibitory cascade. *Journal of anatomy*, 226(2), 150-162.

- Stock, D. W., Weiss, K. M., & Zhao, Z. (1997). Patterning of the mammalian dentition in development and evolution. *Bioessays*, 19(6), 481-490.
- Streelman, J. T., Webb, J. F., Albertson, R. C., & Kocher, T. D. (2003). The cusp of evolution and development: a model of cichlid tooth shape diversity. *Evolution & development*, 5(6), 600-608.
- Tsai, H. P., & Holliday, C. M. (2011). Ontogeny of the alligator cartilago transiliens and its significance for sauropsid jaw muscle evolution. *PLoS One*, 6(9), e24935.
- Tabata, T., & Takei, Y. (2004). Morphogens, their identification and regulation. *Development*, 131(4), 703-712.
- Tucker, A. S., Matthews, K. L., & Sharpe, P. T. (1998). Transformation of tooth type induced by inhibition of BMP signaling. *Science*, 282(5391), 1136-1138.
- Tucker, A., & Sharpe, P. (2004). The cutting-edge of mammalian development; how the embryo makes teeth. *Nature Reviews Genetics*, 5(7), 499.
- Valcourt, U., & Moustakas, A. (2005). BMP signaling in osteogenesis, bone remodeling and repair. *European Journal of Trauma*, 31(5), 464-479.
- Van der Heyden, C., & Huysseune, A. (2000). Dynamics of tooth formation and replacement in the zebrafish (*Danio rerio*)(Teleostei, Cyprinidae). *Developmental dynamics: an official publication of the American Association of Anatomists*, 219(4), 486.
- Viriot, L., Lesot, H., Vonesch, J. L., Ruch, J. V., Peterka, M., & Peterková, R. (2000). The presence of rudimentary odontogenic structures in the mouse embryonic mandible requires reinterpretation of developmental control of first lower molar histomorphogenesis. *The International journal of developmental biology*, 44(2), 233.
- Viriot, L., Lesot, H., Vonesch, J. L., Ruch, J. V., Peterka, M., & Peterková, R. (2002). The presence of rudimentary odontogenic structures in the mouse embryonic mandible requires reinterpretation of developmental control of first lower molar histomorphogenesis. *International Journal of Developmental Biology*, 44(2), 233-240.
- Wake, M. H. (1980). Fetal tooth development and adult replacement in *Dermophis mexicanus* (Amphibia: Gymnophiona): Fields versus clones. *Journal of Morphology*, 166(2), 203-216.

- Woodward, M. F. (1893). Contributions to the study of mammalian dentition.-Part I. On the development of the teeth of the Macropodidae. In Proc. Zool. Soc. London (pp. 450-473).
- Woodward, M. F. (1896). On the teeth of the Marsupialia, with especial reference to the premilk dentition. *Anat. Anz.* 12: 281-291
- Young, N. M., Winslow, B., Takkellapati, S., & Kavanagh, K. (2015). Shared rules of development predict patterns of evolution in vertebrate segmentation. *Nature communications*, 6, 6690.
- Zhao, Z., Weiss, K. M., & Stock, D. W. (2007). 11 Development and evolution of dentition patterns and their genetic basis. *Development, function and evolution of teeth*, 152.
- Ziegler, A. C. (1971). A theory of the evolution of therian dental formulas and replacement patterns. *The Quarterly Review of Biology*, 46(3), 226-249.

Mischief managed

- Marauders: Moony, Wormtail, Padfoot and Prongs

Appendices

For Chapters 2-5

APPENDIX A

Supplementary Figures for Chapter 2

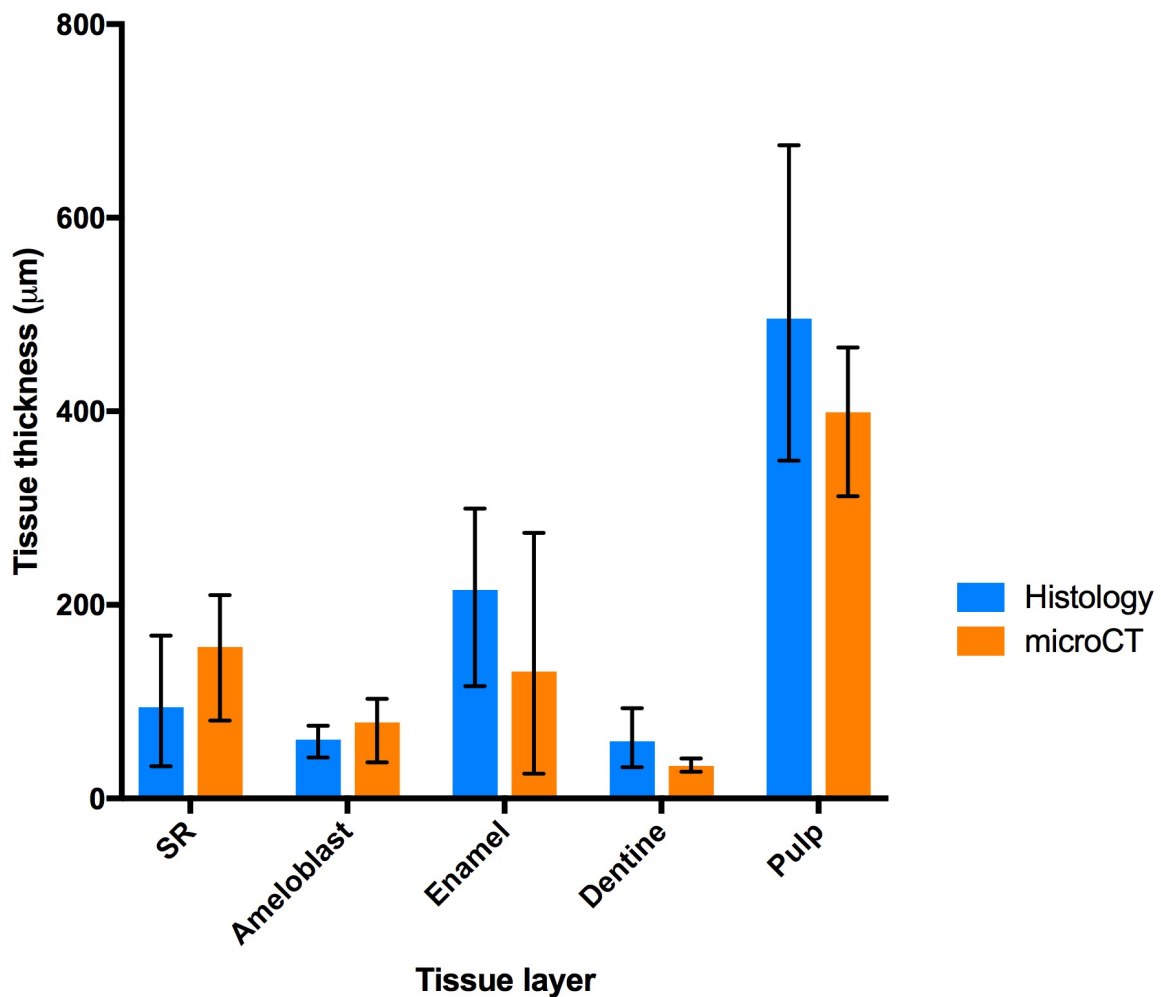


Figure A2.1 Comparison of tissue layer thicknesses between histology sections (blue left columns) and whole-head microCT scans (at 0.39×) (orange right columns) of specimen 5694 (in µm). Bars represent average values, while black lines are min-max ranges. Abbreviation: SR (Stellate Reticulum).

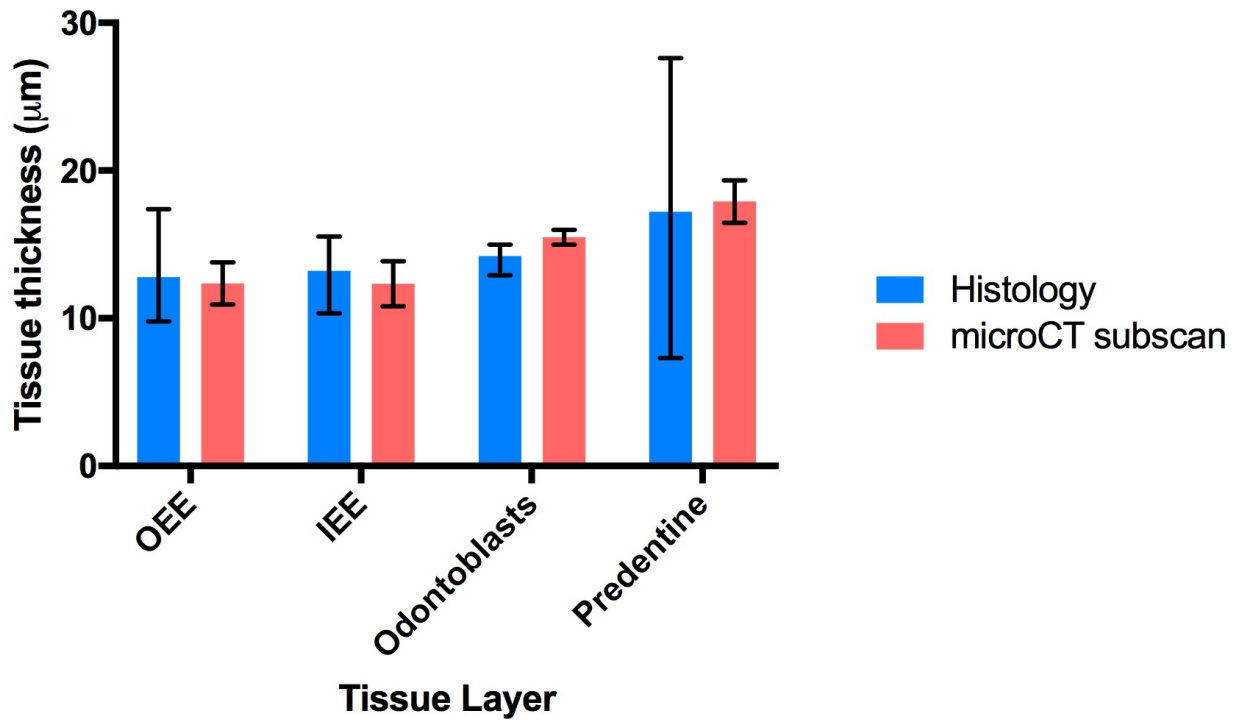


Figure A2.2 Comparison of tissue layer thicknesses between histology sections (blue left columns) and sub-volume microCT scan of single tooth organ (at 4×) (red right columns) of specimen 4946 (in μm). Bars represent average values, while black lines are min-max ranges. Abbreviations: OEE (Outer Enamel Epithelium), IEE (Inner Enamel Epithelium).

Supplementary Tables for Chapter 2

Table A2.1 Staining and scanning parameters used for fourteen tammar wallaby specimens at the XFIG, Monash University, Melbourne Australia (during 2014-2017).

Specimen #	Head Length (mm)	Age (days)	Lugol's staining time (days)	Power (μ A)	Voltage (kV)	Magnification	Projections	Exposure (seconds)	Source (mm)	Detector (mm)	Voxel length (μ m)
11-245	6.13	²³ RP Y	1	7	80	4x	3201	15	149.99	54.99	4.94
6103	7.77	1	2	10	50-130	4x	1601-3201	5-40	150	50	5.09
4180	11.5	11.5	2	10	130	.39-4x	3201	1-5	40.02	200	1.12-10.54
3935	12.36	14	2	10	130	.39x	3201	2	43.03	316.92	8.18
5563	18.77	30	5	7-Oct	80-130	.39x	1601-3201	1.5-5	43.02	232.93	10.68
6543	21.97	36	5	7	80	.39x	3201	3	60	225	14.41
5694	22.02	43	5	40	50	.39x	3201	3	44.02	149.99	15.53
4946	28	57	5	8-Oct	90-130	.39-4x	3201	1-4	50.03	140	4.02-18.03
5470	36.51	70	7	7	80	.39x	3201	3	90	160	24.63
4942	36	74	Unstained /7	7	80	.39x	3201	3	100.98	152.7	27.25
5449	36	82	7	10	130	.39-4x	3201	1.5-10	150.03	90	3.37-42.8
4914	45	120	7	10	130	.39-4x	1601-3201	2.5-20	140	185.19	3.37-29.48
7046	56.7	150	14	10	130	.39x	3201	2	120	90	39.13
6843	83	258	28	10	130	.39x	3201	6	200/60	45/130	21-55.9

Table A2.2 Staining and scanning parameters used for six tammar wallaby specimens using the IMBL, Australian Synchrotron, Melbourne Australia (during 2014).

Specimen #	Head Length (mm)	Age (days)	Lugol's staining time	Exposure (seconds)	Energy (kev)	Voxel Size (μm^3)
MR4180	11.5	11.5	2	0.5	32/34	6.11
MR4946	28	57	5	0.5	34	6.11
MR4942	36	74	unstained	0.5	34	6.11
MR4913	36	81	7	0.5	34	6.11
MR4992	40.5	90	7	0.5	34	6.11
MR4914	45	120	7	0.5	34	6.11

Table A2.3 Organ and tissue thickness comparisons between coronal histology sections and XY slices of Xradia microCT scan of whole heads of specimen 5694, in μm .

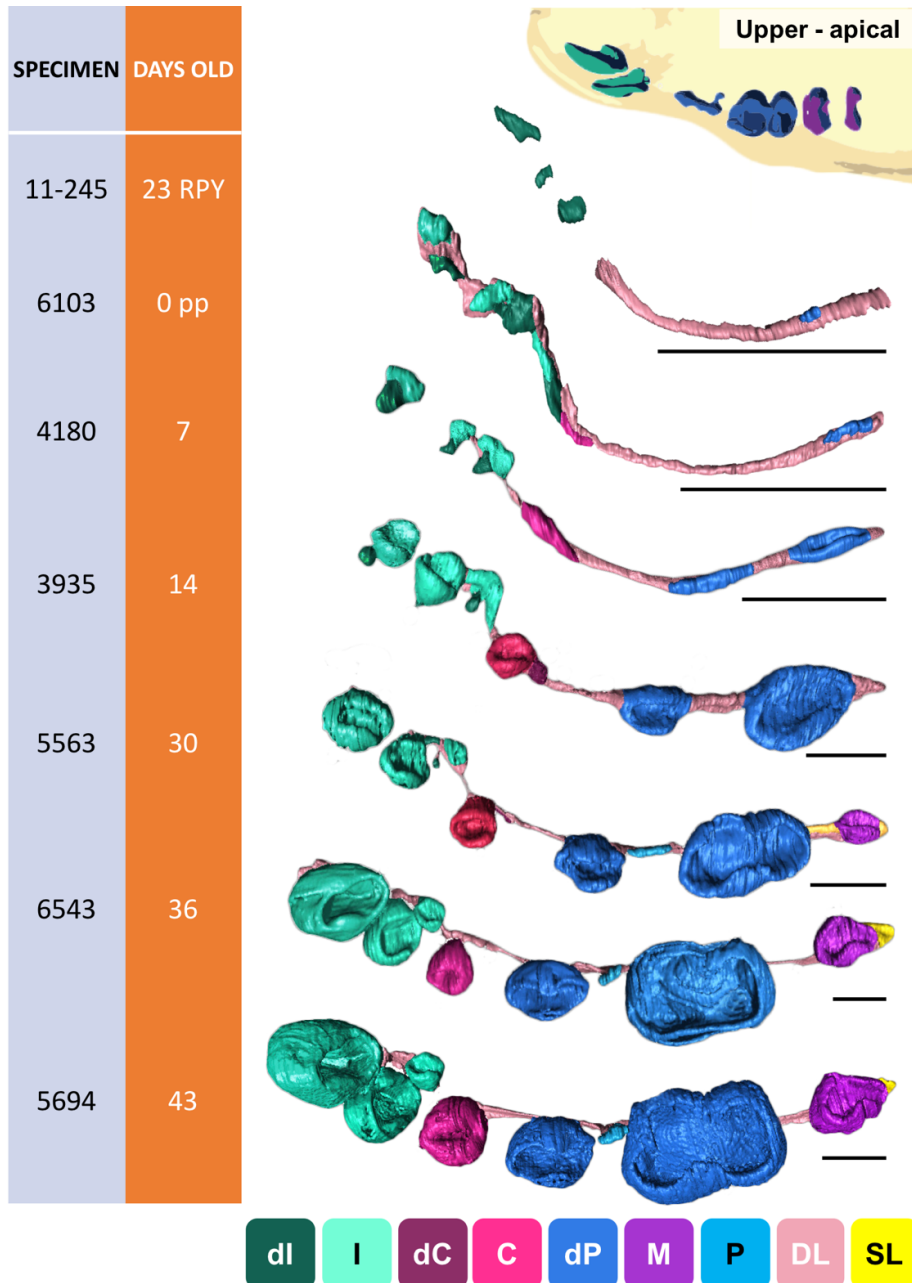
	Histology				MicroCt			
	Length	Average	Min	Max	Length	Average	Min	Max
Head width (coronal)	8356.34				8398.94			
	8313.35	8321.87	8295.92	8356.34	8409.11	8394.42	8375.21	8409.11
	8295.92				8375.21			
Incisor organ width	1574.92				1580.51			
	1607.9	1593.97	1574.92	1607.9	1571.61	1577.61	1571.6	1580.71
	1599.08				1580.71			
Outer enamel epithelium	17.39				63.54			
	9.8	12.8	9.8	17.39	41.31	51.02	41.31	63.54
Stellate reticulum	11.22				48.21			
	33.21				210.21			
	81.54	94.39	33.21	168.42	179.36	156.67	80.44	210.21
Inner enamel epithelium	168.42				80.44			
	15.54				14.26			
	13.76	13.21	10.33	15.54	28.73	27.71	14.26	40.13
Ameloblasts	10.33				40.13			
	42.43				95.45			
	75.3	60.78	42.43	75.3	37.35	78.55	37.35	102.86
Enamel	64.62				102.86			
	299.53				274.31			
	115.95	215.39	115.95	299.53	93.23	131.03	25.54	274.31
Dentine	230.69				25.54			
	93.4				41.2			
	32.23	59.08	32.23	93.4	32.52	33.8	27.69	41.2
Predentine	51.61				27.69			
	27.61				77.88			
	7.3	17.21	7.3	27.61	39.85	56.3	39.85	77.88
Odontoblasts	16.71				51.17			
	14.98				105.86			
	12.91	14.22	12.91	14.98	29.72	65.5	29.72	105.86
Pulp	14.77				60.91			
	674.99				465.95			
	463.07	495.76	349.22	674.99	312.4	399.07	312.4	465.95
	349.22			418.87				

Table A2.4 Organ and tissue thickness comparisons between coronal histology sections and XY slices of Xradia microCT sub-volume scan of single tooth organ of specimen 4946, in μm .

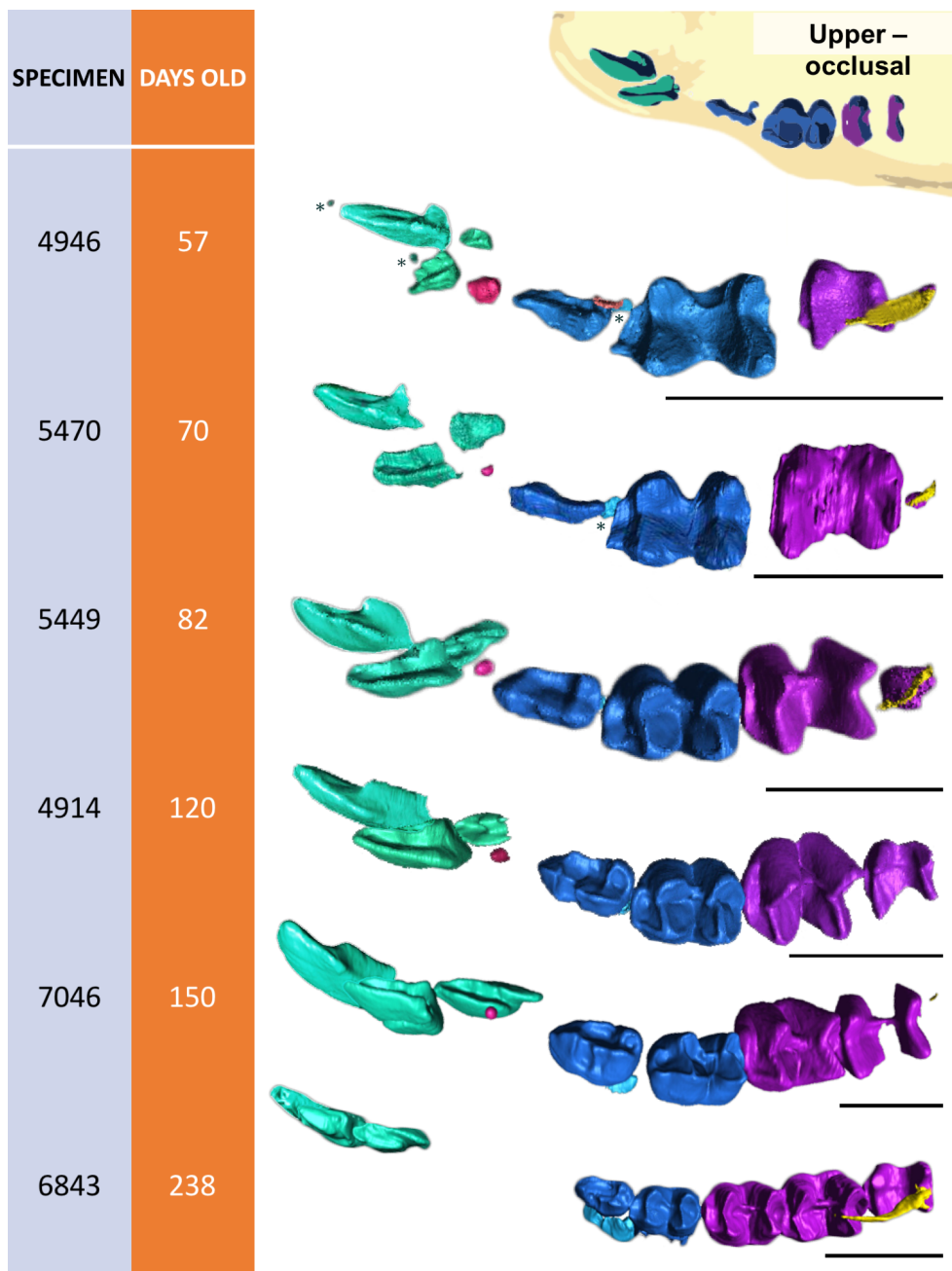
	Histology				MicroCT			
	Length	Average	Min	Max	Length	Average	Min	Max
Outer enamel epithelium	17.39				14.97			
	9.8	12.8	9.8	17.39	10.09	12.36	10.09	14.97
	11.22				12.01			
Inner enamel epithelium	15.54				12.1			
	13.76	13.21	10.33	15.54	9.83	12.34	9.83	15.1
	10.33				15.1			
Ameloblasts	42.43				48.87			
	75.3	60.78	42.43	75.3	44.69	48.66	44.69	52.43
	64.62				52.43			
Dentine	93.4				41.44			
	32.23	59.08	32.23	93.4	56.47	37.75	15.35	56.47
	51.61				15.35			
Predentine	27.61				15.59			
	7.3	17.21	7.3	27.61	17.59	17.9	15.59	20.53
	16.71				20.53			
Odontoblasts	14.98				14.97			
	12.91	14.22	12.91	14.98	16.47	15.49	14.97	16.47
	14.77				15.02			

APPENDIX B

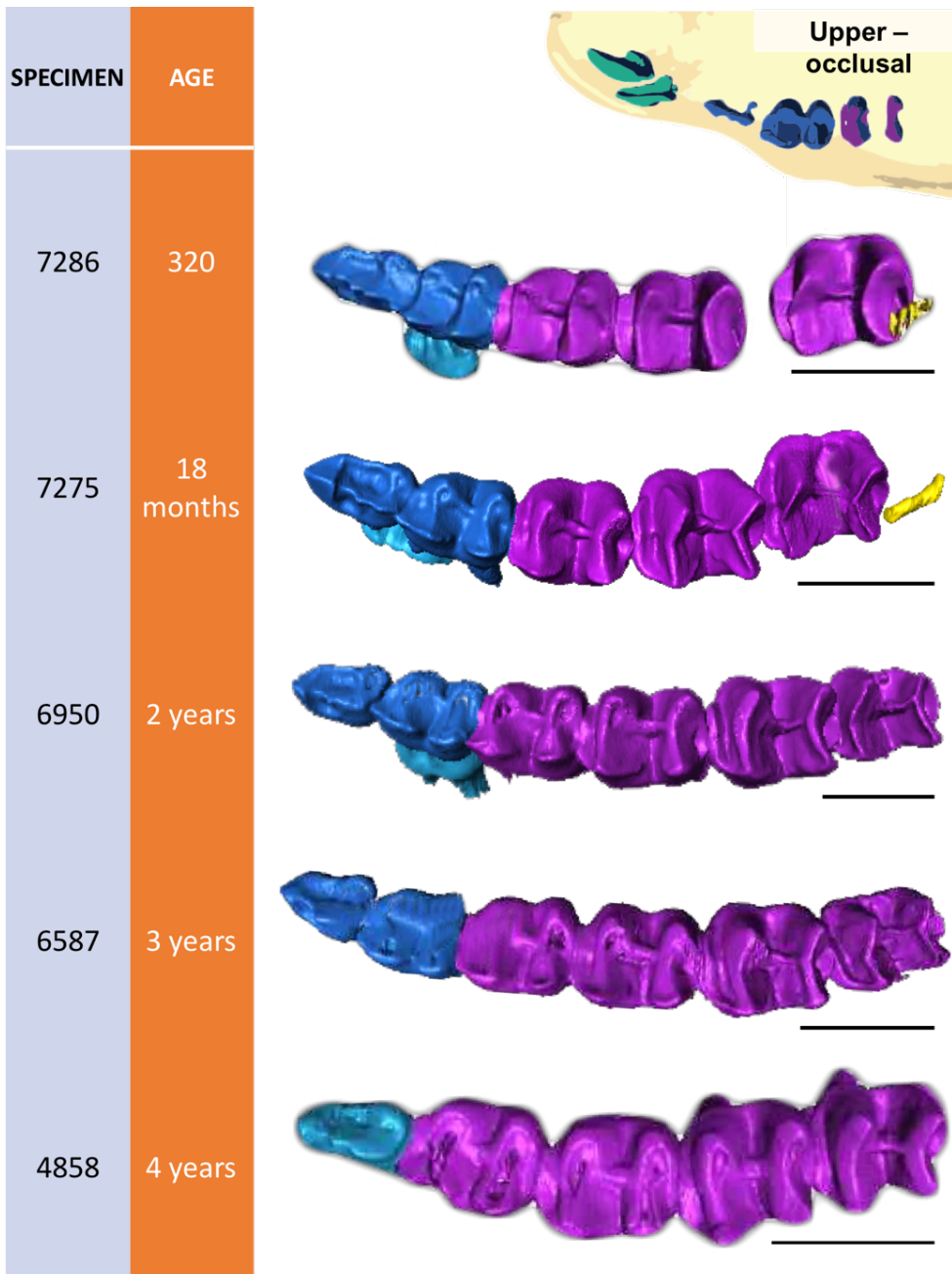
Supplementary Figures for Chapter 3



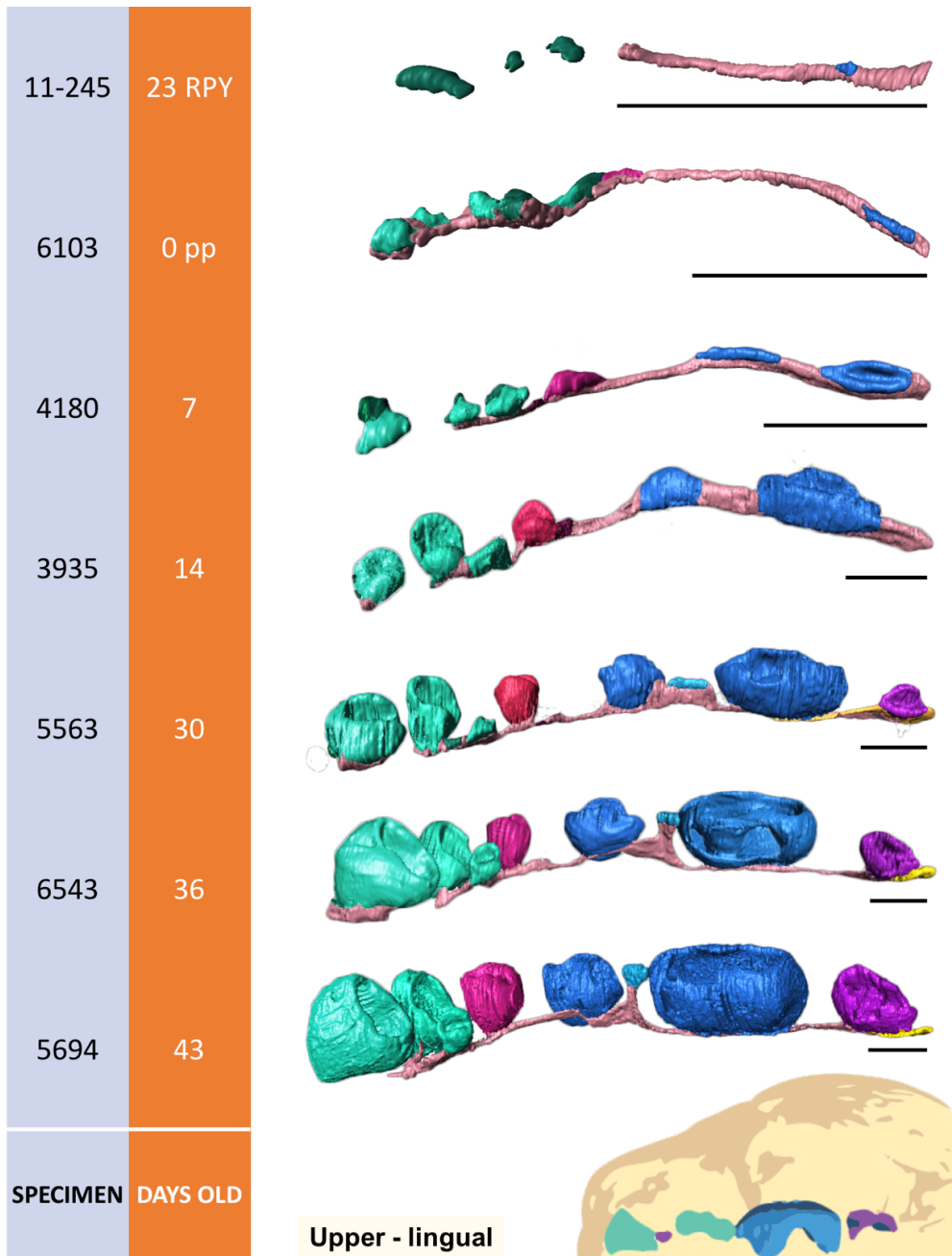
Supplementary Figure A3.1 3D reconstructions of tooth development of soft tissue using diceCT for the upper right jaws of the tammar wallaby, from 23 days RPY to 43 days pp. Models are in apical view (viewing the dental lamina and tooth germs from below, with the dental lamina behind the teeth). Abbreviations: C (Canine), dC (deciduous canine), dI (deciduous incisor), DL (Dental lamina), dP (Deciduous Premolar), I (Incisor), M (Molar), P (Permanent Premolar), SL (successional lamina). Specimens were segmented between the inner (IEE) and outer enamel epithelium (OEE). Scale bars = 1 mm.



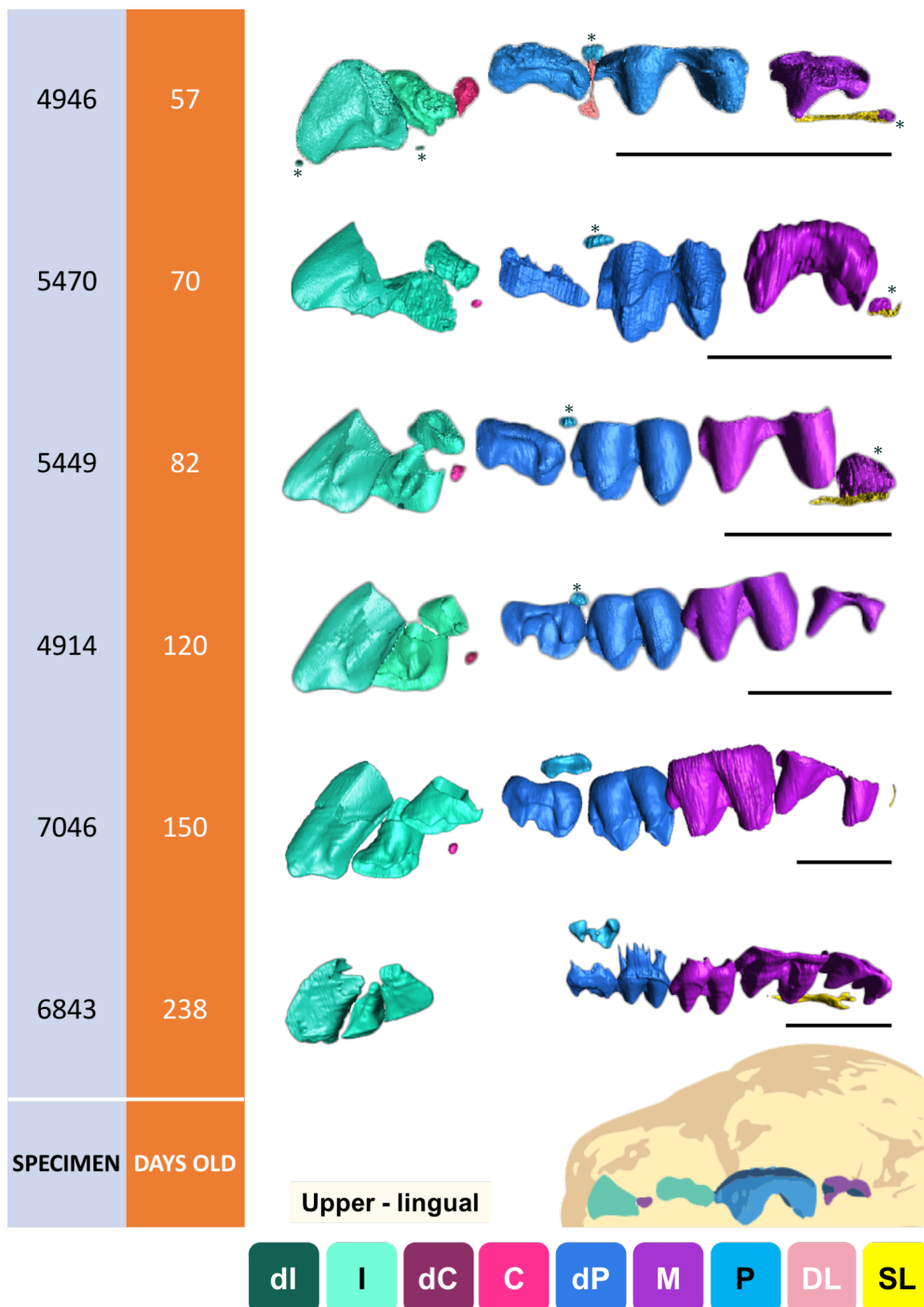
Supplementary Figure A3.2 3D reconstructions of tooth development of soft and mineralised tissue using diceCT for the upper right jaws of the tammar wallaby, from 57 to 238 days. Models are in occlusal views (viewing the tooth crowns from above). Abbreviations: C (Canine), dC (deciduous canine) dI (deciduous incisor), DL (Dental lamina), dP (Deciduous Premolar), I (Incisor), M (Molar), P (Permanent Premolar), SL (successional lamina). Specimens with mineralisation were segmented between the ameloblast and outer enamel layers, where * denotes unmineralised teeth segmented between the inner (IEE) and outer enamel epithelium (OEE). Scale bars = 6 mm.



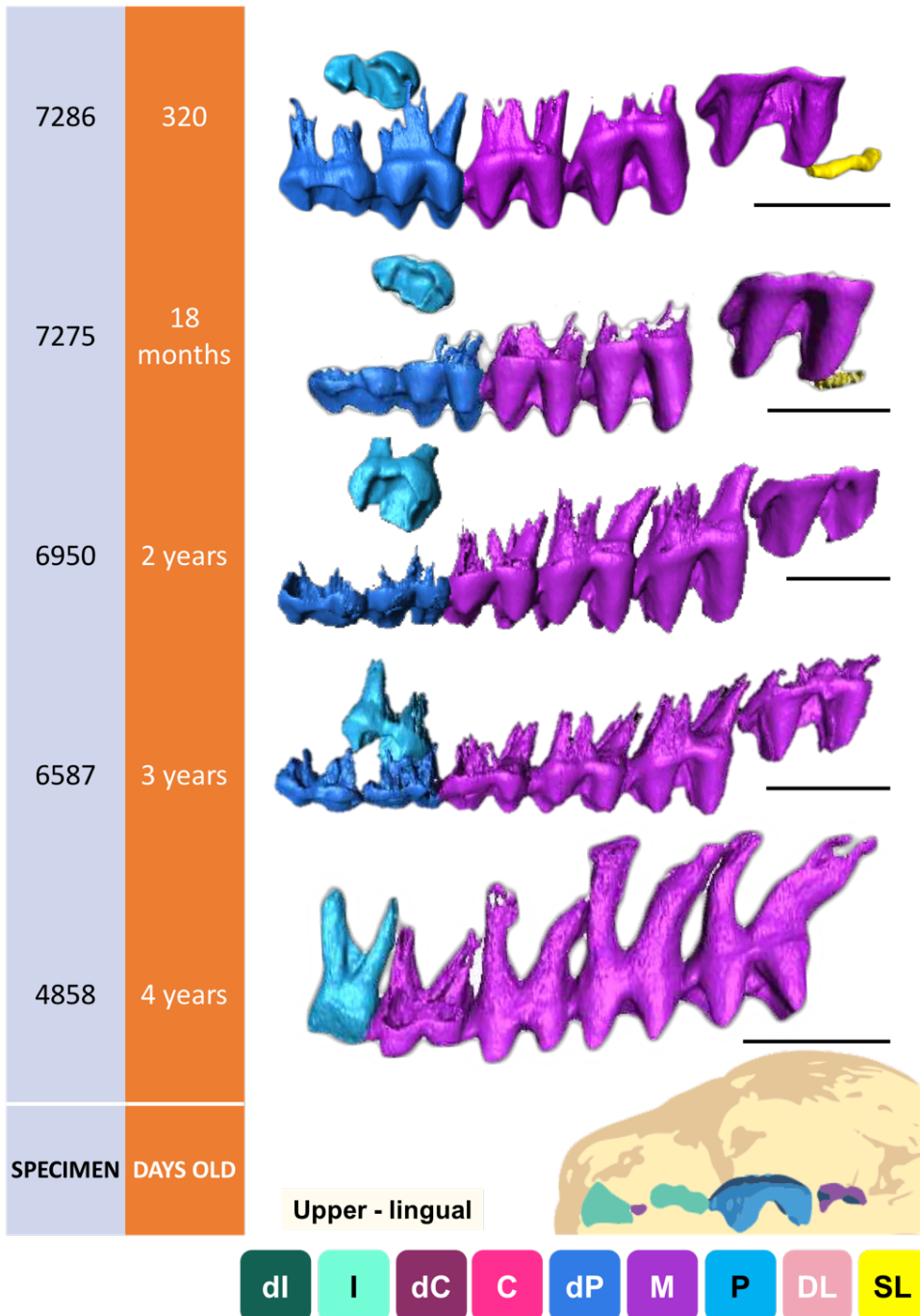
Supplementary Figure A3.3 3D reconstructions of tooth development of soft and mineralised tissue using diceCT for the upper right jaws of the tammar wallaby, from 320 days to four years. Models are in occlusal views (viewing the tooth crowns from above). Abbreviations: C (Canine), dC (deciduous canine) dI (deciduous incisor), DL (Dental lamina), dP (Deciduous Premolar), I (Incisor), M (Molar), P (Permanent Premolar), SL (successional lamina). Incisors were excluded in these models to save space as they had already erupted. Specimens were segmented between the ameloblast and outer enamel layers. Scale bars = 6 mm.



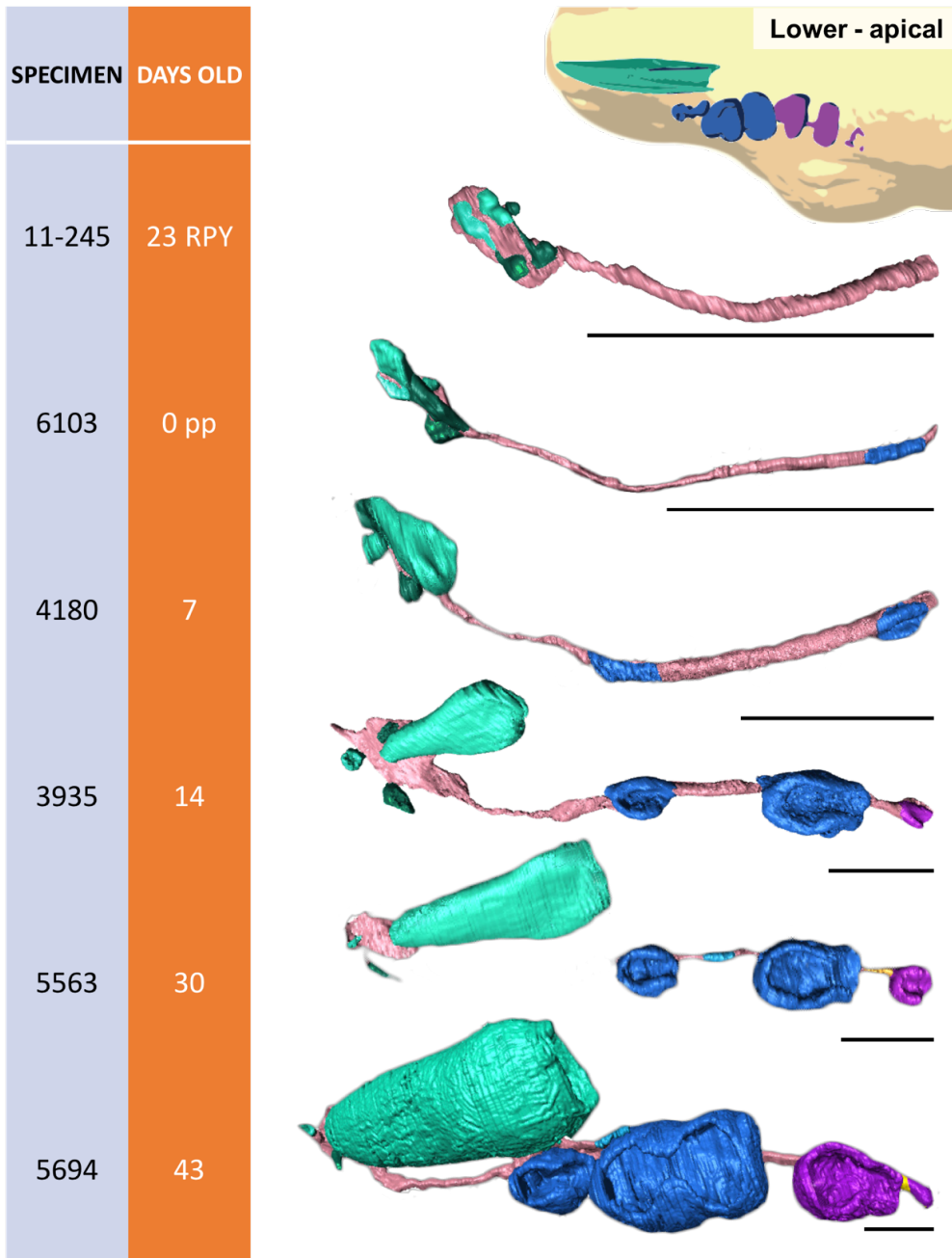
Supplementary Figure A3.4 3D reconstructions of tooth development of soft tissue using diceCT for the upper right jaws of the tammar wallaby, from 23 days RPY to 43 days pp. Models are in lingual view. Abbreviations: C (Canine), dC (deciduous canine) dI (deciduous incisor), DL (Dental lamina), dP (Deciduous Premolar), I (Incisor), M (Molar), P (Permanent Premolar), SL (successional lamina). Specimens were segmented between the inner (IEE) and outer enamel epithelium (OEE). Scale bars = 1 mm.



Supplementary Figure A3.5 3D reconstructions of tooth development of soft and mineralised tissue using diceCT for the upper right jaws of the tammar wallaby, from 57 to 238 days. Models are in lingual views. Abbreviations: C (Canine), dC (deciduous canine) dI (deciduous incisor), DL (Dental lamina), dP (Deciduous Premolar), I (Incisor), M (Molar),/P (Permanent Premolar), SL (successional lamina). Specimens with mineralisation were segmented between the ameloblast and outer enamel layers, where * denotes unmineralised teeth segmented between the inner (IEE) and outer enamel epithelium (OEE). Scale bars = 6 mm.

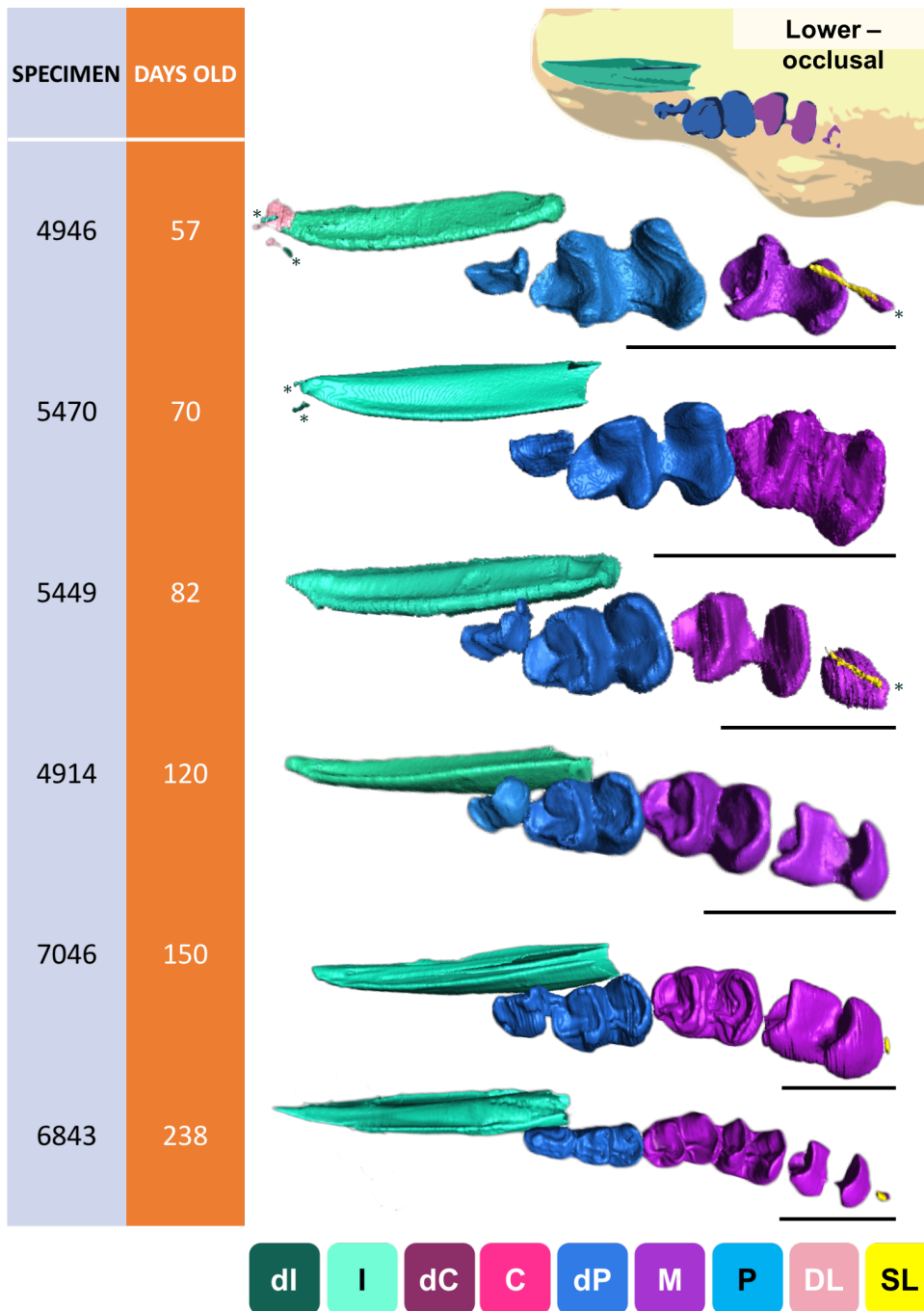


Supplementary Figure A3.6 3D reconstructions of tooth development of soft and mineralised tissue using diceCT for the upper right jaws of the tammar wallaby, from 320 days to four years. Models are in lingual views. Abbreviations: C (Canine), dC (deciduous canine) dI (deciduous incisor), DL (Dental lamina), dP (Deciduous Premolar), I (Incisor), M (Molar), P (Permanent Premolar), SL (successional lamina). Incisors were excluded in these models to save space as they had already erupted. Specimens were segmented between the ameloblast and outer enamel layers. Scale bars = 6 mm.

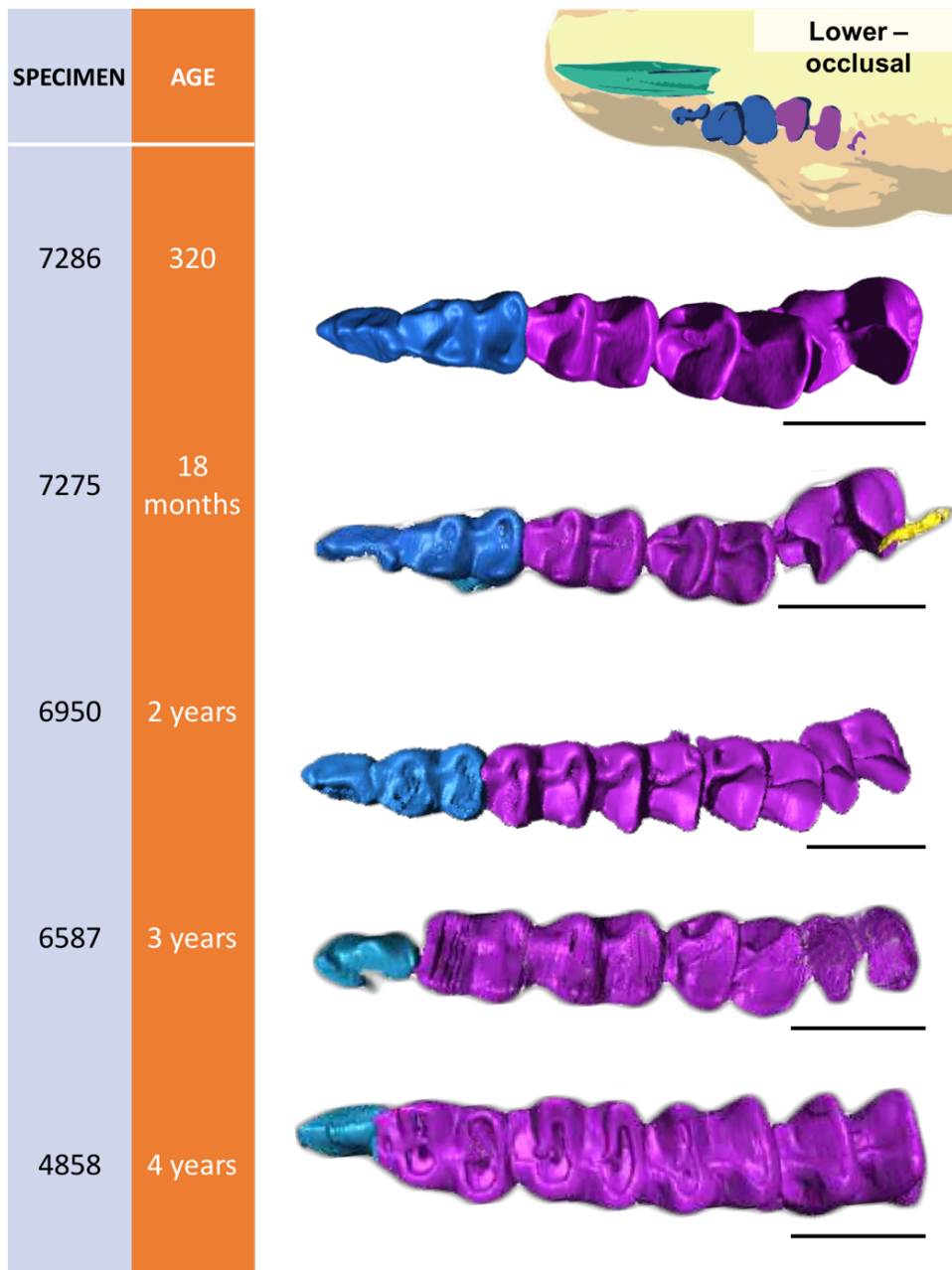


dl I dC C dP M P DL SL

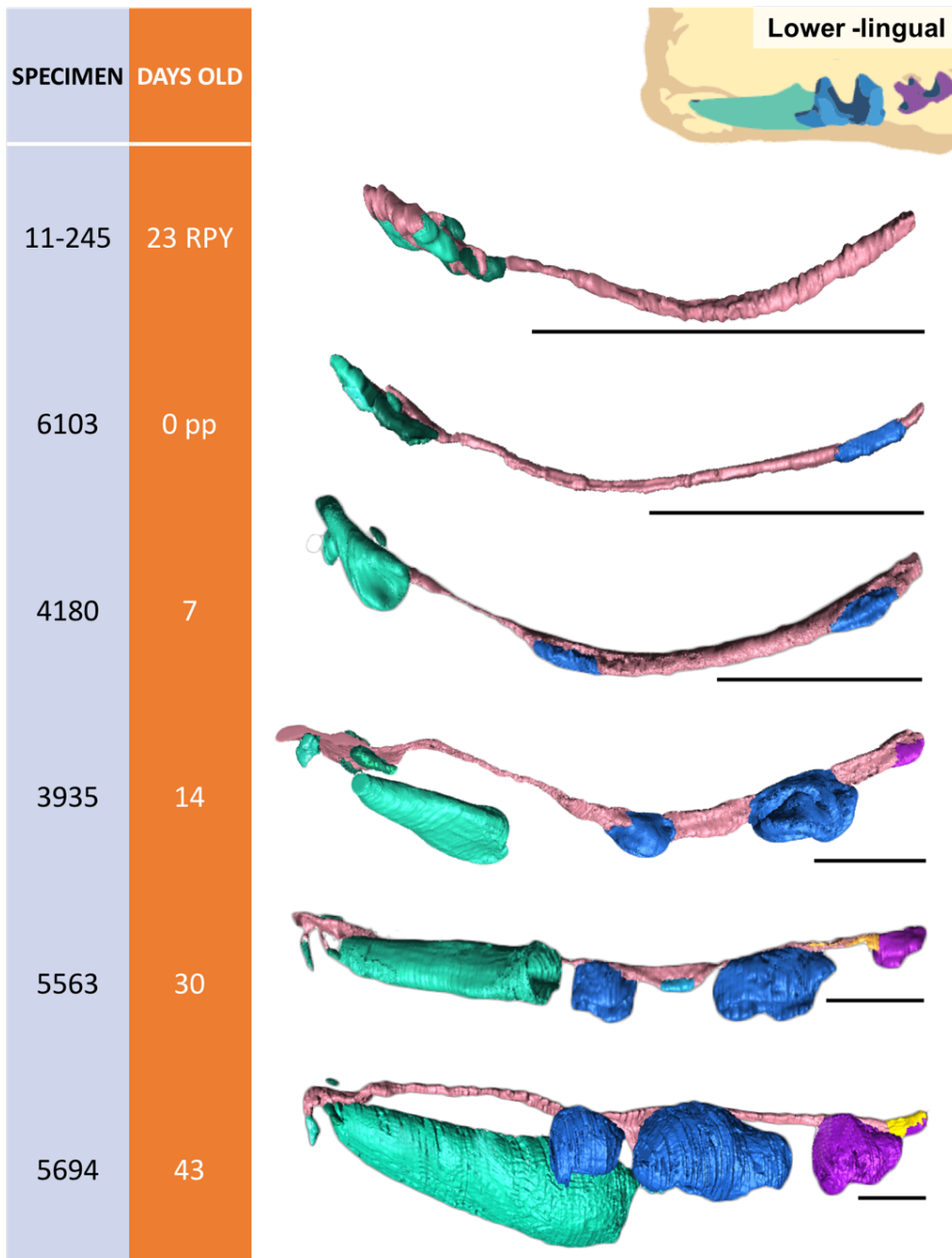
Supplementary Figure A3.7 3D reconstructions of tooth development of soft tissue using diceCT for the lower right jaws of the tammar wallaby, from 23 days RPY to 43 days pp. Models are in apical view (viewing the dental lamina and tooth germs from below, with the dental lamina behind the teeth). Abbreviations: C (Canine), dC (deciduous canine) dI (deciduous incisor), DL (Dental lamina), dP (Deciduous Premolar), I (Incisor), M (Molar), P (Permanent Premolar), SL (successional lamina). Specimens were segmented between the inner (IEE) and outer enamel epithelium (OEE). Scale bars = 1 mm.



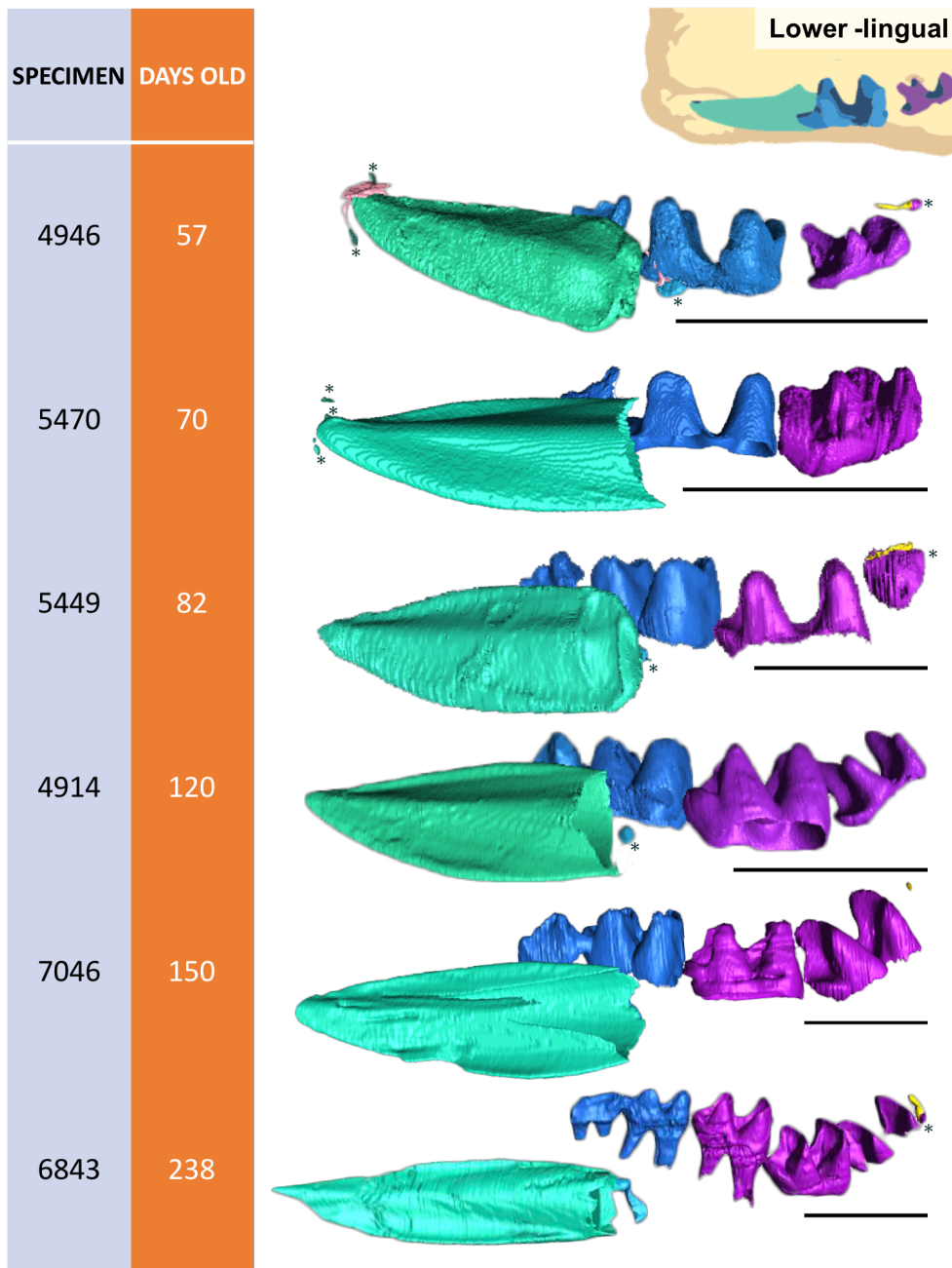
Supplementary Figure A3.8 3D reconstructions of tooth development of soft and mineralised tissue using diceCT for the lower right jaws of the tammar wallaby, from 57 to 238 days. Models are in occlusal views (viewing the tooth crowns from above). Abbreviations: C (Canine), dC (deciduous canine) dI (deciduous incisor), DL (Dental lamina), dP (Deciduous Premolar), I (Incisor), M (Molar), P (Permanent Premolar), SL (successional lamina). Specimens with mineralisation were segmented between the ameloblast and outer enamel layers, where * denotes unmineralised teeth segmented between the inner (IEE) and outer enamel epithelium (OEE). Scale bars = 6 mm.



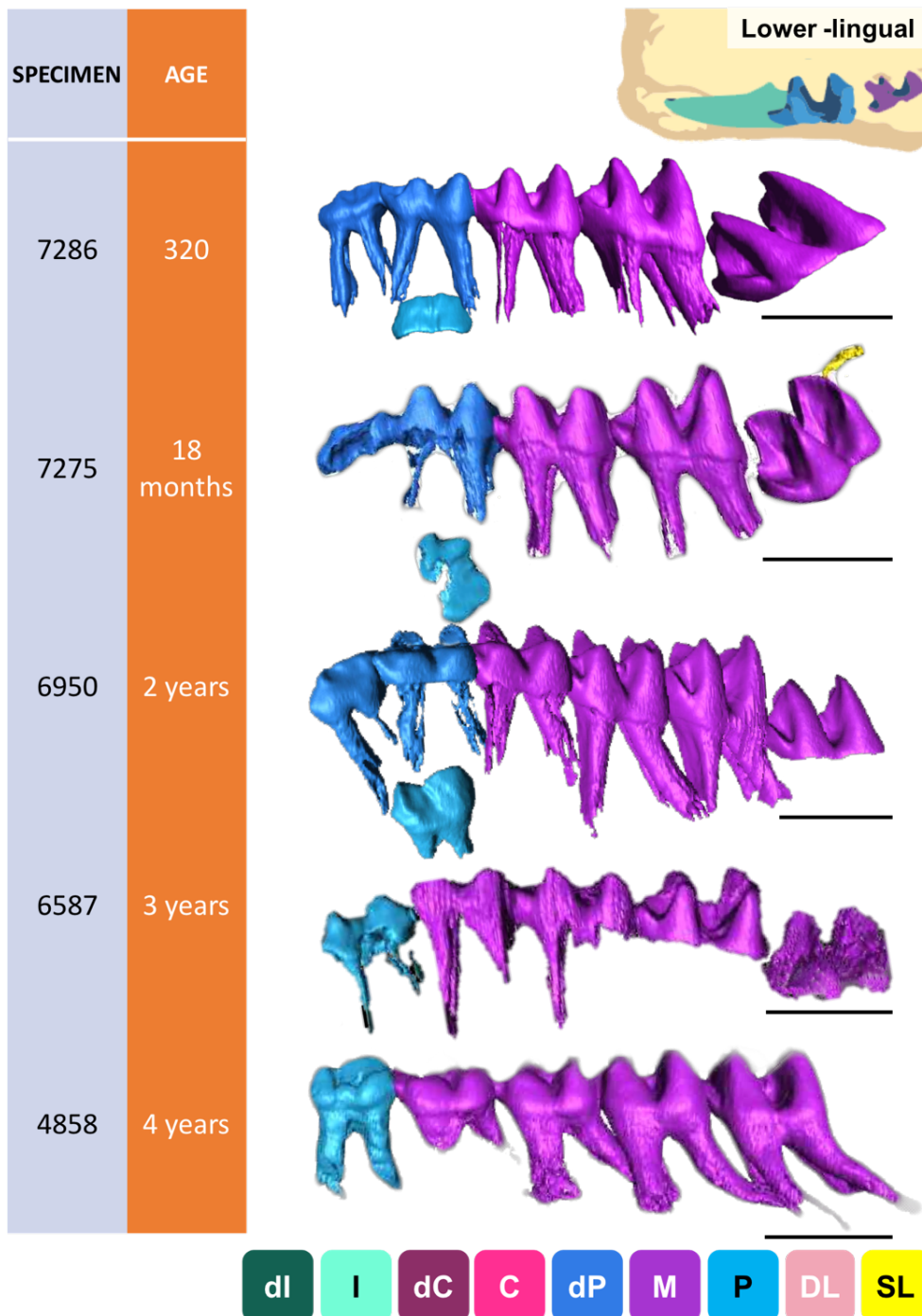
Supplementary Figure A3.9 3D reconstructions of tooth development of soft and mineralised tissue using diceCT for the lower right jaws of the tammar wallaby, from 320 days to four years. Models are in occlusal views (viewing the tooth crowns from above). Abbreviations: C (Canine), dC (deciduous canine) dI (deciduous incisor), DL (Dental lamina), dP (Deciduous Premolar), I (Incisor), M (Molar), P (Permanent Premolar), SL (successional lamina). Incisors were excluded in these models to save space as they had already erupted. Specimens were segmented between the ameloblast and outer enamel layers. Scale bars = 6 mm.



Supplementary Figure A3.10 3D reconstructions of tooth development of soft tissue using diceCT for the lower right jaws of the tammar wallaby, from 23 days RPY to 43 days pp. Models are in lingual view. Abbreviations: C (Canine), dC (deciduous canine) dI (deciduous incisor), DL (Dental lamina), dP (Deciduous Premolar), I (Incisor), M (Molar), P (Permanent Premolar), SL (successional lamina). Specimens were segmented between the inner (IEE) and outer enamel epithelium (OEE). Scale bars = 1 mm. dI₃



Supplementary Figure A3.11 3D reconstructions of tooth development of soft and mineralised tissue using diceCT for the lower right jaws of the tammar wallaby, from 57 to 238 days. Models are in lingual views. Abbreviations: C (Canine), dC (deciduous canine) dI (deciduous incisor), DL (Dental lamina), dP (Deciduous Premolar), I (Incisor), M (Molar), P (Permanent Premolar), SL (successional lamina). Specimens with mineralisation were segmented between the ameloblast and outer enamel layers, where * denotes unmineralised teeth segmented between the inner (IEE) and outer enamel epithelium (OEE). Scale bars = 6 mm.



Supplementary Figure A3.12 3D reconstructions of tooth development of soft and mineralised tissue using diceCT for the upper right jaws of the tammar wallaby, from 320 days to four years. Models are in lingual views. Abbreviations: C (Canine), dC (deciduous canine) dI (deciduous incisor), DL (Dental lamina), dP (Deciduous Premolar), I (Incisor), M (Molar), P (Permanent Premolar), SL (successional lamina). Incisors were excluded in these models to save space as they had already erupted. Specimens were segmented between the ameloblast and outer enamel layers. Scale bars = 6 mm.

Supplementary Tables for Chapter 3

Supplementary Table A3.1 Tooth development and eruption sequence of upper teeth in the tammar wallaby, based on stages from Luckett (1993b). Cessation = ceases to grow, e+d = enamel and dentine distinguishable, - = tooth not visible, + = becomes part of functional dentition.

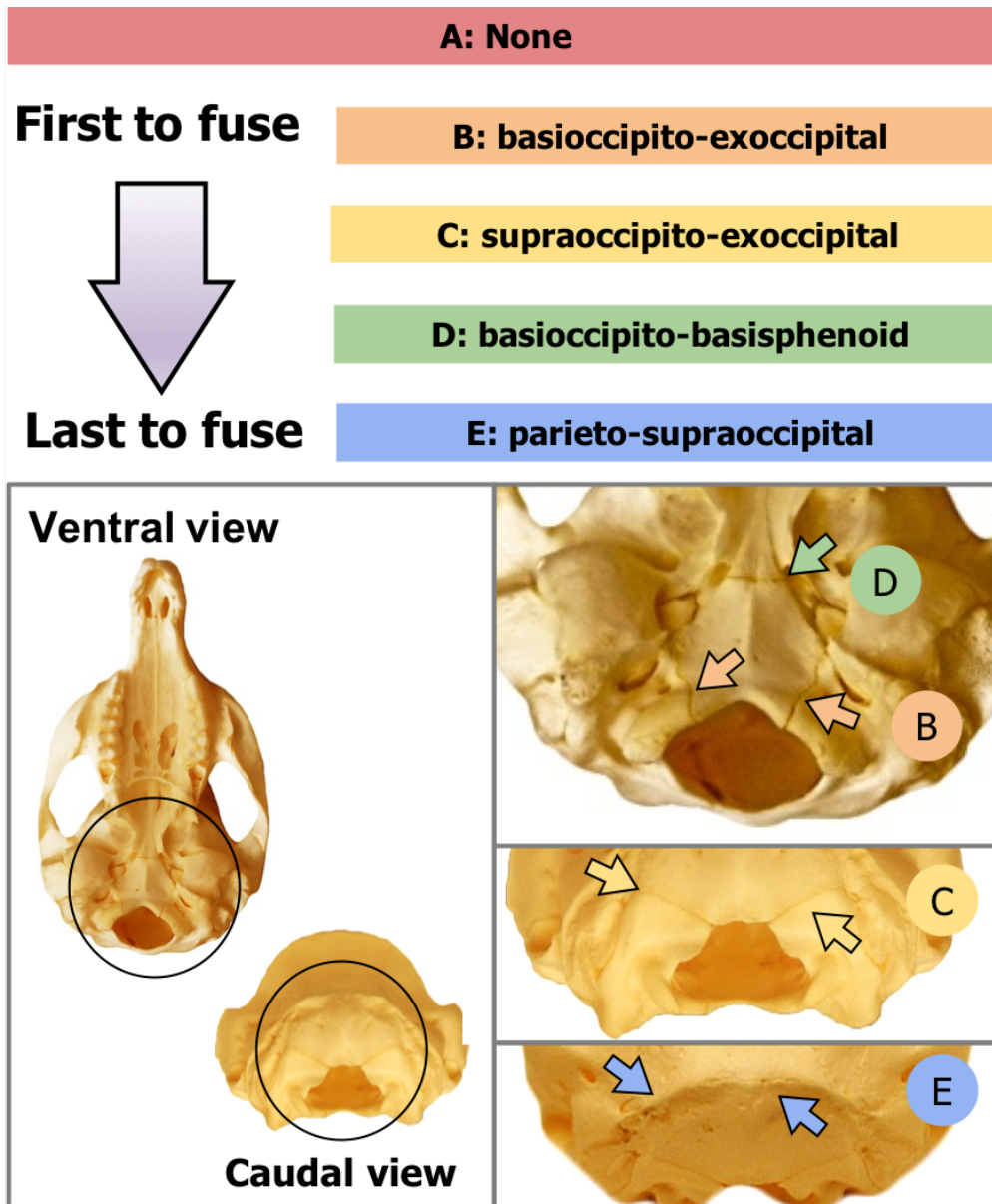
Specimen #	Age	Head Length (mm)	Incisors						Canines		Deciduous Premolar		Permanent Premolar	Molars			
			dl ¹	l ¹	dl ²	l ²	dl ³	l ³	dC ¹	C ¹	dP ²	dP ³	P ³	M ¹	M ²	M ³	M ⁴
11-245	23 days RPY		initiation	-	initiation	-	initiation	-	-	-	initiation	-	-	-	-	-	-
6103	0 days pp	7.77	mid bud	mid bud	early bud	early bud	early bud	early bud	initiation	-	-	mid bud	-	-	-	-	-
4180	7 days	11.5	mid bud	late bud	early bud	early bud	early bud	early bud	initiation	initiation	late cap	late cap	-	-	-	-	-
3935	14 days	12.36	mid bud	mid cap	late bud	late cap	mid bud	late bud	early bud	late cap	early bell	late bell	initiation	-	-	-	-
5563	30 days	18.77	early cap	early bell	early cap	early bell	mid bud	mid cap	-	late bell	late bell	late bell	early bud	late cap	-	-	-
6543	36 days	21.97	mineralisation	condensed	condensed	late bell	-	late cap	-	late bell	late bell	late bell	mid bud	early bell	lamina extension	-	-
5694	43 days	22.02	mineralisation	late bell	condensed	late bell	-	early bell	-	late bell	enamel chord	late bell	mid bud	mid bell	lamina extension	-	-
4946	57 days	28	cessation	mineralised	cessation	late bell	-	late bell	-	late bell	mineralised	mineralised	mid bud	late bell	initiation	-	-
5470	70 days	36.51	-	mineralised	-	late bell	-	late bell	-	mineralised	mineralised	mineralised	late bud	mineralisation	early cap	-	-
4942	74 days	36	-	mineralised	-	mineralised	-	mineralised	-	mineralised	mineralised	mineralised	mid cap	mineralisation	mid cap	-	-
5449	82 days	36	-	e + d	-	mineralised	-	mineralised	-	mineralised	mineralised	mineralised	late cap	e + d	early bell	-	-
4914	120 days	45	-	e + d	-	e + d	-	e + d	-	mineralised	mineralised	mineralised	late bell	e + d	mineralisation	-	-
7046	150 days	56.7	-	e + d	-	e + d	-	e + d	-	condensed	e + d	e + d	mineralisation	e + d	mineralisation	lamina extension	-
6843	238 days	83		erupted	-	erupted	-	erupted	-	-	erupted	erupted	mineralisation	erupted	e + d	bell stage	-
7386	320 days		-	+	-	+	-	+	-	-	+	+	e + d	+	erupted	mineralisation	lamina extension
7275	18 months		-	+	-	+	-	+	-	-	+	+	e + d	+	+	e + d	cap stage
6950	2 years		-	+	-	+	-	+	-	-	+	+	e + d	+	+	erupted	e + d
6587	3 years		-	+	-	+	-	+	-	-	+	+	e + d	+	+	+	e + d
4858	4 years		-	+	-	+	-	+	-	-	replaced	replaced	erupted	+	+	+	erupted

Supplementary Table A3.2 Tooth development and eruption sequence of lower teeth in the tammar wallaby, based on stages from Luckett (1993b). Cessation = ceases to grow, e+d = enamel and dentine distinguishable, - = tooth not visible, + = becomes part of functional dentition.

Specimen #	Age	Head Length (mm)	Incisors					Deciduous Premolar		Permanent Premolar	Molars			
			dl ₁	l ₁	dl ₂	dl ₃	l ₃	dP ₂	dP ₃	P ₃	M ₁	M ₂	M ₃	M ₄
11-245	23 days RPY		initiation	initiation	initiation	initiation	initiation	-	-	-	-	-	-	-
6103	0 days pp	7.77	mid bud	mid bud	early bud	late bud	late bud	-	early bud	-	-	-	-	-
4180	7 days	11.5	late bud	late bud	early bud	early cap	late cap	initiation	mid cap	-	-	-	-	-
3935	14 days	12.36	early bell	early bell	early bud	early cap	late bell	mid cap	early bell	initiation	bud stage	-	-	-
5563	30 days	18.77	late bell	late bell	early bud	early cap	mineralised	late bell	late bell	early bud	early bell	-	-	-
6543	36 days	21.97	late bell	late bell	early bud	-	e + d	late bell	late bell	mid bud	early bell	lamina extension	-	-
5694	43 days	22.02	mineralised	mineralised	mid bud	-	e + d	late bell	late bell	mid bud	mid bell	mid bud	-	-
4946	57 days	28	cessation	cessation	bud	-	e + d	mineralised	mineralised	mid bud	late bell	late bud	-	-
5470	70 days	36.51	cessation	cessation	cessation	-	e + d	mineralised	mineralised	late bud	mineralisation	late cap	-	-
4942	74 days	36	-	-	-	-	e + d	mineralised	mineralised	mid cap	mineralisation	early bell	-	-
5449	82 days	36	-	-	-	-	e + d	mineralised	mineralised	late cap	e + d	late bell	-	-
4914	120 days	45	-	-	-	-	e + d	mineralised	mineralised	late bell	e + d	late bell	-	-
7046	150 days	56.7	-	-	-	-	e + d	e + d	e + d	mineralisation	e + d	late bell	initiation	-
6843	238 days	83	-	-	-	-	erupted	erupted	erupted	mineralisation	erupted	mineralisation	late bell	-
7386	320 days		-	-	-	-	+	+	+	e + d	+	erupted	mineralisation	-
7275	18 months		-	-	-	-	+	+	+	e + d	+	+	e + d	lamina extension
6950	2 years		-	-	-	-	+	+	+	e + d	+	+	erupted	mineralisation
6587	3 years		-	-	-	-	+	replaced	replaced	erupted	+	+	+	e + d
4858	4 years		-	-	-	-	+	-	-	+	+	+	+	erupted

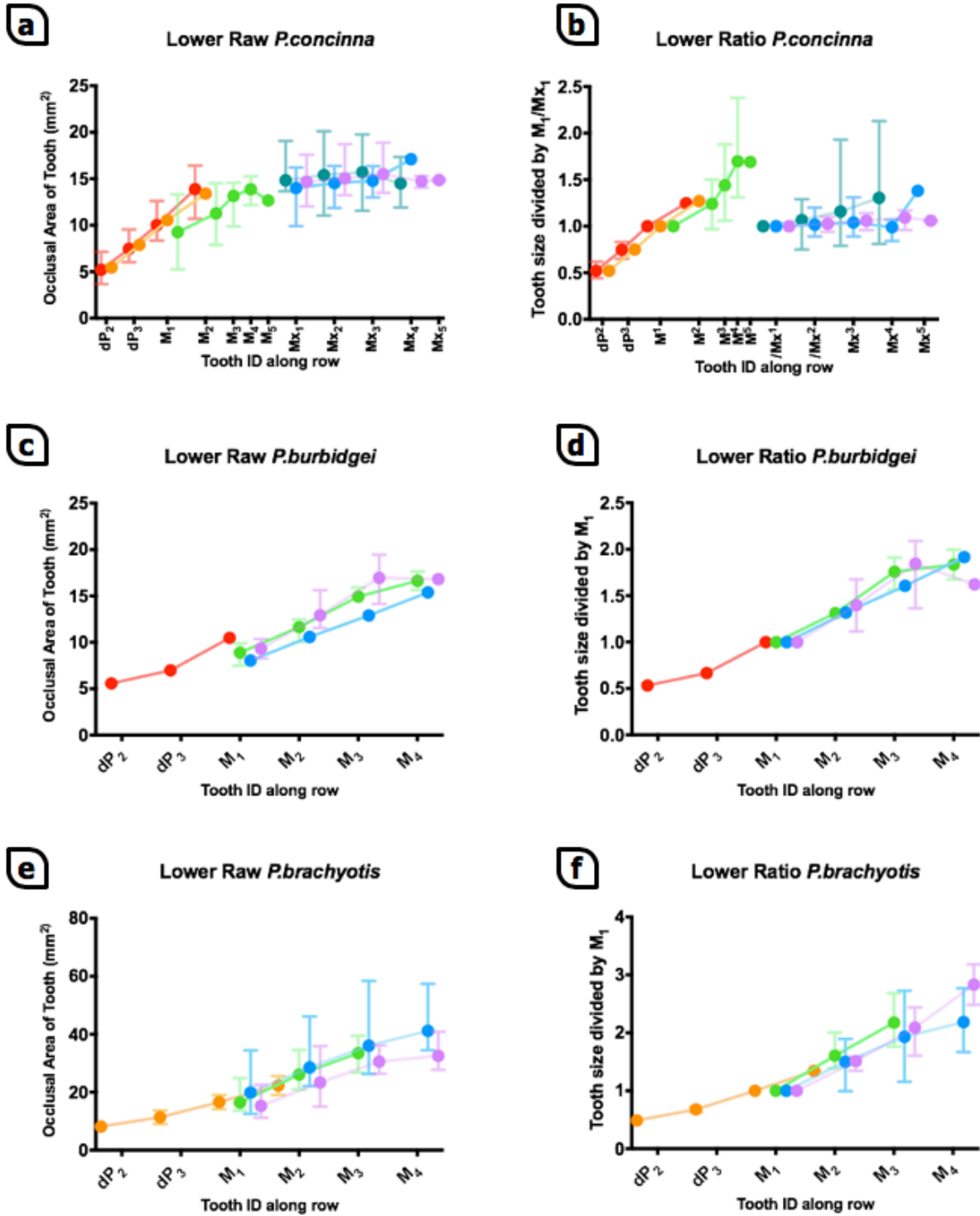
APPENDIX C

Supplementary Figures for Chapter 4

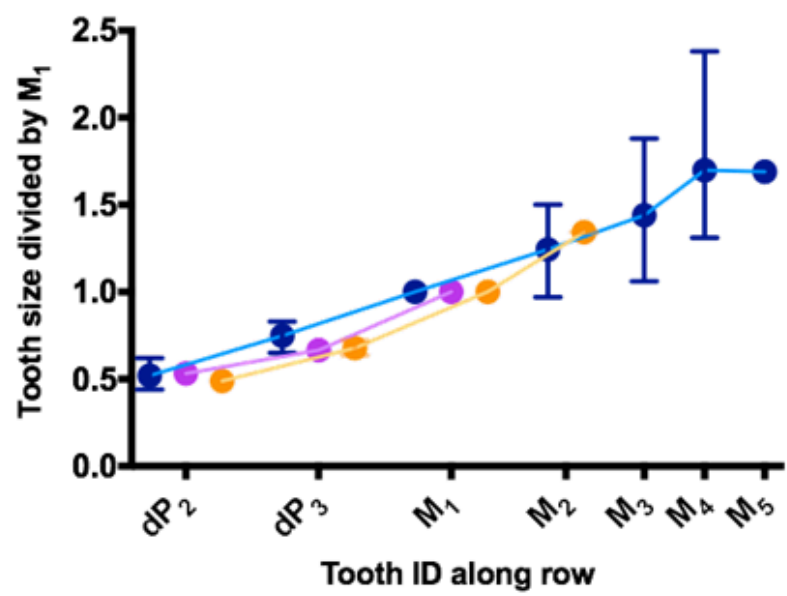
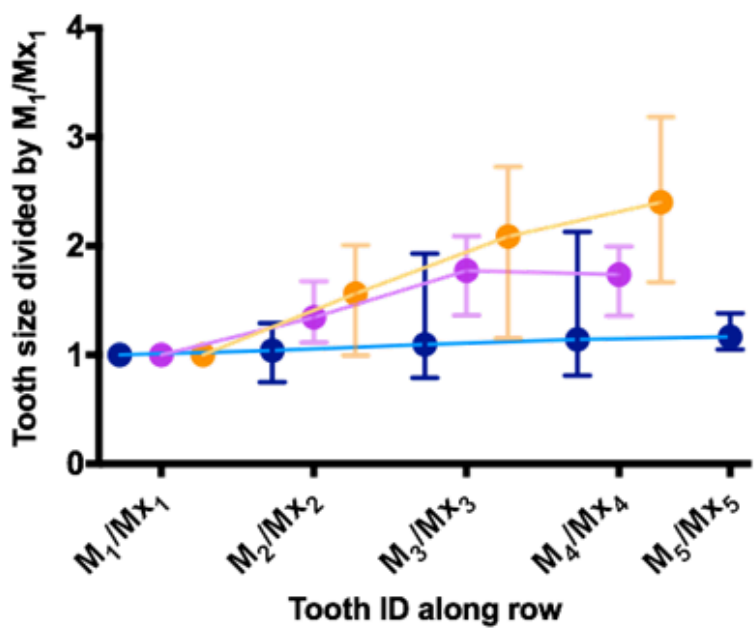


Supplementary Figure A4.1 Suture Closure pattern of *Petrogale* species, based on Rager *et al.* 2014. Suture closure order consisted of five categories (A-E): A) none closed; B-E) each suture closure in order, where the basioccipito-exoccipital is the first, parieto-supraoccipital the last

● A ● B ● C1 ● C2 ● D ● E



Supplementary Figure A4.2 *Petrogale* spp. lower tooth size (occlusal area in mm²) (A, C and E) and tooth ratios (tooth size divided by the M₁ or Mx₁ size) (B, D and F) patterns according to age, indicated by the suture closure stage (A-E). Whiskers represent range (min-max), where ranges smaller are not drawn. Suture stages are colour coded, located above the graphs.

a**Juvenile Petrogale Ratios (Lower)****b****Adult Petrogale Ratios (Lower)**

● *P. concinna* ● *P. burbidgei* ● *P. brachyotis*

Supplementary Figure A4.3 *Petrogale* spp. lower tooth ratios (tooth size divided by M_1/M_{x1} size) for a) juveniles (premolars present) and b) adults (molars only). Whiskers represent range (min-max), where ranges smaller are not drawn.

Supplementary Tables for Chapter 4

Supplementary Table A4.1 List of *Petrogale* spp. specimens used in this study, sorted by museum location. Includes suture closure category (A-E), skull length (mm) and eruption pattern (DP= deciduous premolars present, P= P3 present, M=molars only or P3 worn).¹ Museum abbreviations and locations: Australian Museum (AM), Sydney; Australian National Wildlife Collection (AWRC), Canberra; Museum and Art Gallery of Northern Territory (MAGNT), Darwin; Museums Victoria (MV), Melbourne; Monash University Zoology Research Collection (MZRC), Melbourne; South Australian Museum (SAM), Adelaide; and Western Australian Museum (WAM), Perth. "-" indicates data not available.

Museum and accession prefix	Species	Specimen #	Suture closure stage	Skull length (mm)	Eruption Pattern	Known Age
AM M	<i>P. brachyotis</i>	1254	-	79.00	P	-
AM M	<i>P. brachyotis</i>	7702	D	-	M	-
AM M	<i>P. brachyotis</i>	10363	D	97.00	P	-
AM M	<i>P. burbidgei</i>	22316	E	73.00	p	-
AM M	<i>P. concinna</i>	1222	D	77.00	P	-
AWRC CM	<i>P. brachyotis</i>	6803	B	77.45	P	-
AWRC CM	<i>P. brachyotis</i>	7884	C	92.06	P	-
AWRC CM	<i>P. brachyotis</i>	7921	-	-	P	-
AWRC CM	<i>P. brachyotis</i>	11995	C	100.47	M	-
AWRC CM	<i>P. brachyotis</i>	13577	C	90.66	M	-
AWRC CM	<i>P. brachyotis</i>	15281	D	99.87	P	-
AWRC CM	<i>P. brachyotis</i>	15281	C	100.92	P	-
AWRC CM	<i>P. brachyotis</i>	15283	A	69.30	DP	-
AWRC CM	<i>P. brachyotis</i>	15302	D	100.01	M	-
AWRC CM	<i>P. brachyotis</i>	15305	E	97.07	P	-
AWRC CM	<i>P. brachyotis</i>	15306	C	98.50	P	-
AWRC CM	<i>P. brachyotis</i>	15311	E	96.58	P	-

AWRC CM	<i>P. brachyotis</i>	15313	D	101.97	P	-
AWRC CM	<i>P. brachyotis</i>	15315	C	103.55	P	-
AWRC CM	<i>P. brachyotis</i>	15318	E	105.00	P	-
AWRC CM	<i>P. brachyotis</i>	15320	D	100.06	M	-
AWRC CM	<i>P. brachyotis</i>	15326	D	100.70	M	-
AWRC CM	<i>P. brachyotis</i>	15378	D	99.75	P	-
AWRC CM	<i>P. brachyotis</i>	15380	C	97.25	P	-
AWRC CM	<i>P. brachyotis</i>	15385	E	98.91	P	-
AWRC CM	<i>P. brachyotis</i>	15387	C	94.07	P	-
AWRC CM	<i>P. brachyotis</i>	15388	E	104.10	P	-
AWRC CM	<i>P. brachyotis</i>	15391	C	100.59	M	-
AWRC CM	<i>P. brachyotis</i>	15425	E	104.93	P	-
AWRC CM	<i>P. brachyotis</i>	15510	C	99.09	P	-
AWRC CM	<i>P. brachyotis</i>	15511	E	100.02	M	-
AWRC CM	<i>P. brachyotis</i>	18201	C	95.31	P	-
AWRC CM	<i>P. brachyotis</i>	24234	D	-	M	-
AWRC CM	<i>P. burbidgei</i>	15373	D	69.55	DP	-
AWRC CM	<i>P. burbidgei</i>	15561	E	74.61	P	-
AWRC CM	<i>P. burbidgei</i>	15562	E	72.99	P	-
AWRC CM	<i>P. burbidgei</i>	18037	A	47.39		-
AWRC CM	<i>P. concinna</i>	7603	D	74.97	P	-
AWRC CM	<i>P. concinna</i>	8766	B	67.18	DP	-
AWRC CM	<i>P. concinna</i>	8767	E	74.65	P	-
AWRC CM	<i>P. concinna</i>	8768	E	77.24	P	-
AWRC CM	<i>P. concinna</i>	8785	D	73.20	P	-
MAGNT U	<i>P. brachyotis</i>	103	E	100.67	M	-
MAGNT U	<i>P. brachyotis</i>	484	C	85.68	P	-
MAGNT U	<i>P. brachyotis</i>	497	A	84.22	P	-

MAGNT U	<i>P. brachyotis</i>	1030	E	98.65	P	-
MAGNT U	<i>P. brachyotis</i>	1180	E	96.21	P	-
MAGNT U	<i>P. brachyotis</i>	2002	C	91.76	M	-
MAGNT U	<i>P. brachyotis</i>	3158	A	64.00		-
MAGNT U	<i>P. brachyotis</i>	3160	E	98.37	P	-
MAGNT U	<i>P. brachyotis</i>	3162	A	76.22	P	-
MAGNT U	<i>P. brachyotis</i>	3166	E	87.88	M	-
MAGNT U	<i>P. brachyotis</i>	3171	B	72.01	DP	-
MAGNT U	<i>P. brachyotis</i>	3173	E	88.26	M	-
MAGNT U	<i>P. brachyotis</i>	3175	C	91.35	M	-
MAGNT U	<i>P. brachyotis</i>	3176	-	-	P	-
MAGNT U	<i>P. brachyotis</i>	3177	B	73.05	P	-
MAGNT U	<i>P. brachyotis</i>	3178	D	94.93	M	-
MAGNT U	<i>P. brachyotis</i>	4066	A	75.52	P	-
MAGNT U	<i>P. brachyotis</i>	4067	C	77.04	P	-
MAGNT U	<i>P. brachyotis</i>	4114	B	72.07	DP	-
MAGNT U	<i>P. brachyotis</i>	4120	C	86.20	P	-
MAGNT U	<i>P. brachyotis</i>	4188	C	96.93	P	-
MAGNT U	<i>P. brachyotis</i>	4189	C	-	M	-
MAGNT U	<i>P. brachyotis</i>	4314	C	91.98	P	-
MAGNT U	<i>P. brachyotis</i>	4682	E	90.72	M	-
MAGNT U	<i>P. concinna</i>	3181	E	75.49	P	-
MAGNT U	<i>P. concinna</i>	3183	D	69.51	DP	-
MAGNT U	<i>P. concinna</i>	3185	D	72.67	M	-
MAGNT U	<i>P. concinna</i>	3187	E	73.97	P	-
MAGNT U	<i>P. concinna</i>	6117	E	79.75	P	-
MZRC	<i>P. concinna</i>	4410	C	70.28	DP	-
MZRC	<i>P. concinna</i>	4411	A	65.50	DP	-

MZRC	<i>P. concinna</i>	4412	E	77.27	P	-
MZRC	<i>P. concinna</i>	4413	C	74.33	P	-
MZRC	<i>P. concinna</i>	4630	E	76.98	P	-
MZRC	<i>P. concinna</i>	4631	E	76.88	P	-
MZRC	<i>P. concinna</i>	5495	-	-	M	-
MZRC	<i>P. concinna</i>	5496	-	-	M	-
MZRC	<i>P. concinna</i>	6007	D	77.10	P	-
MZRC	<i>P. concinna</i>	6199	A	53.97	DP	-
MZRC	<i>P. concinna</i>	6225	E	74.94	P	-
MZRC	<i>P. concinna</i>	6295	E	72.28	DP	-
MZRC	<i>P. concinna</i>	6296	E	77.37	P	-
MZRC	<i>P. concinna</i>	6395	D	77.32	P	-
MZRC	<i>P. concinna</i>	6397	C	74.40	P	2 years
MZRC	<i>P. concinna</i>	6398	A	52.78	DP	6 months
MZRC	<i>P. concinna</i>	6399	C	73.94	P	18 months
MZRC	<i>P. concinna</i>	6408	C	72.28	DP	-
MZRC	<i>P. concinna</i>	6409	A	63.97	DP	-
MZRC	<i>P. concinna</i>	6410	A	57.10	DP	6 months
MZRC	<i>P. concinna</i>	6411	E	74.90	P	-
MZRC	<i>P. concinna</i>	6412	D	76.82	P	-
MZRC	<i>P. concinna</i>	6413	D	74.48	P	-
MZRC	<i>P. concinna</i>	6414	E	71.94	DP	-
MZRC	<i>P. concinna</i>	6465	A	42.45	DP	5 months
SAM M	<i>P. brachyotis</i>	81	E	100.00	P	-
SAM M	<i>P. brachyotis</i>	285	B	78.00	P	-
SAM M	<i>P. brachyotis</i>	286	D	86.00	P	-
SAM M	<i>P. brachyotis</i>	287	C	79.00	P	-
SAM M	<i>P. brachyotis</i>	288	-	-	P	-

SAM M	<i>P. brachyotis</i>	5141	B	73.00	P	-
SAM M	<i>P. brachyotis</i>	10157	C	83.00	P	-
VM DTC	<i>P. brachyotis</i>	186	E	89.42	M	-
VM DTC	<i>P. brachyotis</i>	188	E	96.68	P	-
VM DTC	<i>P. brachyotis</i>	190	D		M	-
VM DTC	<i>P. brachyotis</i>	192	E	87.72	M	-
VM DTC	<i>P. brachyotis</i>	196	B		M	-
VM DTC	<i>P. brachyotis</i>	199	A	77.78	P	-
VM DTC	<i>P. brachyotis</i>	201	D		M	-
VM DTC	<i>P. brachyotis</i>	206	E	87.02	P	-
VM DTC	<i>P. brachyotis</i>	207	D	87.50	M	-
VM DTC	<i>P. brachyotis</i>	208	E	88.02	M	-
VM DTC	<i>P. brachyotis</i>	209	E	97.21	P	-
VM DTC	<i>P. brachyotis</i>	210	E	98.41	M	-
VM M	<i>P. brachyotis</i>	26101	D	104.23	DP	-
VM M	<i>P. concinna</i>	6475	C	72.30	P	-
VM M	<i>P. concinna</i>	6478	E	73.15	P	-
VM M	<i>P. concinna</i>	6480	C	72.43	DP	-
WAM M	<i>P. brachyotis</i>	2006	C	96.04	P	-
WAM M	<i>P. brachyotis</i>	3025	C	96.28	P	-
WAM M	<i>P. brachyotis</i>	3128	C	95.36	P	-
WAM M	<i>P. brachyotis</i>	3129	-	-	P	-
WAM M	<i>P. brachyotis</i>	4094	D	105.35	P	-
WAM M	<i>P. brachyotis</i>	4095	C	97.50	M	-
WAM M	<i>P. brachyotis</i>	4142	C	94.74	P	-
WAM M	<i>P. brachyotis</i>	4143	D	102.78	P	-
WAM M	<i>P. brachyotis</i>	4144	D	107.93	P	-
WAM M	<i>P. brachyotis</i>	4145	C	95.24	M	-

WAM M	<i>P. brachyotis</i>	11598	D	-	M	-
WAM M	<i>P. brachyotis</i>	11599	E	103.97	P	-
WAM M	<i>P. brachyotis</i>	11602	C	100.42	M	-
WAM M	<i>P. brachyotis</i>	11603	E	102.02	P	-
WAM M	<i>P. brachyotis</i>	11604	E	99.33	P	-
WAM M	<i>P. brachyotis</i>	11641	C	98.78	P	-
WAM M	<i>P. brachyotis</i>	12398	C	103.33	P	-
WAM M	<i>P. brachyotis</i>	13726	C	96.31	P	-
WAM M	<i>P. brachyotis</i>	14321	D	97.15	P	-
WAM M	<i>P. brachyotis</i>	14323	C	93.97	P	-
WAM M	<i>P. brachyotis</i>	14324	D	102.98	P	-
WAM M	<i>P. brachyotis</i>	14702	C	97.80	P	-
WAM M	<i>P. brachyotis</i>	15355	C	98.00	P	-
WAM M	<i>P. brachyotis</i>	17134	C	108.14	P	-
WAM M	<i>P. brachyotis</i>	17135	C	98.24	M	-
WAM M	<i>P. brachyotis</i>	18106	C	99.58	P	-
WAM M	<i>P. brachyotis</i>	19066	C	88.32	M	-
WAM M	<i>P. brachyotis</i>	19205	C	102.85	M	-
WAM M	<i>P. brachyotis</i>	19206	B	84.63	P	-
WAM M	<i>P. brachyotis</i>	19540	D	100.55	M	-
WAM M	<i>P. brachyotis</i>	19588	C	91.95	P	-
WAM M	<i>P. brachyotis</i>	19865	C	99.95	P	-
WAM M	<i>P. brachyotis</i>	19880	D	94.82	P	-
WAM M	<i>P. brachyotis</i>	24401	C	93.76	P	-
WAM M	<i>P. brachyotis</i>	24402	D	109.38	P	-
WAM M	<i>P. brachyotis</i>	24511	C	87.53	M	-
WAM M	<i>P. brachyotis</i>	32781	C	-	M	-
WAM M	<i>P. brachyotis</i>	47422	D	-	M	-

WAM M	<i>P. brachyotis</i>	54699	C	-	M	-
WAM M	<i>P. brachyotis</i>	55155	D	105.88	P	-
WAM M	<i>P. brachyotis</i>	61261	D	106.91	P	-
WAM M	<i>P. burbidgei</i>	9313	D	71.61	DP	-
WAM M	<i>P. burbidgei</i>	9314	C	67.48	DP	-
WAM M	<i>P. burbidgei</i>	15417	D	71.17	DP	-
WAM M	<i>P. burbidgei</i>	15418	D	-	M	-
WAM M	<i>P. burbidgei</i>	15827	E	78.78	P	-
WAM M	<i>P. burbidgei</i>	15832	C	71.88	DP	-
WAM M	<i>P. burbidgei</i>	24982	C	71.58	DP	-
WAM M	<i>P. burbidgei</i>	52665	C	71.24	DP	-
WAM M	<i>P. burbidgei</i>	54836	C	70.50	DP	-
WAM M	<i>P. burbidgei</i>	55191	-	-	P	-
WAM M	<i>P. burbidgei</i>	55235	C	75.02	P	-
WAM M	<i>P. concinna</i>	558	A	58.49	DP	-
WAM M	<i>P. concinna</i>	2007	-	-	P	-
WAM M	<i>P. concinna</i>	3185	A	56.68	DP	-
WAM M	<i>P. concinna</i>	4168	C	75.98	P	-
WAM M	<i>P. concinna</i>	4169	D	78.06	P	-
WAM M	<i>P. concinna</i>	4170	C	72.12	DP	-
WAM M	<i>P. concinna</i>	4171	-	-	P	-
WAM M	<i>P. concinna</i>	4172	C	71.25	DP	-
WAM M	<i>P. concinna</i>	4174	B	72.53	DP	-
WAM M	<i>P. concinna</i>	4540	C	71.34	DP	-
WAM M	<i>P. concinna</i>	8499	-	-	P	-
WAM M	<i>P. concinna</i>	9288	C	71.82	DP	-
WAM M	<i>P. concinna</i>	9346	B	69.36	DP	-
WAM M	<i>P. concinna</i>	9360	C	68.25	DP	-

WAM M	<i>P. concinna</i>	10317	-	-	P	-
WAM M	<i>P. concinna</i>	10319	B	-	M	-
WAM M	<i>P. concinna</i>	12400	C	77.97	P	-
WAM M	<i>P. concinna</i>	12401	A	66.61	DP	-
WAM M	<i>P. concinna</i>	17416	C	76.55	P	-
WAM M	<i>P. concinna</i>	24423	C	70.81	DP	-
WAM M	<i>P. concinna</i>	26845	C	77.07	P	-
WAM M	<i>P. concinna</i>	55215	-	-	P	-

APPENDIX D

Supplementary Materials and Methods

Reagents

For Tissue Dissection

1. Dulbecco's phosphate-buffered saline (PBS), pH 7.4
2. 70% ethanol, in a spray bottle at room temperature (RT)

For Tissue Culture

The tissue culture media comprised of:

1. Dulbecco's phosphate-buffered saline, modified (D-PBS) (Thermofisher Scientific) with the following added:
 - a. 1% v/v/ GlutaMAX supplement (Gibco/ Thermofisher Scientific)
 - b. 10% v/v heat-inactivated Fetal Bovine Serum (FBS; Gibco/Thermo Scientific, USDA-approved regions)
 - c. 0.1% (v/v) PS (Gibco/Thermofisher Scientific, 10,000 U/mL), streptomycin 10,000 µg/mL
2. F-12 (Ham's F-12 Nutrient Mix, Gibco/Thermofisher)

We combined the DMEM media and F-12 at a 1:1 ratio. For samples that included tooth germs e16 or older, we also added 100–150 µg/mL Ascorbic acid (Merck, Darmstadt, DE, for analysis EMSURE® ACS,ISO,Reag. Ph Eur) which is required for tooth mineralisation.

For details on solutions preparation and storage, see Närhi and Thesleff (2010).

Materials

All glassware and metal instruments were sterile. We used autoclaved glassware. For sterilization of forceps and scissors we used Steri 250 glass bead sterilizer (Simon Keller Ltd. Burgdorf, CH) or when not available, coated equipment in 70% ethanol and burned off through a Bunsen flame. The following are lists of materials that we used that we recommend for these methods:

For Tissue Dissection

1. Stainless steel sterilised watch-makers forceps (at least two pairs), perforated spoon and surgical scissors
2. Glass (10cm diameter, autoclaved) or disposable plastic bacteriological petri dishes (90mm Petri Dish, Techno PLas, Pacific Laboratory Products) (NOTE: Glass does not get scratched but may not be sterile)
3. Disposable 19-gauge needles (Terumo, Neolus) and 1-mL plastic syringes (Terumo).

For Tissue Culture

1. Culture dishes: 35 mm/10 mm plastic Petri dishes (Falcon 100 mm Cell Culture Dish, In Vitro Technology).
2. Metal grids: were made using a medical grade stainless-steel sheet (0.66mm Aperture - 0.19mm Wire Diameter, The Mesh Company), cut into 4x4cm squares, wrapped around the lid of a 15mL falcon tube, bending down the sides to produce a ~30mm diameter platform with 3mm high sides. We used curved secateurs to cut away the excess corners to ensure the sides were of equal height. The grids were then stored in ethanol in a 50mL falcon tube. Unlike Närhi and Thesleff (2010), we did not pierce holes in the mesh for photographs.
3. Filters: 25-mm diameter, 0.2µm pore size, Isopore polycarbonate track-etched Membranes (Millipore, Sigma-Aldrich). These were cut using sterilised surgical scissors into ~4x4mm square piece and stored in ethanol in a 50mL falcon tube.
4. Incubator: (Forma Scientific 3111, model) was set at 37°C, in an atmosphere of 5% CO₂ in air and 90–95% humidity.

Methods

Preparation of Culture Plates

1. We placed metal grids in the 35-mm culture dishes. We then added 2-3mL of culture medium (See Item 1 in Tissue Culture Reagents above) by pipetting through the grid and avoiding air bubbles.
2. We pierced a hole at the top of the mesh, as well as marked the culture dish with a permanent marker, to help keep track of orientation of the tissues during culturing.

Removal of Embryos

1. After spraying the belly of the mouse with 70% ethanol, we used tweezers and surgical scissors to cut open the mouse abdomen, revealing the uterine horn. With tweezers we raised the uterine horn out of the abdomen while removing the connective tissue with the surgical scissors. The uterus was able to be removed in-tact. We placed the uterus immediately into a 10cm disposable petri-dish, filled with chilled (4°C) D-PBS.
2. We cut open the uterine horn by holding one side with the tweezers and cutting through the individual fetal membranes with the surgical scissors to release the embryos. If the correct angle was found, this could be done in a single continuous action. Depending on the size of the embryos (e14 in particular), we used a stereo-microscope to help remove the embryos.
3. Using a sterilised metal scoop or forceps, we transferred the embryos to a fresh disposable petri-dish filled with 4°C D-PBS. We cut off the heads using disposable needles attached to disposable syringes, passing the sharp sides of the needles against each other.
4. The heads were then stored together in one D-PBS-filled petri dish on ice and in a 4°C fridge. We occasionally separated the embryos into a 12-well plate, when there is more than 1 litter.

Dissection of Tissues

1. Taking one head at a time from the chilled D-PBS, we transferred the heads to a fresh glass or disposable plastic petri dish, and quarter-filled the dish with 4°C D-PBS. This prevented the tissue from floating, making dissection easier.

2. Laying the head to its side, we began with first making a coronal cut behind the ears, to remove the back of the head.
3. Then turning the snout to face upwards, we held one side with one needle, and cut a slice between the upper and lower jaws, through the cheek. This was repeated on the other side so that the mandible became separated (with tongue still intact).
4. We cut around one side of the tongue, separating one lower tooth bud from the other (still attached to the tongue). This helped to find the next tooth bud and also helped identify right from left for replicates. We then proceeded to dissect out the isolated lower tooth germ, first removing the cartilage and excess tissue, holding down the tissue with one needle, and cutting with the other. We removed as much of the jaw mesenchyme layer as possible.
5. To pick up the isolated tooth bud, we used tweezers to hold a cut square of filter paper, placed it into the D-PBS, ensuring its completely submerged in liquid, and scoop up the tooth bud. Using the microscope, we corrected the orientation of the bud with the epithelium side facing up. We then placed the tooth bud and paper on the prepared petri dish, and into the incubator.

Culturing Combinations

Due to difference in litter ages (depends when the female is mated), we trialled between both e16 and e17 M2s. Also due to limited numbers of litters, we were not able to repeat each control for both e16 and e17 experimental treatments. We cultured e16 M2 alone as the control for e16 M2 anterior to e14 M1 treatment (distal end of anterior tooth faced mesial end of posterior tooth). For both e16 M2s and e17 M2s we had an anterior and posterior treatment (to the e14 M1) to determine whether position has an effect on growth. For the e17 M2s we also had a control where we simply separated it from its e17 M1, and cultured it, to see whether the simple act of separating the teeth apart affected growth (Figure 5.2). See Tables A5.1 to A5.4 for more details on conditions and number of replicates.

Culturing and Recording

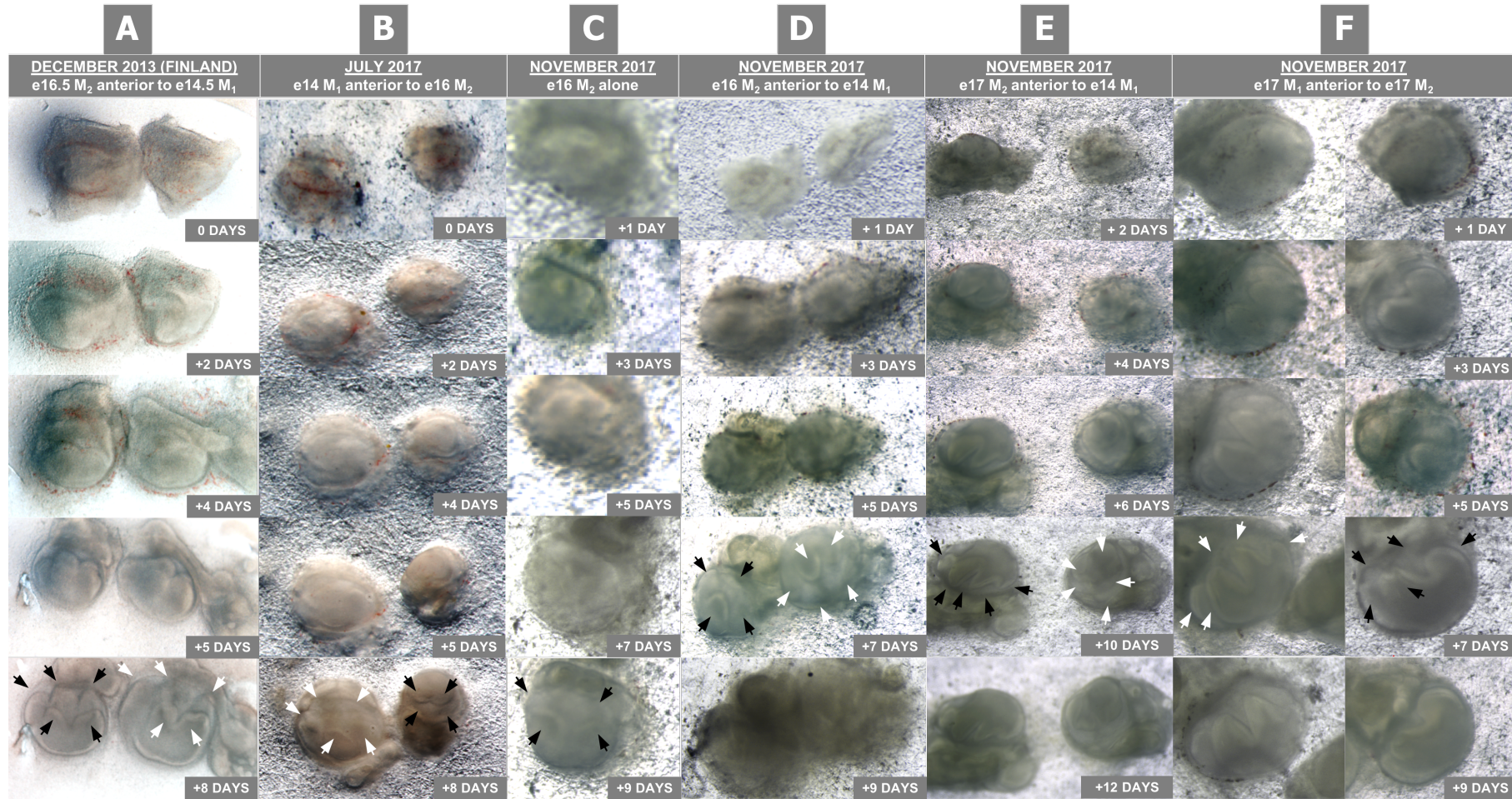
1. Tissues were cultured for a minimum of 5 days up to 2 weeks (see Table A5.1 – A5.4, for culture lengths of each replicate).

2. In the first 1-2 days of culturing, the tooth germs may have moved from their initial orientations, which were corrected using needles to gently push them back into place. After this period they did not move and fixed in position on the filter paper.
3. Culture media was changed every second day. We removed the old media by pipetting through the grid and pipetting fresh pre-warmed media back through the grid.
4. Photos were taken every day using the Zeiss Stereo Discovery V20 with an Axio 506 colour camera. To take photos, we lifted the filter papers holding the tissues off, and placed them on a sterile petri dish to take photos. We found with the original method from Närhi and Thesleff (2010), of taking photos through the holes in the metal grids, that our tissues would soon outgrow the width of the holes, and be required to be lifted off the grid eventually. For our photos we used the dark field settings to reduce reflections coming off the wet tissue surfaces.

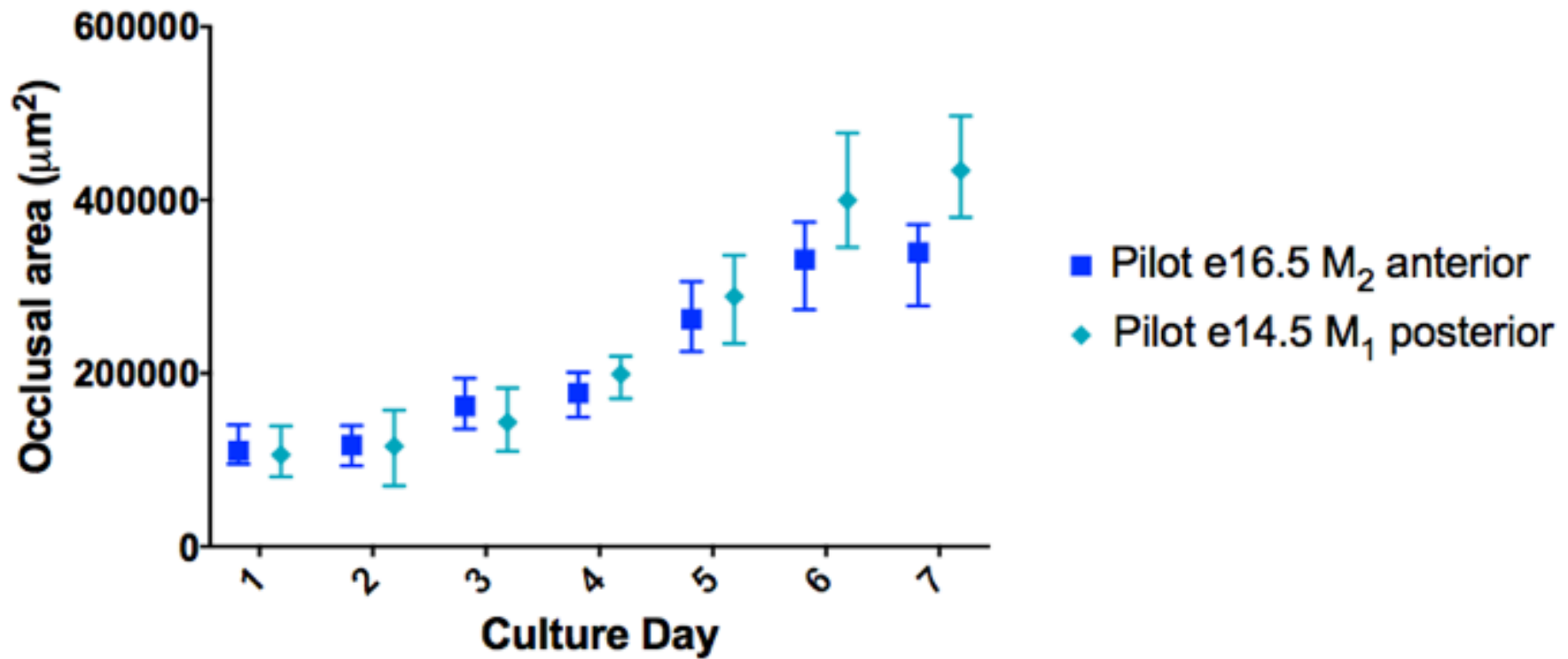
Measurements and Analyses

1. Using the photographs, we measured outlines of the tooth buds at the maximum occlusal perimeter. These were created using the polygonal tool within Fiji V 2.0.0 (Schindelin *et al.* 2012). A scale was set for each photo and then the area was measured (in μm^2). Paired two-tailed t-tests were conducted on e16 and e17 M2 growths between different control and experimental treatments using Prism version 7.0d (for Mac OS X. GraphPad Software, La Jolla California USA, www.graphpad.com).
2. The final number of tooth cusps formed for each bud were tabulated. As *in-vitro* cultured teeth do not reach its final cusp morphology, we counted the presence of one cusp of the bi-cuspid teeth as present for that structure, including the anteroconid. If a minimum of one of the two were not present, then they were recorded as absent.

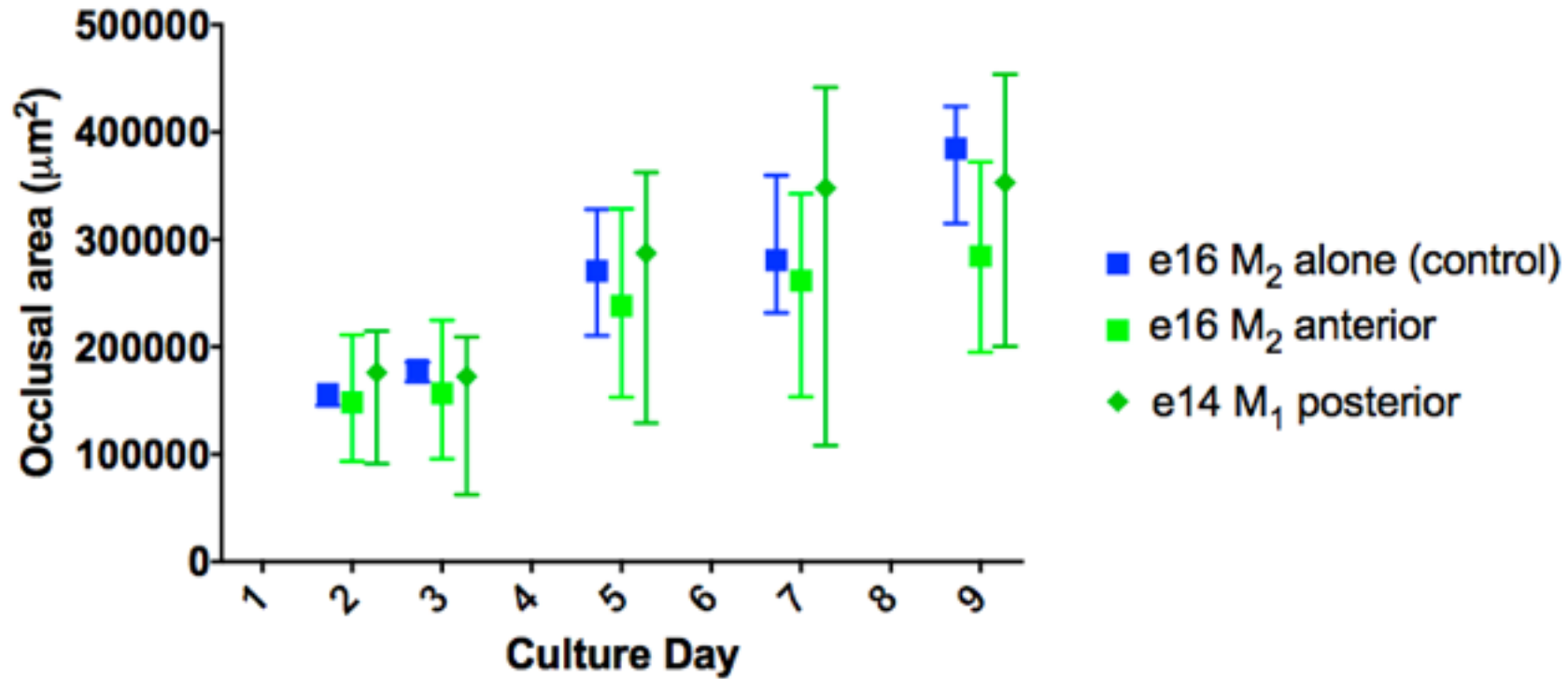
Supplementary Figure for Chapter 5



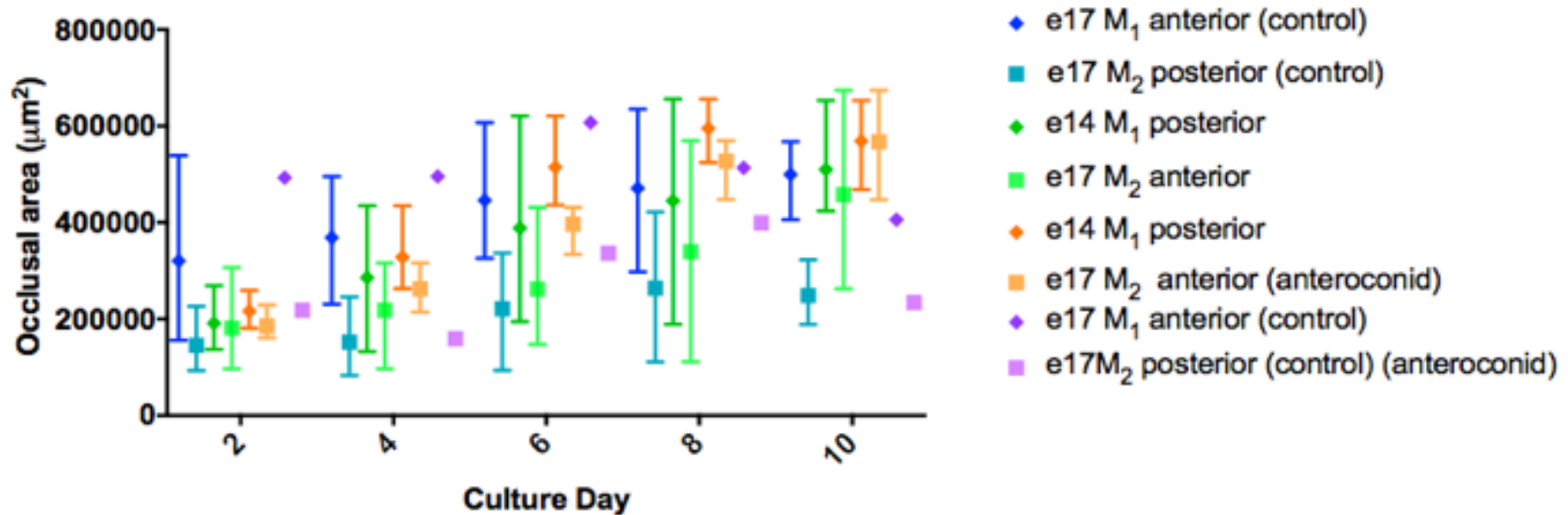
Supplementary Figure A5.1 Tissue culture growths of pilot (A) and main (B-F) experiments. Cultures were conducted over 8-12 days. Cusp number was counted, where arrows indicate numbers of cusps on M₁s (white) and M₂s (black).



Supplementary Figure A5.2 Mean outline area (µm²) of E14.5 M₁s cultured posteriorly to e16.5 M₂s. Sizes measured from culture day 1 to 7. Squares=M₂s, diamonds=M₁s, Anterior/posterior indicates orientation during culturing. Whiskers give ranges of measurements (min-max). Conducted at the University of Helsinki, Finland, from the 5th December, 2013.



Supplementary Figure A5.3 Mean maximum outline area (μm^2) of E14 M₁s cultured posteriorly to E16 M₂s, and e16 M₂s cultured alone. Sizes measured from Culture Day 2 to 9. Squares=M₂s, diamonds=M₁s, experimental pairs are colour coded to match. Anterior/posterior indicates orientation during culturing. Whiskers give ranges of measurements (min-max). Conducted at the Monash University, Australia, from the 23rd November 2017.



Supplementary Figure A5.4 Mean maximum outline area (μm^2) of e14 M₁s cultured posteriorly and e17 M₁s cultured anteriorly to e17 M₂s. E17 M₂s that produced an additional cusp are labelled as separate “anteroconid” series. Sizes measured from Culture Day 2 to 10. Squares=M₂s, diamonds=M₁s, experimental pairs are colour coded to match. Anterior/posterior indicates orientation during culturing. Whiskers give ranges of measurements (min-max). Conducted at the Monash University, Australia, from the 24th November 2017.

Supplementary Tables for Chapter 5

Supplementary Table A5.1 Finland tissue culture measurements and samples started on the 5th December 2013

Occlusal outline size (μm^2)										
Sample #	Tooth	Initial Tooth Age	5th Dec	6th Dec	7th Dec	8th Dec	9th Dec	10th Dec	11th Dec	Final Cusp Count
1	M ₁	e14.5	80888.47	70080.05	143337.3	211741.9	331606.9	477265	497123.1	5
1	M ₂	e16.5	107548.8	114204	139834.8	201127.2	305761.9	374684.5	371707.1	5*
2	M ₁	e14.5	139173.1	117303.2	137595	170881.4	252019.2	369680.9	380018.5	5
2	M ₂	e16.5	97894.26	93123.87	194360.8	176393.4	269042.2	341990.3	366344.5	5*
3	M ₁	e14.5	109926.7	157368.3	110114.6	193886.1	234456	345432.5	389992.8	5
3	M ₂	e16.5	140658.6	139765.8	135813.6	181402.1	225269.2	273496.3	277937.7	5*
4	M ₁	e14.5	93786.01	118454.2	183160.4	219599.1	336288.1	406730.9	468784.4	5
4	M ₂	e16.5	95587.66	121763.8	178589.6	149144.7	249879.2	335046.9	342123.8	5*

Supplementary Table A5.2 Australian tissue culture measurements and samples started on the JULY 2017. Conditions were e16 M₂ posterior to e14 M₁.

Sample #	Tooth	Initial Tooth Age	Final Cusp Count
1	M ₁	e14	4
1	M ₂	e16	5
2	M ₁	e14	4
2	M ₂	e16	5
3	M ₁	e14	4
3	M ₂	e16	5
4	M ₁	e14	4
4	M ₂	e16	5
5	M ₁	e14	4
5	M ₂	e16	5
6	M ₁	e14	4
6	M ₂	e16	5
7	M ₁	e14	4
7	M ₂	e16	5
8	M ₁	e14	4
8	M ₂	e16	5
9	M ₁	e14	4
9	M ₂	e16	5
10	M ₁	e14	-
10	M ₂	e16	-
11	M ₁	e14	4
11	M ₂	e16	5

Supplementary Table A5.3 Australian tissue culture measurements and samples started on the 23rd November 2017. Conditions were e16 M₂ anterior to e14 M₁, and e16 M₂ cultured alone.

Samples #	Condition	Tooth	Initial Tooth age	Occlusal outline size (µm ²)					Final Cusp Count
				Day 2	Day 3	Day 5	Day 7	Day 9	
1	M ₁ -M ₂ transplant	M ₂	e16	93535.83	97264.89	153106.867	153678.842	195027.165	4
1	M ₁ -M ₂ transplant	M ₁	e14	91272.575	62455.415	129038.404	108127.666	200422.14	5
2	control M ₂ only	M ₂	e16	145343.224	167391.863	328093.163	359800.253	415475.184	4
3	M ₁ -M ₂ transplant	M ₂	e16	138098.489	224719.243	328663.622	342685.547	337482.243	4
3	M ₁ -M ₂ transplant	M ₁	e14	193682.27	184542.421	360407.353	401166.209	453850.047	5
5	M ₁ -M ₂ transplant	M ₂	e16	164106.584	182257.564	240624.58	248370.462	210833.341	4
5	M ₁ -M ₂ transplant	M ₁	e14	187597.518	202228.65	260899.08	352432.098	242983.456	5
6	control M ₂ only	M ₂	e16	165449.586	183134.511	210425.729	251196.088	424004.216	4
7	M ₁ -M ₂ transplant	M ₂	e16	211205.738	95849.22	170062.332	226117.218	372480.187	4
7	M ₁ -M ₂ transplant	M ₁	e14	214894.483	209420.638	323769.683	436214.571	438103.14	5
9	M ₁ -M ₂ transplant	M ₂	e16	135379.7	184220.219	298500.254	338298.972	306576.695	4
9	M ₁ -M ₂ transplant	M ₁	e14	193437.551	203958.57	362566.364	441618.198	430229.345	5
10	control M ₂ only	M ₂	e16	158025.548	185647.168	274322.612	231698.149	314962.707	4

Supplementary Table A5.4 Australian tissue culture measurements and samples started on the 24th November 2017. Conditions were e17 M₂ cultured anteriorly to e14 M₁, and e17 M₂ cultured posteriorly to e17 M₁. * denotes additional cusp development, - means uncountable.

Occlusal outline size (µm ²)								
Samples #	Condition	Tooth	Day 2	Day 4	Day 6	Day 8	Day 10	Final cusp count
1	M ₁ -M ₂ transplant	M ₂	232289.385	249975.178	279101.536	319396.16		4
1	M ₁ -M ₂ transplant	M ₁	242590.03	314991.789	222220.191	298742.828		5
2	control M ₂ only	M ₂	73035.376	51743.191				4
2	control M ₁ only	M ₁	155641.948	123073.4				5
3	M ₁ -M ₂ transplant	M ₂	136316.989	178311.491	191076.692	282531.556		4
3	M ₁ -M ₂ transplant	M ₁	173042.883	176947.789	272405.219	350687.389		5
4	control M ₂ only	M ₂	155214.718	111363.924	198484.013	240986.468		4
4	control M ₁ only	M ₁	297800.191	302901.811	420929.732	365868.155		5
5	M ₁ -M ₂ transplant	M ₂	248178.71	177586.318	231012.869	296816.23		4
5	M ₁ -M ₂ transplant	M ₁	233148.189	263814.061	392023.425	428842.654		5
6	control M ₂ only	M ₂	226053.414		291603.707	301896.754		4
6	control M ₁ only	M ₁	162443.713		334753.683	399167.592		5
7	M ₁ -M ₂ transplant	M ₂	216295.215	306199.934	334062.64	510217.451		5*
7	M ₁ -M ₂ transplant	M ₁	149644.596	355973.151	403178.475	531259.623		5
8	control M ₂ only	M ₂	95277.186	82861.811	187833.514	143715.631		4
8	control M ₁ only	M ₁	318589.58	230510.74	415437.151	457695.231		5
9	M ₁ -M ₂ transplant	M ₂	173646.872	139928.194	286521.153	263660.693		4
9	M ₁ -M ₂ transplant	M ₁	139028.648	293105.387	370242.146	408305.55		5
10	control M ₂ only	M ₂	123255.724	109889.092	93759.644	111216.007		4
10	control M ₁ only	M ₁	377835.041	377242.372	370400.537	335997.769		5
11	control M ₂ only	M ₂						-
11	control M ₁ only	M ₁						-
12	M ₁ -M ₂ transplant	M ₂	306513.992	279107.972	209621.18	268097.46		4

12	M ₁ -M ₂ transplant	M ₁	247455.181	244464.909	375219.958	470913.101			5
13	control M ₂ only	M ₂	77526.617	61511.134					4
13	control M ₁ only	M ₁	255518.855	214176.765					5
14	M ₁ -M ₂ transplant	M ₂	96640.356	199666.343	210383.755	377214.584			4
14	M ₁ -M ₂ transplant	M ₁	268926.155	275112.661	399221.262	315971.863			5
15	control M ₂ only	M ₂	182249.522	131955.915	246378.046	296270.902			4
15	control M ₁ only	M ₁	193026.953	382952.456	517488.038	546145.642			5
16	M ₁ -M ₂ transplant	M ₂	228815.406	316509.089	424908.19	564957.922	579058.568		5
16	M ₁ -M ₂ transplant	M ₁	259126.013	434742.568	620536.753	655805.178	652806.893		5
17	control M ₂ only	M ₂	148040.25	245852.876		422067.216			4
17	control M ₁ only	M ₁	538905.098	383749.317		565299.441			5
18	M ₁ -M ₂ transplant	M ₂	167380.485	214755.323	333673.102	447894.972	447148.897		4
18	M ₁ -M ₂ transplant	M ₁	209793.943	286774.255	436236.728	605630.131	585923.419		5
19	control M ₂ only	M ₂	125684.264						-
19	control M ₁ only	M ₁	96055.242						-
20	M ₁ -M ₂ transplant	M ₂	169559.459	183573.557	188725.379	223291.511	262581.904		4
20	M ₁ -M ₂ transplant	M ₁	151316.052	224055.497	237611.683	320363.463	424047.872		5
21	control M ₂ only	M ₂	119275.268	107755.854	175256.183	179401.689	188409.282		4
21	control M ₁ only	M ₁	340513.546	364671.252	420028.658	562953.717	525646.222		5
22	M ₁ -M ₂ transplant	M ₂	171495.161	96700.988	147390.885	111251.83			-
22	M ₁ -M ₂ transplant	M ₁	140435.859	132638.49	194617.664	188824.101			-
23	control M ₂ only	M ₂	54946.232	64729.151					-
23	control M ₁ only	M ₁	223817.815	275137.553					-
24	M ₁ -M ₂ transplant	M ₂	115563.26	197739.709	198822.332	247470.595			4
24	M ₁ -M ₂ transplant	M ₁	152594.991	399464.989	431390.541	607345.162			5
25	control M ₂ only	M ₂	93008.397	205706.256	186155.608	264835.126			4
25	control M ₁ only	M ₁	155826.189	352412.906	326051.667	297829.471			5

26	M ₁ -M ₂ transplant	M ₂	161121.23	255678.233	431336.363	569655.512	674423.516	5*
26	M ₁ -M ₂ transplant	M ₁	180802.053	262739.873	487945.189	524613.548	468250.022	5
27	control M ₂ only	M ₂	104115.04	169663.105	297265.751	311711.555	322905.186	-
27	control M ₁ only	M ₁	382250.932	452627.871	581527.522	635164.263	567312.879	-
28	M ₁ -M ₂ transplant	M ₂	120533.503	211732.843	240270.91	235560.307	390260.184	4
28	M ₁ -M ₂ transplant	M ₁	137079.01	270727.856	378916.821	364944.281	428764.217	5
29	control M ₂ only	M ₂	218375.513	159269.693	336582.44	399132.691	234318.621	5*
29	control M ₁ only	M ₁	492902.675	495653.043	607394.62	513437.625	405980.72	5
30	M ₁ -M ₂ transplant	M ₂	174844.232	264465.473	280784.923	396305.1	395274.269	5*
30	M ₁ -M ₂ transplant	M ₁	177966.365	345974.441	549046.693	583579.519	499590.875	5
31	control M ₂ only	M ₂	133351.626	194741.728	201307.73	230584.556		4
31	control M ₁ only	M ₁	263243.139	345616.154	466439.389	501780.317		5